SUMMARY REPORT OF PHYSICS
MEASUREMENTS ON SM-1 CORE I

By:
S. H. Weiss

Approved By:
M. H. Dixon, Project Engineer

Issued: February 6, 1962

ABSTRACT

This report summarizes all core physics experiments performed on SM-1 Core I and SM-1 Rearranged and Spiked Core I throughout core life. These measurements were obtained on site during the 16. 4 MWYR lifetime of SM-1 Core I and 1. 6 MWYR lifetime of SM-1 Rearranged and Spiked Core I. SM-1 Core I was the first stainless steel - UO_2 dispersion core to burn out in the Army Nuclear Power Program. Experimental techniques are described and a complete history of fuel movements in the core presented.

Measurements include control rod bank positions during all core conditions, temperature and pressure coefficients, control rod calibrations, transient poison effects, source multiplication, and stuck rod positions. The effect of core re-arrangement and spiking on core reactivity and core life is also reported. Applicable measurements from the SM-1 zero power experiments are included.

ACKNOWLEDGEMENTS

TABLE OF CONTENTS

TABLE OF CONTENTS (CONT'D)

TABLE OF CONTENTS (CONT'D)

TABLE OF CONTENTS (CONT'D)

TABLE OF CONTENTS (CONT'D)

LIST OF FIGURES

LIST OF FIGURES (CONT'D)

xvi

LIST OF FIGURES (CONT'D)

LIST OF FIGURES (CONT'D)

xviii

LIST OF FIGURES (CONT'D)

LIST OF FIGURES (CONT'D)

LIST OF TABLES

LIST OF TABLES (CONT'D)

LIST OF TABLES (CONT'D)

SUMMARY

This report provides a comprehensive summary of all core physics data obtained during burnup of SM-1 Core I and SM-1 Rearranged and Spiked Core I. SM-1 Core I, the first stainless steel-UO_2 dispersion core to burn out in the Army Nuclear Power Program, reached end of life after 16.4 MWYR energy release; the core was then rearranged and spiked for an additional potential 2.7 MWYR energy release. These measurements will serve as a basis for analysis to establish the accuracy of design methods and to develop improvements in reactor core performance that will result in improved plant reliability, economy of operation, and reduced fuel cost.

Physics tests were performed at intervals of approximately 2 to 3 MWYR core energy release to determine the variation of core parameters with lifetime. Measurements include control rod bank positions during all core conditions, temperature and pressure coefficients, control rod calibrations, transient poison effects, source multiplication, and stuck rod positions. The following table summarizes some of the important experimental results:

SM-1 Core I energy release	16.4 MWYR*
SM-1 Rearranged and Spiked Core I	
A) Actual energy release	1.6 MWYR
B) Estimated potential energy release	2.7 MWYR
Reactivity increase due to core rearrangement and spiking	$2.7
Temperature coefficient at 440°F, low xenon concentration	-3.6 ± 0.1¢/°F
Hot to cold reactivity change with low xenon concentration	
A) SM-1 Core I	$6.7 ± 0.5
B) SM-1 Rearranged and Spiked Core I	$7.2 ± 0.4
Five rod bank integral worth, 0 MWYR, 70°F	$27.4 ± 1.0
Seven rod bank integral worth, 0 MWYR, 70°F	$34.0 ± 2.0
Shutdown margin, five-rod bank and rods A and B, 0 MWYR, 70°F	$10.2
Excess reactivity of core, 0 MWYR, 70°F	23.8

* The energy release of the SM-1 Core I unperturbed by the insertion of two new elements at 2/3 core life is estimated at 16.1 MWYR.

SUMMARY (CONT'D)

Time required to reach peak xenon concentration after
reduction from full-power operation   7-9 hr.

Time required to reach peak xenon and decay back to
equilibrium xenon concentration after reduction from
full-power operation   19-21 hr.

The conclusions section of the report (6. 0) presents more fully the
principal results and indicates their significance. Appendix E summarizes
at greater length, the SM-1 Core I experimental data. Recommendations for
improved core physics measurements and techniques are given in section 6. 3.

1.0 INTRODUCTION

The end of life of SM-1 Core I was reached after 16.4 MWYR energy release. This was the first stainless steel - UO_2 dispersion core to burn out in the Army Nuclear Power Program. The core was then rearranged and spiked for an additional potential 2.7 MWYR energy release.

Extensive experiments were performed throughout SM-1 Core I life and at the beginning and end of life of the SM-1 Rearranged and Spiked Core I. These experiments were sufficient to completely define the control rod bank position during all core conditions. In addition, temperature and pressure coefficients were measured along with control rod calibrations, transient poison effects, source multiplication, and stuck rod positions.

The purpose of this report is to provide a comprehensive summary of all core physics data obtained during the burnup of the SM-1 Core I and the Rearranged and Spiked Core I. Analysis of these measurements will serve as a basis for establishing the accuracy of design methods and to develop a basis for improvements of reactor core performance that will result in improved plant reliability, economy of operation and reduced fuel cost.

Work was performed under Item 2.2 of the Fiscal Year 1961 Program Plan for Engineering Support and Development of the Army PWR Power Plants.

2.0 DESCRIPTION OF SM-1 CORE I

2.1 GENERAL DESCRIPTION[1]

The SM-1 Core I consists of a 7 x 7 array of fixed and control rod fuel elements with the four-corner elements missing as shown in Fig. 2.1. The core contains 38 fixed fuel elements and 7 control rod assemblies of the fuel follower type. Figure 2.2 shows a plan view of the core layout and core lattice and control rod designations. The central rod is designated C, the two close packed rods A and B, and the eccentric rods 1, 2, 3 and 4. The fuel elements consist of fuel plates containing a dispersion of fully enriched UO_2 as fuel and B_4C as a burnable poison contained in a stainless steel matrix clad with 5 mils of stainless steel. The fuel plates in the fixed fuel elements are arranged in sub-assemblies containing 18 fuel plates brazed into side plates as shown in Fig. 2.3. The control rods shown in Fig. 2.4 consist of a tube containing an absorber section and fuel element follower, such that insertion of the absorber section into the reactor core displaces a fuel element. The control rod fuel elements consist of 16 fuel plates per element as illustrated in Fig. 2.5. An absorber section drawing is shown in Fig. 2.6. Figure 2.7 presents an overall view of the reactor and primary shield arrangement.

2.2 HISTORY OF SM-1 CORE I

The SM-1 Core I attained initial criticality on April 8, 1957[2]. At the end of 2/3 core life (approximately 10.5 MWYR), the following changes were made:[3]*

1. Because of swelling, those absorbers containing boron in control rods 1, 2, 3, 4 and C as shown in Fig. 2.2 were replaced by absorbers containing Eu_2O_3

2. One fixed element in a position adjacent to the reflector was replaced by a new Core I element (ref. Appendix A).

3. One control rod element was replaced by a new Core II control rod element.

Both of the removed fuel elements and two of the absorber sections were sent to ORNL for hot cell and metallographic examination.

---

* Details presented in Appendix A.
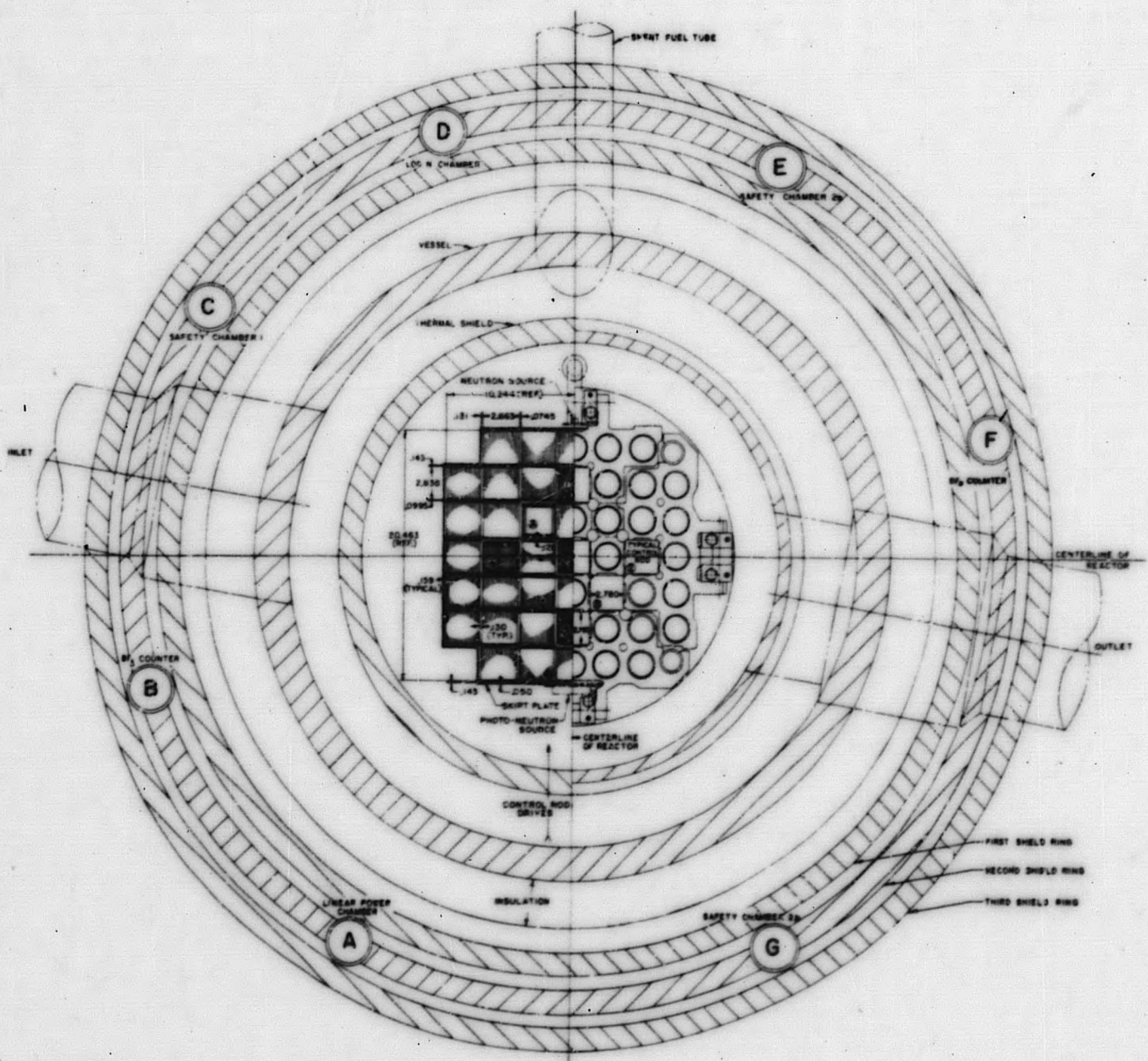
Figure 2. 1.   Reactor Core Cross Section
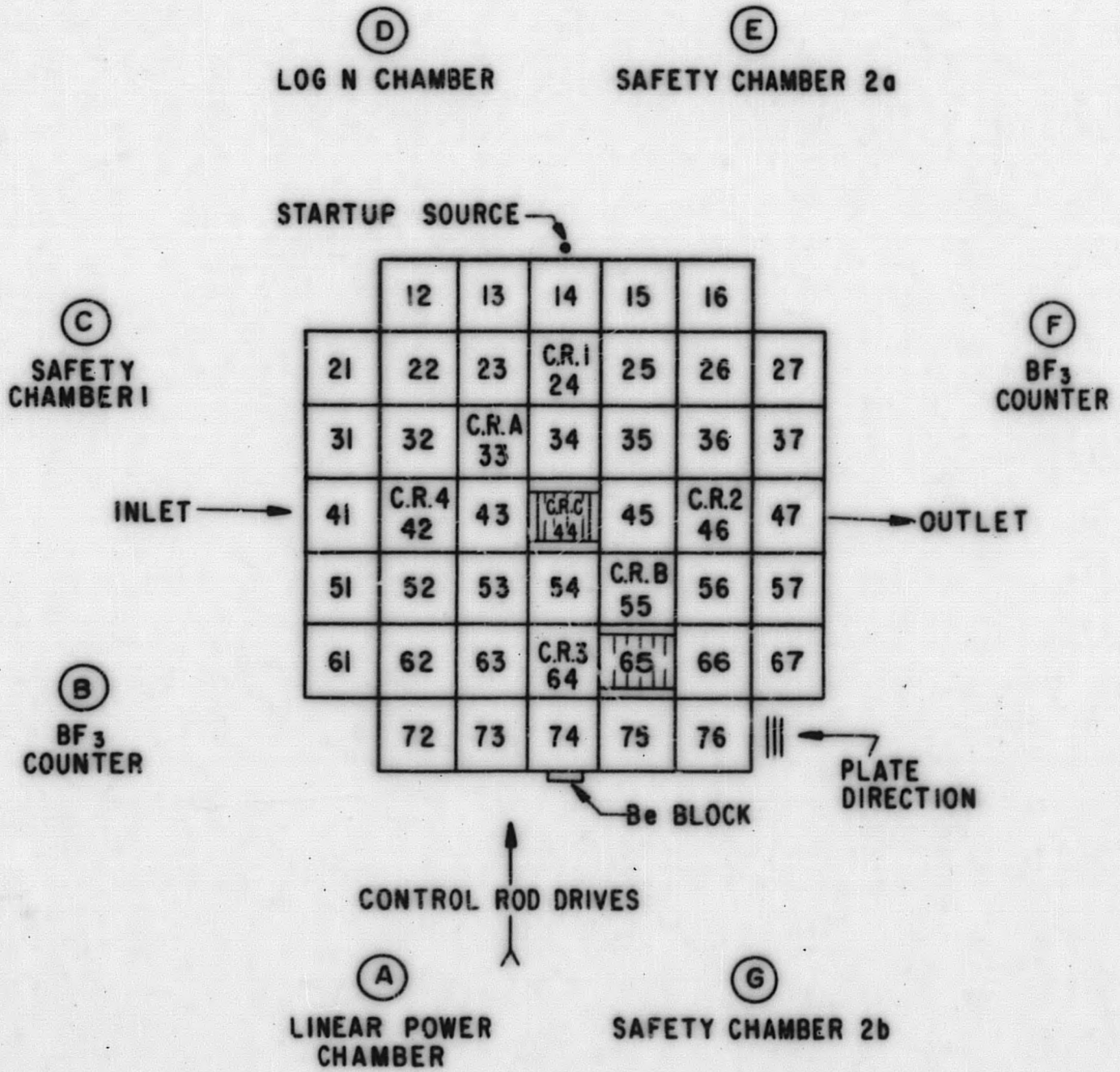
Figure 2.2.   SM-1 Core Layout

Figure 2.3. Stationary Fuel Element, Core I
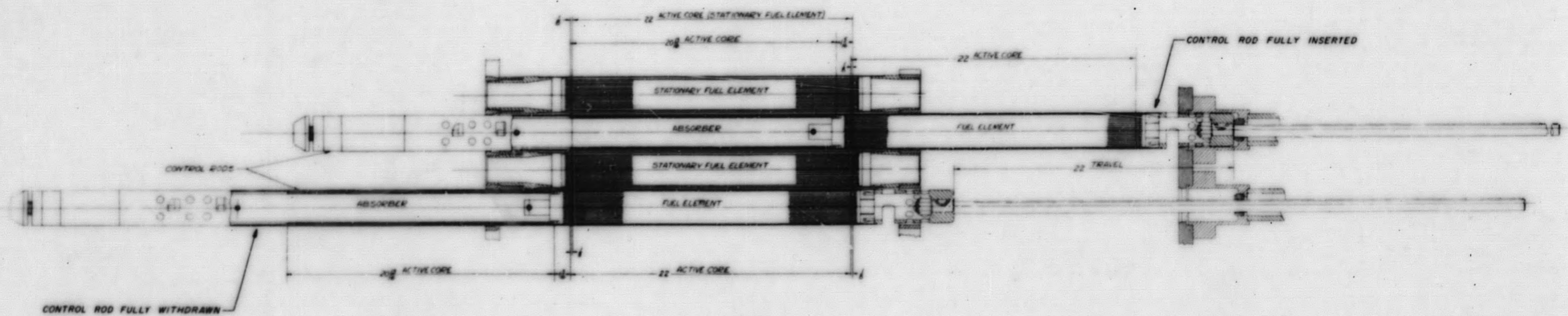
Figure 2. 4.   Control Rod Positions

ASSEMBLED ELEMENT MUST FIT WITHIN A THEORETICAL STRAIGHT BOX OF THESE DIMENSIONS 25" LONG WITHOUT INTERFERENCE.

2.450 MAX.

2.450 MAX.

2.624 ±.002

2.619 ±.002

SECTION A-A

COAST METALS NP BRAZING ALLOY

.005 CLEARANCE

SECTION AT B
SCALE 4 X SIZE

HANDLE
B9-13-2021
2 REQUIRED

SIDE PLATE
D9-13-2011
2 REQUIRED

PIN
A9-13-2020
1 REQUIRED

COMB
A9-13-2012
2 REQUIRED

FUEL PLATE
D9-13-2006
14 REQUIRED

FUEL PLATE, LONG
A9-13-2009
2 REQUIRED

(EACH LEG OF HANDLES)

24 13/16 ±1/64 (REF.)

METHOD OF ASSEMBLY
1- HELI-ARC HANDLES TO SIDE PLATES AS SHOWN.
2- ASSEMBLE SIDE PLATES (WITH HANDLES) FUEL PLATES AND COMBS.
3- FURNACE BRAZE FUEL PLATES TO SIDE PLATES AND COMBS TO FUEL PLATES.
4- HELI-ARC PIN TO HANDLES AS SHOWN.

Figure 2.5. Control Rod Fuel Element, Core I

ABSORBER PLATE (DRILLED)
B9-13-2017
2 REQUIRED

PIN
A9-13-2019
1 REQUIRED

2.624
2.616

2.650 MAX

2.624
2.616

2.650 MAX

ABSORBER PLATE
A9-13-2018
2 REQUIRED

ASSEMBLED SECTION MUST FIT WITHIN
A THEORETICAL STRAIGHT BOX OF THESE
DIMENSIONS 26 1/2 LONG WITHOUT INTERFERENCE.

26 1/16 (REF)
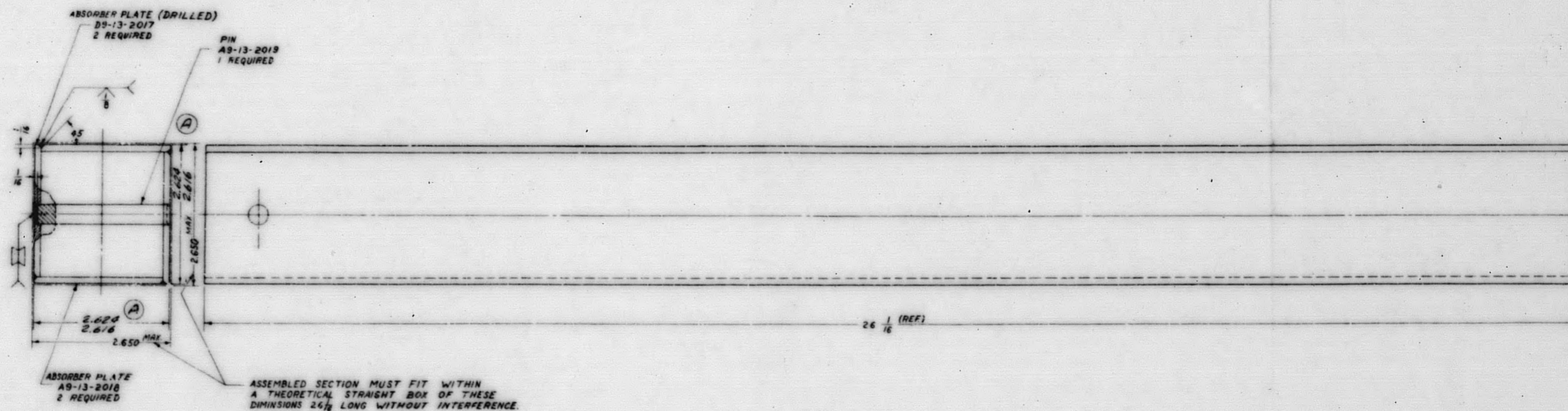
Figure 2.6. Control Rod Absorber Section, Core I
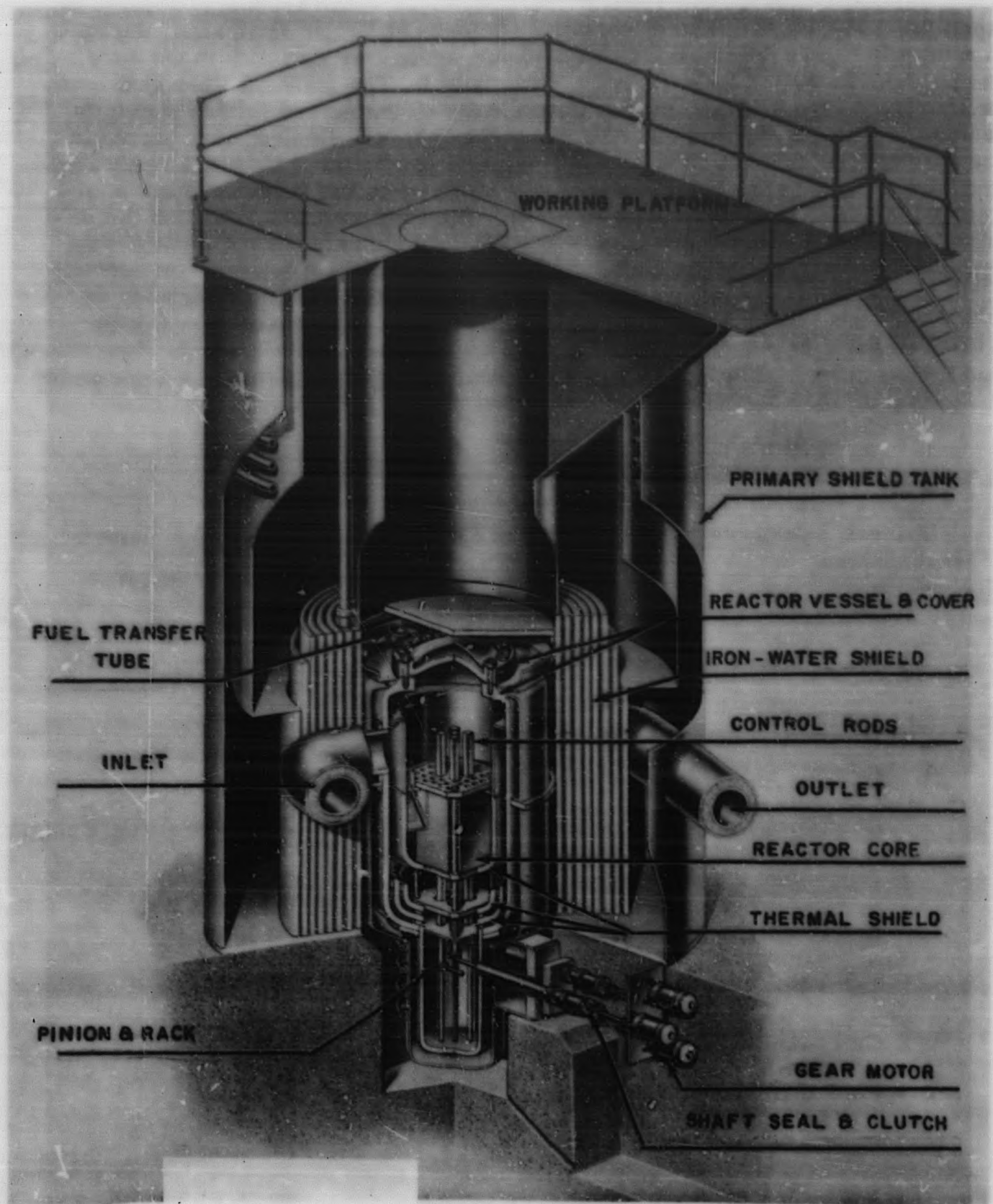
Figure 2.7. Reactor and Primary Shield Arrangement

The end of SM-1 Core I life occurred after 16.4 MWYR energy release on April 28, 1960. [4], [5]   End of core life was defined as that time when, during normal full-power operation with equilibrium xenon concentration in the core, the full load of 2050 KWe could not be maintained.   The plant was then shut down and the fixed elements rearranged (interchange of center and outside elements). [6] In addition, an SM-2B type element and a PM-1-M fuel element were placed in the core and referred to as spikes.   The initial operation of the SM-1 Rearranged and Spiked Core I resulted in a significant increase in the fission product concentration in the primary coolant of SM-1.   The core was shut down and the release of fission products localized to the PM-1-M element.   This element was then removed and an SM-2A element inserted.   Appendix A presents the fuel element locations for the various loadings.   Operation was continued for another 1.6 MWYR until April 11, 1961, before shutdown for core changeover.   It is estimated that, at this time, there was still available 1.1 MWYR in the Rearranged and Spiked Core I.   The SM-1 Core I and Rearranged and Spiked Core I operated for a total of 18.0 MWYR and had a potential of 19.1 MWYR energy release.

2.3   SM-1 CORE I DESCRIPTION

Table 2.1 presents a summary of the SM-1 Core I geometry and material characteristics.

TABLE 2.1
SM-1 CORE I GEOMETRY AND MATERIAL CHARACTERISTICS

A.   GEOMETRY

1.   Overall

Configuration	7 x 7 with corners missing
Equivalent diameter, (in.)	22.2
Active core height, (in.)	21.75
Total No. of cells	45
Cell size (in.)	2.9375 x 2.9375

2.   Fuel Elements (Fixed)

Number	38
Active length, (in.)	21.75 $\pm$ .75
Total length, (in.)	33.625

Cross section, (in.)	2. 863 x 2. 844
Shipping length (in.)	33. 625
Lift handle on assembly	Dowel pin on upper end box

3. **Fuel Elements (Control Rod)**

Number	7
Active length (in.)	21. 125 $\pm$ .625
Total length, (in.)	26. 44
Cross section, (in.)	2. 624 x 2. 619
Shipping length, (in.)	26. 625
Lift handle on assembly	Handle on upper end

4. **Fuel Plates (Fixed)**

Type of fuel	UO_2 (Geneva)
No. of plates/element	18
Size of fuel plates, overall, (in.)	0. 30 x 2. 778 x 23
Type of cladding	304L SS
Wall thickness of cladding (in.)	0. 005
Meat width, (in.)	2. 540
Meat thickness, (in.)	0. 020
Active volume per plate (in.^{3})	1. ⌐
Size of UO_2 fuel particles (microns)	44 to 88
Water gap between fuel plates, (in.)	0. 133

5. Fuel Plates (Control Rod)

Type of fuel	UO_2 (Geneva)
No. of plates/element	16
Size of fuel plates, overall, (in.)	0.030 x 2.558 x 23
Type of cladding	304L SS
Wall thickness of cladding (in.)	0.005
Meat width, (in.)	2.320
Meat thickness (in.)	0.020
Active volume per plate, (in.^{3})	0.98
Size of UO_2 fuel particles, (microns)	44 to 88
Water gap between fuel plates, (in.)	0.133

B. COMPOSITION AND LOADING

1. Core

Total weight of U^{235} in core (kg)	22.50
Total weight of B^{10} in core, (gm)	** 15.75
Enrichment of U^{235} (%)	93.07
Total weight of SS in core, (kg)	*208.92

2. Fuel Element (Fixed)

Weight of U^{235} per element, (gm)	515.16
Weight of UO_2 per element, (gm)	630.36
Weight of SS per element, (kg)	* 4.263
Weight of B_4C per element (gm)	** 2.626
Weight of B^{10} per element (gm)	** 0.3605
Weight of B^N per element, (gm)	** 1.9926

* Includes cladding.
** Best estimate of actual boron content in fabricated plates and core. [7]

3. Fuel Element (Control Rod)

Weight of U^{235} per element, (gm)	417. 76
Weight of UO_2 per element, (gm)	512. 16
Weight of SS per element, (kg)	* 6. 704
Weight of B_4C per element (gm)	** 2. 132
Weight of B^{10} per element (gm)	** 0. 2926
Weight of B^N per element, (gm)	** 1. 8176

4. Fuel Plate (Fixed)

Weight of U^{235} per plate, (gm)	28. 62
Weight of UO_2 per plate,(gm)	35. 02
Weight of SS in meat per plate, (gm)	99. 80
Weight of B_4C per plate, (gm)	** 0. 1459
Weight of B^{10} per plate, (gm)	** 0. 02003
Weight of B^N per plate, (gm)	** 0. 1107

5. Fuel Plate (Control Rod)

Weight of U^{235} per plate, (gm)	26. 11
Weight of UO_2 per plate,(gm)	32. 01
Weight of SS in meat per plate (gm)	91. 56
Weight of B_4C per plate (gm)	** 0. 1332
Weight of B^{10} per plate (gm)	** 0. 01829
Weight of B^N per plate (gm)	** 0. 1011

---

* Includes cladding.
** Best estimate of actual boron content in fabricated plates and core. [7]

2.4 CORE SUPPORT STRUCTURE

The core support structure functions to:

1. Locate and orient the stationary fuel elements.

2. Enclose the core so that the entire primary coolant flow is directed through it.

3. Provide the upper guides for the control rod.

4. Provide the dashpot for deceleration of the control rod during scram.

The core support structure[1] consists of an upper mounting flange, upper and lower grid plates, a skirt, four tie rods, pinion bearing support carrier and seven pinion bearing supports. The upper grid plate (in the form of four hinged doors) and the lower grid plate locate, orient and hold the stationary fuel elements. The upper grid plate also provides upper guides for the control rods. The skirt (0.050 in.), which encloses the entire core, is sandwiched between the upper mounting flange and the lower grid plate. The photoneutron source (0.5 x 3 x 3 in. Be block) is mounted on the skirt.

2.5 REACTOR VESSEL

The reactor vessel contains the active core, its supporting structure and thermal shielding. It is a cylindrical vessel 47-1/2 in. ID, approximately 5-1/2 ft long with a 22 in. ID extension approximately 4 ft long on the bottom. The latter part of the structure houses the control rod racks and their associated pinions and support structures. Wall thicknesses of the vessel and the extension are 2-3/4 and 1-1/2 in., respectively.

An ellipsoidal head is welded to the lower end of the vessel. The upper end of the vessel is closed, thus providing a closure by means of a dish-type cover 2-3/4 in. thick, which is secured to the vessel by means of a flange and gasket and stud bolts. Total height, including cover, is 13 ft, 6 in. The opening at the upper end of the vessel is 28 in. diam to permit insertion of the fully assembled core structure.

Primary water enters at 427.7°F, makes one upward pass through the core, and leaves the vessel at 448°F and 1200 psia. The inlet and outlet nozzles are stainless steel and are located above the core and near the top of the large cylindrical section. Seven tubes penetrate the lower pressure vessel section at right angles to permit connection of the control rod drives. A mounting flange ties these tubes together 41 in. from the centerline of the vessel. The seals and drive mechanisms are bolted to this flange.

2-20

Structural support for the pressure vessel is by means of a ring attached to the outside diameter of the cylindrical section just below the inlet and outlet pipes. This ring rests on a support ring welded to the inner steel shielding ring, which in turn, rests on a concrete structure in the bottom of the vapor container.

2.6 REACTOR INSTRUMENTS

Five ionization chambers and two BF_3 counters are used on the SM-1. The chambers are mounted in wells next to the inner wall of the shield tank as shown in Figs. 2.1 and 2.2. In the first critical experiment at SM-1, neutron counters were mounted temporarily within the pressure vessel next to the core.

There are three uncompensated ionization chambers which serve to actuate the safety level scram system. One compensated ionization chamber is connected to the log N and period meters. The second compensated ionization chamber provides a signal to the linear power channel.

2.7 DOCUMENTS REPORTING SM-1 CORE I EXPERIMENTAL PHYSICS DATA

The SM-1 Core I was fabricated according to specifications documented in ORNL-2225, "Specifications for Army Package Power Reactor (APPR-1) Fuel and Control Rod Components," by R. J. Beaver, et al. These specifications were based on analytical work reported in APAE No. 7, "Reactor Analysis for the Army Package Power Reactor No. 1," edited by J. G. Gallagher. Following is a summary of documents relating to measurements performed in the design and development work and operation of the SM-1 Core I:

By	Title	No.	Dated
Williams, D. V. P., et al	Army Package Power Reactor Critical Experiment.	ORNL 2128	8-8-56
Noaks, J. W., and Johnson, W. R.	Army Package Power Reactor Zero Power Experiments, ZPE-1.	APAE #8	2-8-57
Noaks, J. W., editor	Extended Zero Power Experiments on the Army Package Power Reactor, ZPE-2	APAE #21	11-15-57
Meem, J. L., editor	Initial Operation and Testing of the Army Package Power Reactor APPR-1.	APAE #18	8-9-57

By	Title	No.	Dated
MacKay, S. D., et al	SM-1 Research and Development Program, Interim Report on Core Measurements, Task No. VII. (Summary of core physics measurements through 9.1 MWYR energy release.)	APAE Memo #178	3-1-59
MacKay, S. D. et al	SM-1 Research and Development Program, Interim Report No. 2 on Core Measurements, Task No. VII. (Core physics measurements at 10.5 MWYR energy release.)	APAE Memo #206	6-30-59
Obrist, C. H. et al	SM-1 Reactor Core Inspection at 2/3 Core Life.	APAE #55	1-13-60
MacKay, S. D. and Tubbs, D. C.	SM-1 Research and Development Program Test Report, Core Physics Measurements, Tests 301-316. (Core physics measurements at 12.1 MWYR energy release.)	-	9-30-59
Tubbs, D. C. et al	SM-1 Research and Development Program Test Report Core Physics Measurements at 13.5 MWYR, Tests 301-316.	-	3-23-60
Kemp, S. N. et al	SM-1 Research and Development Program Test Report, Core Physics Measurements at 16.43 MWYR, Tests 301-317, 319, 320. (End of life of SM-1 Core I physics measurements).	AP Note #291	10-15-60
Kemp, S. N., et al	PWR Research and Development Program, Test Report, Gamma Scanning Spent SM-1 Core I Fuel Elements, Test 318.	APAE Memo #281	4-6-61

2-22

By	Title	No.	Dated
Kemp, S. N. et al	PWR Research and Development Program Test Report, Core Physics Measurements at Startup of the Rearranged and Spiked SM-1 Core.	AP Note #309	12-6-6(
Hasse, R. A. , et al	Army PWR Support and Development Program Test Report, Flux Mapping of SM-1 Spent, Rearranged and Spiked Cores - Test 321.	AP Note #321	1-5-61

3.0 EXPERIMENTAL TECHNIQUES

3.1 INTRODUCTION

The core physics test program is designed to provide experimental data which can be used to establish the reactivity associated with various xenon concentrations and core parameters, and verify the reliable operation of the SM-1 nuclear plant.

Physics tests are performed at intervals of approximately 2 to 3 MWYR core energy release to determine the variation of core parameters with lifetime. Knowledge of reactor behavior with time provides a basis for improving the design models and evaluating the accuracy of the analytical techniques used to predict core burnup behavior.

3.2 PROBLEMS OF POWER REACTOR CORE PHYSICS MEASUREMENTS

The problems in making core physics measurements on a power reactor are twofold:

1. Some of the difficulties present in performing physics measurements on a high temperature, high power level reactor are:

   a. The core must supply power to heat the primary system; the xenon thus built up complicates xenon transient, temperature coefficient and low xenon concentration measurements.

   b. Temperature corrections must be applied to all measurements due to the large temperature coefficient.

   c. The reactor must operate at a minimum of approximately 1 percent of full power to maintain operating temperature.

   d. Any change in power level will induce a temperature change and a resulting reactivity change.

2. Special problems encountered in performing tests on a prototype of a reactor designed to meet the requirements of a remote military base.

   a. Reactor operations are carried out by the military operating crew at all times, including core physics measurements. Portions of the data are also collected by the military operating crew.

   b. There is an estimated uncertainty of ± 0.03 in in determining a control rod position.

c. There is an estimated uncertainty of $\pm$ 2°F in determining the reactor inlet and outlet temperatures.

d. There is an estimated uncertainty of $\pm$ 10 percent in determining the core energy release.

e. Necessity of streamlining test procedures to minimize plant down-time rather than maximizing information yield.

3.3 SM-1 CORE I CORE PHYSICS TESTS

3.3.1 Summary of Core Physics Tests

Table 3.1 summarizes the core physics tests performed on the SM-1. A description of each test and its objective is presented in Appendix B.

TABLE 3.1
SUMMARY OF SM-1 CORE PHYSICS TESTS

Test	Title
A-301	Transient Xenon
A-302	Equilibrium Xenon
A-303	Five Rod Bank Position; Peak Xenon Concentration, 440°F
A-304	Five Rod Bank Position; Equilibrium Xenon Concentration, 440°F
A-305	Five Rod Bank Position; Low Xenon Concentration, 440°F
A-306	Five Rod Bank Position; Low Xenon Concentration, Low Temperature
A-307	Control Rod A Calibration at Peak Xenon, 440°F
A-308	Control Rod A Calibration at Low Xenon, 440°F
A-309	Control Rod A Calibration at Low Xenon, Low Temperature
A-310	Control Rod C Calibration at Low Xenon, 440°F
A-311	Temperature Coefficient
A-312	Source Multiplication
A-312-A	Neutron Source Evaluation
A-313	Gamma Heating in Pressure Vessel
A-314	Five Rod Bank Calibration; Peak to Equilibrium Xenon
A-315	Five Rod Bank Calibration from Rod A Calibration; Low Xenon, 440°F
A-316	Five Rod Bank Calibration from Rod A Calibration; Low Xenon, Low Temp.
A-317	Spent Core Rearrangement
A-318	Gamma Scanning of Spent Fuel Elements
A-319	Danger Coefficient Measurements
A-320	Xenon Over-ride by Temperature Compensation
A-321	Flux Mapping
A-322	Shutdown Neutron Source Evaluation
A-325	Calibration of Five Rod Bank

3.4 NOMENCLATURE AND EXPLANATIONS

3.4.1 Active Core

The active core is that region defined by upper and lower average limits of U-235 distribution in stationary fuel elements and cell boundaries of the outer row of stationary elements.

3.4.2 Control Rod Withdrawal

This refers to the withdrawal of the absorber section of the control rod from the active core and consequent simultaneous insertion of fuel.

3.4.3 Control Rod Position

Control rod positions are reported as the distance withdrawn from the position of deepest insertion measured in inches. Deepest insertion represents the control rods in the scrammed position resting on the carrier plate of the core support structure; the point at which the control rod indicator dials are set to zero. At the position of deepest insertion the control rod fuel element upper fuel boundary is located 1/8 in. above the bottom of the active core as shown in Fig. 2.4.

Bank positions result from the average of positions of the individual rods comprising the bank.

3.4.4 Core Energy Release

The core thermal release is reported in MWYR; if the SM-1 were operated at full power of 10.77 MW* for one year, the core energy release would be 10.77 MWYR. If operated at 50% of full power for three years, the core energy release would be 16.16 MWYR.

---

* Ref. (2) - Heat balance number 2 with a coolant flow of 3862 gpm, core outlet temperature of 448°F, and core $\triangle T$ of 20.3°F.

4.0 CORE PHYSICS MEASUREMENTS ON SM-1 CORE I

4.1 BANK POSITIONS DURING CORE LIFE

4.1.1 Introduction

The SM-1 reactor is normally operated with five control rods, (1, 2, 3, 4, and C as shown in Fig. 2.2), positioned as a bank; the two remaining rods (A and B) act as safety rods and are nearly fully withdrawn from the core. The safety rods were positioned at 20 in. during the initial startup and testing of the SM-1 rather than fully withdrawn to 22 in.* to meet coolant flow criteria. At the completion of the startup tests, this position was changed to 19 in. withdrawal in order to obtain a faster rate of reactivity decrease in the event of a scram.

4.1.2 Uncertainty in Measurements

In determining control rod positions, there is an experimental error of ± 0.03 in. in the position of a single rod. This is due both to the uncertainty in reading the rod position indicator and the uncertainty in actual control rod location due to backlash in the indicating mechanism.

During the physics measurements, the control rods in the bank were kept within 0.1 in. of one another. The average position of the bank then has a maximum experimental error of ± 0.015 in. Appendix C presents a discussion of the error analysis techniques employed

The core inlet and outlet temperature recorders have an accuracy of $\pm 1.5^{\circ}F$ according to the manufacturer's specifications. However, because these instruments cannot be calibrated regularly, it is estimated that there is an uncertainty of $\pm 2^{\circ}F$ in determining the core inlet and outlet temperature.

The core energy release is obtained from a Δt integrator. Comparison of integrator readings and generator output readings and estimates by plant personnel indicate that there is an estimated uncertainty of $\pm 10\%$ in the core energy release reported in MWYR. Appendix D illustrates the conversion of Δt integrator readings in $^{\circ}F$ days to MWYR.

---

* Rod travel is 22 in. as seen in Fig. 2.4. This means that at 22 in. withdrawal the control rod upper fuel boundary is 3/8 in. above the stationary element upper fuel boundary and the control rod lower fuel boundary is 1 in. above stationary element lower fuel boundary.

4.1.3 Initial Criticality

Prior to the initial startup of the SM-1, zero power experiments were performed at the Alco Products, Inc. Critical Facility, utilizing an SM-1 ZPE Core.[8] This core was manufactured to identical specifications as SM-1 Core I at Ft. Belvoir and used the same core support structure. The ZPE measurements provided a check of the analytical techniques used in designing the core.

Initial criticality, in both cases, was reached with a minimum core loading of 17 elements containing 8.07 Kg U-235. Following initial criticality, further fuel additions were made until the fully loaded 45 element core was reached. Table 4.1 and Fig. 4.1 present the five and seven rod bank critical positions as a function of total number of elements in the core during the approach to the fully loaded condition. Figure 4.2 presents the critical configurations from initial criticality to the fully loaded core for the SM-1 ZPE Core and the SM-1 Core I. Differences in critical positions are probably due to different element configurations, and the boron losses during fuel element manufacture may have been different for the two cores.

TABLE 4.1
CRITICAL BANK POSITIONS VS. NUMBER OF ELEMENTS IN CORE
FOR SM-1 CORE I AND SM-1 ZPE CORE

Total Number of Elements	SM-1 Core I		SM-1 ZPE Core	
	Five Rod Bank Position (in.)	Seven Rod Bank Position (in.)	Five Rod Bank Position (in.)	Seven Rod Bank Position (in.)
17	17.83	18.08		
18			15.74	
19	13.99	14.40	14.09	
21	11.48	12.00	11.51	
22			10.82	
23			10.33	
24	10.21	10.75	9.81	
25			9.43	
26			8.96	
27	8.73	9.44	8.59	
28			8.20	
29			7.91	
30	7.35	8.36	7.58	
31			7.25	
32			6.96	
33	6.48	7.57	6.66	
36	5.71	6.81		
39	5.19	6.39		
42	4.60	6.03		
45	3.70	5.50	3.64	5.31
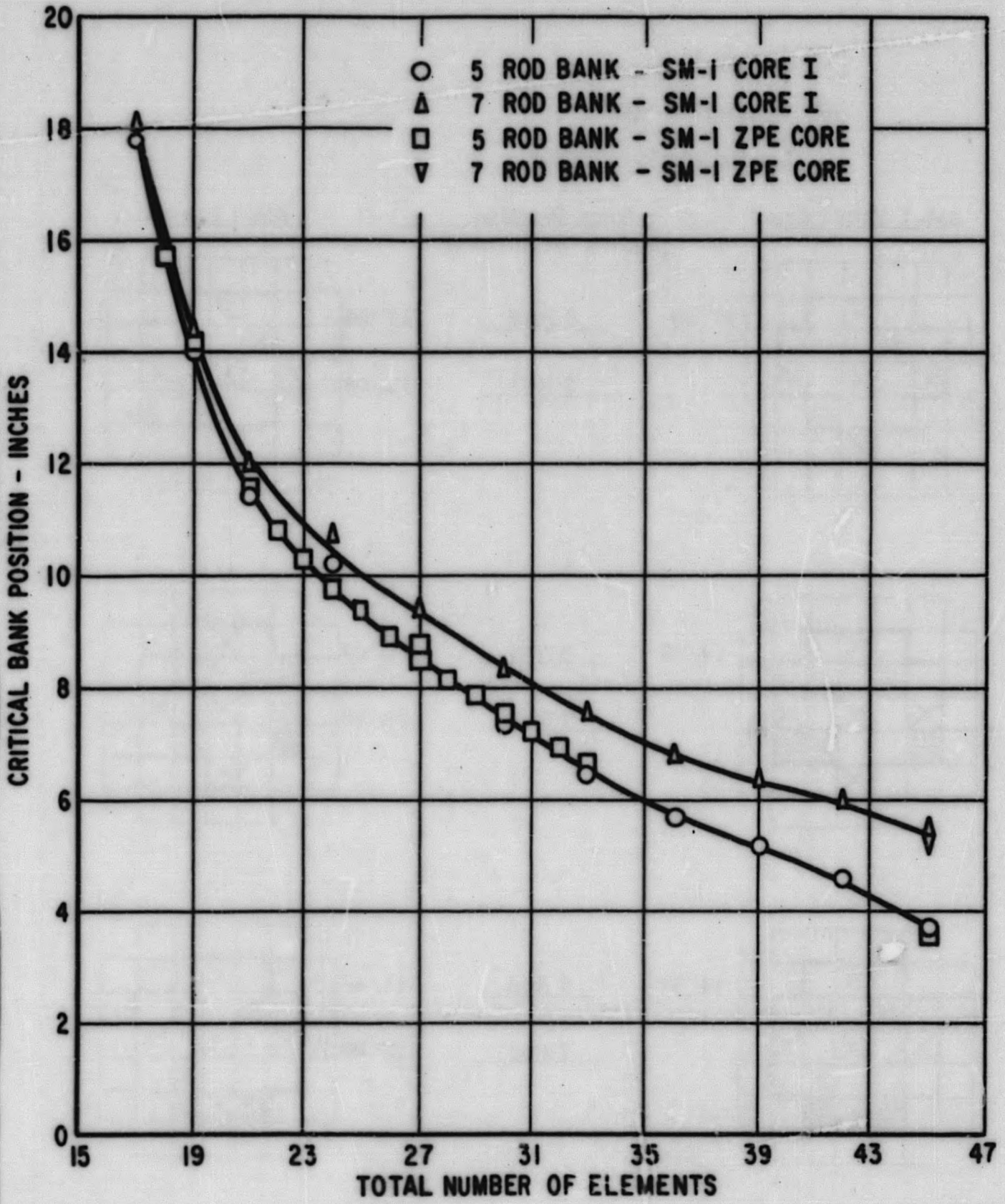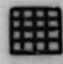
Figure 4.1. Critical Bank Position as a Function of Total Number of Elements Loaded, 68°F
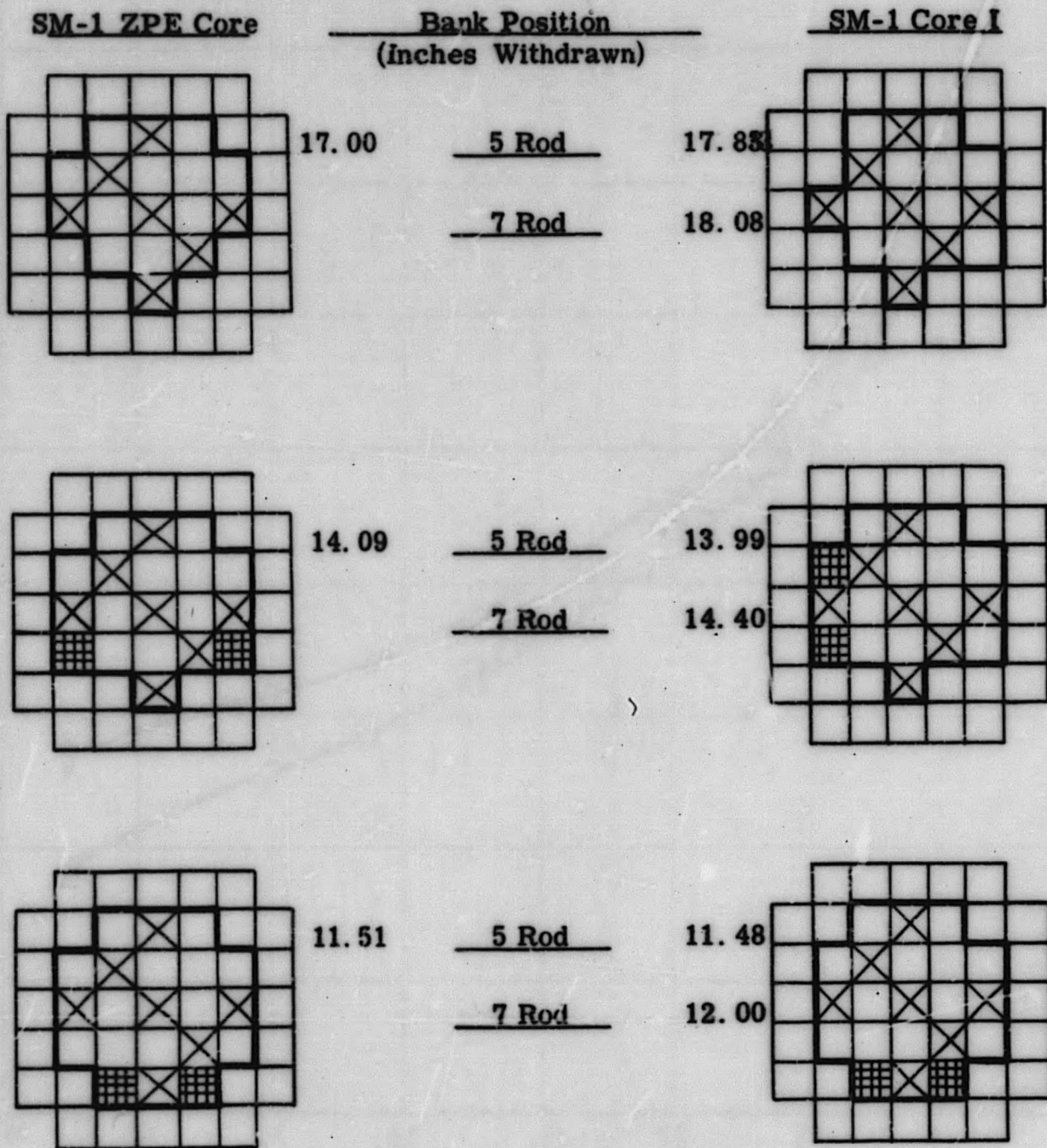
Figure 4.2. Critical Configurations From Initial Criticality
To Fully Loaded Core
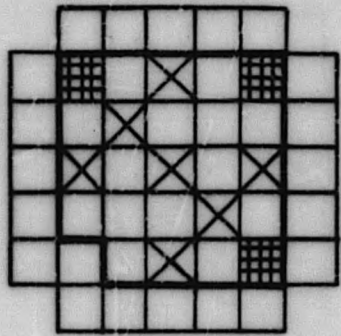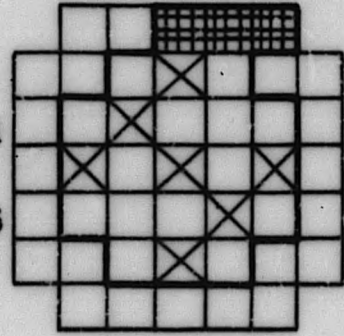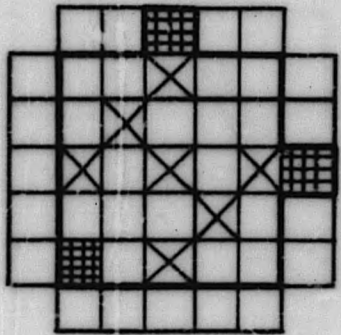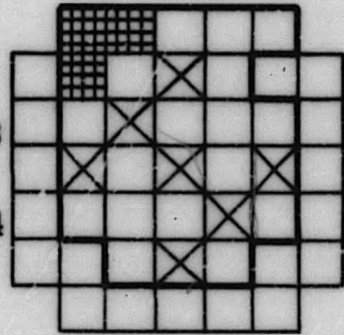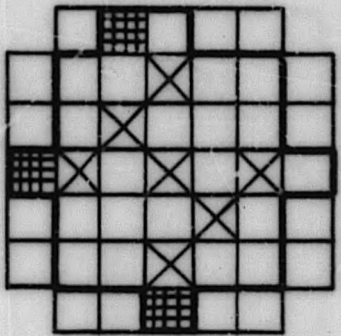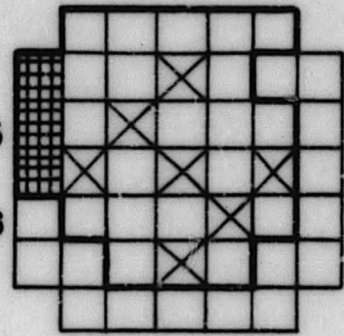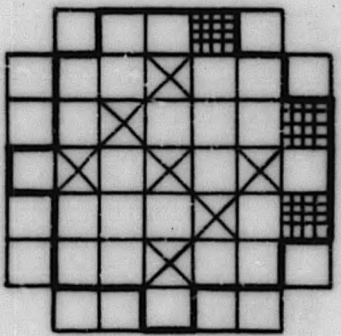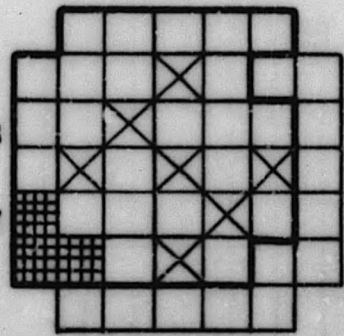
SM-1 ZPE Core   SM-1 Core I

                          Bank Position
                       (Inches Withdrawn)
              9.81   5 Rod   10.21

                            7 Rod   10.75

              8.59   5 Rod   8.73

                            7 Rod   9.44

              7.58   5 Rod   7.35

                            7 Rod   8.36

              6.66   5 Rod   6.48

                            7 Rod   7.57

Figure 4.2. (Continued)

4-5

SM-1 ZPE Core

Bank Position
(Inches Withdrawn)

SM-1 Core I

	Bank Position (Inches Withdrawn)	
5 Rod		5.71
7 Rod		6.81
5 Rod		5.19
7 Rod		6.39
5 Rod		4.60
7 Rod		6.03
3.64	5 Rod	3.70
5.31	7 Rod	5.50
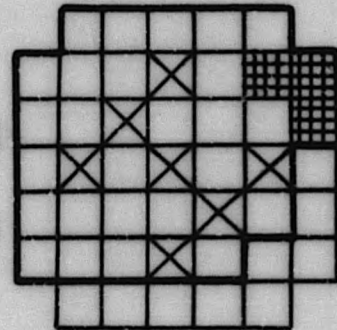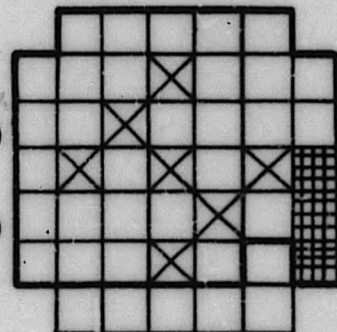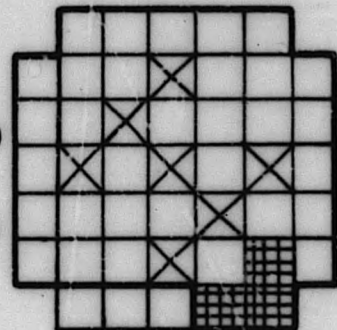
Figure 4.2. (Continued)

4-6
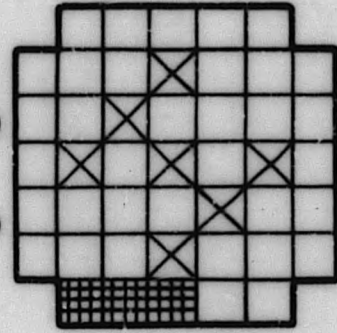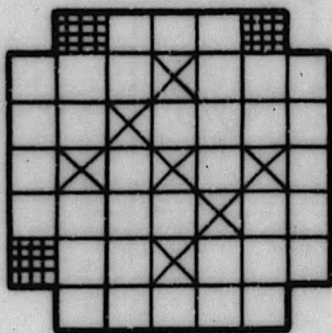
4.1.4 Five Rod Bank Critical Positions as a Function of Core Energy Release

The five rod bank critical position is a function of core burnup, core temperature, and the concentration of xenon and other fission products. To study the behavior of the bank as a function of core life, measurements were made of the five rod bank critical position during core burnup for various core operating conditions (Tests A-303, A-304, A-305, and A-306). The point in life was determined from Δt integrator readings converted to MWYR as in Appendix D.

Table 4.2 presents the measured five rod bank critical positions at equilibrium xenon concentration and $440^\circ F$ as a function of core energy release. This data is presented on Fig. 4.3. At 10.5 MWYR, two fuel elements were removed and replaced by two fresh fuel elements. *[3] Based on calculations performed with the CANDLE-2, IBM-704 code,[9] the replacement of the two depleted elements with two fresh elements results in an increase in core life of 0.35 MWYR. The dashed curve on Fig. 4.3, therefore, represents the burnup of an unmodified core.

Figure 4.4 presents the five rod bank critical positions measured as a function of energy release for low xenon, $70^\circ F$, low xenon, $440^\circ F$, equilibrium xenon, $440^\circ F$ and peak xenon, $440^\circ F$.

The equilibrium xenon, $440^\circ F$ curve shows that initially the reactivity of the core decreased as Sm-149 buildup was superimposed on the B-10 and U-235 burnup. After Sm-149 equilibrium concentration was attained, at approximately 1 MWYR, the reactivity of the core increases slightly as the burnup of B-10 more than compensates for U-235 burnup. After 1.5 MWYR, the shape of the curve was governed by the burnup of U-235 and the buildup of fission products other than Sm-149.

The low xenon, $440^\circ F$, measurements were made approximately 60 hr after power reduction with an estimated 12 cents of reactivity due to the remaining xenon concentration.[10] The low xenon, $70^\circ F$, data has been corrected for temperature (from the lowest temperature reached during cooldown to $70^\circ F$).

4.1.5 Conclusions

1. Evaluation of bank position data as a function of core burnup indicates a steady decrease in core reactivity with core burnup to approximately 1 MWYR energy release. Beyond this point there is a slight increase in core reactivity to approximately 2 MWYR. However, the total core reactivity never exceeds that at the startup condition. This effect is

---

* Appendix A, Figure A.2

TABLE 4.2
SM-1 CORE I MEASURED EQUILIBRIUM XENON BANK POSITIONS
(440 ± 2°F, A and B at 19 In.)

Core Energy Release MWYR ± 10%	Five Rod Bank Position Inches ± 0.02
0	8.3*
0.39	8.41*
0.79	8.54
1.00	8.51
1.41	8.50
1.62	8.52
2.21	8.63
2.77	8.73
3.16	8.82
3.49	8.97
3.80	9.00
4.16	9.07
4.44	9.21
4.79	9.32
5.41	9.60
5.77	9.77
6.15	10.00
6.70	10.20
7.22	10.59
8.21	11.22
8.73	11.45
8.89	11.53
9.10	11.69
9.77	12.10
10.70	12.86
11.03	13.23
11.71	13.90
11.88	14.05
12.10	14.38
13.50	16.03
14.35	16.96
15.26	18.28
16.21	20.70**
16.43	22.0 ***

* A and B at 20 in.
** A and B at 20.20 in.
*** A and B at 22.0 in.
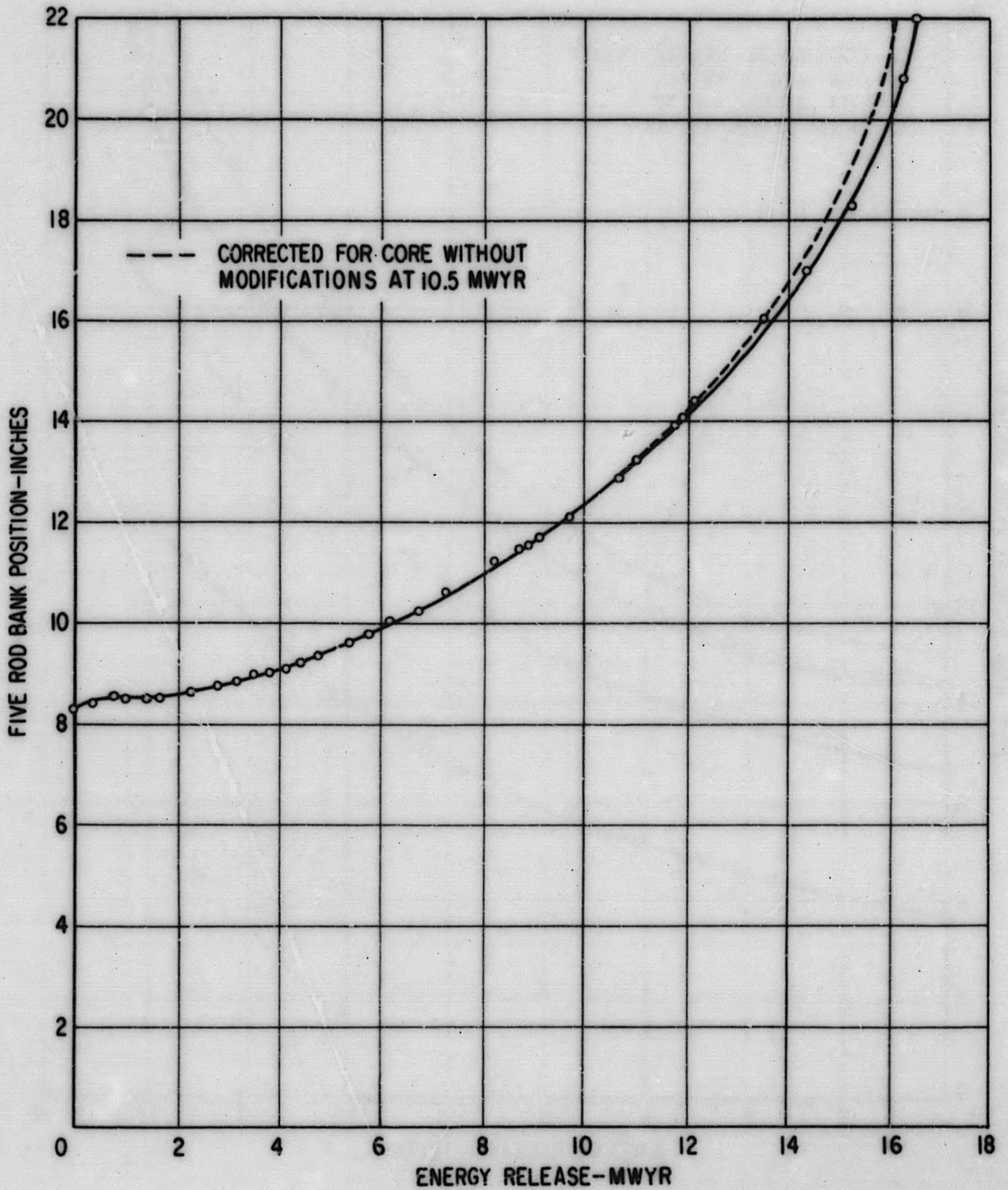
Figure 4.3. SM-1 Core I Five Rod Bank Position as a Function of Energy Release, Equilibrium Xenon, 440°F
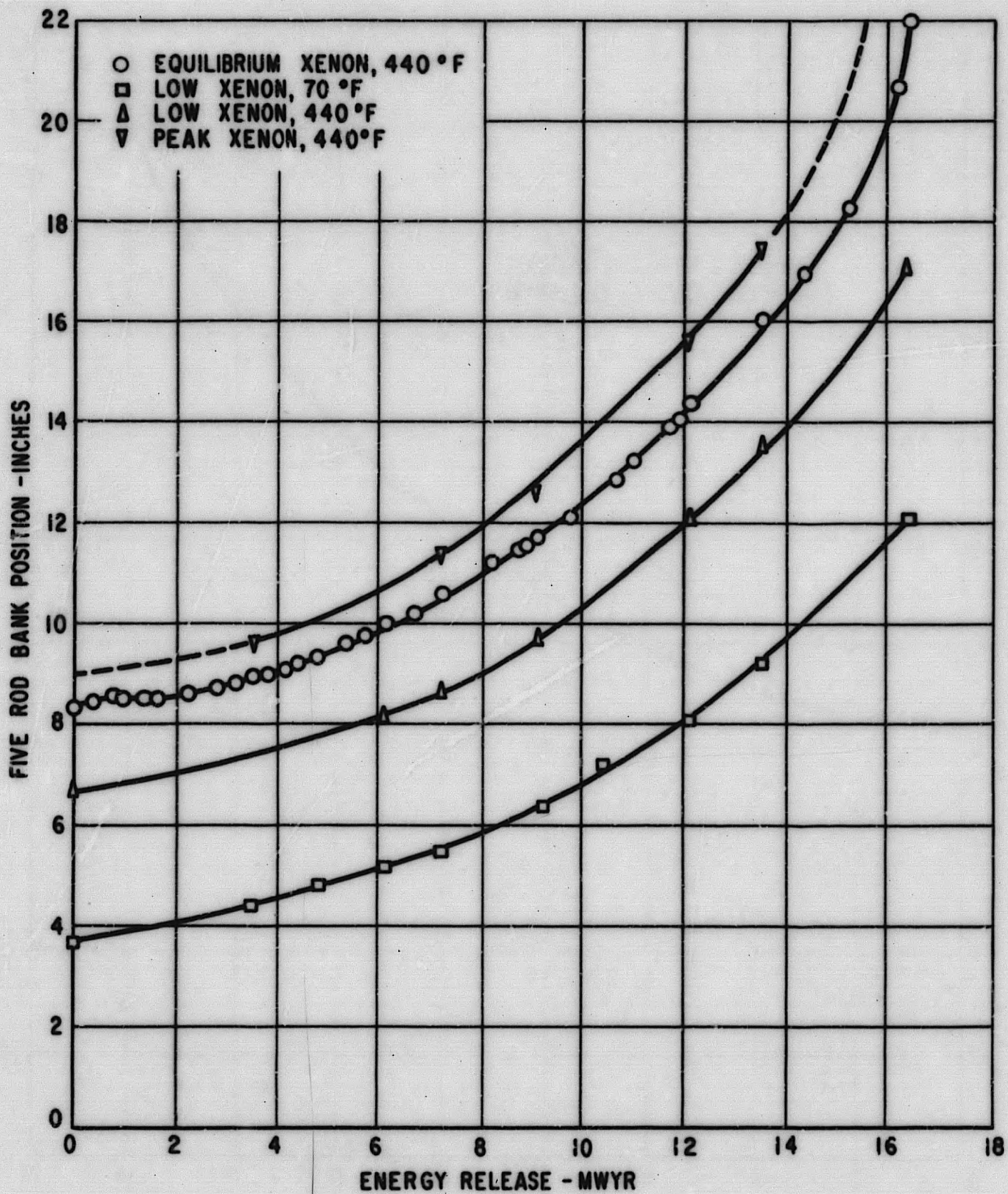
Figure 4.4. SM-1 Core I Five Rod Bank Position as a Function of Energy Release, Various Core Conditions

attributed to initial buildup of fission product poisons Xe and Sm. Beyond the point where saturation fission product concentration is reached in the core, the core reactivity increases slightly as the burnable poison B-10 burns out more rapidly than the U-235.

2. The motion of the five rod bank necessary to override the increase in core temperature from 70^OF to 440^OF, at low xenon, increased from 3.0 to 4.8 in. with core life. The five rod bank movement necessary to override the increase in xenon concentration from low xenon to equilibrium xenon, at 440^OF, increased from 1.6 to 3.4 in. during burnup. The motion of the five rod bank necessary to override the increase in xenon concentration from equilibrium xenon to peak xenon, at 440^OF, increased from 0.7 to 1.7 in.

3. The modifications made at 10.5 MWYR, replacement of two elements with two fresh elements, resulted in an estimated increase in core life of 0.35 MWYR.

4. End of core life was reached at 16.4 MWYR energy release when during normal full power operation, with equilibrium xenon concentration in the core, the full load of 2050 KWe could not be maintained.

5. Extrapolating the bank position as a function of energy curves to 22 in. rod withdrawal indicates that the SM-1 Core I would have a core life of 18 and 21 MWYR if operated at low xenon, 440^OF, and low xenon, 70^OF, respectively.

6. After approximately 15.6 MWYR energy release, the SM-1 Core I could no longer override peak xenon concentration in the core.

4.2 TEMPERATURE COEFFICIENT DURING CORE LIFE

4.2.1 Introduction

The temperature coefficient of reactivity was determined as a function of temperature over the lifetime of the core. Measurements were made as the core was cooled down from operating temperature to room temperature, and the reactivity change associated with the change in core temperature was evaluated from the motion of calibrated control rods.

4.2.2 Test Method

The general test method is to follow the change in reactivity during temperature change with a calibrated control rod. During core life, three variations of test procedure A-311 were used in determining the temperature coefficient.

At startup, during the initial operation and testing of the SM-1, the temperature coefficient was determined during heatup using an outside steam source for heat. As the temperature increased, the bank was kept at a constant position and criticality maintained with control rod C. After the critical position was determined, rod C was then withdrawn slightly to put the reactor on a positive period and obtain a rod calibration point. In this manner, the rod worth was measured at the proper core temperatures.

The temperature coefficient, $\frac{\Delta K}{\Delta T}$, was calculated as follows:

$$\frac{\Delta K}{\Delta T} = \frac{\Delta X}{\Delta T} \cdot \frac{\Delta K}{\Delta X} = \text{cents per } {}^{\circ}F$$

where the ratio of the change in rod position, $\Delta X = X_2 - X_1$, to the change in temperature, $\Delta T = T_1 - T_2$, is $\frac{\Delta X}{\Delta T}$ in inches per ${}^{\circ}F$. $\frac{\Delta K}{\Delta X}$ is the rod worth in cents per inch obtained from the rod calibration curve at the average rod position, $\frac{X_1 + X_2}{2}$. The temperature coefficient value is considered to apply at an average temperature of $\frac{T_1 + T_2}{2}$.

Temperature coefficient tests using the above test procedure were run several times, during the initial startup testing program of the SM-1, with the bank located at a different position for each run. Rod C was recalibrated as a function of temperature for each new configuration. There was excellent agreement among the temperature coefficient data for the various runs. [2]

In the periodic core physics measurements performed during the interval from startup to 7.22 MWYR, the test method was modified slightly and a program was written for the IBM-650 to calculate the temperature coefficient as a function of temperature from the test data. [11] It was also necessary to perform the test without the use of an outside heat source.

During cooldown from operating temperature to low or room temperature, the rate of change of rod A position with time $\Delta X/\Delta t$, was determined as the calibrated control rod was adjusted to maintain criticality. The change in core temperature as a function of time, $\Delta T/\Delta t$, was also recorded. The temperature coefficient, $\frac{\Delta K}{\Delta T}$, was calculated as follows:

$$\frac{\Delta K}{\Delta T} = \frac{\Delta K}{\Delta X} \cdot \frac{\Delta X}{\Delta t} \cdot \frac{1}{\frac{\Delta T}{\Delta t}} = \text{cents per } {}^{\circ}F,$$

where $\frac{\Delta K}{\Delta X}$ is the rod A worth in cents per inch at the average position,

$\frac{X_1 + X_2}{2}$. The temperature coefficient value is plotted at the average temp-

erature, $\frac{T_1 + T_2}{2}$. Rod A was calibrated as a function of the bank position at

both operating temperature and the lowest temperature reached during cooldown.

Values of rod A worth, $\frac{\Delta K}{\Delta X}$, at intermediate temperatures in the temperature

coefficient calculations are obtained by linear interpolation.

Using this method, difficulties were encountered in maintaining a con-
stant cooldown rate so as to obtain an adequate and uniform temperature de-
crease as a function of time. There was also considerable uncertainty in the
rod worth used because the rod calibration curve is a dual function of the bank
position and the core temperature. Use of a rod calibration curve for configur-
ations with a different bank position will at best give only a first order approxi-
mation of the actual rod worth.

The temperature coefficient procedures were again modified after 7.22
MWYR. The changes incorporated some of the advantages of the two preceding
methods. The change in reactivity with temperature is followed with control
rod A; control rod A being calibrated as a function of the five rod bank position
at both operating temperature and the lowest temperature reached during cool-
down. The temperature coefficient was calculated in the same manner as in the
initial procedure; however, the choice of a rod calibration curve from which the
rod worth is obtained is governed by matching bank configurations rather than
core temperature. *

4.2.3 Temperature Coefficient Results

Figure 4.5 presents the measured temperature coefficients versus
temperature, obtained as a function of core life. The data was obtained using
the three previously described techniques; however there were no cases in
which more than one technique was used at the same core energy release. The
curve shown is the best estimate through the data as fitted by eye. At 7.22
MWYR, 11 measurements of the temperature coefficient were made at 443°F;
the average calculated value was -3.5 cents per °F with a probable error of
± 0.1 cents per °F. The data points shown on Fig. 4.5 were, in general,
evaluated over 25 degree increments.

---

* Described in Section 5.4.2
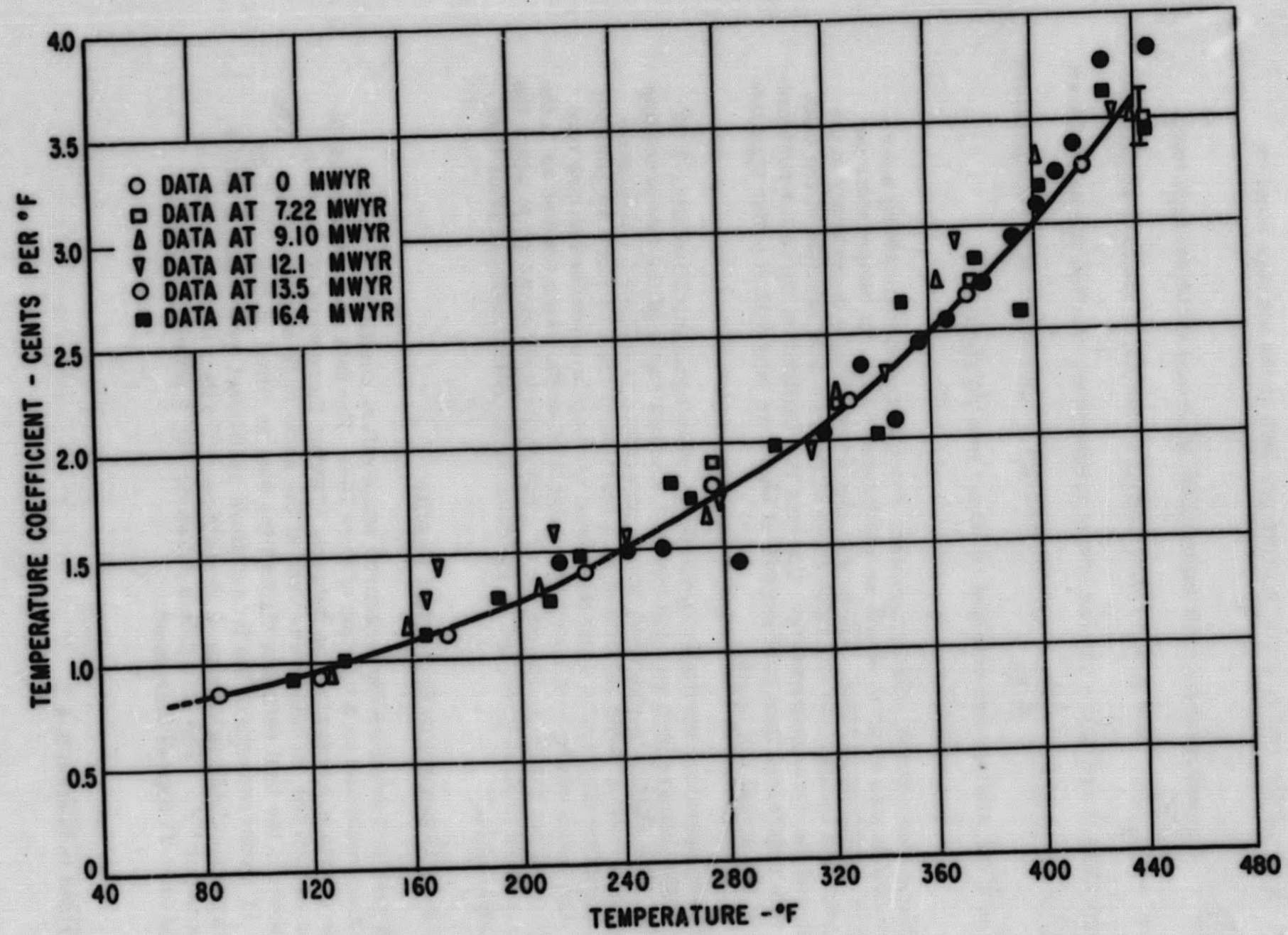
Figure 4.5.   SM-1 Core I Temperature Coefficient vs. Temperature
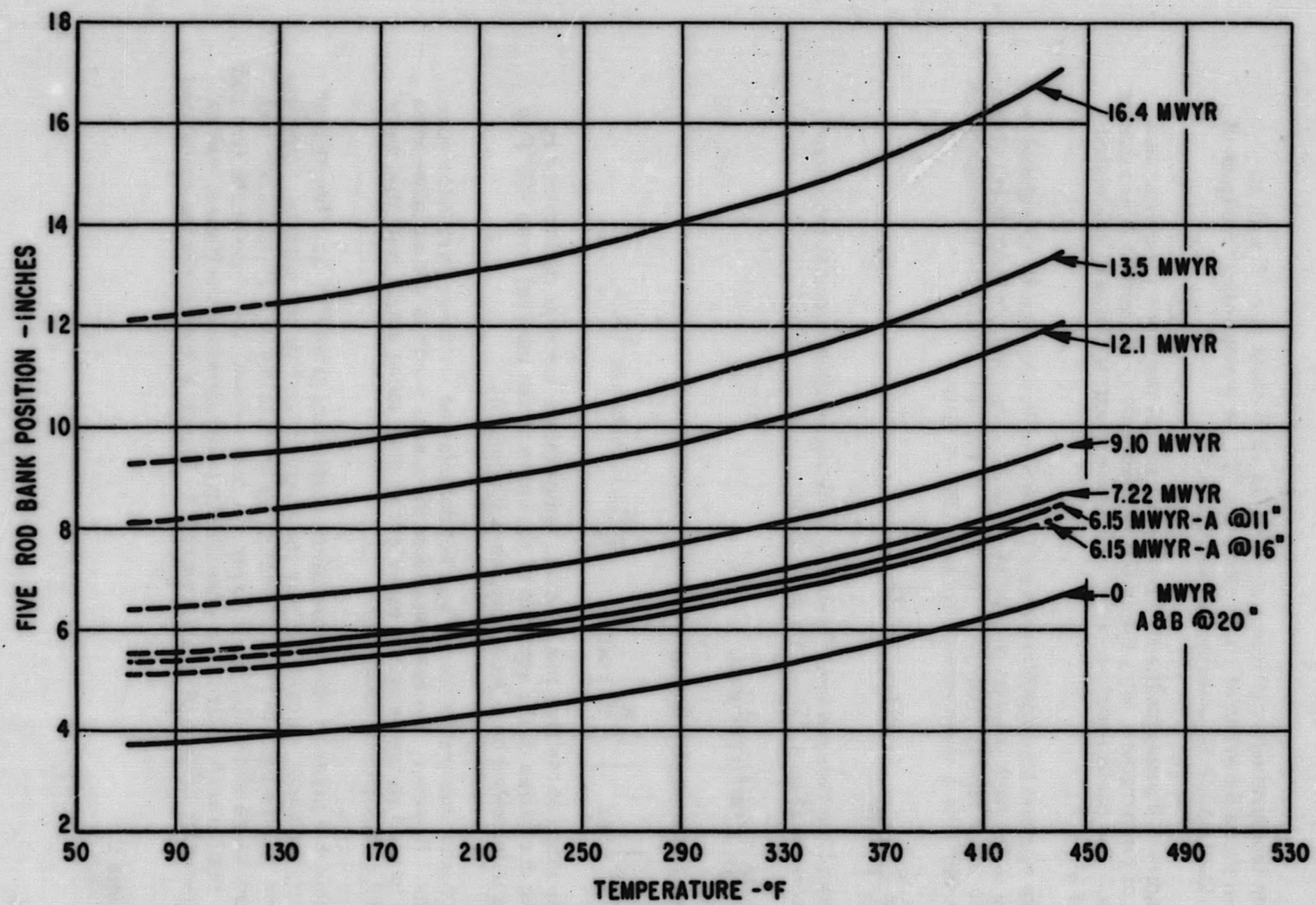
Figure 4. 6.   SM-1 Core I Five Rod Bank Position Vs. Temperature, Rods A and B
at 19", Low Xenon Concentration

The temperature coefficient at 440°F is -3.6 cents per °F with an estimated probable error of ± 0.1 cents per °F. A typical error analysis of the individual points is presented in Section 5.4.2.

Figure 4.6 presents the five rod bank critical positions measured as a function of temperature, with low xenon concentration, at various times during core life. The dashed portion of the curves were extrapolated to calculated positions at 70°F.

The temperature coefficient as a function of burnup can be calculated from the slope of the bank position vs. temperature curves and the bank worth obtained at the same energy release. The slope of the bank positions vs temperature curve at 440°F at a given energy release (Fig. 4.6) is

$$\left[\frac{\Delta X}{\Delta T} \right]_{440} = \text{inches per } °F$$

The worth of the five rod bank (from the bank calibration curve at the same energy release (Fig. 4.35) at this position is

$$\frac{\Delta K}{\Delta X} = \text{cents per inch.}$$

The temperature coefficient at 440°F is therefore

$$\left[\frac{\Delta K}{\Delta T} \right]_{440} = \left[\frac{\Delta X}{\Delta T} \right]_{440} \cdot \frac{\Delta K}{\Delta X} = \text{cents per } °F.$$

The slope of the five rod bank vs. temperature curve is determined by taking the derivative of the equation of the curve in the interval from 400°F to 440°F as determined by a least squares polynomid fit.

The bank calibration curve was not determined for these particular core conditions. However, the deviation from the actual worth is not as large when the bank is used as the deviation experienced when using single rods that were calibrated at other core conditions.

Table 4.3 presents the temperature coefficient at 440°F, as a function of core energy release, calculated from the slope of the five rod bank vs. temperature curve and the bank worth. Assuming an uncertainty of ± 10 cents per inch in the bank worth and a negligible error, in comparison, the slope of the five rod bank vs. temperature curve, the uncertainty in temperature coefficient was calculated using the method of least squares. * Figure 4.7 presents the calculated

---

* Appendix C

4-16
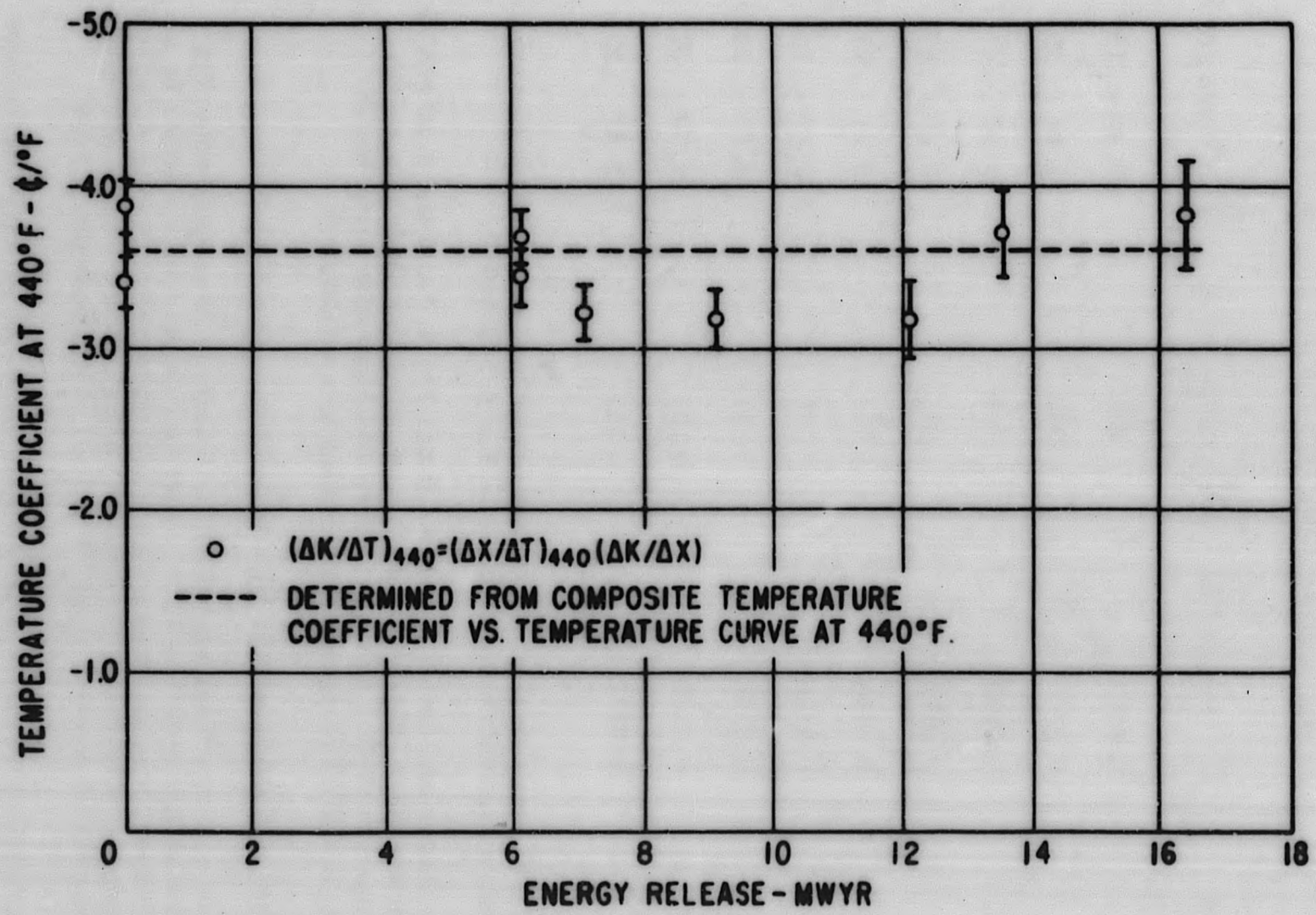
Figure 4.7. SM-1 Core I Temperature Coefficient at 440°F as a Function of Energy Release

TABLE 4.3
TEMPERATURE COEFFICIENT DETERMINATION AT 440°F
AS A FUNCTION OF LIFETIME

Burnup-MWYR	$\frac{\Delta X}{\Delta T}$, in. per °F	$\frac{\Delta K}{\Delta X}$, cents per in. $\pm 10¢/\text{in.}$	$\frac{\Delta K}{\Delta T}$, cents per °F
0	0.0157	216	-3.40 ± .16
0	0.0157	246	-3.87 ± .16
6.15	0.0173	198	-3.43 ± .17
6.15	0.0173	213	-3.68 ± .17
7.22	0.0168	191	-3.21 ± .17
9.10	0.0180	176	-3.17 ± .18
12.1	0.0242	131	-3.17 ± .24
13.5	0.0270	137	-3.70 ± .27
16.4	0.0331	115	-3.81 ± .33

temperature coefficient values at 440°F and respective uncertainties in comparison with the value obtained from the curve in Fig. 4.5 at 440°F.

The repeated points shown in Table 4.3 and Fig. 4.6 at 0 and 6.15 MWYR energy release are due to the two possible bank worth curves in this region (Fig. 4.35, composite ZPE-1 and CE-1 curve and composite curve based on data obtained during 9.1 MWYR operation at various core conditions).

4.2.4 Hot to Cold Reactivity Change

The hot to cold reactivity change is the reactivity associated with core temperature change from 440° to 70°F. This may be determined either by integrating the temperature coefficient versus temperature curve (Fig. 4.5) from 440°F to 70°F, or by integrating the five rod bank calibration curve over the interval from the critical position at 440°F to the critical position at 70°F.

The measured temperature coefficient as a function of temperature data showed little variation, within experimental error, during core life; as a result, a single curve was drawn through the data. Therefore, it follows that the hot

to cold reactivity change as determined from the integral of the temperature coefficient is also constant during core life. Integrating the temperature coefficient curve from 440°F to 70°F yields a reactivity change of $6.66 with an estimated uncertainty of $\pm$ $0.50.

The accuracy of the hot to cold change as determined by integrating the five rod bank calibration curve over the interval from the critical position at 440°F to the critical position at 70°F is a function of the accuracy of the bank calibration curves. Figure 4.35 shows the five rod bank calibration curves obtained at intervals during core life, which were integrated from the hot critical position to the cold critical position to determine the hot to cold reactivity change at these respective intervals.

Table 4.4 lists the hot to cold reactivity change obtained from the change in hot to cold bank position and bank worths. The uncertainties listed are estimated and are due to the uncertainties in the bank calibration.

<div align="center">

TABLE 4.4

HOT TO COLD REACTIVITY CHANGE AS DETERMINED FROM CHANGE IN SM-1 CONTROL ROD BANK POSITION

</div>

Energy Release, MWYR	Hot to Cold Reactivity Change, Dollars
0	7.15 + .20 - .50
6.15	6.62 $\pm$ .50
7.22	6.76 $\pm$ .50
9.10	6.55 $\pm$ .40
12.1	6.71 $\pm$ .40
13.5	6.36 $\pm$ .40
16.4	6.77 $\pm$ .40

4.2.5 Conclusions

Within experimental error, the temperature coefficient remained constant with core life, and at 440°F is -3.6 cents/$^\circ$F with an estimated probable error of $\pm$ 0.1 cents/$^\circ$F. This result is contrary to that experienced at the PWR,[12] where the temperature coefficient became less negative with core life.

The experimental uncertainties in the SM-1 temperature coefficient measurements are sufficiently large that it may not have been possible to see a small change during core life. However, the temperature coefficient as determined by the slope of the five rod bank vs. temperature curve and the bank worth serves as a further check that any change in temperature coefficient experienced during the SM-1 Core I lifetime was probably quite small and may be assumed constant within the inherent experimental uncertainties.

Figure 4.8 summarizes the various values of hot to cold reactivity change as a function of core life, and shows that within the estimated uncertainties, the hot to cold reactivity change remained constant.

4.3 PRESSURE COEFFICIENT

4.3.1 Test Method

The pressure coefficient of reactivity was measured during the initial startup and testing of the SM-1[2] and at the end of 4.79 MWYR energy release.[10] The general test method is to follow the change in core reactivity due to pressure change (using the pressurizer) with a calibrated control rod, while maintaining all other core parameters constant.[2]

4.3.2 Experimental Results

Because the pressure coefficient was quite small, it was necessary to make pressure changes of the order of 200 psi to obtain a sufficient difference in control rod positions. Table 4.5 presents the pressure coefficient data obtained at the SM-1. The two integral measurements were made by quickly increasing the pressure and measuring the resulting period in seconds and then converting to reactivity in cents.

4.3.3 Conclusions

The inherent uncertainties present in all reactivity measurements together with the very small differences measured here indicate that the probable error in each measured pressure coefficient value is quite large, estimated at + 30 percent. As seen in Table 4.5, the pressure coefficient within the probable errors, at approximately the same temperature (84°F and 115°F), remained constant with burnup. In going from low temperatures to operating temperatures, there is a definite increase in the pressure coefficient. The average pressure coefficient at low temperature is 1.06 + 0.33* cents per 100 psi and at operating temperature is 3.35 ± 0.68* cents per 100 psi.

---

* Probable errors

4-20
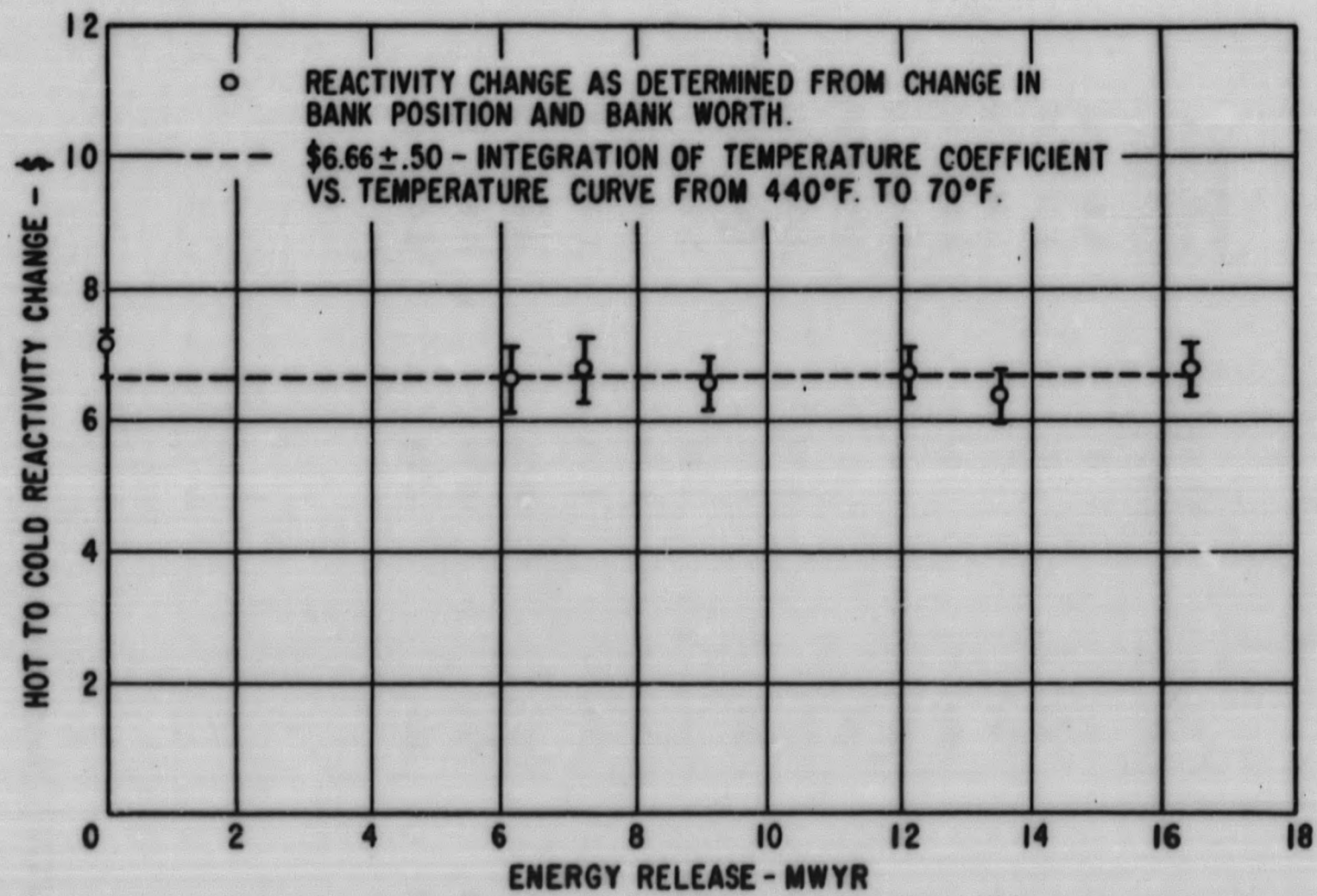
Figure 4. 8.   SM-1 Core I Hot to Cold Reactivity Change as a Function of Energy
Release

TABLE 4.5
SM-1 CORE I PRESSURE COEFFICIENT DATA

Pressure, psi	Core Temperature, $^\circ$F	Burnup, MWYR	Pressure Coefficient, ¢/100 psi*
112	84	0	0.69 ± .21
305	84	0	1.16 ± .35
500	84	0	1.11 ± .33
700	450	0	2.05 ± .62
900	450	0	2.67 ± .80
1100	450	0	5.32 ± 1.60
200	115	4.79	1.31 ± .39
400	115	4.79	1.03 ± .31
600	115	4.79	1.24 ± .37
800	115	4.79	1.02 ± .31
1000	115	4.79	1.11 ± .33
1200	115	4.79	0.94 ± .28
Integral Run 1	115	4.79	0.98 ± .29
Integral Run 2	115	4.79	1.08 ± .32

* Errors listed are probable errors.

4.4 CONTROL ROD CALIBRATION

4.4.1 Introduction

Calibrated control rods form the basis for all reactivity measurements performed at the SM-1. Reactivity in dollars or cents is determined by the change in critical position of a calibrated control rod and the average control rod worth in cents per inch over this interval.

Due to the very large worth of the individual control rods, there is a large interaction between rods; hence, the rod worths are most accurate for the exact configuration used.

4.4.2 Calibration Techniques

Control rod calibrations are performed using the period technique.[13] Criticality is achieved with the core in a steady state condition; a control rod is then withdrawn a small amount, resulting in a supercritical condition and positive reactor period. The positive reactor period is interpreted as reactivity in cents by means of in-hour equation calculations. Rod worth is calculated from the reactivity change divided by the rod position change and plotted at the average rod position. A calibration over the length of a control rod is accomplished by varying a core parameter or the position of the other control rods.

4.4.3 Control Rod Calibrations

Control rods A and C were calibrated at various times during core life, as a function of the five rod bank position with low xenon concentration in the core at operating temperature and at a low core temperature. Calibrations were also obtained as a function of xenon concentration with the five rod bank at a constant position at operating temperature.

Figures 4.9 to 4.14 summarize all the rod A calibration curves obtained during the SM-1 Core I life. Table 4.6 indicates the position of the five rod bank and control rod B, and core conditions during the rod A calibrations.

TABLE 4.6
FIVE ROD BANK POSITION DURING ROD A CALIBRATION
AT VARIOUS CORE CONDITIONS, SM-1 CORE I

Core Energy Release, MWYR	Temperature °F	Rod B Position Inches	Xenon Condition	Five Rod Bank Position, Inches
4.79	120	19	Low	4.85 to 5.10
6.15	440	19	Low	8.39 to 8.60
6.15	120	19	Low	5.30 to 5.57
7.22	120	19	Low	5.74 to 7.27
7.22	440	19	Low	9.05 to 11.21
9.10	120	19	Low	6.57 to 8.26
9.10	440	19	Low	9.91 to 12.52
10.5	70	19	Low	7.18 to 9.03
12.1	130	19	Low	8.43 to 10.43
12.1	440	19	Low	12.85 to 15.39
12.1	440	19	Transient	16.16
13.5	120	19	Low	9.54 to 11.58
13.5	440	19	Low	13.69 to 17.25
13.5	440	19	Transient	19.66 and 15.30
16.4	120	19	Low	12.66 to 14.95
16.4	440	19	Low	17.75 to 22.00
16.4	370	22	Transient	22.00

Figure 4.15 summarizes all the rod C calibration curves obtained during the SM-1 Core I life. Table 4.7 indicates the position of the four rod bank and the core conditioning during the rod C calibrations.
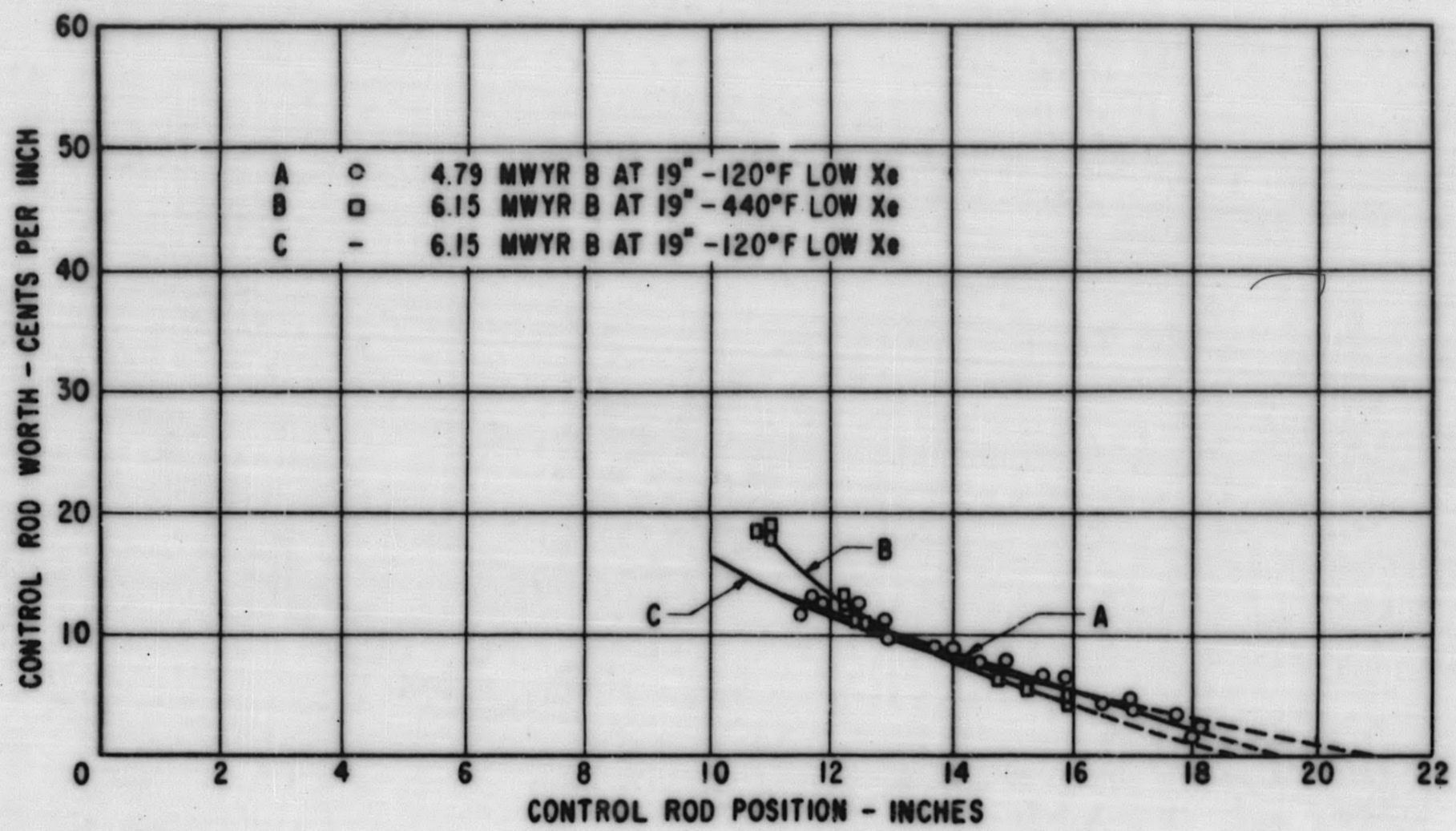
Figure 4.9. SM-1 Core I Control Rod A Calibration Curves
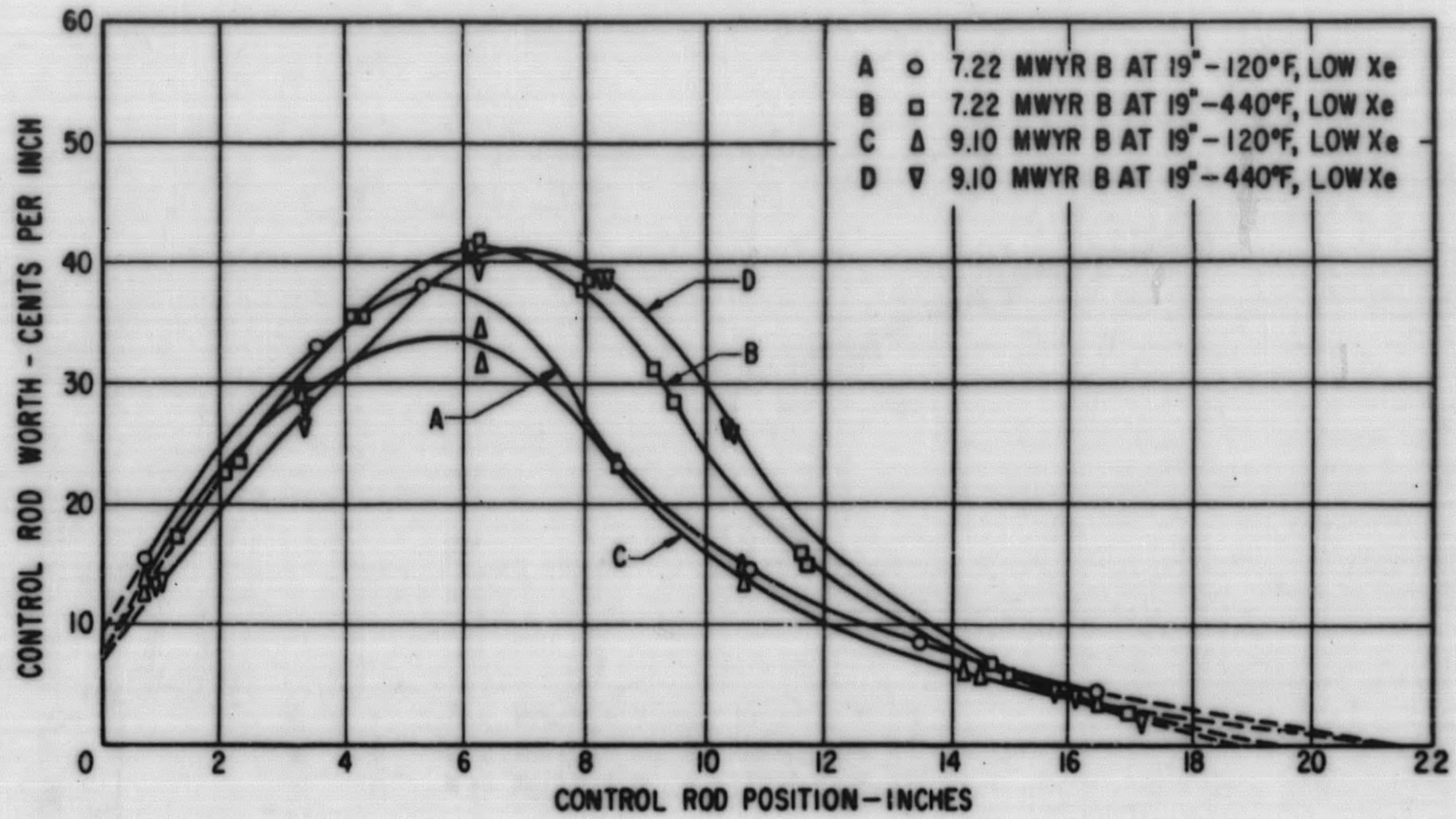
Figure 4. 10.   SM-1 Core I Control Rod A Calibration Curves
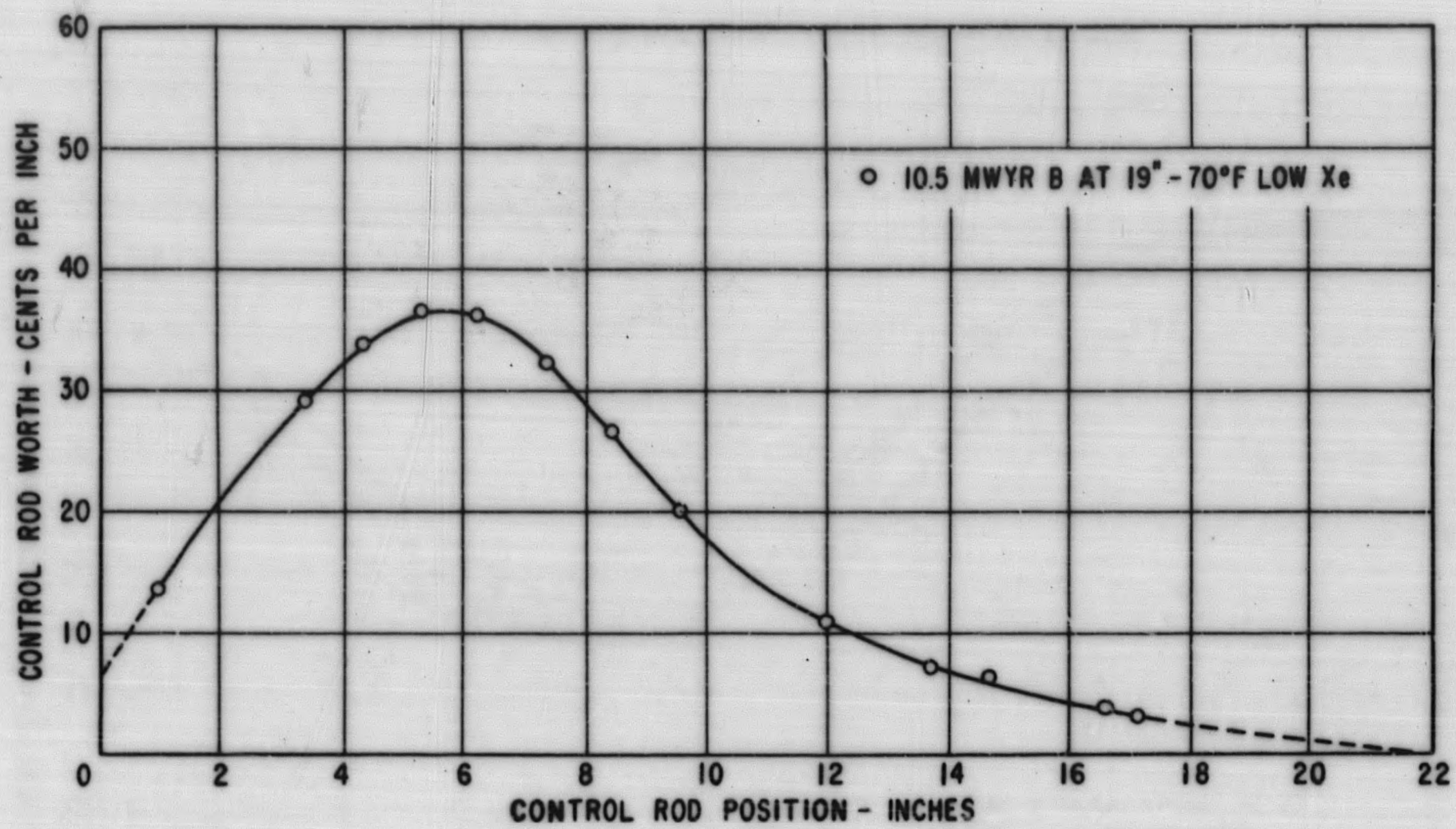
Figure 4.11.   SM-1 Core I Control Rod A Calibration Curves

4-28
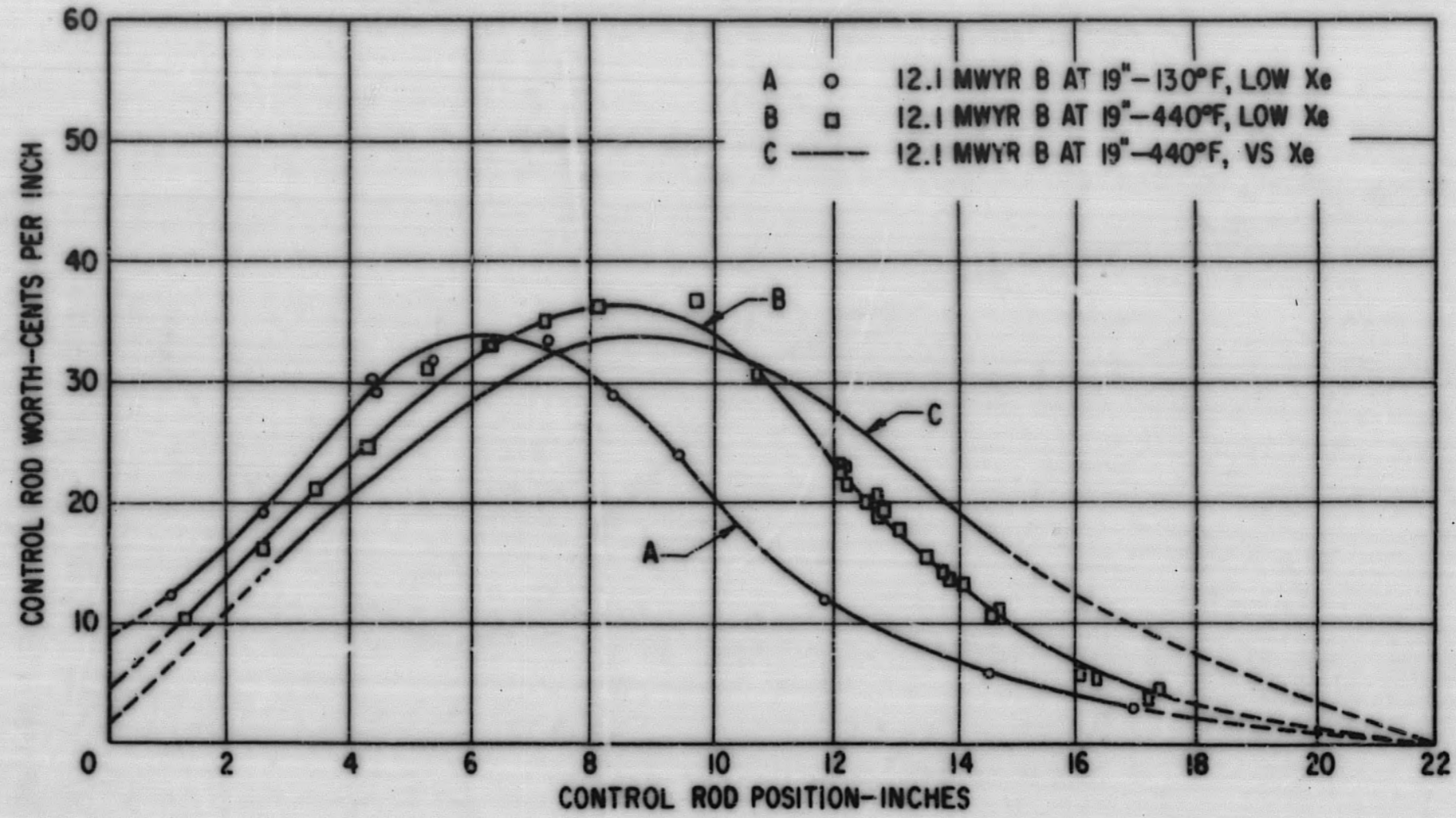
Figure 4.12.   SM-1 Core I Control Rod A Calibration Curves
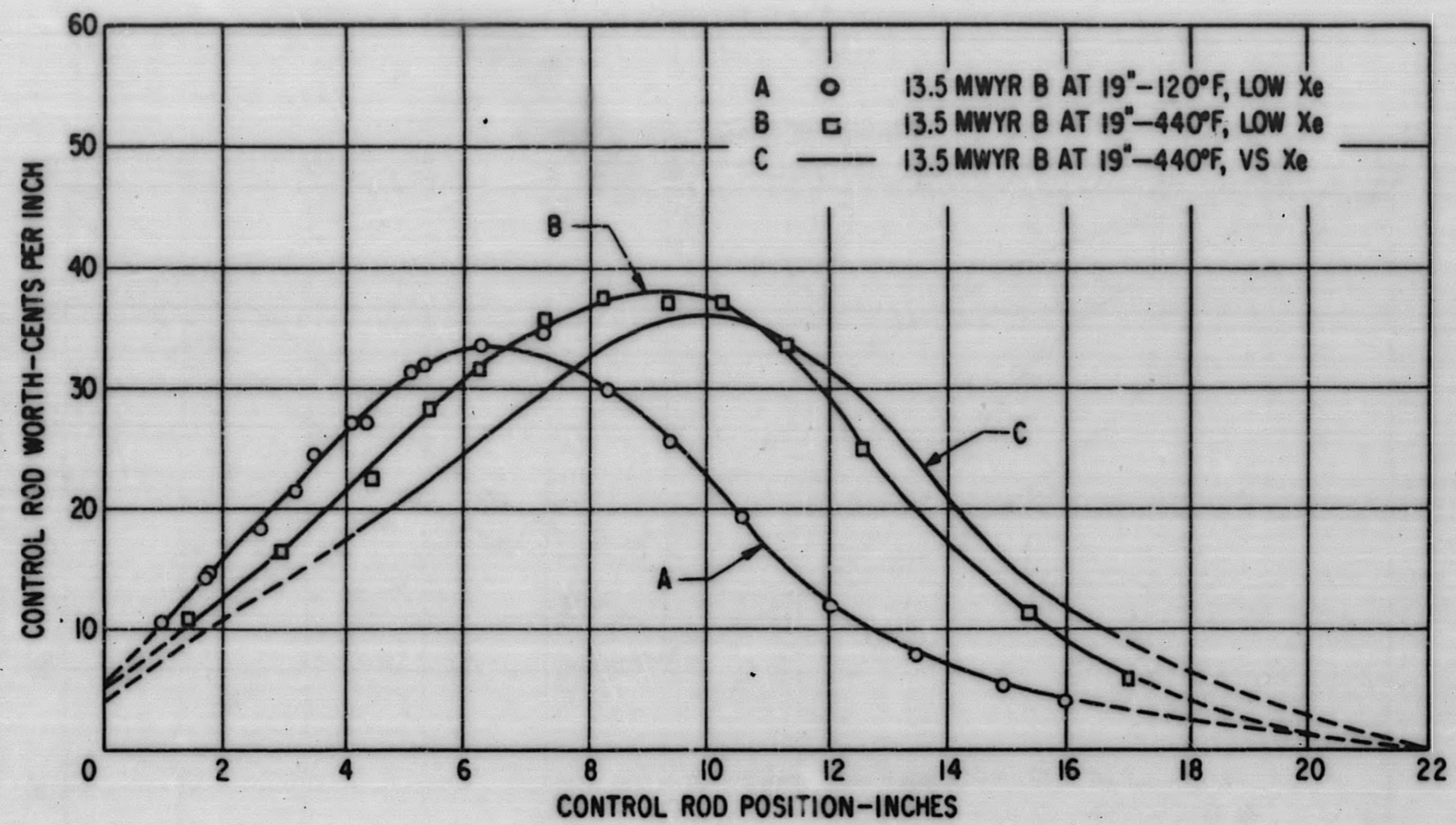
Figure 4.13.   SM-1 Core I Control Rod A Calibration Curves
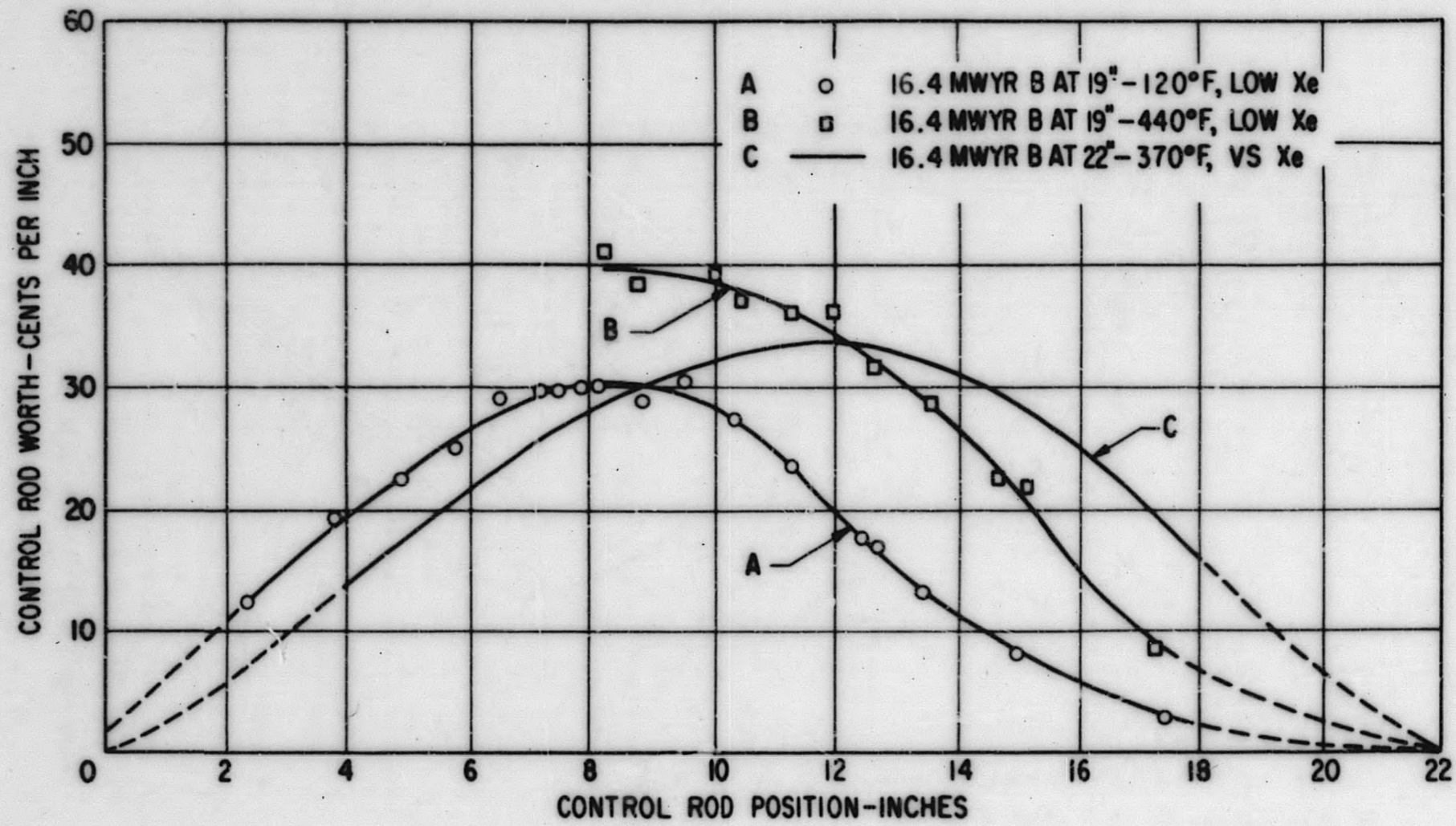
Figure 4.14. SM-1 Core I Control Rod A Calibration Curves
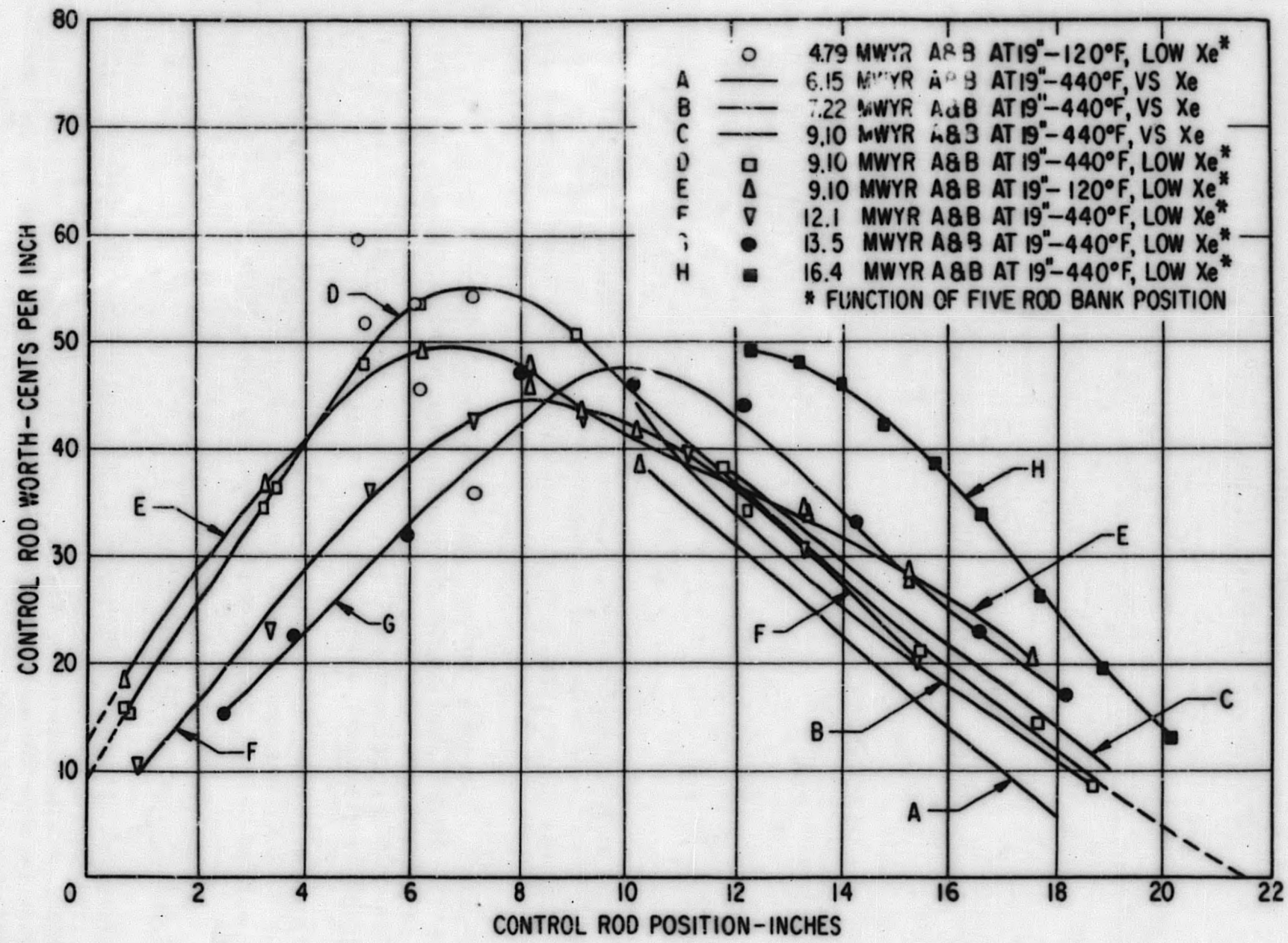
Figure 4.15.   SM-1 Core I Control Rod C Calibration Curves

TABLE 4.7
FOUR ROD BANK POSITION DURING ROD C CALIBRATION
AT VARIOUS CORE CONDITIONS, SM-1 CORE I

Core Energy Release, MWYR	Temperature °F	Rod A & B Position, Inches	Xenon Condition	Four Rod Bank Position, Inches
6.15	440	19	Transient	7.72
7.22	440	19	Transient	10.47
9.10	120	19	Low	3.59 to 8.18
9.10	440	19	Transient	9.74 to 12.69
9.10	440	19	Low	8.70 to 13.59
12.1	440	19	Low	11.35 to 16.58
13.5	440	19	Low	12.70 to 19.36
16.4	440	19	Low	16.70 to 22.00

Figure 4.16 presents the rod C calibration curves obtained during SM-1 ZPE-1.[8] Rod C was calibrated as a function of the four rod bank position (rods 1, 2, 3, and 4) for a clean core and cores with three different B-10 poison loadings.

Figure 4.17 presents the rod C calibration curves obtained during SM-1 ZPE-2.[14] Rods 1, 2, 3, 4 A and B were kept fully withdrawn and rod C calibrated as the core was poisoned with B-10 and stainless steel. Figure 4.18 shows the critical position of rod C as a function of B-10 and stainless steel loading with the remaining control rods fully withdrawn.

Figure 4.19 presents the rod 3 calibration curves obtained during SM-1 ZPE-1.[8] Rod 3 was calibrated as a function of the four rod bank position (rods 1, 2, 4 and C) for a clean core and cores with three different B-10 poison loadings.

4.4.4 Control Rod Integral Worth

Figures 4.20 through 4.29 present the integral worth of the rod calibration curves presented in the previous section. Table 4.8 lists the integrated worth of the respective calibration curve, the uncertainty is estimated at + 30 cents, and is based on the experimental uncertainties in the calibration data points and possible inaccuracies in drawing the calibration curves.

TABLE 4.8
CONTROL ROD INTEGRAL WORTH

Rod	Energy Release MWYR	Temperature °F	Core Conditions	Five Rod Bank Position, Inches	Integral Worth, Dollars
A	7.22	120	Low Xe	5.74 to 7.27	3.49
A	7.22	440	Low Xe	9.05 to 11.21	3.82
A	9.10	120	Low Xe	6.57 to 8.26	3.16
A	9.10	440	Low Xe	9.91 to 12.52	3.87
A	10.5	70	Low Xe	7.18 to 9.03	3.27
A	12.1	130	Low Xe	8.43 to 10.43	3.13
A	12.1	440	Low Xe	12.85 to 15.39	3.73
A	12.1	440	Transient Xe	16.16	3.97
A	13.5	120	Low Xe	9.54 to 11.58	3.18
A	13.5	440	Low Xe	13.69 to 17.25	3.89
A	13.5	440	Transient Xe	19.66 and 15.30	3.88
A	16.4	120	Low Xe	12.66 to 14.95	3.11
A	16.4	370	Transient Xe	22.00	4.20
C	9.10	120	Low Xe	3.59 to 8.18*	6.75
C	9.10	440	Low Xe	8.70 to 13.59*	6.46
C	12.1	440	Low Xe	11.35 to 16.58*	5.18
C	13.5	440	Low Xe	12.70 to 19.36*	5.84
C	SM-1 ZPE-1	68	8.964 gm B-10 added	4.07 to 8.19*	7.34
C	SM-1 ZPE-1	68	17.928 gm B-10 added	7.60 to 12.90*	5.62
C	SM-1 ZPE-1	68	26.892 gm B-10 added	12.26 to 20.53*	5.11
C	SM-1 ZPE-2	68	B-10 poisoned core	6 rods fully withdrawn	5.68
C	SM-1 ZPE-2	68	SS poisoned core	6 rods fully withdrawn	6.71
3	SM-1 ZPE-1	68	8.964 gm B-10 added	4.09 to 6.70**	5.72
3	SM-1 ZPE-1	68	17.928 gm B-10 added	8.17 to 10.58**	3.80
3	SM-1 ZPE-1	68	26.892 gm B-10 added	12.56 to 16.38**	2.97

* 4 rod bank (rods 1, 2, 3, and 4)

** 4 rod bank (rods 1, 2, 4, and C)
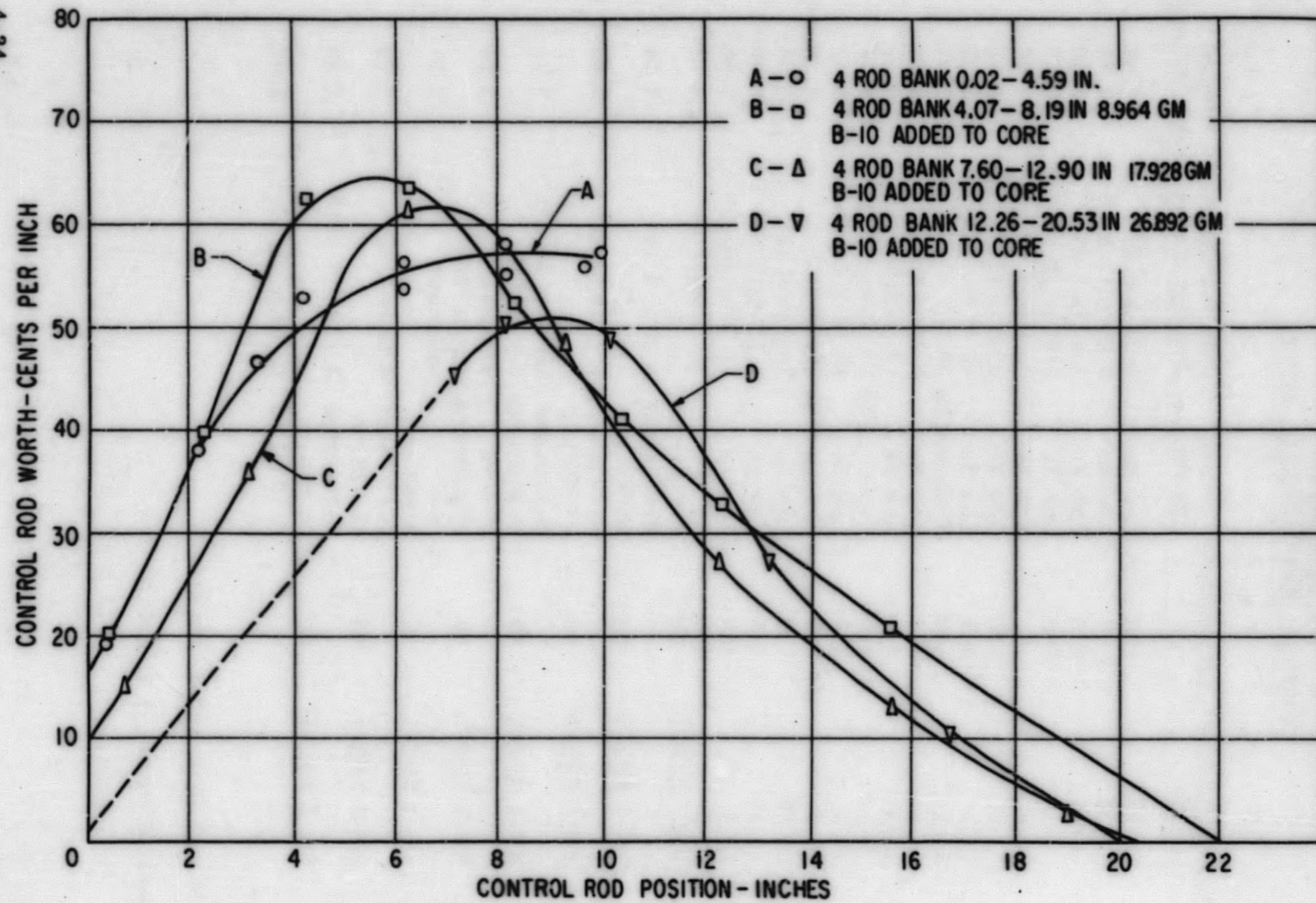
Figure 4.16. Control Rod C Calibration Curves, SM-1 ZPE-1, 68°F
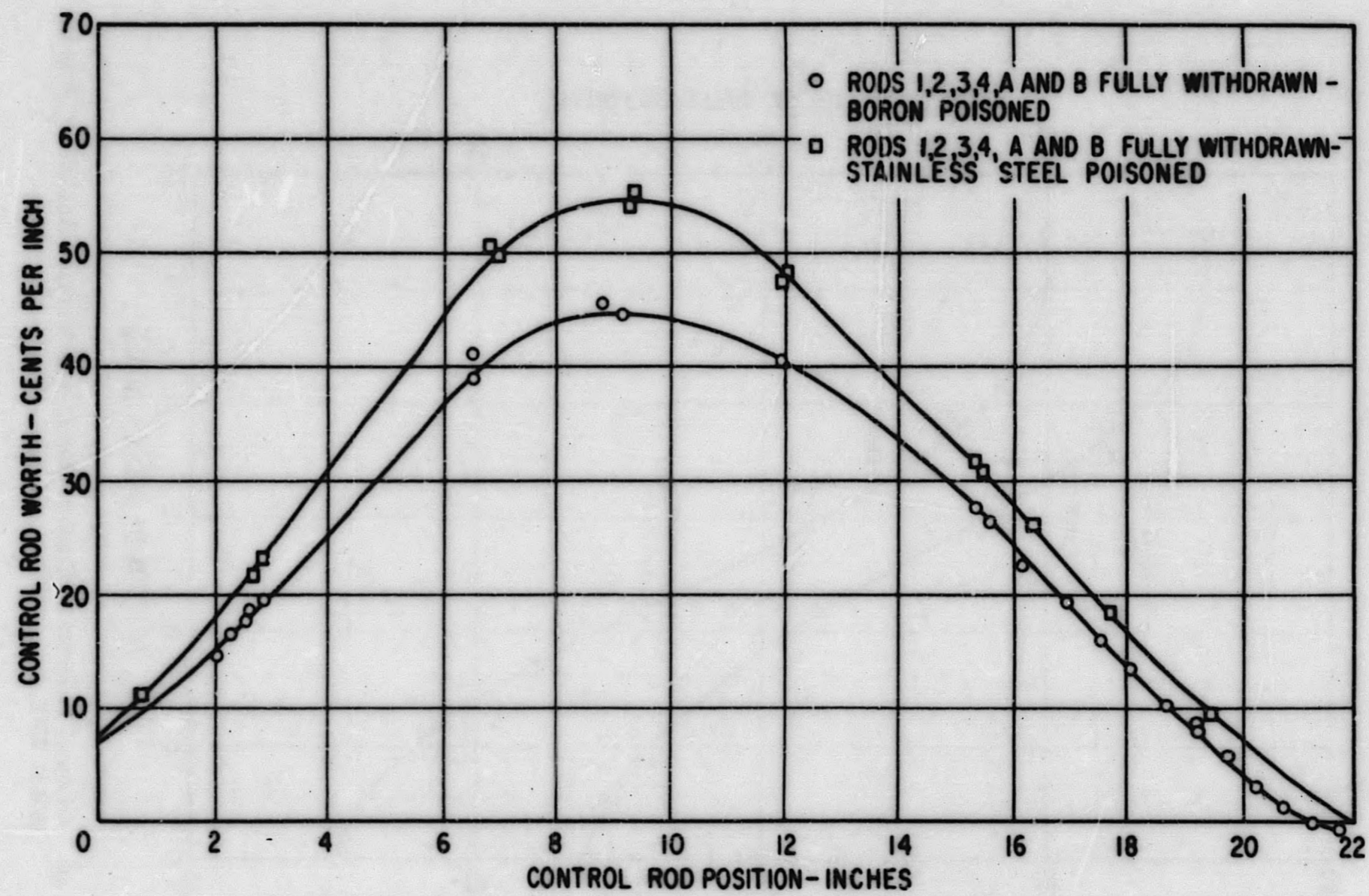
Figure 4.17.   Control Rod C Calibration Curves, SM-1 ZPE-2
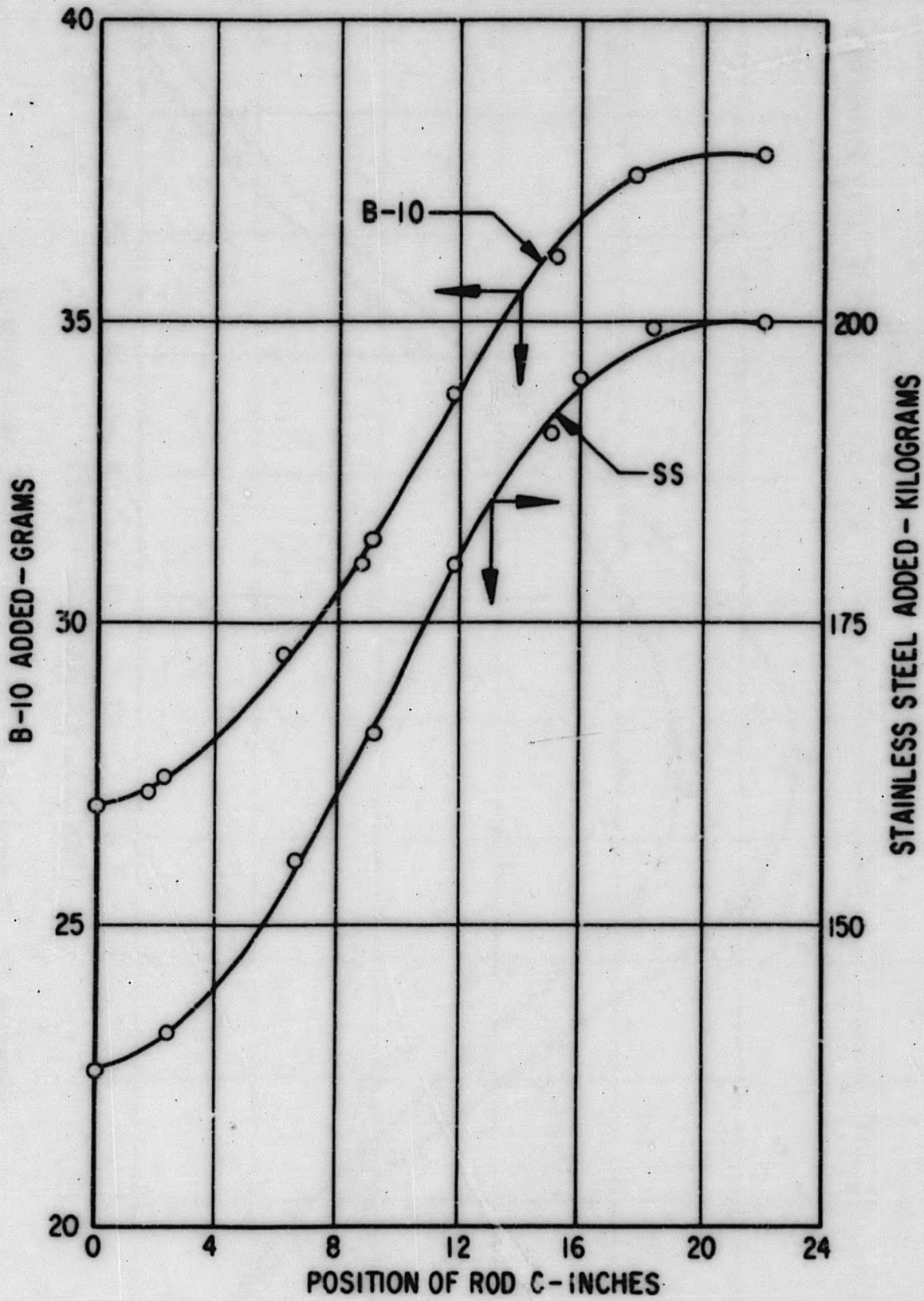
Figure 4.18.   Critical Position of Control Rod C with Varying Amount of Poison, SM-1 ZPE-2
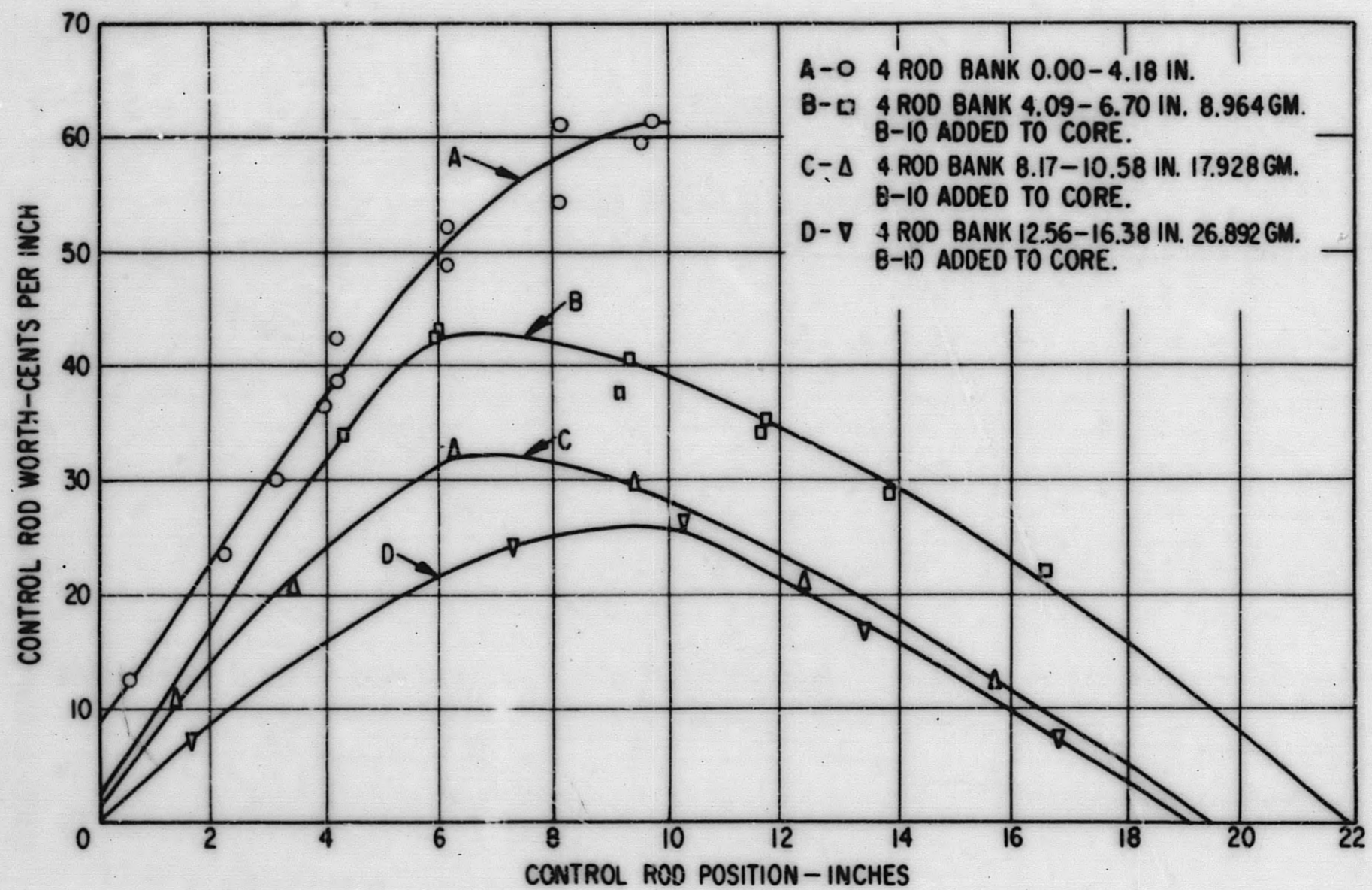
Figure 4.19.   Control Rod 3 Calibration Curves, SM-1 ZPE-1, 68°F
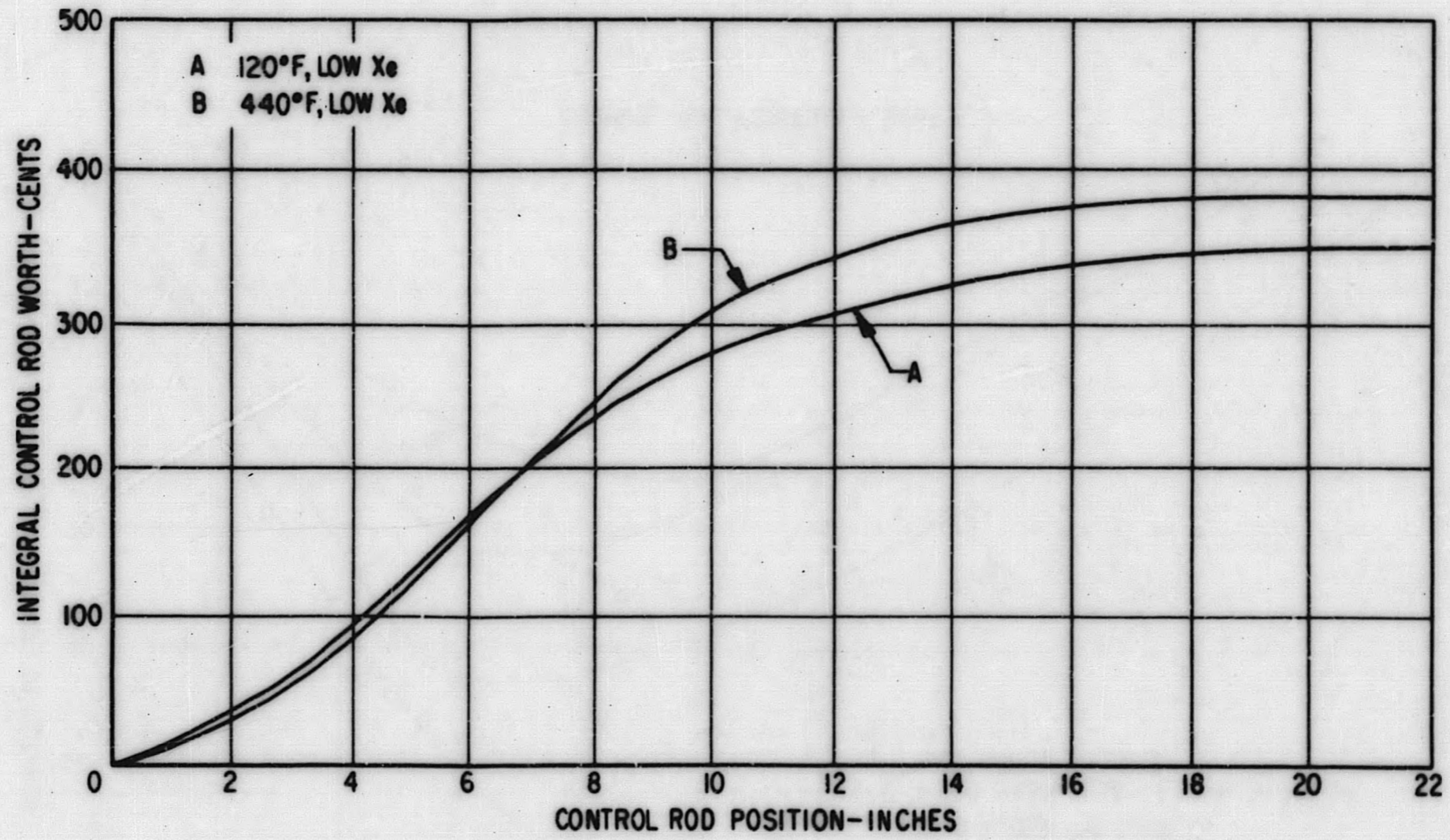
Figure 4.20.   Control Rod A Integral Worth, 7.22 MWYR, SM-1 Core I
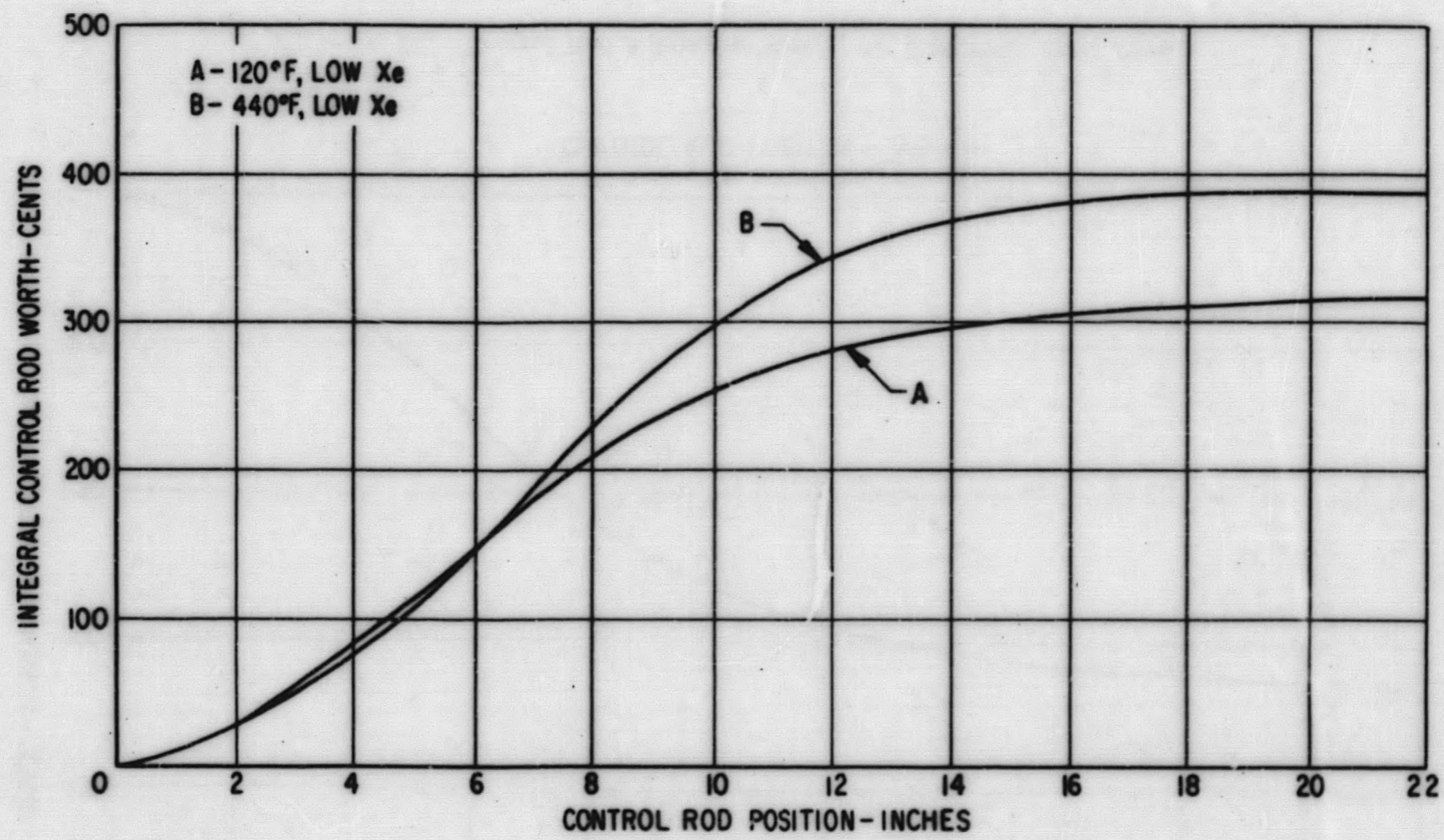
Figure 4.21.   Control Rod A Integral Worth, 9.10 MWYR, SM-1 Core I
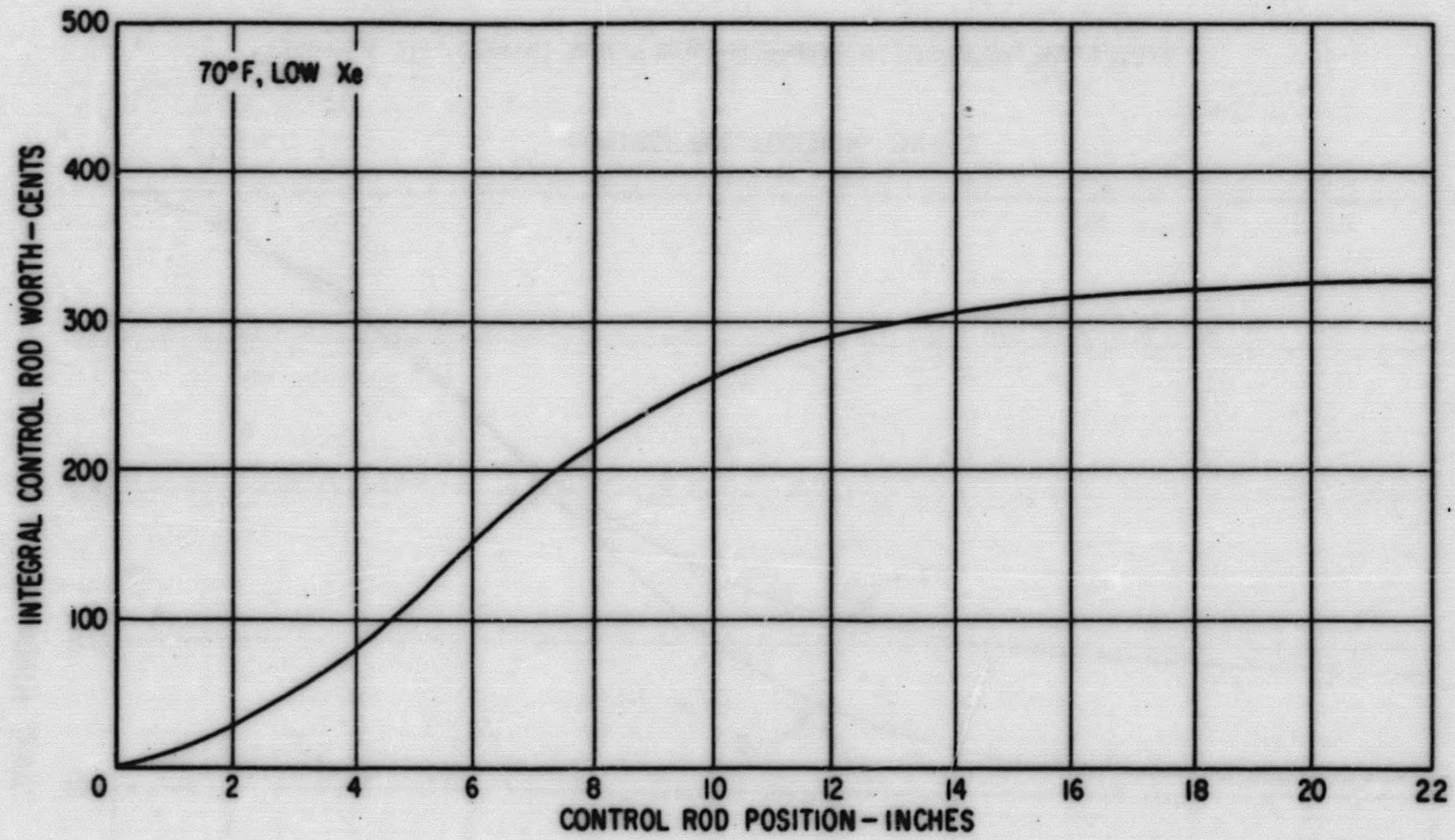
Figure 4.22. Control Rod A Integral Worth, 10.5 MWYR, SM-1 Core I
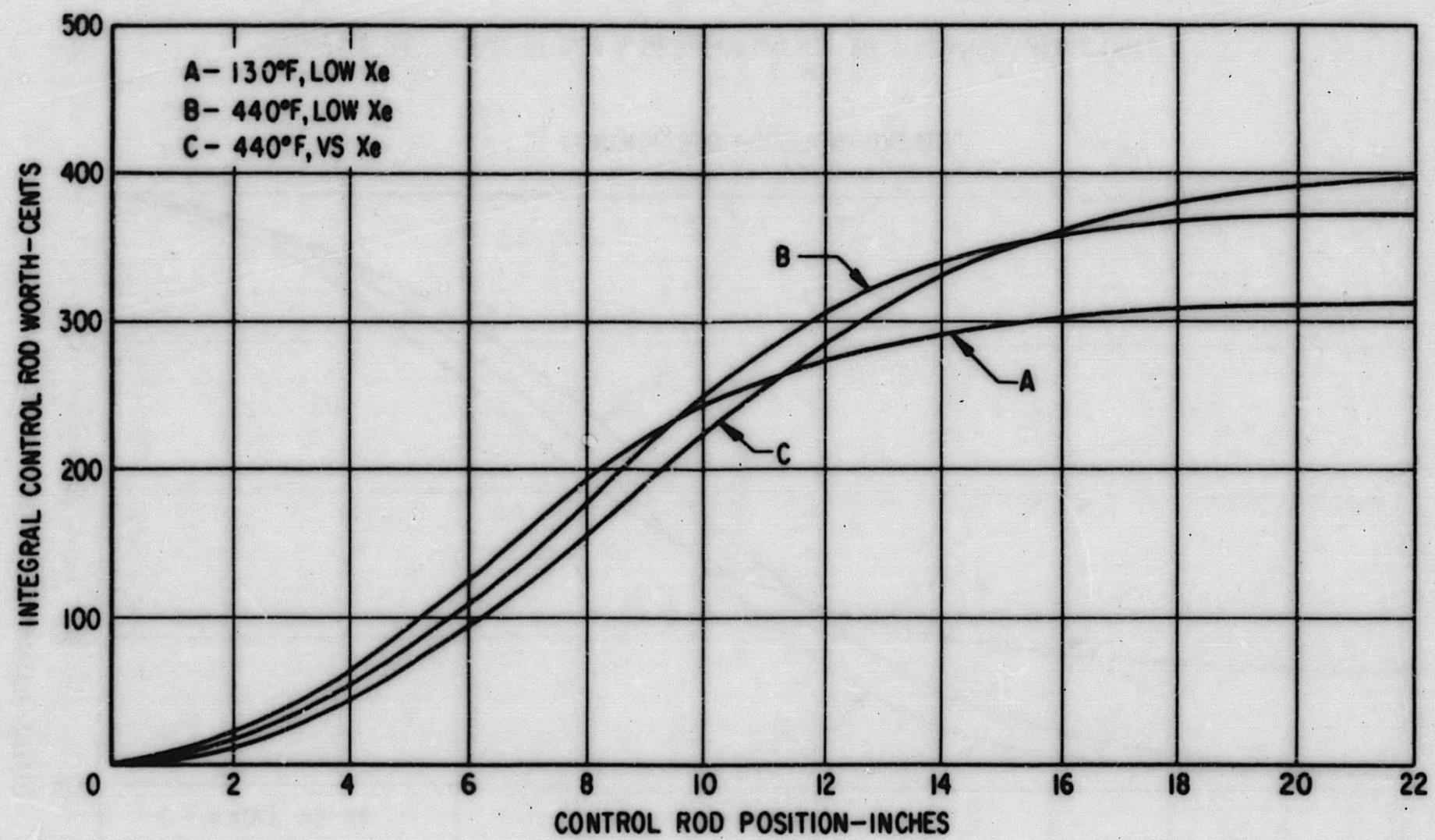
Figure 4.23.   Control Rod A Integral Worth, 12.1 MWYR, SM-1 Core I
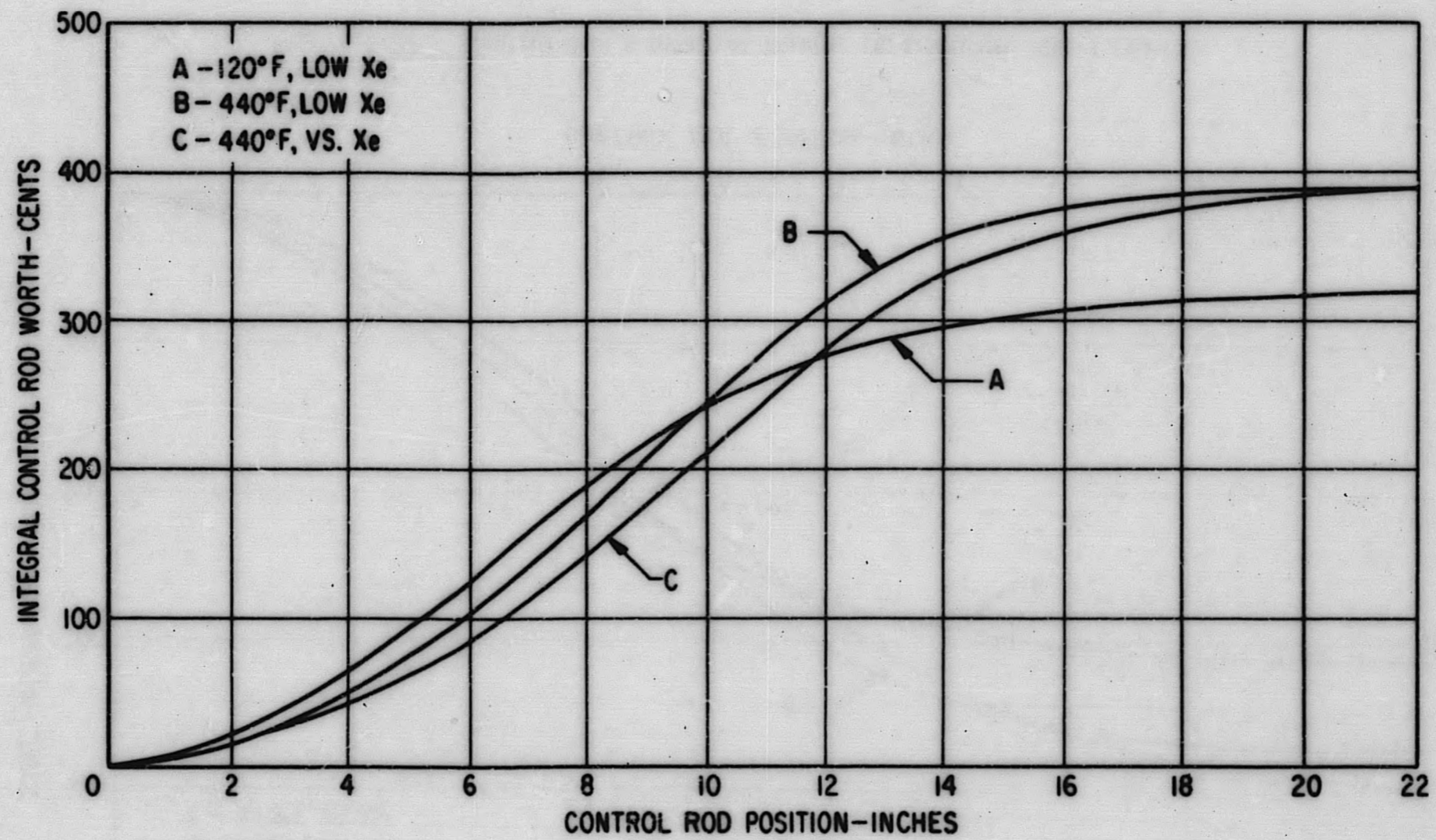
Figure 4.24.   Control Rod A Integral Worth, 13.5 MWYR, SM-1 Core I
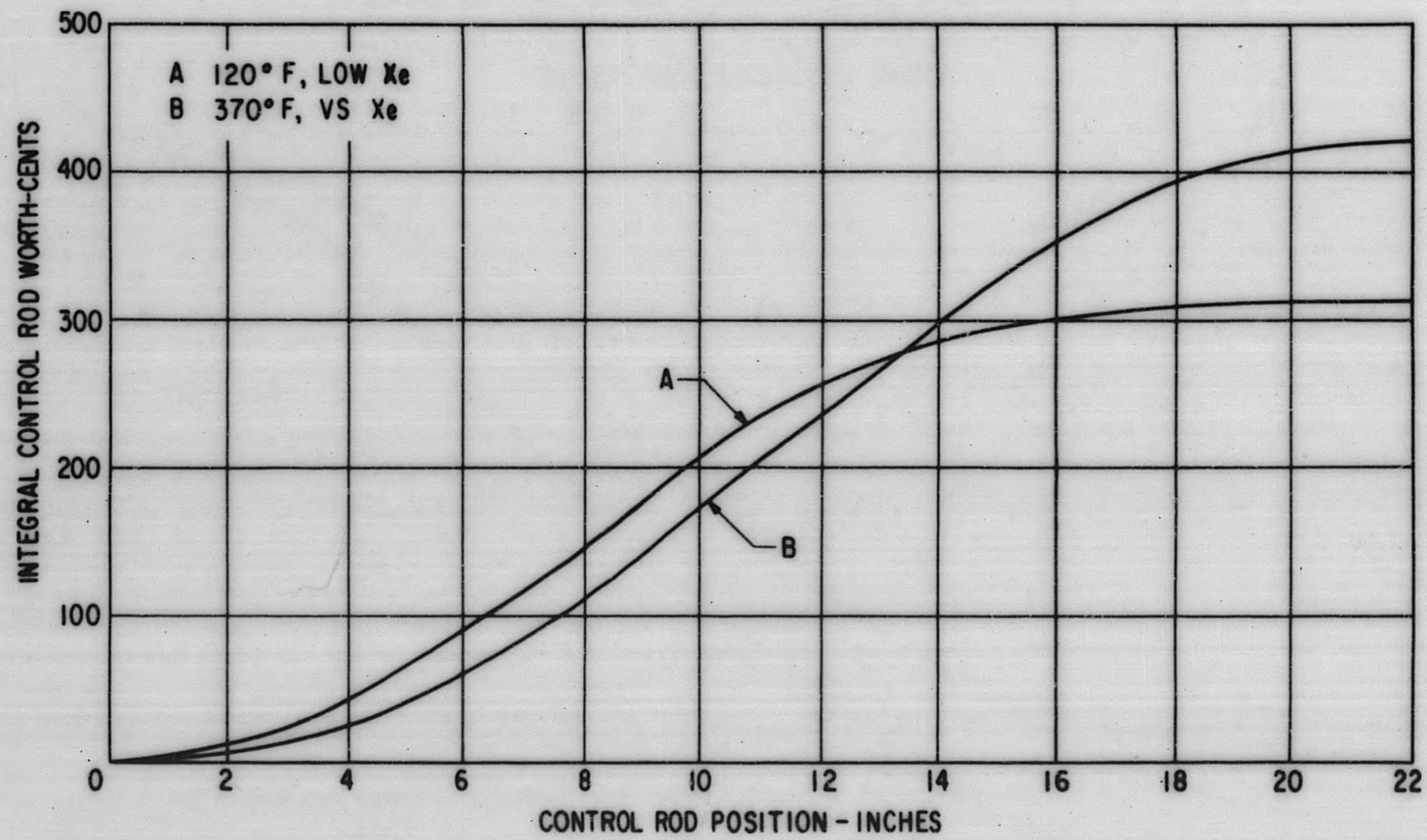
Figure 4.25. Control Rod A Integral Worth, 16.4 MWYR, SM-1 Core I
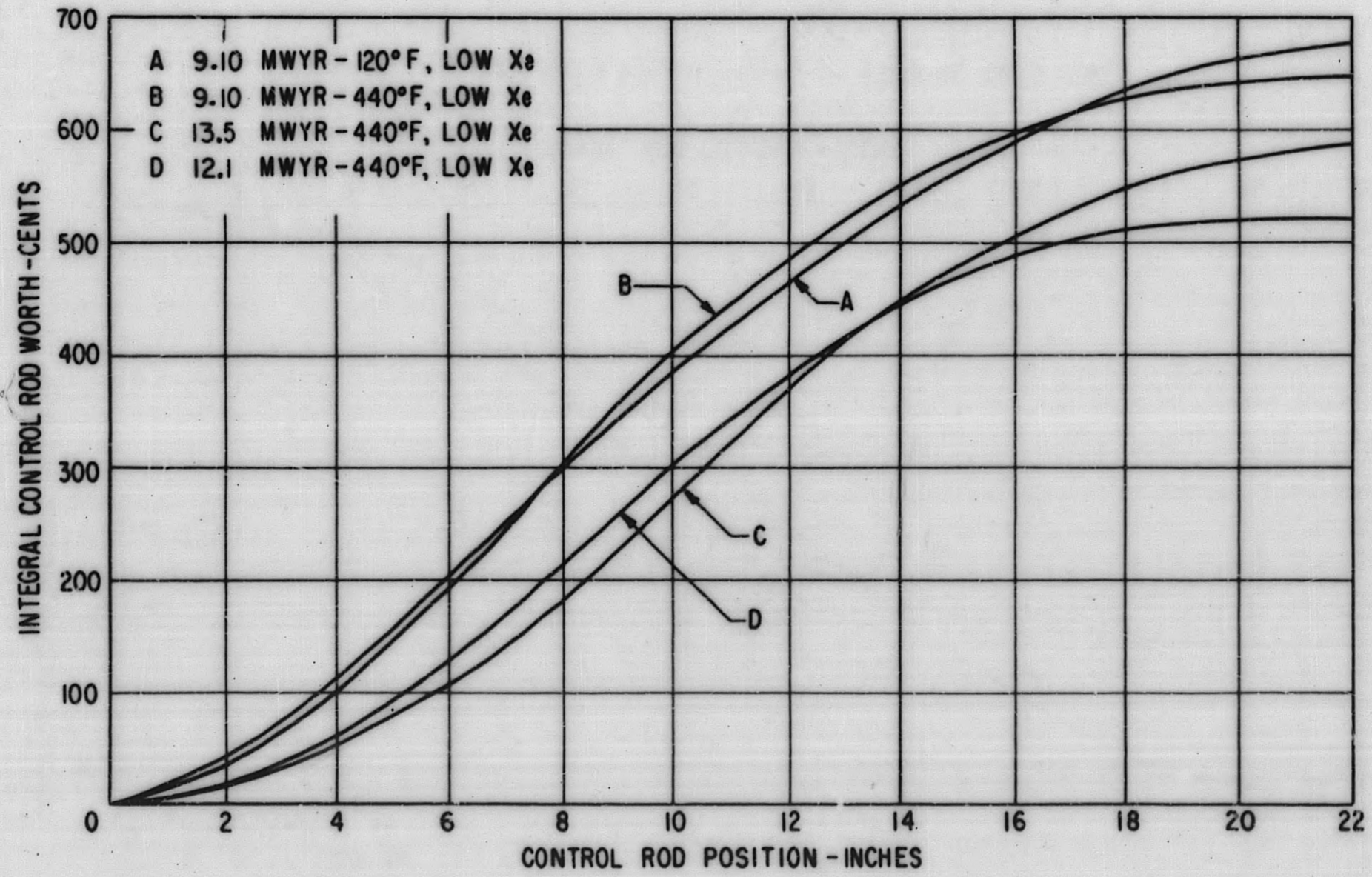
Figure 4.26. Control Rod C Integral Worth, SM-1 Core I
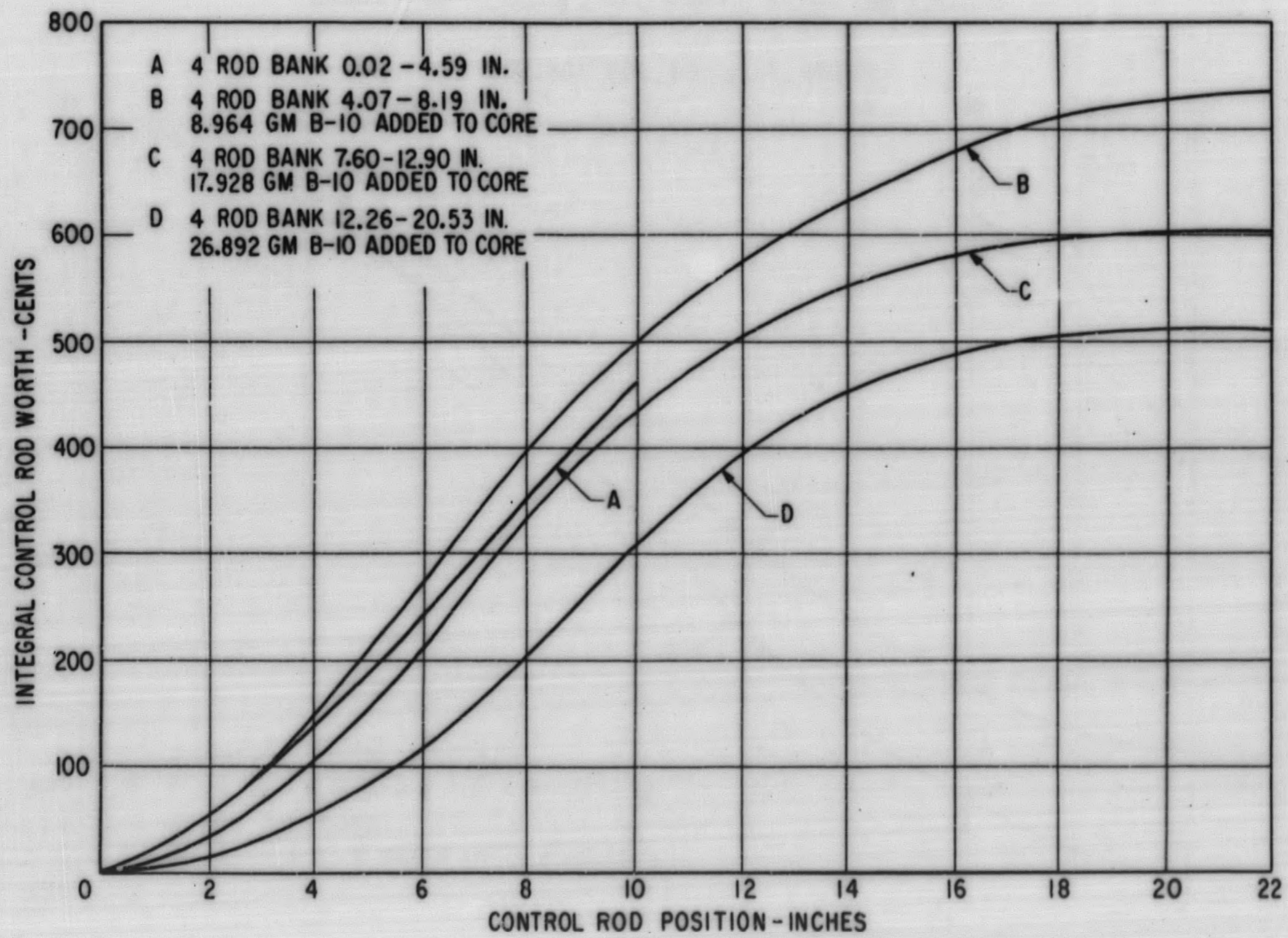
Figure 4.27. Control Rod C Integral Worth, SM-1 ZPE-1

The figure shows a graph with the following legend:

A 4 ROD BANK 0.02 – 4.59 IN.

B 4 ROD BANK 4.07 – 8.19 IN.
   8.964 GM B-10 ADDED TO CORE

C 4 ROD BANK 7.60 – 12.90 IN.
   17.928 GM B-10 ADDED TO CORE

D 4 ROD BANK 12.26 – 20.53 IN.
   26.892 GM B-10 ADDED TO CORE

Y-axis: INTEGRAL CONTROL ROD WORTH – CENTS (0 to 800)

X-axis: CONTROL ROD POSITION – INCHES (0 to 22)
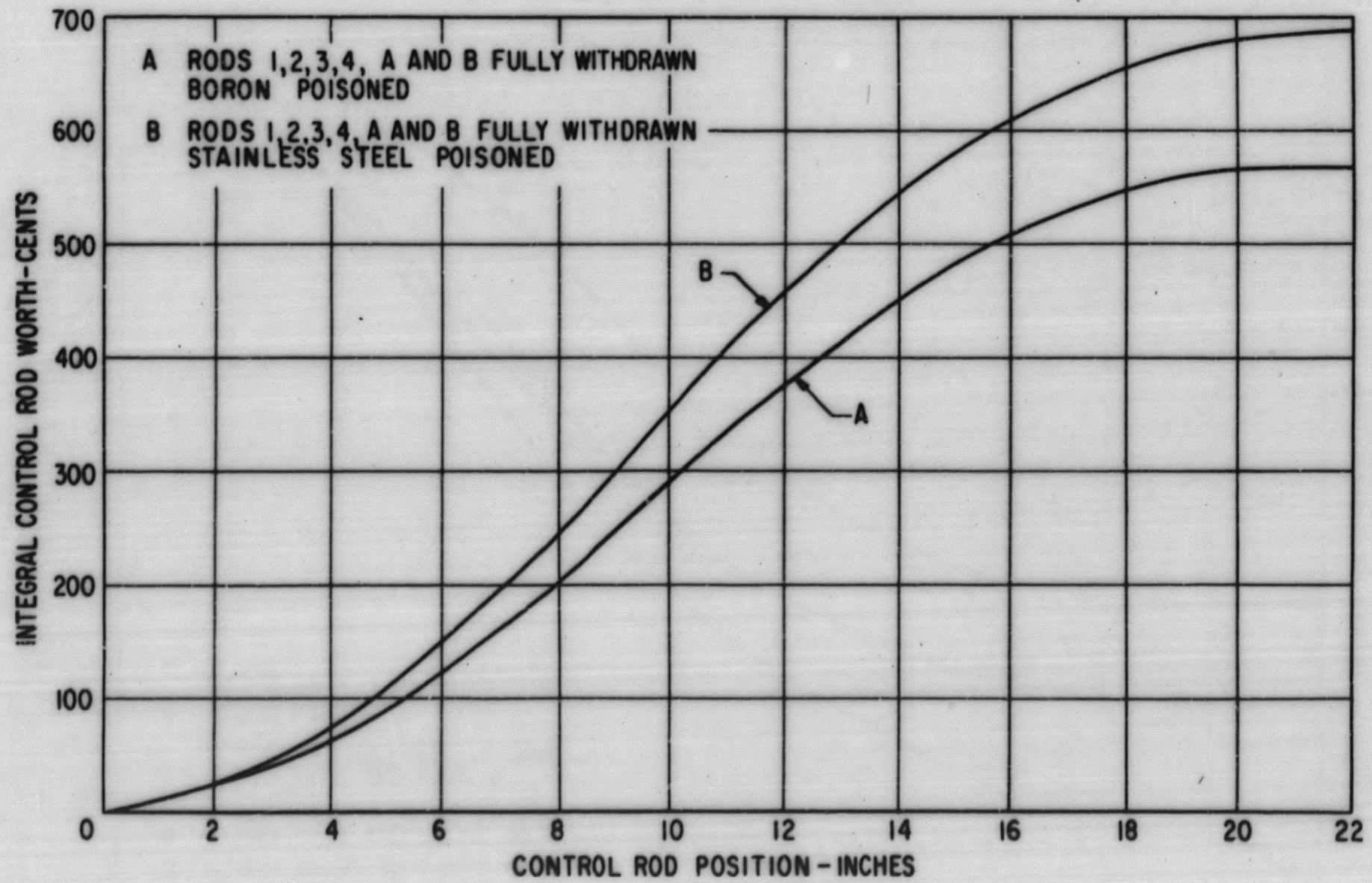
Figure 4.28.   Control Rod C Integral Worth, SM-1 ZPE-2
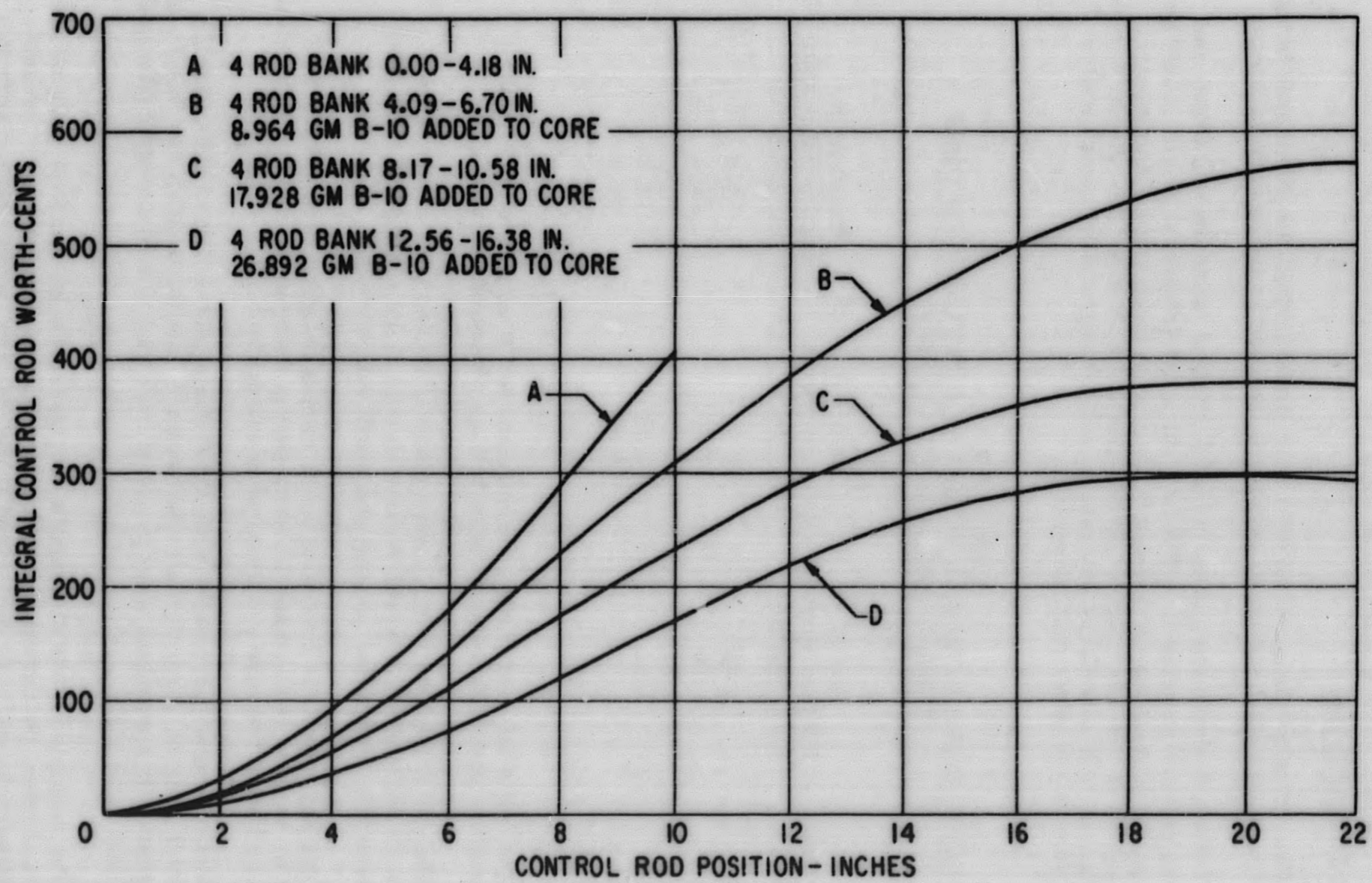
Figure 4.29.   Control Rod 3 Integral Worth, SM-1 ZPE-1

4.4.5 Conclusions

1. The rod calibration curves over core lifetime show the worth peak being displaced toward the upper portion of the core as the bank is withdrawn.

2. Table 4.9 shows the change in Rod A integral worth over lifetime, and the percent increase in rod A integral worth from cold to hot. Considering the uncertainty of $\pm$ 30 cents attached to these values, the integral worths of rod A hot showed little variation with core life. Except for the data at 7.22 MWYR the increase in rod A integral worth from cold to hot is of the order of 20 percent.

TABLE 4.9
CONTROL ROD A INTEGRAL WORTH AS A FUNCTION OF CORE
ENERGY RELEASE SM-1 CORE I

Energy Release MWYR	Rod A Integral Worth, Cold, Dollars	Rod A Integral Worth, Hot, Dollars	Increase in Integral Rod Worth, Cold to Hot, %
7.22	3.49	3.82	9.5
9.10	3.16	3.87	22.5
10.5	3.27	--	--
12.1	3.13	3.73	19.2
13.5	3.18	3.89	22.3
16.4	3.11	--	--

3. The rod A integral worths measured at $440^{\circ}F$ as a function of bank position and of Xe concentration are approximately equal.

4. The rod C integral worth curves obtained during core life indicate a 4.4% decrease in integral worth with cold to hot change and a tendency toward a decreasing integral rod worth with burnup.

5. The rod C and rod 3 integral worth curves obtained during SM-1 ZPE-1 with various B-10 poison loadings show a decrease in rod worth as poison is added to the core and the bank is withdrawn.

6. Measurements performed with rod C during SM-1 ZPE-2 show that the total integral worth with all other control rods fully withdrawn was $1.03 greater in a stainless steel poisoned core than in a boron-steel poisoned core.

7. The multiple effects of temperature, core burnup, and bank position and their effect on control rod calibrations cannot be separated at present. Measurements to be performed at the Critical Facility may clarify this matter.

4.5   CONTROL ROD BANK CALIBRATION

4.5.1   Introduction

In general, the SM-1 Core I five rod bank was not calibrated directly because of the large reactivity that it controlled and the difficulty in obtaining accurate supercritical bank positions by the period technique. Bank calibrations were determined from the integrated reactivity values of calibrated single control rods.

4.5.2   Five Rod Bank Calibration Techniques

The calibration of a single control rod as a function of the five rod bank position involves a change in reactivity corresponding to the change in bank position. The reactivity change is measured by the change in position of the rod being calibrated, calibration points being obtained by the period technique for each new critical position of the rod. Integrating the rod calibration curve, therefore, not only gives the rod worth over its length of travel, but also the worth of the five rod bank over the interval it had to be moved to balance the individual rod movement. The bank calibration in cents per inch is, therefore, determined by dividing the worth obtained from integrating the single rod calibration curve over the interval the rod was moved by the corresponding distance the bank was moved to balance it, and plotted at the average bank position.

Similar bank calibration points were determined from the reactivity introduced by transient xenon. Transient xenon was previously evaluated by maintaining criticality with a calibrated control rod during the xenon buildup and decay. The xenon reactivity worth and five rod bank position were then plotted as a function of time, and the motion of the five rod bank related to reactivity.

4.5.3   Experimental Results

Figure 4.30 shows the composite five rod bank calibration curve obtained during ZPE-1[8] and CE-1[15] at the Alco Critical Facility. The ZPE-1 calibration points were obtained utilizing the period technique as described in Section 4.4.2 for the five rod bank instead of a single rod. The bank was calibrated as a function of position, where the bank position was varied by the addition of nuclear poisons which were added to the core in the form of boron stainless steel strips.

During CE-1, the SM-1 Core I was mocked up using SM-2 fuel plates and boron in the form of impregnated Mylar tape which was attached to the face of the fuel plates. By lowering the B-10 loading, it was possible to obtain bank calibration points in the previously extrapolated region between 0 to 3.7 inches.

Figures 4.31 to 4.34 present the calibration curves obtained on-site as a function of core burnup. The calibration points were obtained from the integrated reactivity values of calibrated single rods (Figures 4.9 to 4.14) as a function of bank position, the reactivity worth of transient xenon as a function of bank position,

and the reactivity due to temperature change as a function of bank position. Figure 4.31 is a composite curve based on measurements at various core conditions through 9.1 MWYR energy release. Figures 4.32, 4.33 and 4.34 present the bank calibrations obtained at 12.1, 13.5, and 16.4 MWYR energy release, respectively, and under varying core conditions as described above.

The spread in data obtained at each interval during core life did not permit quantitative evaluations of data obtained under the identical core conditions. The curves drawn are the best fit by eye through all the data points assuming the calibration curve goes to zero at 22 inches. Because of the indirect manner in which the bank was calibrated and the variety of core conditions at which the calibrations were made, the uncertainty in each of the curves is estimated to be $\pm$ 10 percent. The uncertainty in the bank worth at 22 in. is estimated to be + 10 cents per inch. It should be stated that the use of these curves implies that the calibrations are not a strong function of Xe distribution, temperature or rod used for calibration.

Figure 4.35 summarizes the SM-1 Core I five rod bank calibration curves obtained as a function of core life, and indicates that the worth of the five rod bank increases with core burnup.

Only two curves have been obtained for the entire length of travel of the five rod bank, the composite ZPE-1 and CE-1 curve and the composite curve based on data obtained during 9.1 MWYR operation. Figure 4.36 presents the integral worths of these curves, $27.4 $\pm$ 1.0 and $26.2 $\pm$ 1.0 respectively.

4.5.4 Excess Reactivity Available as a Function of Core Life

The excess reactivity available of the core is determined by integrating the bank calibration curve from the critical bank position to the fully withdrawn position (22 inches). Tables 4.10 through 4.13 list the excess reactivity of the SM-1 Core I as a function of burnup for the low Xenon-70°F, low Xenon-440°F, equilibrium Xenon-440°F, and peak Xenon-440°F core conditions, respectively. These data are shown on Figure 4.37.

· The composite ZPE-1 and CE-1 bank calibration curve was used to determine the excess reactivity until 9.10 MWYR burnup. The calibration curves obtained at 12.1, 13.5 and 16.4 MWYR were used to determine the excess reactivity at these intervals respectively. The bank positions used were obtained from Figure 4.4.
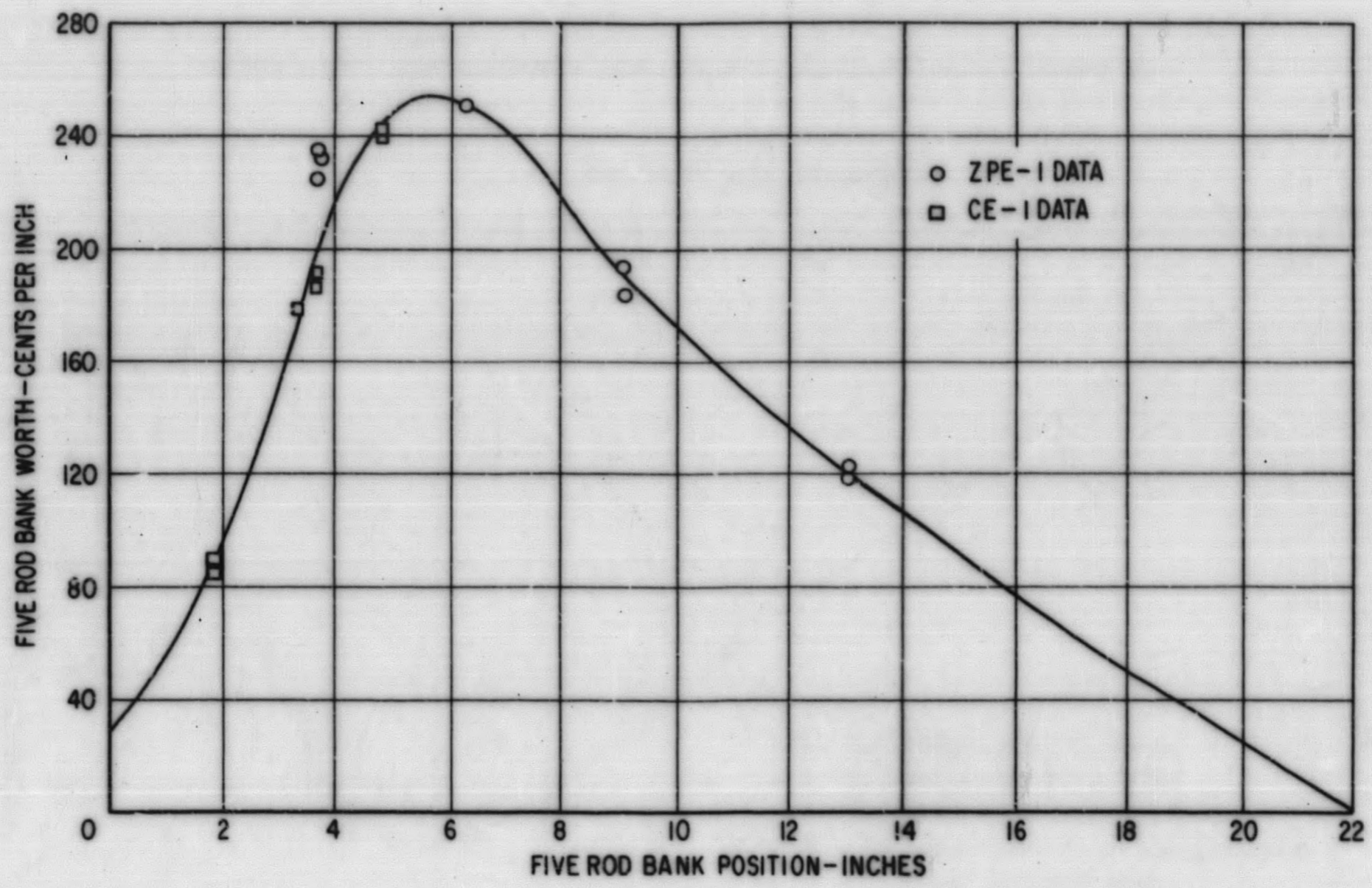
Figure 4.30.   SM-1 Core I Composite ZPE-1 and CE-1 Five Rod Bank
Calibration Curve

FIVE ROD BANK WORTH – CENTS PER INCH

280

240

200

160

120

80

40

0

0   2   4   6   8   10   12   14   16   18   20   22

FIVE ROD BANK POSITION – INCHES

○   O   MWYR – BANK VS ROD C VS TEMPERATURE
      90°F – 440°F
□   6.15 MWYR – ROD A VS BANK
△   7.22 MWYR – ROD A VS BANK
▲   7.22 MWYR – BANK VS Xe CONCENTRATION
▽   7.22 MWYR – SUB-CRITICAL, 100°F.
●   9.10 MWYR – ROD A VS BANK
▼   9.10 MWYR – ROD C VS BANK
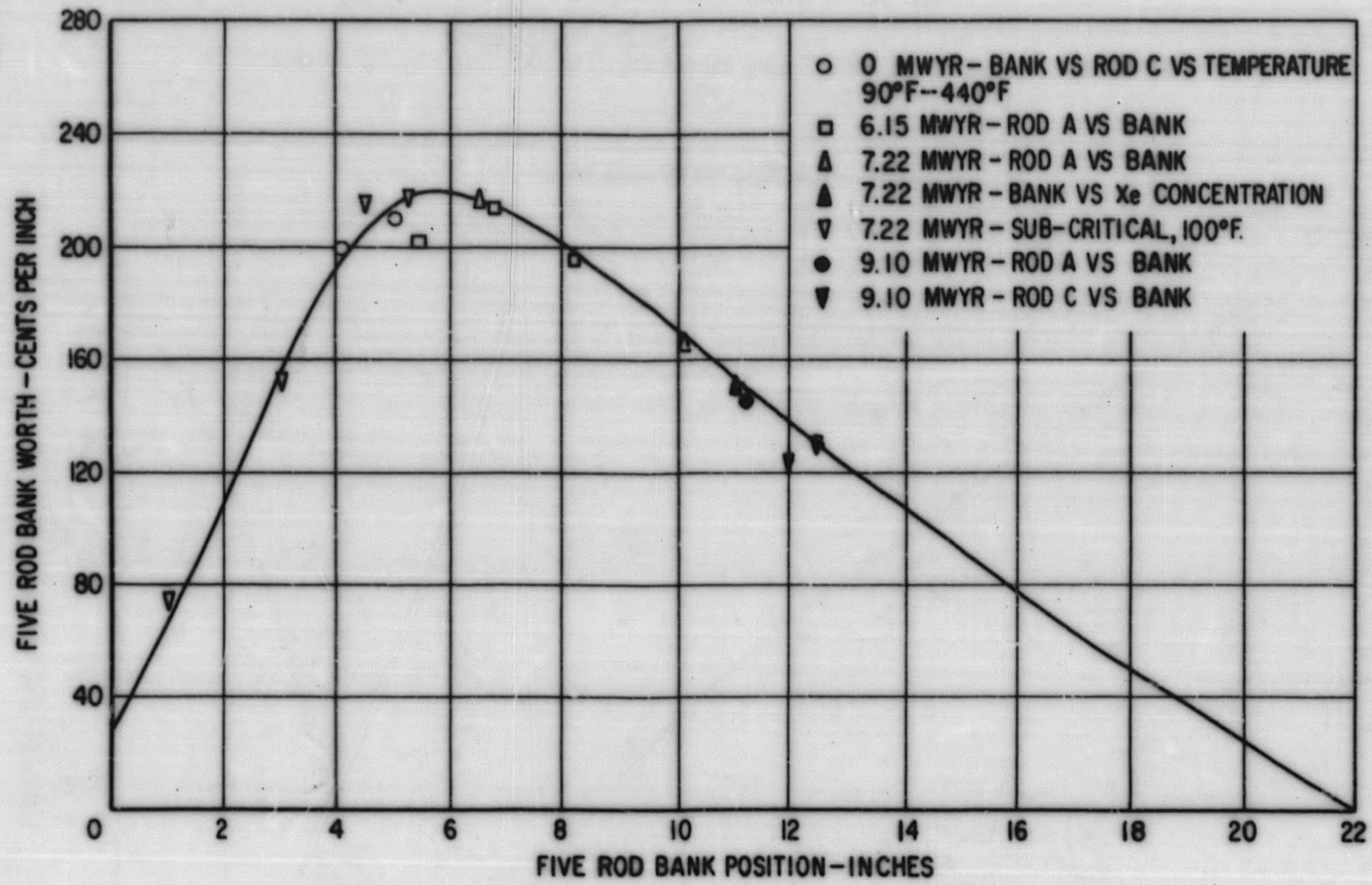
Figure 4.31.   SM-1 Composite Five Rod Bank Calibration Curve through 9.10
MWYR
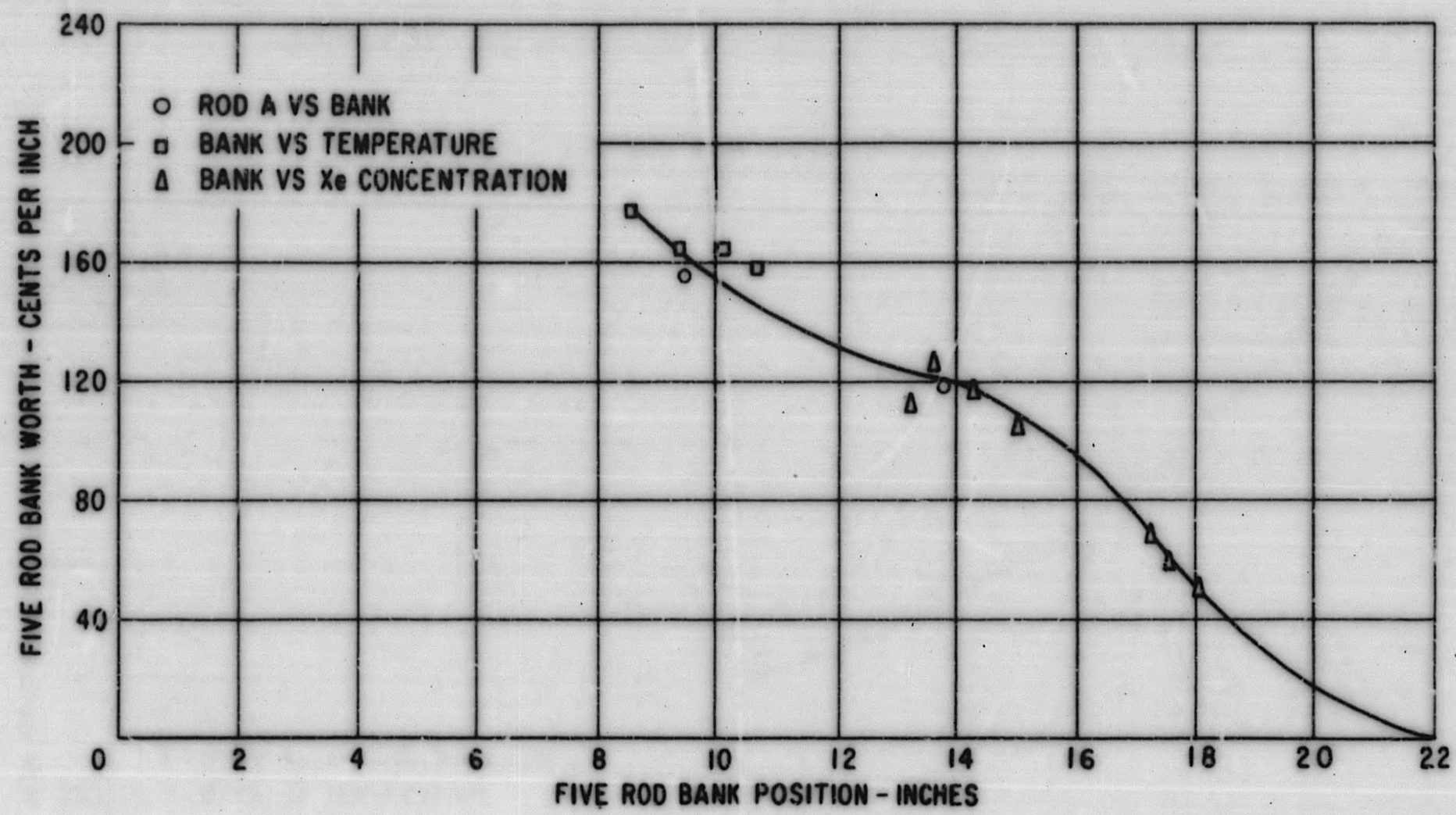
Figure 4.32. SM-1 Core I Five Rod Bank Calibration Curve 12.1 MWYR
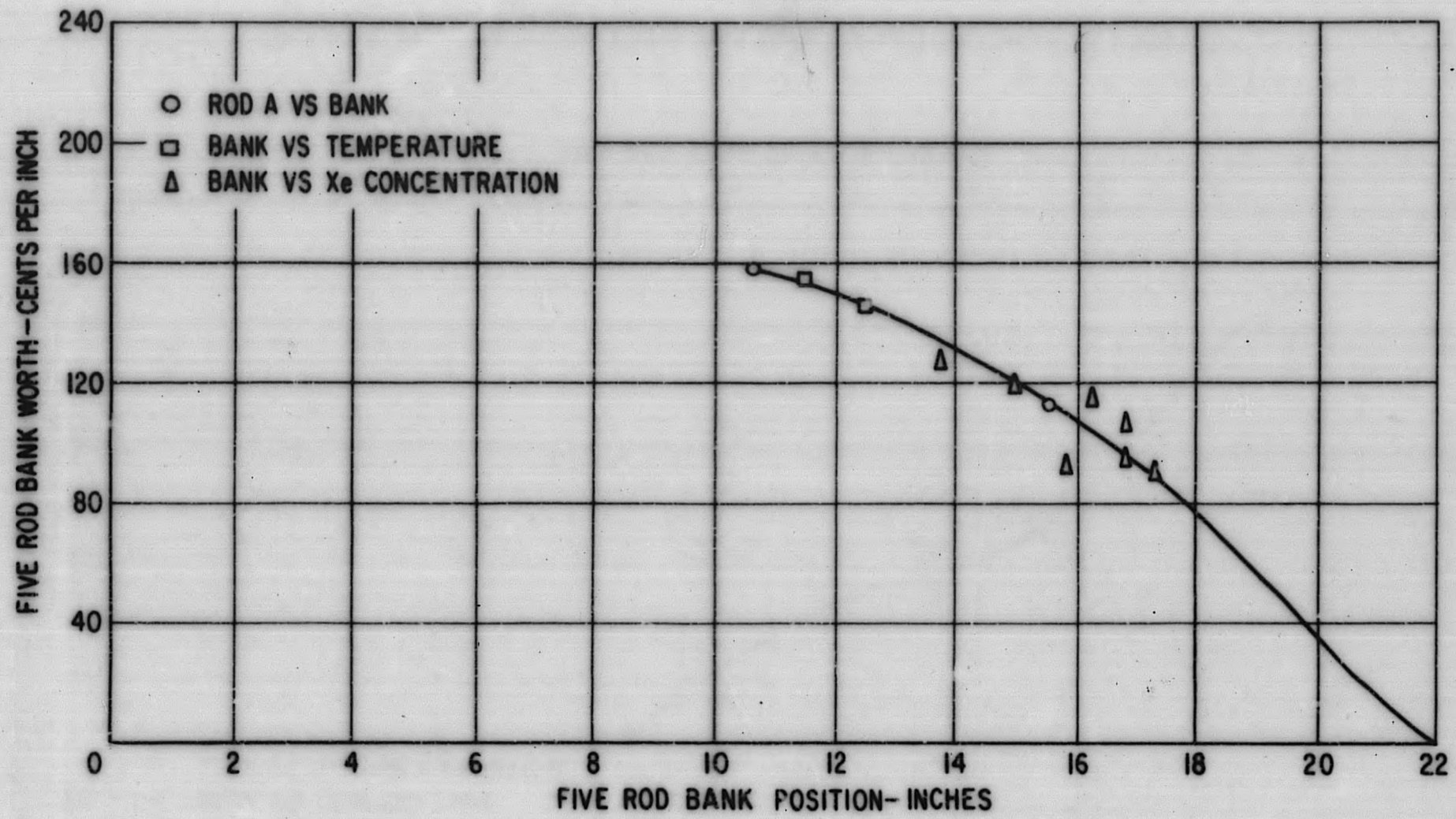
Figure 4. 33.   SM-1 Core I Five Rod Bank Calibration Curve 13. 5 MWYR
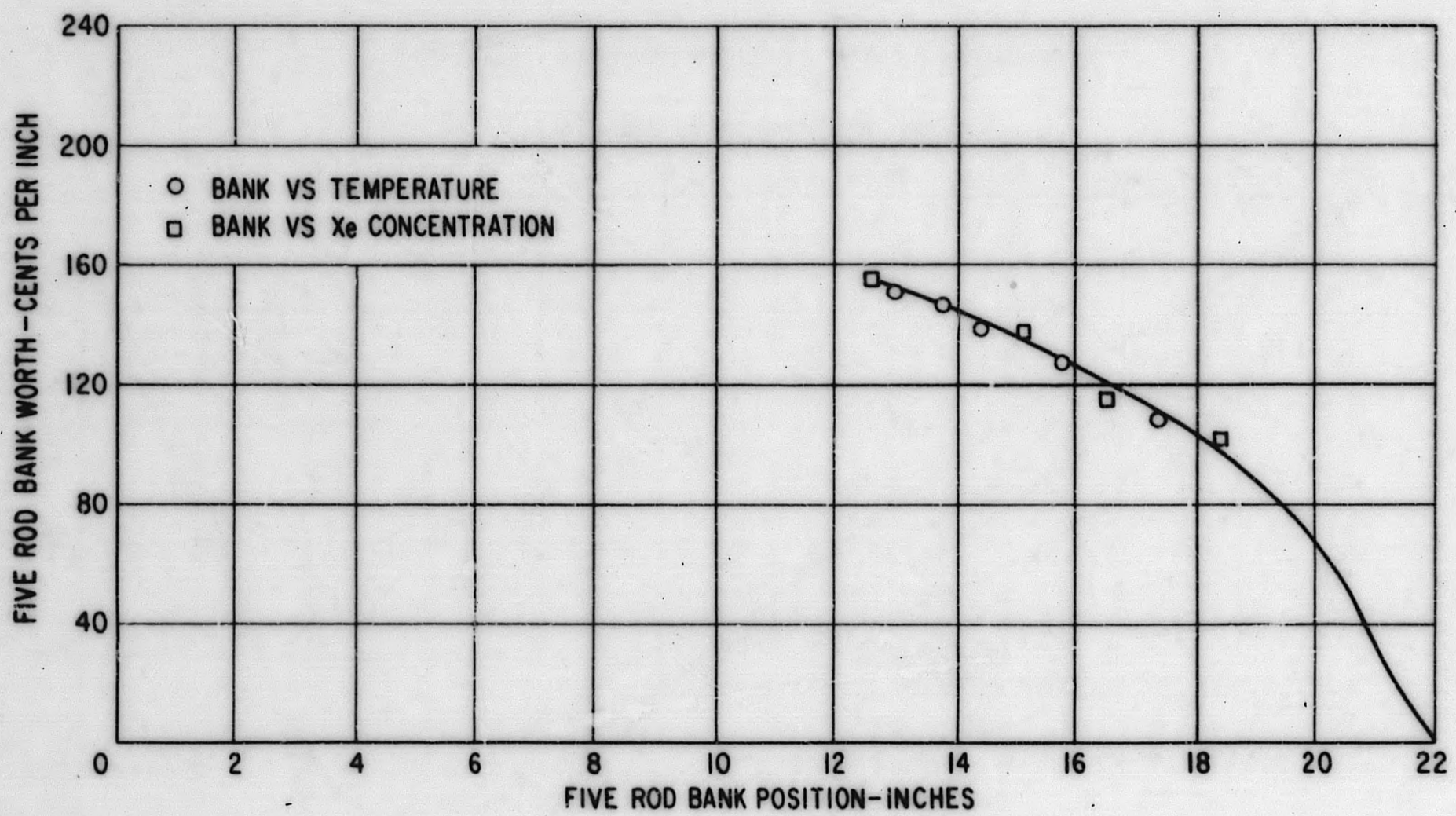
Figure 4.34.   SM-1 Core I Five Rod Bank Calibration Curve 16.4 MWYR
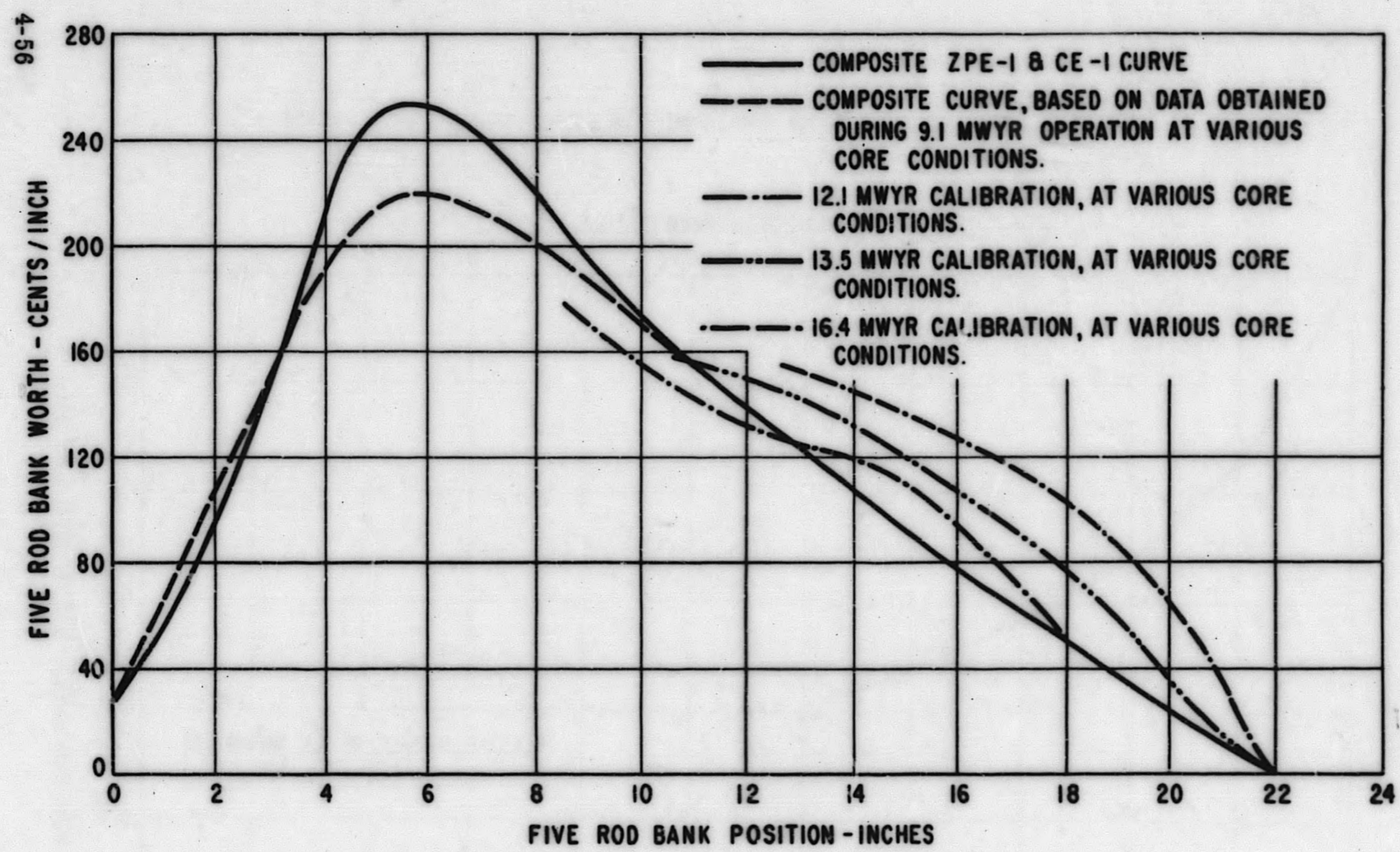
Figure 4.35.   Calibration of SM-1 Core I Five Rod Bank
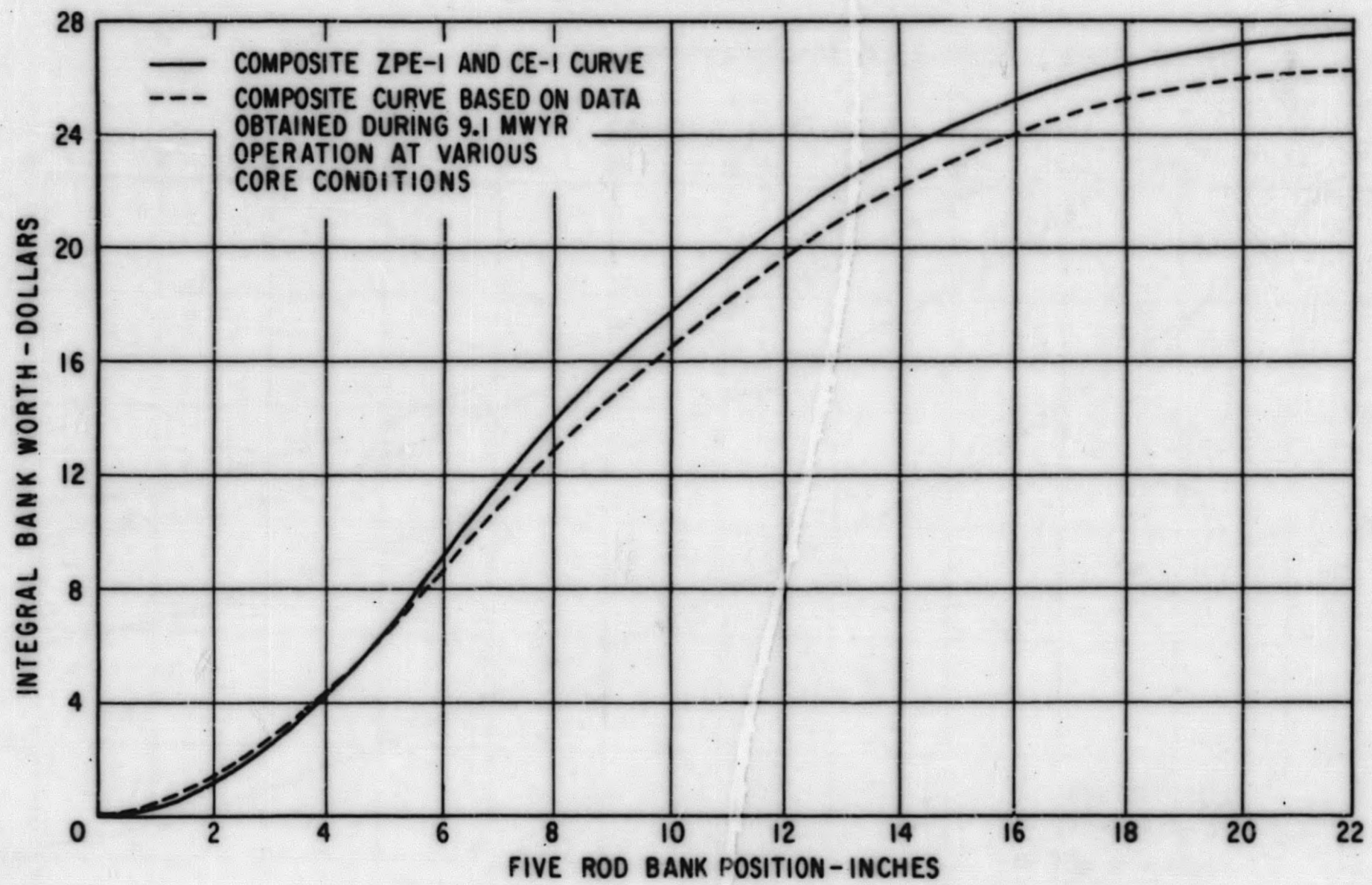
Figure 4.36. SM-1 Core I Five Rod Bank Integral Worth
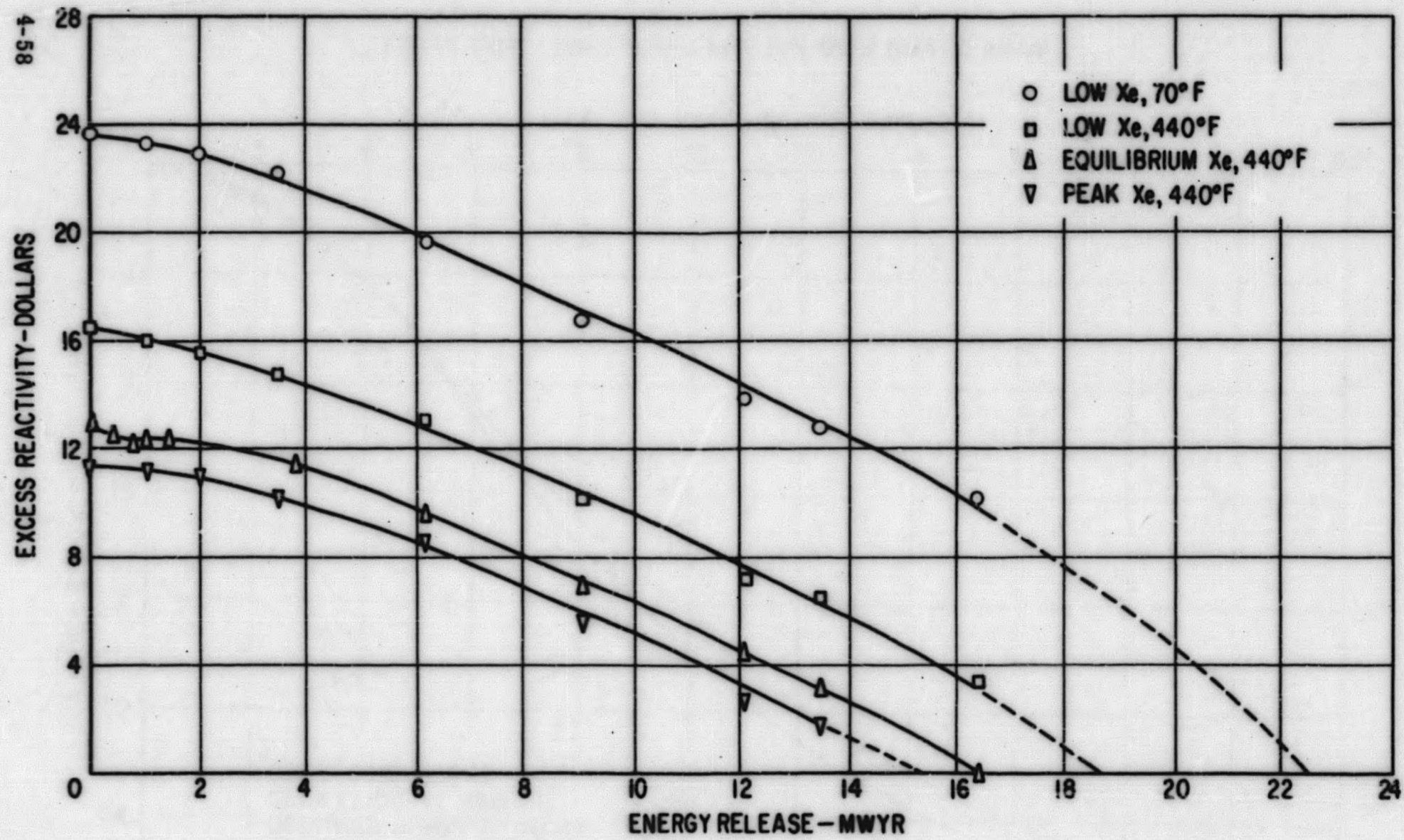
Figure 4.37. SM-1 Core I Excess Reactivity as a Function of Energy Release

TABLE 4.10
EXCESS REACTIVITY AS A FUNCTION OF SM-1 CORE I ENERGY RELEASE
Low Xenon - 70°F

Energy Release - MWYR	Excess Reactivity - Dollars*
0	23.8
1.00	23.4
2.00	23.0
3.50	22.3
6.15	19.7
9.10	16.8
12.1	13.9
13.5	12.9
16.4	10.2

TABLE 4.11
EXCESS REACTIVITY AS A FUNCTION OF SM-1 CORE I ENERGY RELEASE
Low Xenon - 440°F

Energy Release - MWYR	Excess Reactivity - Dollars*
0	16.5
1.00	16.1
2.00	15.6
3.50	14.8
6.15	13.1
9.10	10.2
12.1	7.2
13.5	6.5
16.4	3.4

* Estimated uncertainty of $\pm$ 5%

TABLE 4.12
EXCESS REACTIVITY AS A FUNCTION OF SM-1 CORE I ENERGY RELEASE
Equilibrium Xenon - 440°F

Energy Release - MWYR	Excess Reactivity - Dollars*
0	12.9
0.39	12.6
0.79	12.3
1.00	12.4
1.41	12.4
3.80	11.5
6.15	9.7
9.10	7.0
12.1	4.5
13.5	3.2
16.4	0

TABLE 4.13
EXCESS REACTIVITY AS A FUNCTION OF SM-1 CORE I ENERGY RELEASE
Peak Xenon - 440°F

Energy Release - MWYR	Excess Reactivity - Dollars*
0	11.5
1.00	11.2
2.00	11.0
3.50	10.2
6.15	8.6
9.10	5.6
12.1	2.7
13.5	1.8

* Estimated uncertainty of $\pm$ 5%

4.5.5 Seven Rod Bank Calibration

During ZPE-1,[8] the core was uniformly poisoned with boron steel strips and critical five and seven rod bank positions determined as a function of the B-10 loading. From the change in five and seven rod bank positions and the five rod bank worth, it was possible to determine the seven rod bank worth. Figure 4.38 presents the calculated seven rod bank calibration points as a function of bank position. The extrapolated portions of the calibration curve were estimated using similarity of shape to the five rod bank calibration. The seven rod bank integral worth curve is shown on Figure 4.39.

4.5.6 Conclusions

1. The five rod bank calibration curves were determined under varying core conditions. Use of these curves implies that the calibrations are not a strong function of Xe distribution, temperature or rod used for calibration.

2. A summary of the five rod bank calibration curves during SM-1 Core I life indicates that the worth of the five rod bank increases with burnup in the upper regions of the core. In the interval from 13 to 22 in., the bank worth increased from $5.2 at 0 MWYR to $9.0 at 16.4 MWYR.

3. The five rod bank calibration curve denoted as the composite ZPE-1 and CE-1 curve is the best estimate of the SM-1 Core I five bank calibration at 0 MWYR. The five rod bank integral worth of 0 MWYR is $27.4 ± 1.0.

4. The excess reactivity available in the SM-1 Core I as a function of core life, when plotted for various core conditions, indicates that the hot to cold reactivity change and the reactivity changes due to peak and equilibrium xenon concentrations did not vary significantly during core life. This is further shown in the sections on hot to cold reactivity change and transient xenon.

5. At 0 MWYR the seven rod bank integral worth is $34.0 ± 2.0.

6. The integral worth of rods A and B is $6.6 ± 2.2, as determined by the difference in integral worth between the seven and five rod banks.

7. Assuming no interactions between rods, the integral worth of rods A and B is (2 x $3.2) $6.4 cold and (2 x $3.8) $7.6 hot, using an average of the values in Table 4.9.

8. The shutdown margin of the five rod bank plus rods A and B at 0 MWYR and 68°F is ($3.6 + $6.6) $10.2.
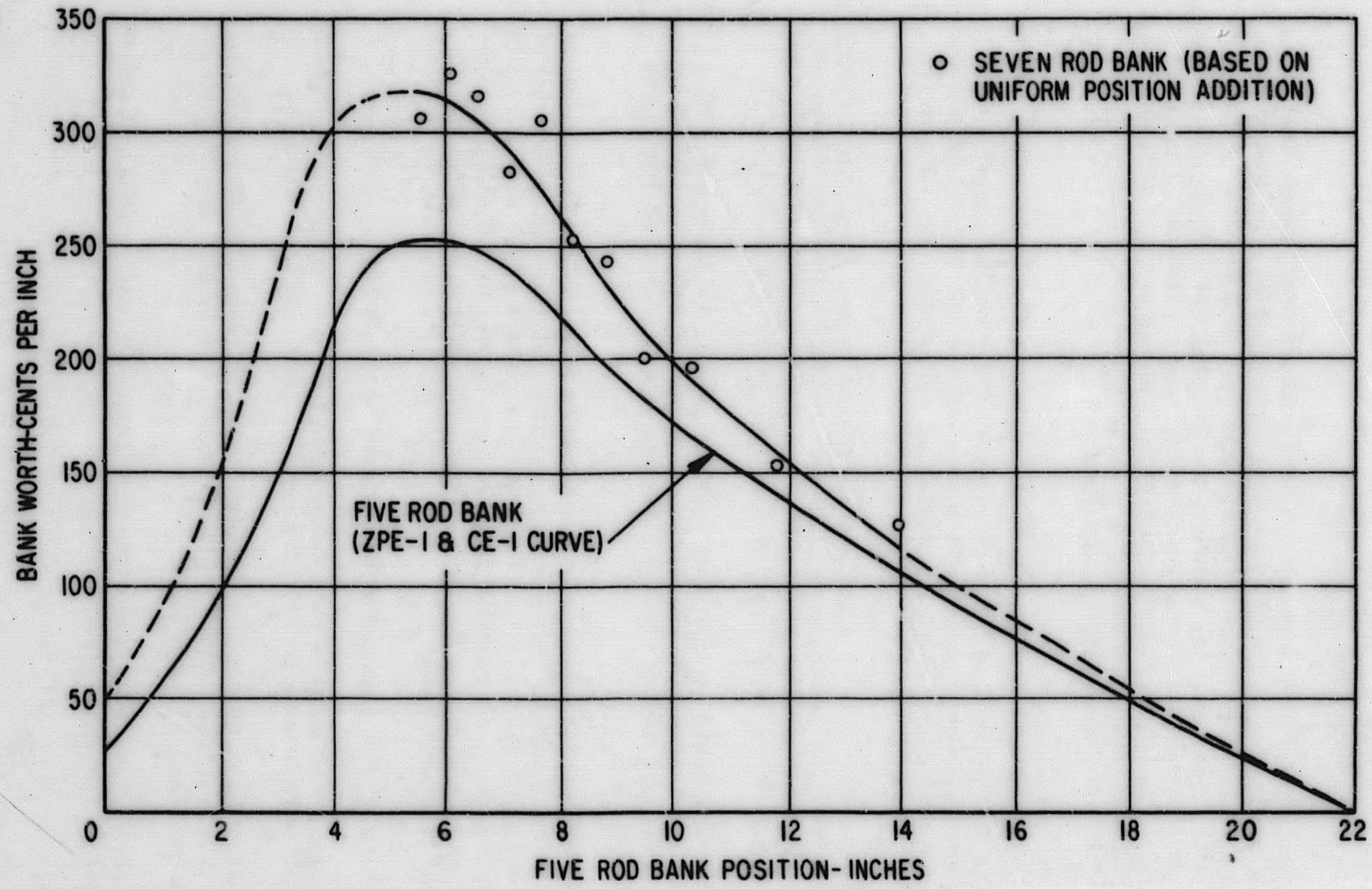
Figure 4.38. SM-1 Core I Five and Seven Rod Bank Calibrations
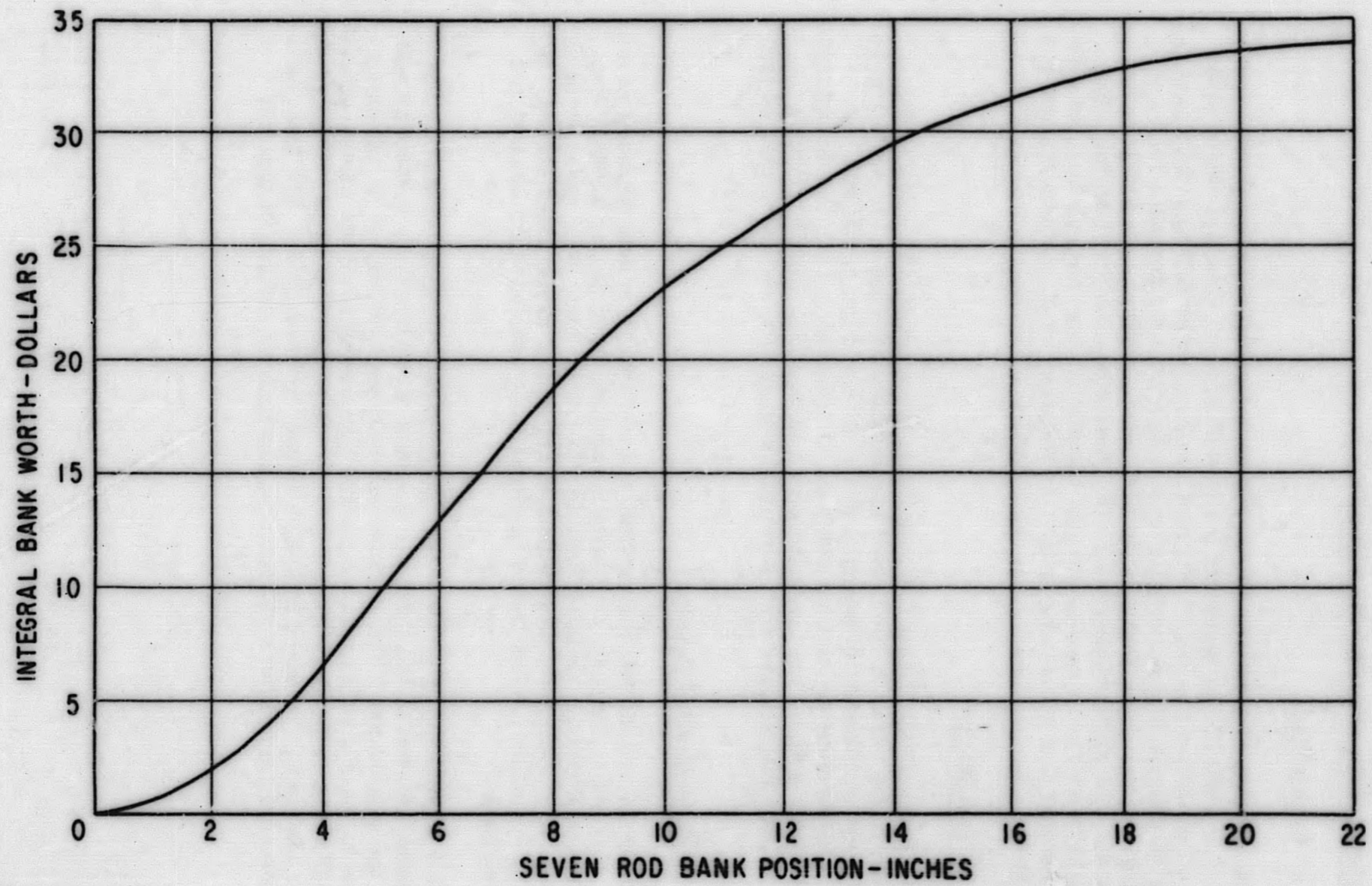
Figure 4.39.   SM-1 Core I Seven Rod Bank Integral Worth

4.6   CRITICAL ROD CONFIGURATIONS

4.6.1   Introduction

Measurements of various critical rod condifigurations were performed
as a function of core life to ascertain that t'e 80 percent contract requirement
for stuck rod shutdown was met. 80 percent stuck rod shutdown is interpreted
as meaning 80 percent of the available rod motion starting from the fully with-
drawn configuration. Thus, 80 percent of 7 control rods means 5.6 rods can
be inserted and 1.4 rods withdrawn or all 7 rods 20 percent withdrawn. The
1.4 rods withdrawn can be met by several situations, one rod can be fully with-
drawn and another 0.4 withdrawn or any combination which yields a total of 1.4
rods withdrawn.

4.6.2   Test Method

Critical rod configuration measurements were made with a low xenon
concentration in the core, at the lowest temperature reached after cooldown.
Six control rods would be fully inserted in the core and the remaining rod
withdrawn to determine the critical position. If criticality could not be achieved
with this rod fully withdrawn, an additional rod was then withdrawn until
criticality. The critical positions were recorded and the rod calibrated at this
position.

4.6.3   Experimental Results

Tables 4.14 to 4.20 list the critical rod configuration data obtained as a
function of core life. The data at 0 MWYR was measured during ZPE-1[8] at
the Alco Critical Facility; as Core I and the ZPE core have been shown to be
very similar, it is assumed that this data is applicable to the SM-1 Core I. In
these tables, rods that are not listed as either fully withdrawn or critical rod
are fully inserted.

Table 4.21 and Fig. 4.40 show the excess reactivity associated with the
partially withdrawn rod of the three worst cases of one rod fully withdrawn and
critical on the second rod. The excess reactivity was calculated by assuming a
linear shape to the rod calibration curve and integrating from the measured cali-
bration point at the critical position to zero cents per inch at 22 in. The calculated
values have also been corrected to a core temperature of 68°F. The shift in re-
activity between configurations reflects the non-uniform burnup of the core.

TABLE 4.14
CRITICAL ROD CONFIGURATIONS - ZERO MWYR[8]
68°F, Atmospheric Pressure

Case	Rods Fully Withdrawn	Critical Rod	Critical Position Inches	Worth, ¢/in.
A	1	A	9.5	-
B	1	2	10.09	40.0 @ 10.09
C	A	1	11.97	56.9 @ 11.97
D	3	C	13.87	23.1 @ 13.87
E	1	4	15.06	24.0 @ 15.06
F	C	3	16.21	27.3 @ 16.21
G	A, C	1	3.36	34.6 @ 3.36
H	A, B	3	9.84	50.0 @ 9.84
I	A, B	C	9.98	50.6 @ 9.98
J	3, A	Subcrit.	-	-
K	1, 3	Subcrit.	-	-

TABLE 4.15
CRITICAL ROD CONFIGURATIONS - 3.50 MWYR[16]
68°F, 80 psia

Case	Rods Fully Withdrawn	Critical Rod	Critical Position Inches	Worth, ¢/in.
A	1	A	11.31	40.9 @ 11.52 40.4 @ 11.54
B	1	2	12.08	37.8 @ 12.32 37.2 @ 12.39
C	A	1	13.67	55.6 @ 13.80 54.4 @ 13.85
D	3	C	17.91	8.2 @ 18.99 8.1 @ 18.94
E	1	4	20.31	2.1 @ 21.17 2.5 @ 21.14
F	C	3	19.14	8.8 @ 19.56 8.6 @ 20.18
G	A, C	1	5.78	53.0 @ 5.94 52.5 @ 5.96
H	A, B	3	11.37	56.1 @ 11.56 56.4 @ 11.43
I	A, B	C	12.04	47.4 @ 12.24 47.4 @ 12.24
J	3, A	B	8.30	38.4 @ 8.56 37.6 @ 8.51
K	1, 3	C	6.97	29.7 @ 7.33 29.0 @ 7.29

TABLE 4.16
CRITICAL ROD CONFIGURATIONS - 3.50 MWYR[17]
120°F, 110-375 psia

Case	Rods Fully Withdrawn	Critical Rod	Critical Position Inches	Worth, ¢/in.
A	1	A	11.93	40.8 @ 12.16 41.9 @ 12.23
B	1	2	12.68	37.3 @ 12.97 35.7 @ 13.06
C	A	1	14.12	49.4 @ 14.31 49.8 @ 14.38
D	3, C	1	2.29	7.1 @ 3.63
E	1, 4	C	3.01	14.0 @ 3.47 14.8 @ 3.55
F	3, C	Subcritical	-	-
G	A, C	1	6.32	58.3 @ 6.44 59.7 @ 6.46
H	A, B	3	11.83	58.3 @ 12.06 57.5 @ 12.03
I	A, B	C	12.55	47.1 @ 12.67 43.7 @ 12.98
J	3, A	B	8.99	39.8 @ 9.21 39.7 @ 9.20
K	1, 3	C	7.76	23.8 @ 7.99 23.9 @ 8.07

TABLE 4.17
CRITICAL ROD CONFIGURATIONS - 4.79 MWYR
120°F, 220-520 psia

Case	Rods Fully Withdrawn	Critical Rod	Critical Position Inches	Worth, ¢/in.
A	1	A	13.20	36.6 @ 13.47 37.0 @ 13.46
B	1	2	14.11	31.8 @ 14.50 34.8 @ 14.42
C	A	1	15.23	45.3 @ 15.49 50.9 @ 15.46
D	3, C	Subcritical	-	-
E	1, 4	Subcritical	-	-
F	C, 3	Subcritical	-	-
G	A, C	1	7.13	68.4 @ 7.32 55.3 @ 7.30
H	A, B	3	12.67	-
I	A, B	C	13.91	43.0 @ 14.13 50.44 @ 14.17
J	3, A	Subcritical	-	-
K	1, 3	Subcritical	-	-

TABLE 4.18
CRITICAL ROD CONFIGURATIONS - 7.22 MWYR
110-170 psia

Case	Rods at 19 Inches	Critical Rod	Critical Position Inches	Worth, ¢/in.	Temp., °F
A	1	A	18.89	3.12 @ 20.39	120
A	1	A	17.44	13.39 @ 18.06	99
B	1	2	19.45	6.86 @ 20.68	120
C	A	1	18.91	16.60 @ 19.57	120
C	A	1	18.18	23.72 @ 18.60	99
D	3, C*	Subcritical	-	-	-
E	1, 4*	Subcritical	-	-	-
F	C, 3*	Subcritical	-	-	-
G	A, C	1	9.59	65.33 @ 9.74	120
G	A, C	1	9.33	70.31 @ 9.53	99
H	A, B	3	15.10	43.43 @ 15.30	99
				45.90 @ 15.31	99
I	A, B	C	18.18	16.92 @ 18.67	99
				16.90 @ 18.82	99
J	3, A*	Subcritical	-	-	-
K	1, 3*	Subcritical	-	-	-

TABLE 4.19
CRITICAL ROD CONFIGURATIONS - 9.1 MWYR
108°F, 220 psia

Case	Rods at 19 Inches	Critical Rod	Critical Position Inches	Worth, ¢/in.
A	1, A*	Subcritical	-	-
B	1, 2*	Subcritical	-	-
C	A, 1*	Subcritical	-	-
D	3, C*	Subcritical	-	-
E	1, 4*	Subcritical	-	-
F	C, 3*	Subcritical	-	-
G	A, C	1	11.78	65.38 @ 11.97
				60.69 @ 11.98
H	A, B	3	18.80	16.46 @ 18.61
				15.97 @ 19.58
I	A, B, C*	Subcritical	-	-
J	3, A*	Subcritical	-	-
K	1, 3*	Subcritical	-	-
A'	1, A	C	6.59 @ 80°F	27.11 @ 6.80
A"	1*, A*	C	4.42 @ 80°F	-
B'	1, 2	C	7.88 @ 80°F	22.52 @ 9.07
B"	1*, 2*	C	5.26 @ 80°F	15.27 @ 6.05
I'	A, B, C	1	6.21 @ 80°F	-
I'	A*, B*, C*	1	5.05 @ 80°F	30.62 @ 5.46

*Rods fully withdrawn

TABLE 4.20
CRITICAL ROD CONFIGURATIONS - 13.5 MWYR*
117°F, 260 psia

Run	Rods at 19 Inches	Critical Rod	Critical Position Inches	Worth, ¢/in.
1	A, B, C	3	15.95	-
2	2, 4, A	C	15.18	-
3	1, 4, A	C	0.84	-
4	4, A, C	3	8.19	-
5	4, A, B	3	15.14	-
6	2, 3, A, C	B	5.51	-
7	1, 2, 3	A	10.50	-
8	1, 4, C	A	9.59	-
9	2, 3, A, C	B	5.54**	-
10	1, 3, C	A	15.94	-

* Verification that no criticality hazards would be introduced during the proposed spent core rearrangement.

** Repeat of Run #6

TABLE 4.21
EXCESS REACTIVITY ASSOCIATED WITH PARTIALLY WITHDRAWN
ROD OF CRITICAL ROD CONFIGURATION, 68°F

Energy Release, MWYR	Rod Fully Withdrawn	Rod Partially Withdrawn	Excess Reactivity of Partially Withdrawn Rod, Dollars
0	1	A	2.8
3.50	1	A	2.2
4.79	1	A	2.1
7.22	1	A	0.5
0	1	2	2.4
3.50	1	2	1.9
4.79	1	2	1.8
7.22	1	2	0.6
0	A	1	2.9
3.50	A	1	2.3
4.79	A	1	2.1
7.22	A	1	0.8
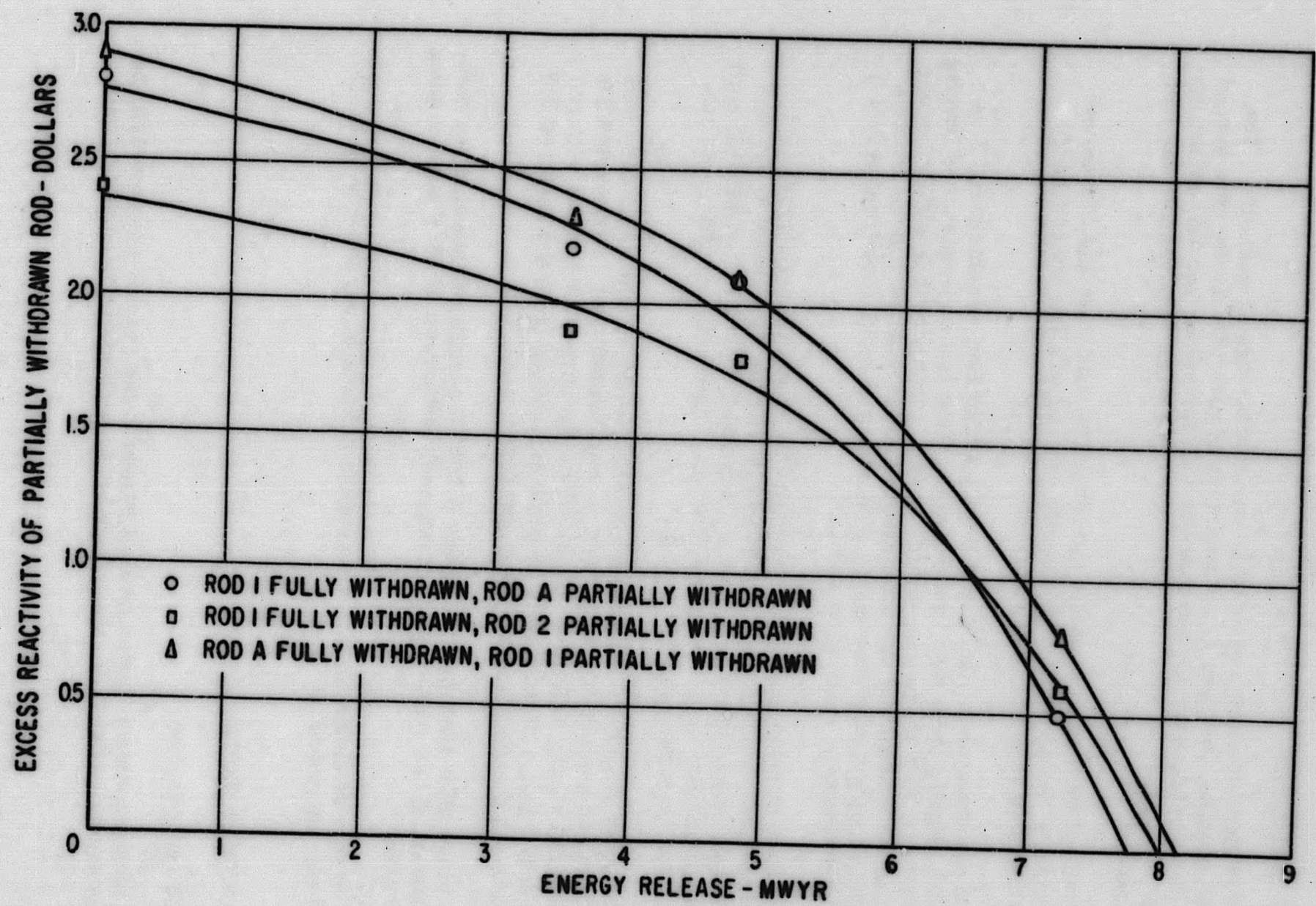
Figure 4.40. Excess Reactivity Associated with Partially Withdrawn Rod of Critical
Rod Configuration, SM-1 Core I, 68°F

4.6.4 Conclusions

1. The 80 percent stuck rod criteria was met throughout core life. The most reactive core was at the beginning of core life; as the core burned out it was necessary to withdraw the rods further to maintain criticality; thus the margin by which the 80 percent shutdown requirement was met increased with core life.

2. It was not until approximately the end of one-half core life that the excess core reactivity was sufficiently reduced to allow subcriticality with rods A, B and C fully withdrawn.

3. It is noted that with rods A and B fully withdrawn, eccentric rod 3 is worth slightly more than center rod C. This is a consequence of leaving effectively half of the core unrodded when control rods A and B plus one eccentric control rod are withdrawn. This is a slightly more reactive configuration than a core with a ring of four control rods (rods A and B fully withdrawn, critical on rod C.

4. The case of seven rods each inserted 80 percent of their travel (4.4 in. withdrawn) results in the largest safety margin. As shown in Fig. 4.2, the fully loaded SM-1 Core I at startup and 68^OF did not go critical until the seven rods were withdrawn 5.50 in., approximately 350 cents subcritical from the required 4.4 in.

5. The most reactive configuration is the case where one rod is fully withdrawn and another 0.4 withdrawn (8.8 in. withdrawn). At zero MWYR with rod 1 fully withdrawn and at 68^OF, the core went critical with rod A at 9.5 in., approximately 30 cents subcritical from the required 8.8 inches in the most reactive configuration.

6. It is not until after approximately 8 MWYR energy release that any combination of two rods could be completely withdrawn at 68^OF without going critical.

7. The core is within $2.8 of meeting the criteria of any two rods full out at startup and 68^OF.

4.7 TRANSIENT XENON

4.7.1 Introduction

The most important fission product poison in the reactor is xenon-135, because of its exceptionally large absorption cross section for thermal neutrons.

The main proportion of Xe-135 is produced from the precursor I-135 by beta decay,

$$Te^{135} \xrightarrow{2m} I^{135} \xrightarrow{6.68h} Xe^{135} \xrightarrow{9.13h} Cs^{135} \xrightarrow{2\times10^4 y} Ba^{135} \text{ (stable)}.$$
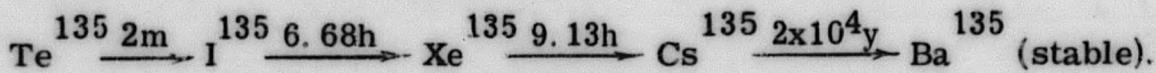
The short half-life of the tellurium-135 allows simplication of the analysis by assuming that iodine-135 is produced directly in fission. The fission decay chain in which Xe-135 arises is then:[18]
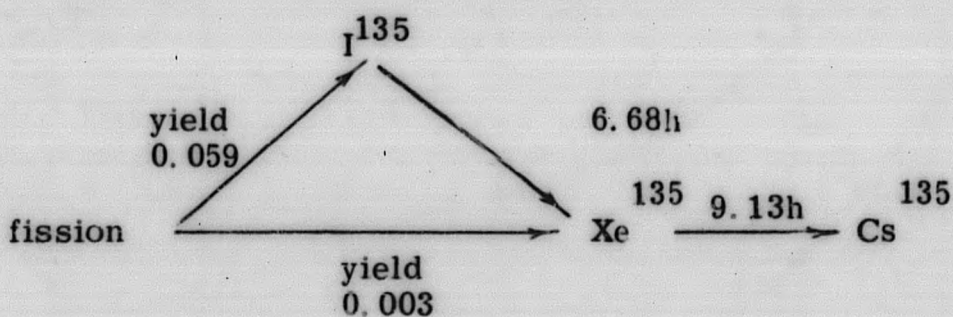
After continuous operation for approximately 50 hours at constant power, the Xe-135 concentration will reach an equilibrium value, as production by direct fission and decay of I-135 will be balanced by burnout by neutron absorption and radioactive decay. If the reactor is now shut down or the power level reduced to a very low value, the removal of Xe-135 by neutron absorption is sharply reduced and the Xe-135 concentration will build up through the decay of I-135 until a peak concentration is reached. At peak xenon concentration, the production of Xe-135 by I-135 decay exactly matches Xe-135 radioactive decay to Cs-135. After reaching peak xenon concentration the xenon concentration will start to decrease as the buildup of Xe-135 by I-135 decay is less than its radioactive decay, since no more I-135 is being produced.

4.7.2 Test Method

The general test method is to operate the reactor continuously at full power for at least 50 hr to build up equilibrium conditions. The power is then reduced to 100 KW to allow the xenon concentration to increase while maintaining temperature. The reactivity associated with the xenon transient is followed with a control rod which is calibrated as a function of xenon concentration during the run. Critical five rod bank positions are determined approximately every four hours.

4.7.3 Experimental Results

Figure 4.41 shows the position of the five rod bank as a function of time after power reduction at various times during core life. The data at 0.19 MWYR

4-71
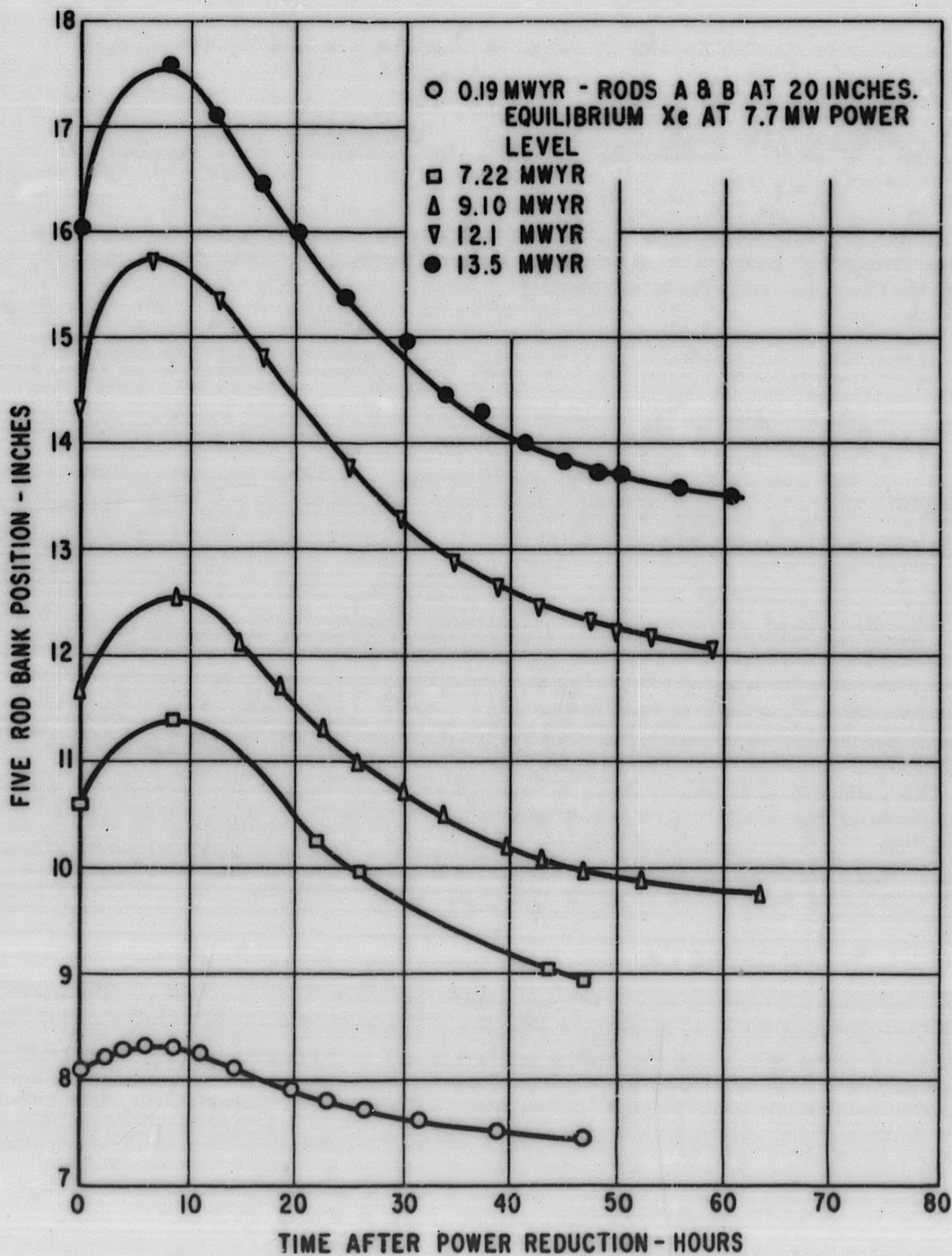
Figure 4.41. Xenon Transient, Five Rod Bank Position Vs. Time after Power Reduction, Rods A and B at 19 Inches, Temperature 440°F

was obtained after reaching equilibrium conditions at the 7.7 MW power level with control rods A and B at 20 inches. The remaining data was obtained after attaining equilibrium conditions at a power level of 10.77 MW with control rods A and B at 19 inches.

Figure 4.42 presents the reactivity introduced by transient xenon as a function of time after power reduction. Except for the values at 7.22 and 9.10 MWYR, the reactivity was determined from the change in critical position of the control rod that is being calibrated as a function of xenon concentration. The values at 7.22 and 9.10 MWYR energy release were determined from the change in bank position during the xenon transient and the bank worth. The data as a function of core energy release shows that except at peak xenon concentration, the various curves are essentially identical within experimental uncertainty.

Table 4.22 lists the reactivity due to equilibrium xenon relative to low xenon and the reactivity due to peak xenon relative to equilibrium xenon. The reactivity at a selected energy release was calculated from the change in bank position at different xenon concentrations and the bank calibration curves. The bank position values were obtained from the curves in Fig. 4.4 and the bank

TABLE 4.22

REACTIVITY DUE TO XENON CONCENTRATION AS A FUNCTION OF
SM-1 CORE I ENERGY RELEASE, 440°F

Energy Release, MWYR	Reactivity Due to Equilibrium Xe Relative to Low Xenon, Dollars*	Reactivity Due to Peak Xe Relative to Equilibrium Xe, Dollars*
0	-3.52	-1.33
2.00	-3.14	-1.39
3.50	-3.06	-1.42
6.15	-3.25	-1.30
7.22	-3.28	-1.44
9.10	-3.16	-1.50
10.5	-2.87	-1.52
12.1	-2.83	-1.43
13.5	-3.10	-1.55
15.0	-3.25	-1.58
16.4	-3.35	---

* Estimated uncertainty of ± 6%.
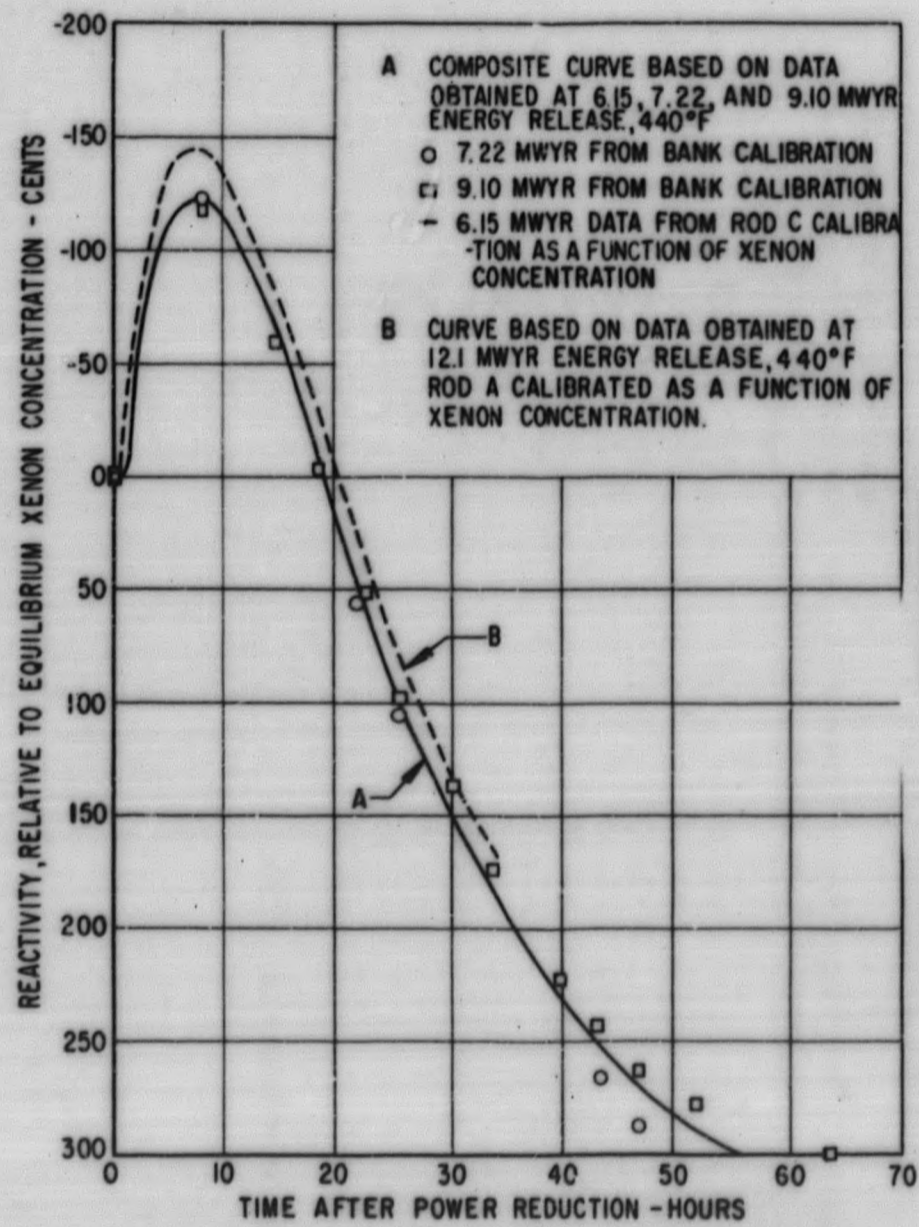
FIGURE 4.42A SM-1 CORE I REACTIVITY INTRODUCED BY TRANSIENT XENON
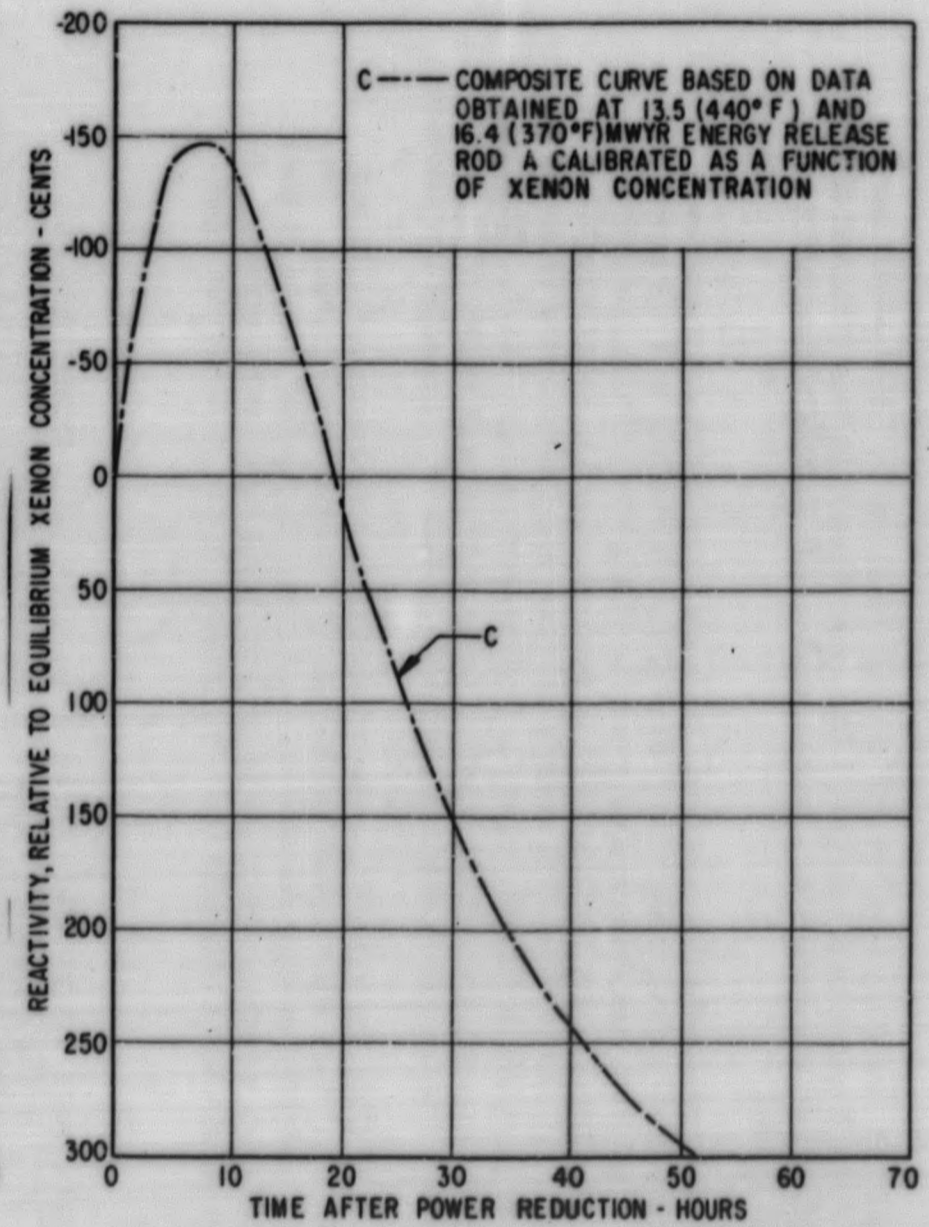
FIGURE 442B SM-1 CORE I REACTIVITY INTRODUCED BY TRANSIENT XENON

Figure 4.42.   SM-1 Core I Reactivity Introduced by Transient Xenon

worths from Fig. 4.35 (using the curve corresponding to the selected energy release interval). Taking the low xenon bank position data off the curves rather than using the measured positions partially corrects for the fact that the low xenon measurement during core life was made with varying amounts of xenon present in the core. *

The reactivity values as a function of core energy release are presented in Fig. 4.43. The equilibrium relative to low xenon and peak relative to equilibrium xenon data have been fitted by least squares linear fits; their sum is the reactivity of peak xenon relative to low xenon.

4.7.4 Conclusions

1. Peak xenon concentration, reached 7 to 9 hr after power reduction, decayed to equilibrium concentration after a total of 19 to 21 hours.

2. The reactivity of peak xenon relative to equilibrium xenon concentration varied from -130 ± 8 cents to -155 ± 10 cents over core lifetime.

3. The reactivity of equilibrium xenon relative to low xenon concentration varied from -283 ± 17 cents to -352 ± 21 cents over core lifetime.

4. Least squares linear fits of the data indicate:

   a. A slight decrease in the reactivity of equilibrium xenon relative to low xenon concentration of from 325 cents to 309 cents during 16.4 MWYR.

   b. A slight increase in the reactivity of peak xenon relative to equilibrium xenon concentration of from 133 cents to 157 cents during 16.4 MWYR.

   c. A slight increase in the reactivity of peak xenon relative to low xenon concentration of from 458 cents to 466 cents during 16.4 MWYR.

4.8 AXIAL NEUTRON FLUX DISTRIBUTION

4.8.1 Introduction

Perturbation theory indicates that the worth of a thermal absorber is proportional to the product of the thermal regular flux and the adjoint flux. Assuming

---

* Low xenon concentration refers to an estimated 10 to 20 cents negative reactivity from the ideal xenon-free condition.
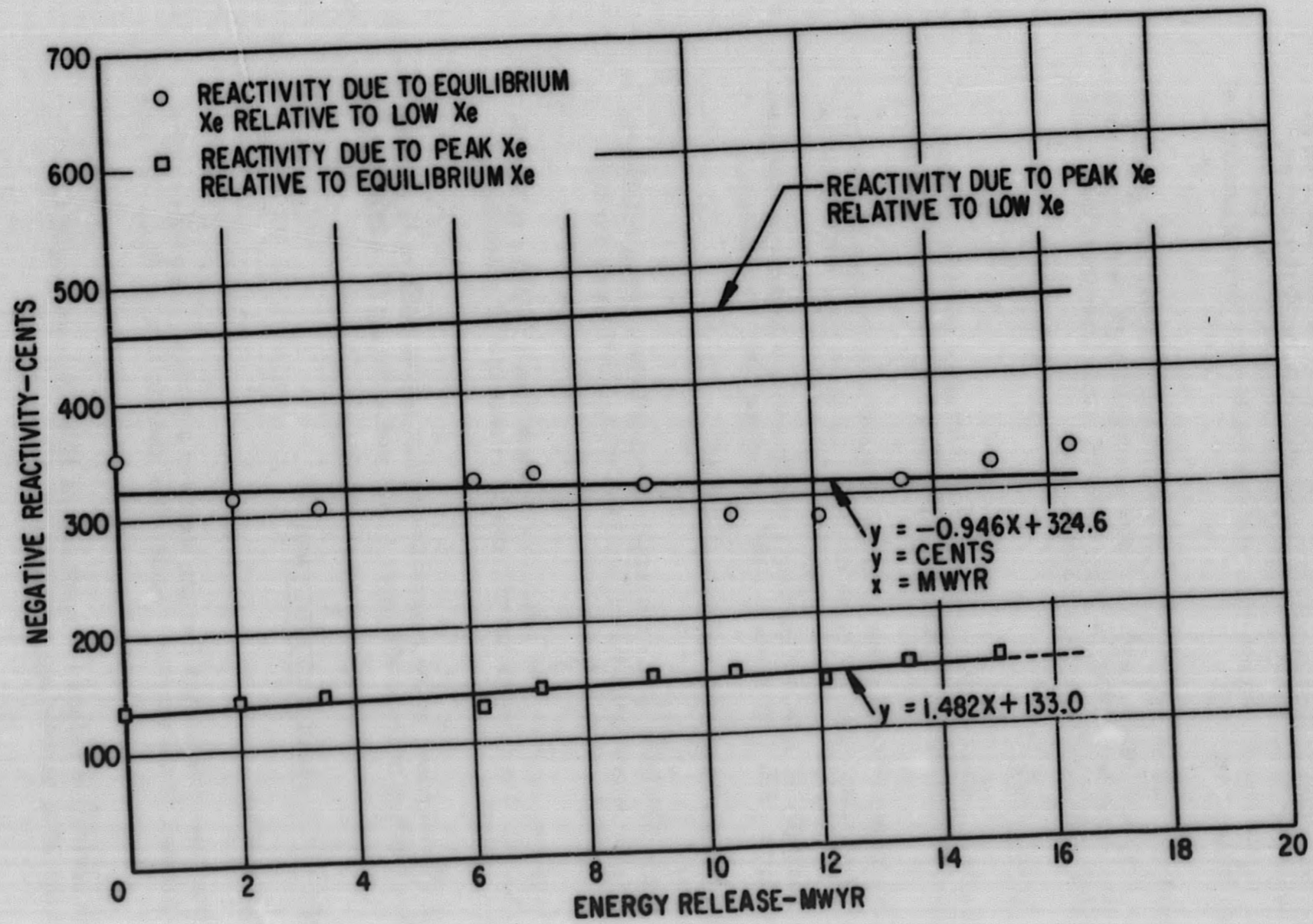
Figure 4.43.   Reactivity Due to Xenon Concentration as a Function of SM-1 Core I
Energy Release

the regular and adjoint fluxes to have the same shape (which is true for a bare reactor) and the control rods sufficiently withdrawn so that the perturbed flux is proportional to the unperturbed flux, and assuming a control rod to be essentially a thermal absorber, the worth of a control rod is proportional to the square of the local thermal flux. Therefore, an indication of the axial flux shape can be obtained from the square root of a control rod calibration curve.

4.8.2 Experimental Results

As a check on the above assumptions, the neutron flux as determined from bare gold activation in the zero power experiments[8] with the bank at 6.3 in. is shown on Fig. 4.44 in comparison with the relative axial flux as determined from the square root of the rod A calibration curves obtained at 7.22 MWYR. There is seen to be close agreement between the gold foil data obtained at a bank position of 6.3 in. and the curve obtained from the rod A calibration with a bank position from 5.74 to 7.27 inches. The values are normalized to an axial average neutron flux of unity. It should be noted that the bare gold foil does not measure only the thermal neutron flux; however, we may conclude that within the experimental errors, the square root of the rod worth as a function of position gives a good indication of the overall relative axial neutron flux distribution.

Figures 4.44 to 4.47 present the relative axial neutron flux distributions determined from the square root of the rod A calibration curves at various times during core life. Table 4.23 shows the shift in the axial location of the flux peak as the bank is withdrawn from the core, and the variation in peak to average ratio during core life.

<div align="center">

TABLE 4.23

LOCATION OF AXIAL NEUTRON FLUX PEAK IN SM-1 CORE I AS A
FUNCTION OF BANK POSITION AT VARIOUS CORE CONDITIONS

</div>

Location of Axial Flux Peak, Inches	Bank Position, Inches	Core Energy Release, MWYR	Core Temp., °F	Neutron Flux Peak to Average Ratio
5.6	5.74 to 7.27	7.22	120	1.71
5.7	6.57 to 8.26	9.10	120	1.72
6.3	8.43 to 10.43	12.1	130	1.72
6.4	9.05 to 11.21	7.22	440	1.63
6.6	9.54 to 11.58	13.5	120	1.68
6.9	9.91 to 12.52	9.10	440	1.70
8.3	12.66 to 14.95	16.4	120	1.57
8.5	12.85 to 15.39	12.1	440	1.58
9.4	13.69 to 17.25	13.5	440	1.57

4-78   Figure 4.44.   SM-1 Core I Axial Flux Distribution, 7.22 MWYR

A   SQUARE ROOT ROD A CALIBRATION
     130°F BANK 8.43 TO 10.43 IN.
B   SQUARE ROOT ROD A CALIBRATION
     440°F BANK 12.85 TO 15.39 IN.

RELATIVE AXIAL FLUX NORMALIZED TO AXIAL AVERAGE = 1.0

POSITION ABOVE BOTTOM OF CORE -INCHES

4-80   Figure 4.46.   SM-1 Core I Axial Flux Distribution, 12.1 MWYR
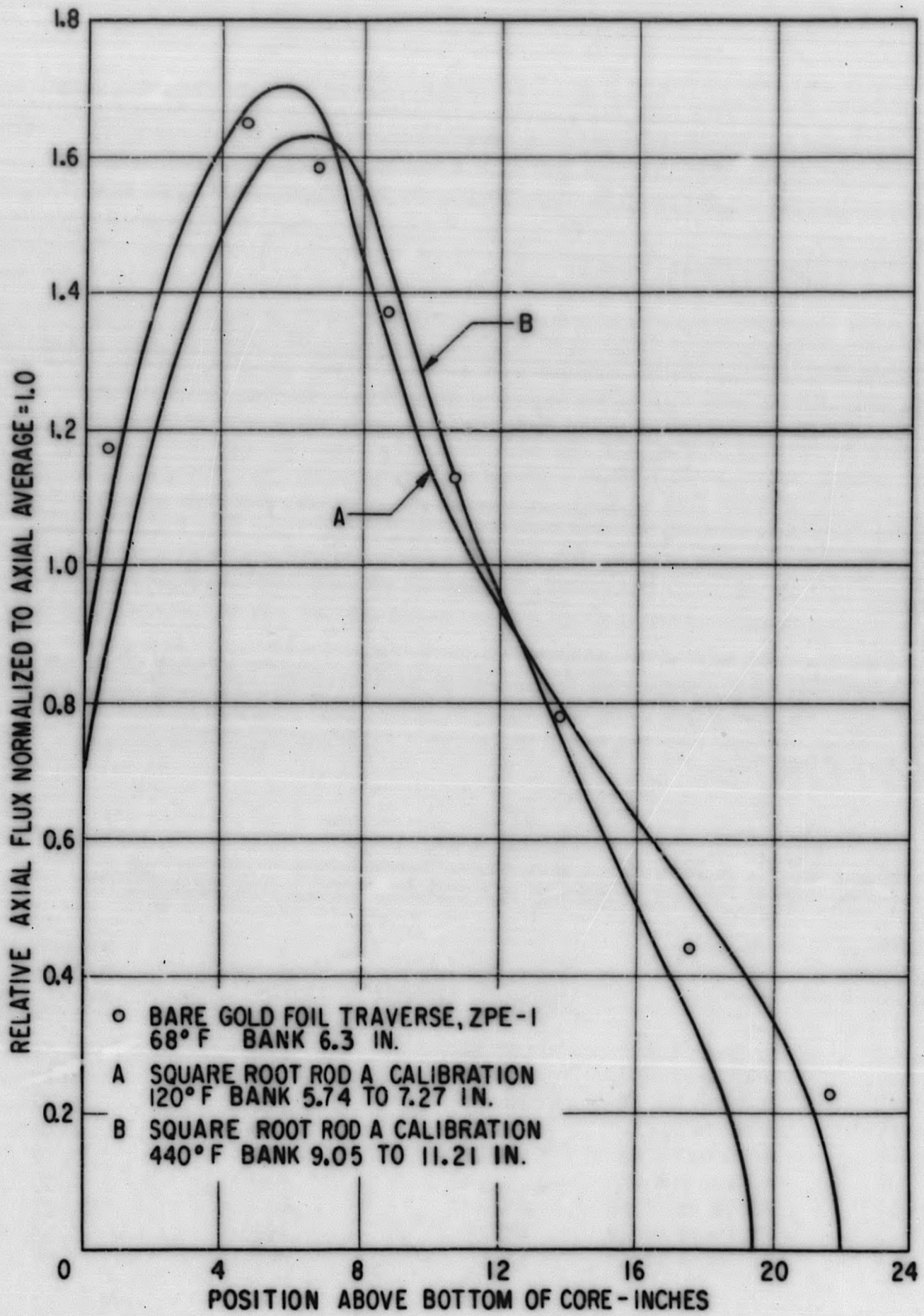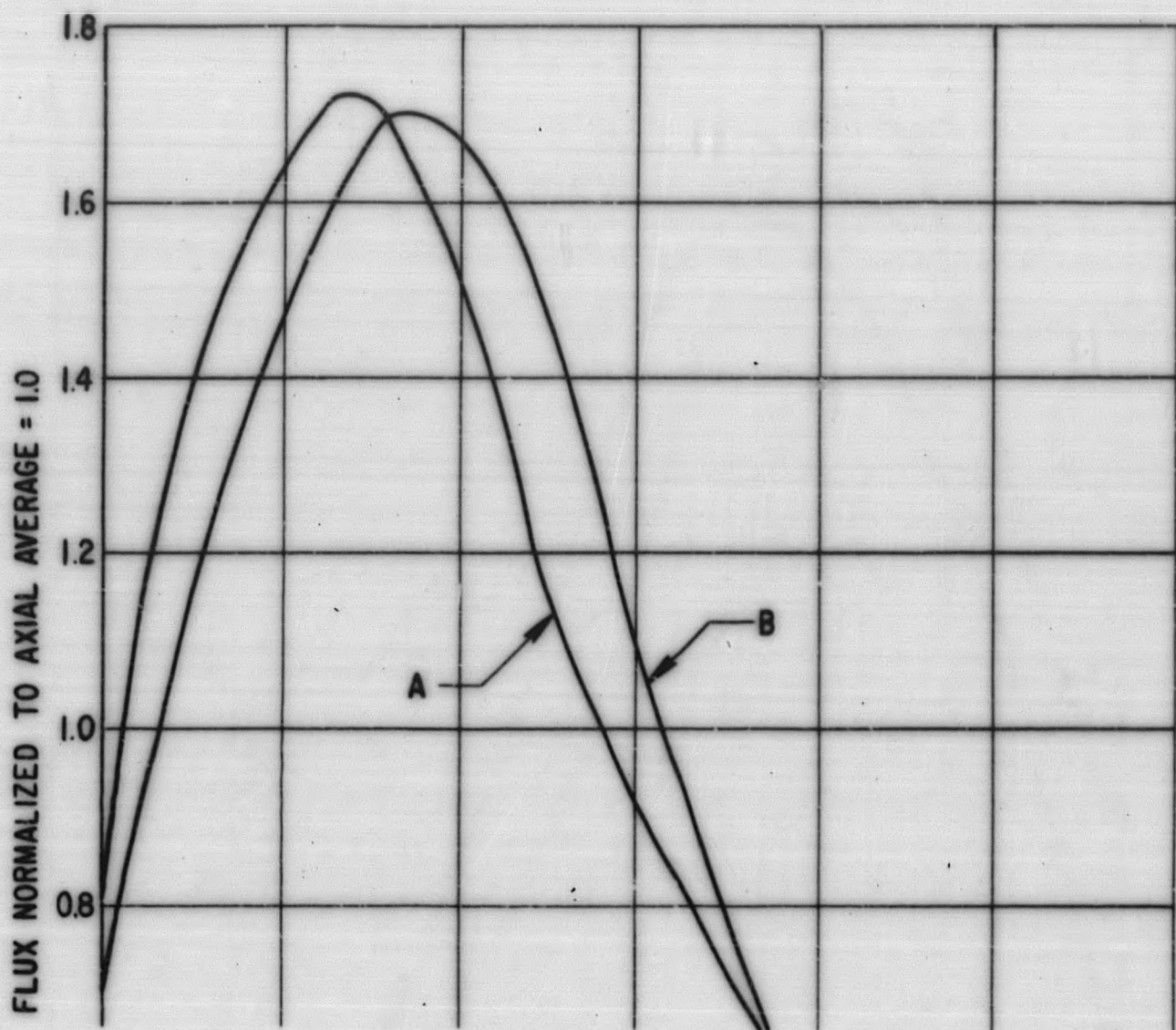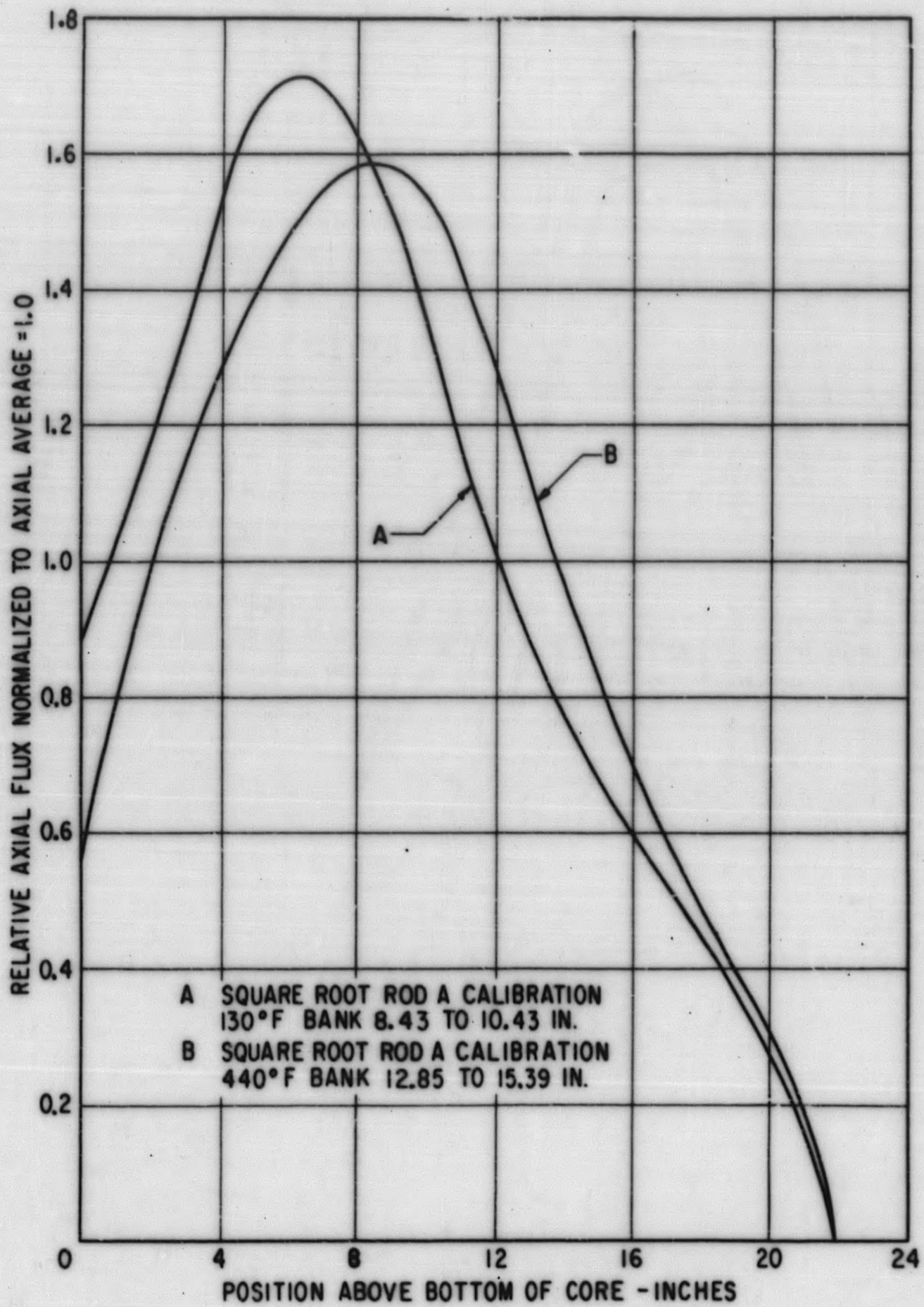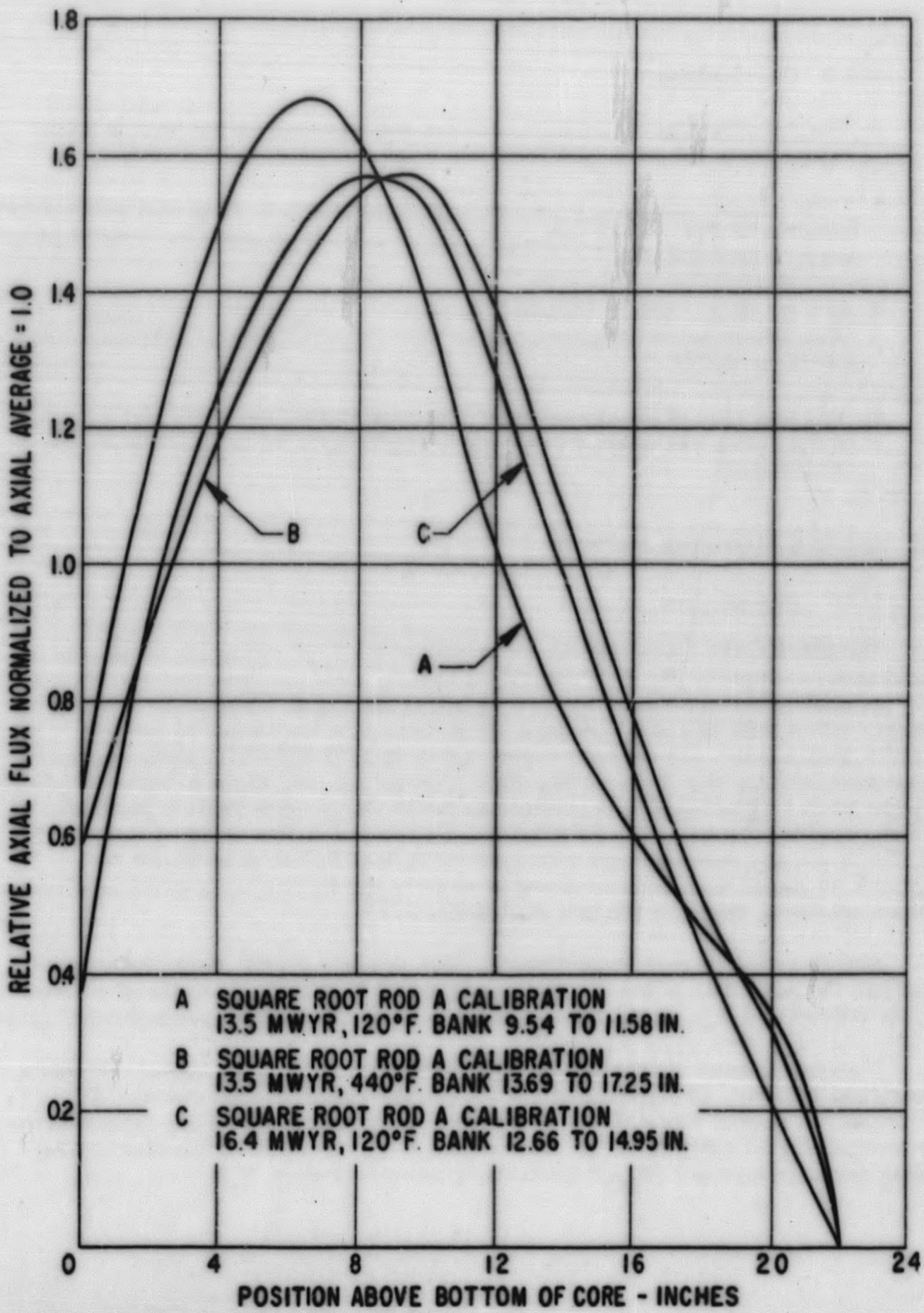
Figure 4.47. SM-1 Core I Axial Flux Distribution, 13.5 and 16.4 MWYR   4-81

4.8.3 Conclusions

1. The relative flux distribution curves indicate that as the bank is withdrawn from the core, the location of the flux peak moves upward.

2. Core temperature and core energy release seem to have only secondary effects, if any, on the flux peak location; the bank position being of primary importance.

3. At a constant energy release, the peak to average ratio decreased (flux distribution flattened) as the core temperature was increased from $120^{\circ}F$ to $440^{\circ}F$.

4. As a function of energy release, the peak to average ratio had a tendency to decrease; the scatter in the data prevented a more quantitative determination.

4.9 SOURCE MULTIPLICATION

4.9.1 Introduction

The SM-1 Core I was initially provided with a 15.5 curie Po-Be source (calibrated on January 25, 1957 and rated at 4.11×10^7 n/sec)and a 0.5 x 3 x 3 in. Be plate photoneutron source, located as shown on Fig. 2.1 and 2.2. The Po-Be source, with a half-life of 138.4 days, had decayed to less than 10 percent of its initial strength after 460 days; however, after about 2 MWYR reactor operation, the gamma activity due to fission product buildup was sufficient to make the photoneutron source significant with respect to the Po-Be source and the photoneutron source provided the neutrons for startup. At the end of life of SM-1 Core I, the old Po-Be source was replaced with a 45 curie dual Po-Be plus Sb-Be source.[4] Figure 4.48 shows a calculated curve of neutron production as a function of continuous operating time for the new dual source.[19]

Source multiplication experiments, test number A-312, were designed to establish the adequacy of the neutron sources and to provide a means of estimating the subcritical K_{eff} of the core at startup using the startup channel count rate.

If an extraneous source of neutrons, S neutrons/sec., is introduced into a subcritical reactor, the neutron flux will approach some steady value. If the reactor is nearly critical, the number of neutrons produced per second from the source is S directly from the source plus $S K_{eff}$ from the immediately preceding generation plus $S (K_{eff})^2$ from the generation before that, etc.; i.e.,
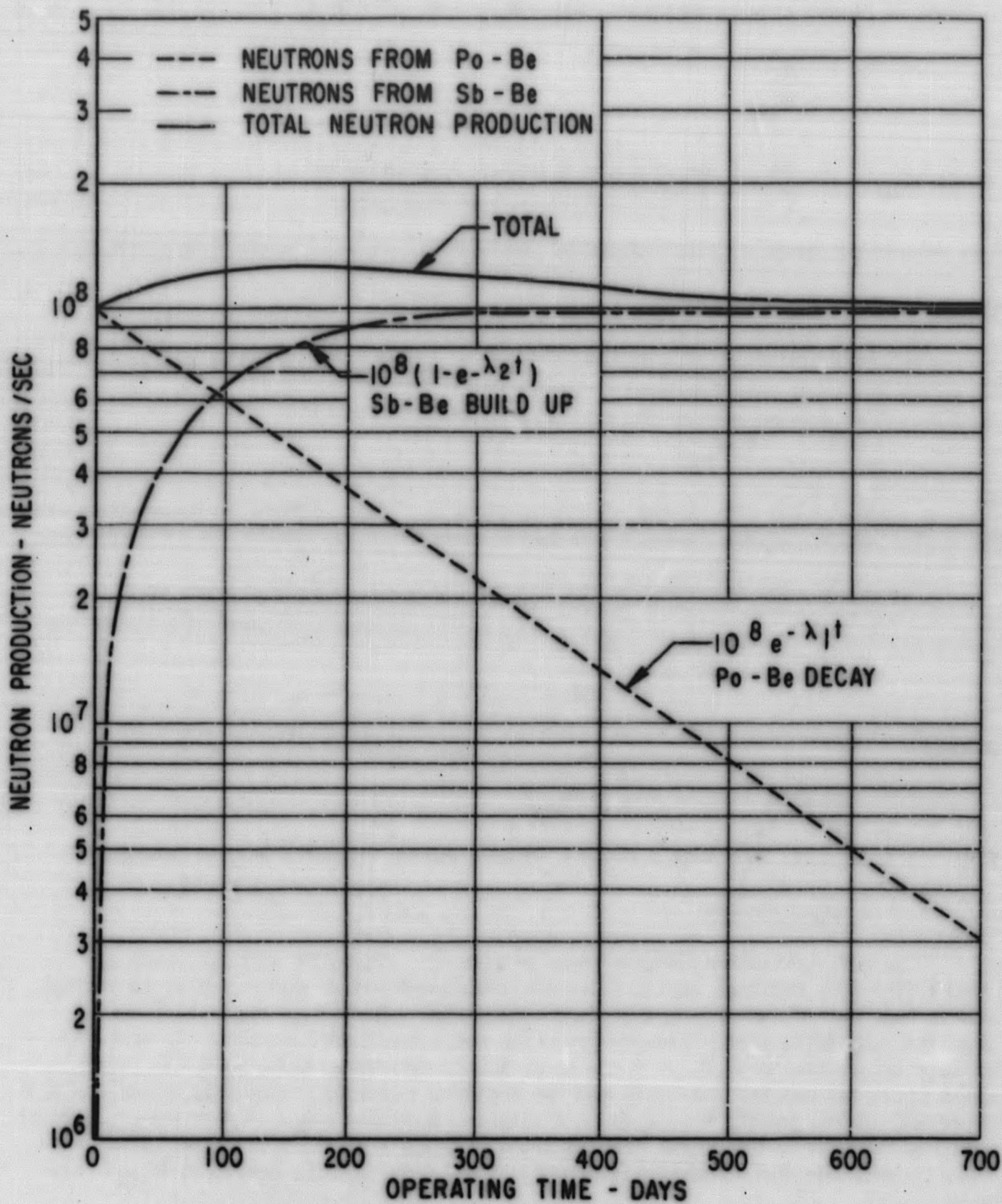
Figure 4.48. Neutron Production from Po-Be and Sb-Be Source as a Function of Operating Time

number of neutrons born per sec $+ S(1 + K_{eff} + K_{eff}^2 + K_{eff}^3 + \ldots\ldots)$

$$= \frac{S}{1-K_{eff}}$$

where $K_{eff} = \dfrac{\text{No. of neutrons born in } (n + 1) \text{ generation}}{\text{No. of neutrons born in } n \text{ generation}}$.

The source production is increased by the factor $\dfrac{1}{1-K_{eff}}$ by the sub-critical chain reaction.

The multiplication, M, of the subcritical reactor is defined as:

$$M = \frac{1}{1-K_{eff}} :$$

This is strictly true only if the source is distributed throughout the reactor in the same manner as the fissions are distributed when the reactor is critical.[20]

The count rate recorded on the startup channels is proportional to M.

$$C.R. = a \; M = \frac{a}{1-K_{eff}}$$

so that

$$\ln C.R. = \ln a - \ln (1-K_{eff})$$

which is a straight line with a slope of minus one on logarithmic coordinates.

4.9.2 Test Method

The test procedure followed was to achieve criticality with six rods as a bank (the five rod bank and previously calibrated rod A) and rod B at 19 inches. Rod A was then inserted stepwise and subcritical count rates recorded; the negative reactivity was evaluated from the rod A calibration curve. It was previously shown that $\ln C.R. = \ln a - \ln (1-K_{eff})$. Plotting the subcritical count rates from the startup channels and the negative reactivity* obtained when rod A is inserted, on log paper, we expect a straight line with a slope of minus one. Extrapolating the data to the count rate obtained with all rods fully inserted, it is possible to estimate the shutdown reactivity of the core and the shutdown K_{eff} of the core.

---

* When K_{eff} is close to one, the negative reactivity may be evaluated in terms of $1-K_{eff}$.

4.9.3 Experimental Results

Figures 4.49 through 4.54 present the source multiplication data obtained at 6.15, 7.22, 9.10, 12.1, 13.5 and 16.4 MWYR energy release, respectively. Startup channel count rate is shown plotted against $1-K_{eff}$. Figures 4.55 and 4.56 present the source multiplication data obtained at 16.4 MWYR for the Be photoneutron source alone without the old Po-Be source, and for the Be photoneutron source with the new dual Po-Be plus Sb-Be 45 curie source, respectively.

Table 4.24 summarizes the startup channel shutdown count rates and the shutdown K_{eff}, as estimated from Fig. 4.49 through 4.56 during core life.

It should be noted that the chamber response was not the same for all tests. The experimental conditions during burnup were varied by radiation effects on the chambers, changing of chambers, different electronic equipment, and changes in the discriminator level in the pulse amplifier and the high voltage applied to the chamber.

4.9.4 Worth of Rods A and B from Shutdown K_{eff} Data

The shutdown margin of the core as a function of core life was determined from Fig. 4.49 through 4.56 for the seven rod bank and the five rod bank, and is listed in Table 4.25. The difference in shutdown margin between the seven rod bank and the five rod bank is the worth of rods A and B and is also presented in Table 4.25 as a function of core life. Neglecting the data at 16.4 MWYR energy release, which shows considerable scatter, rods A and B are worth an average of $6.5 with an external probable error of $\pm$ $0.2. This corresponds to a worth of $6.6 + 2.2 for rods A and B as determined in section 4.5.6 from the integral worths of the five and seven rod banks.

4.9.5 Conclusions

1. It is noted that in some cases the slope of the best line drawn through the data points differs considerably from minus one. The following errors are inherent in this experiment:

   A. Loss of counts at high count rates in the counting system.

   B. Large statistical errors at low count rates.

   C. Gamma ray response of chambers was generally not known during most of these measurements.

   D. Source is not distributed throughout the reactor in the same manner as the fissions are when the reactor is critical.
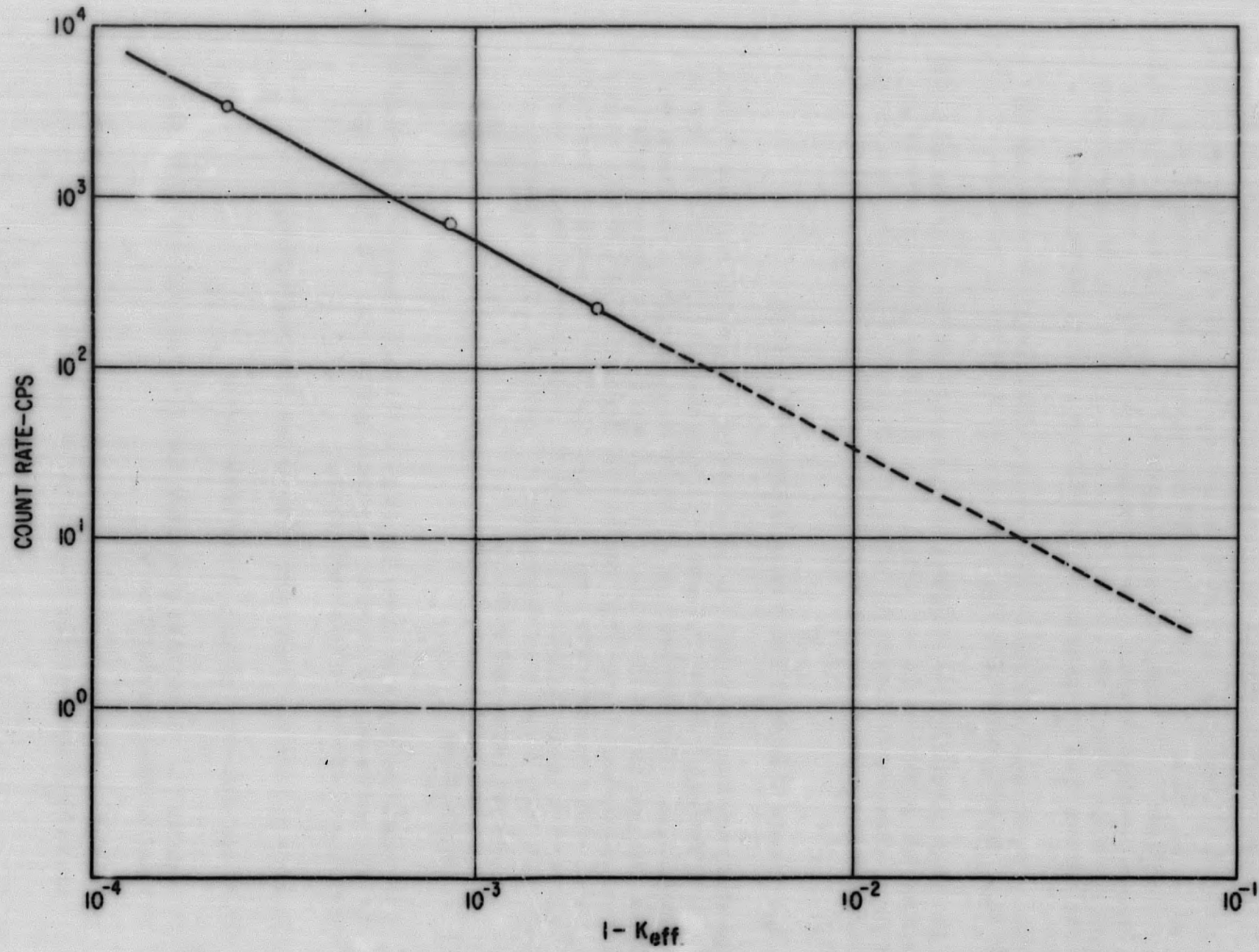
Figure 4.49. Startup Channel Count Rate as a Function of 1-K_{eff}, 6.15 MWYR, 110°F, 122 Hours after Shutdown, SM-1 Core I
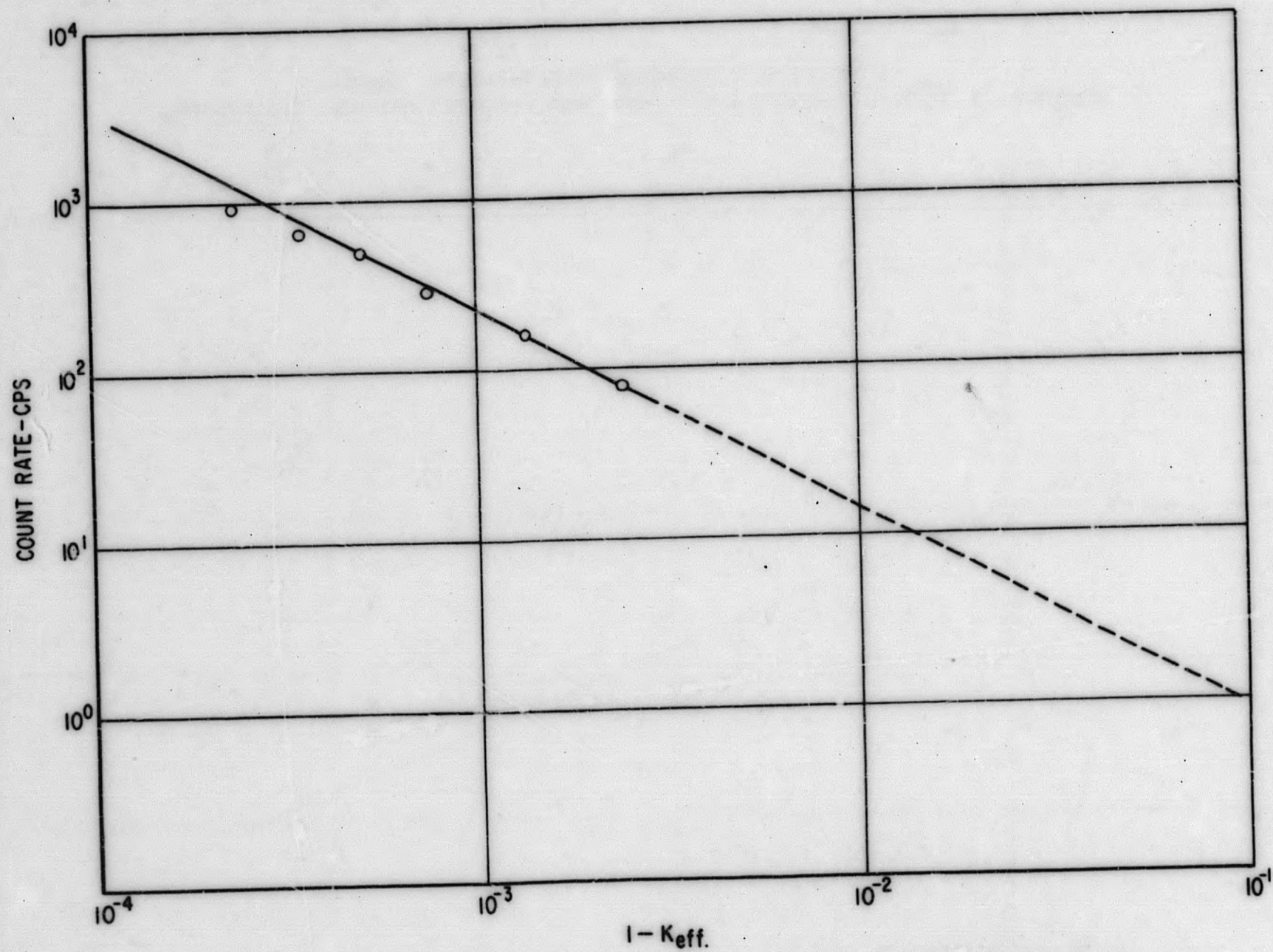
Figure 4.50. Startup Channel Count Rate as a Function of $1-K_{eff}$, 7.22 MWYR, $100^{O}F$, 156 Hours after Shutdown, SM-1 Core I
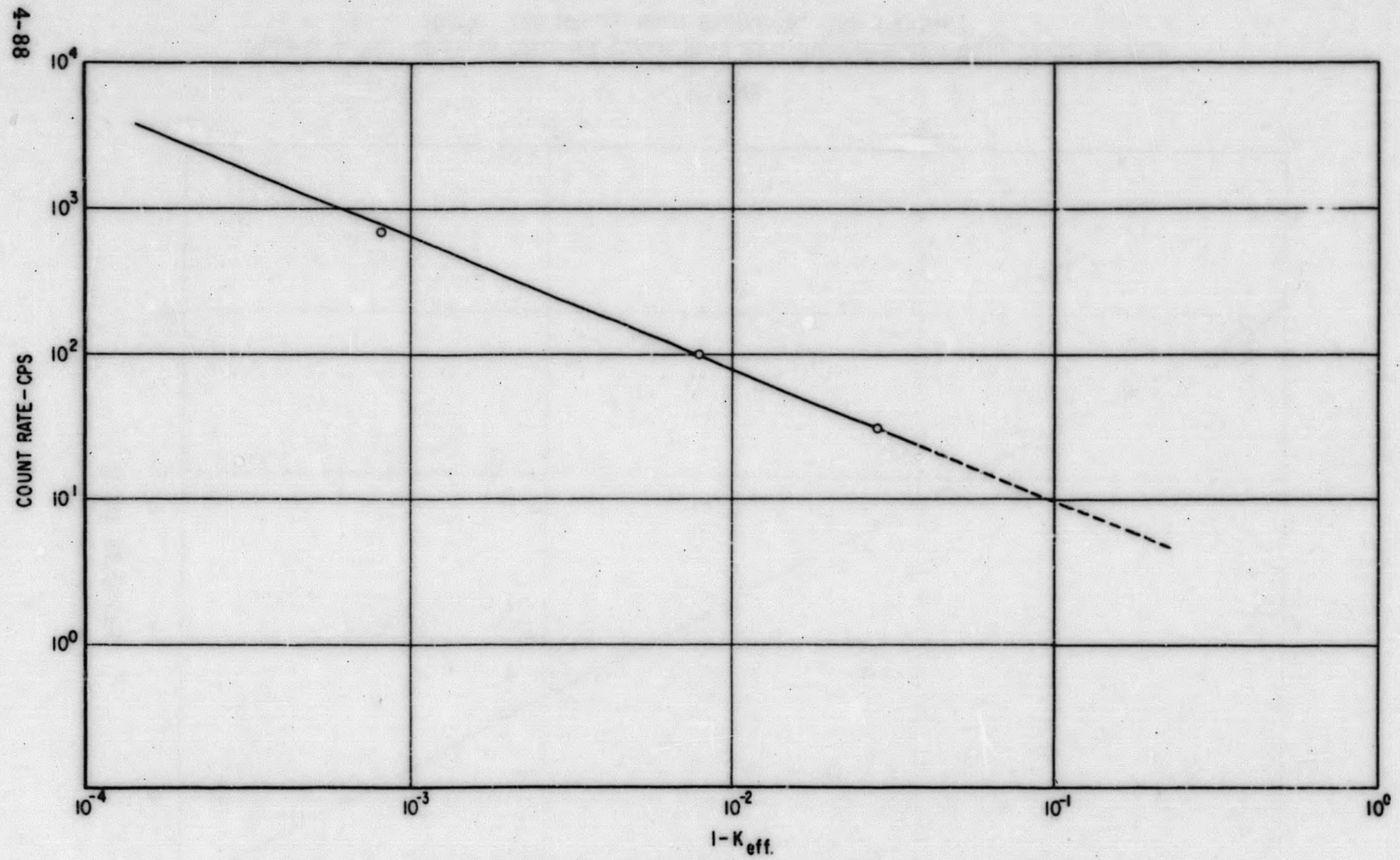
Figure 4.51. Startup Channel Count Rate as a Function of 1-K_{eff}, 9.10 MWYR, 115°F, 88 Hours after Shutdown, SM-1 Core I
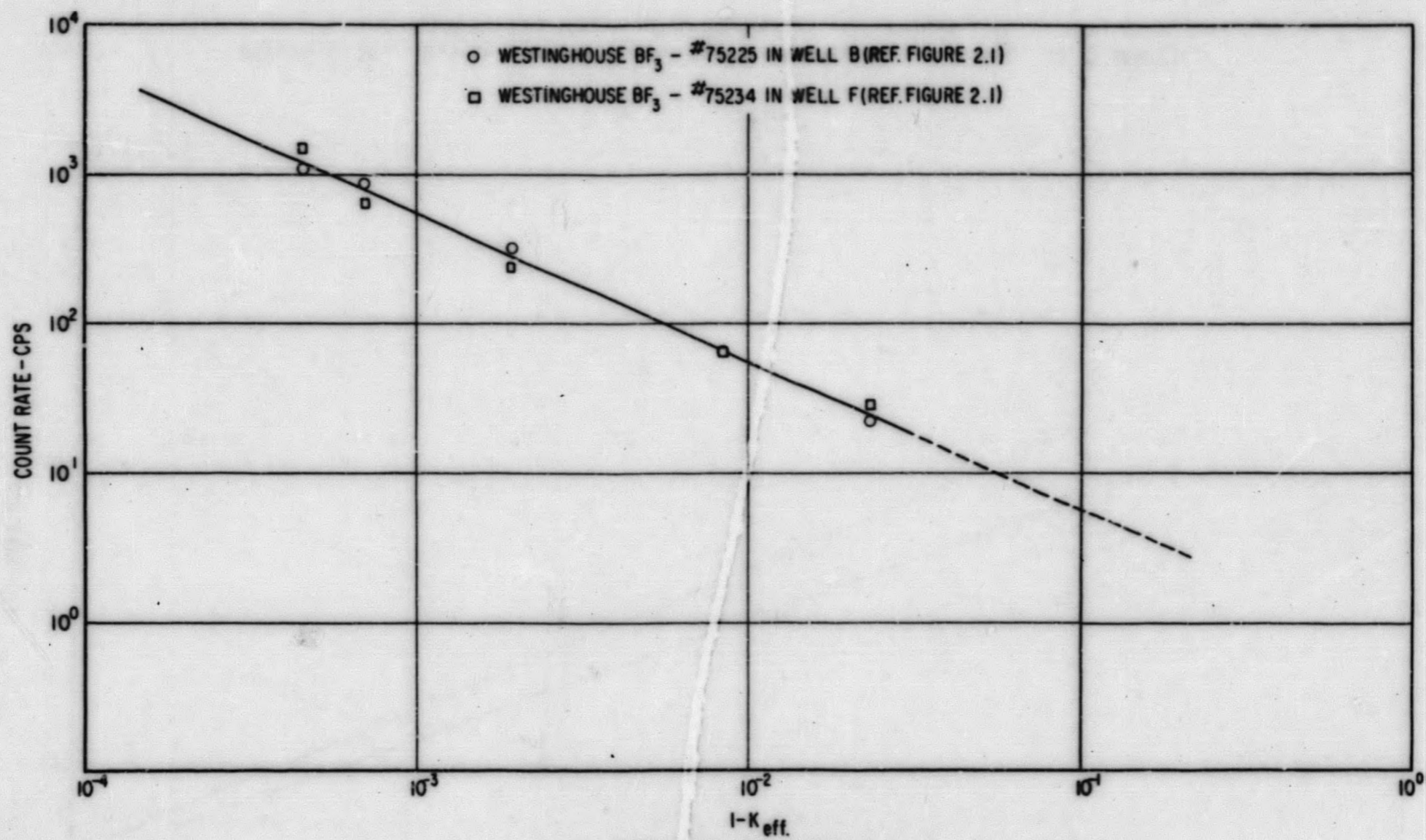
Figure 4.52. Startup Channel Count Rate as a Function of $1-K_{eff}$, 12.1 MWYR, 130°F, 97 Hours after Shutdown, SM-1 Core I
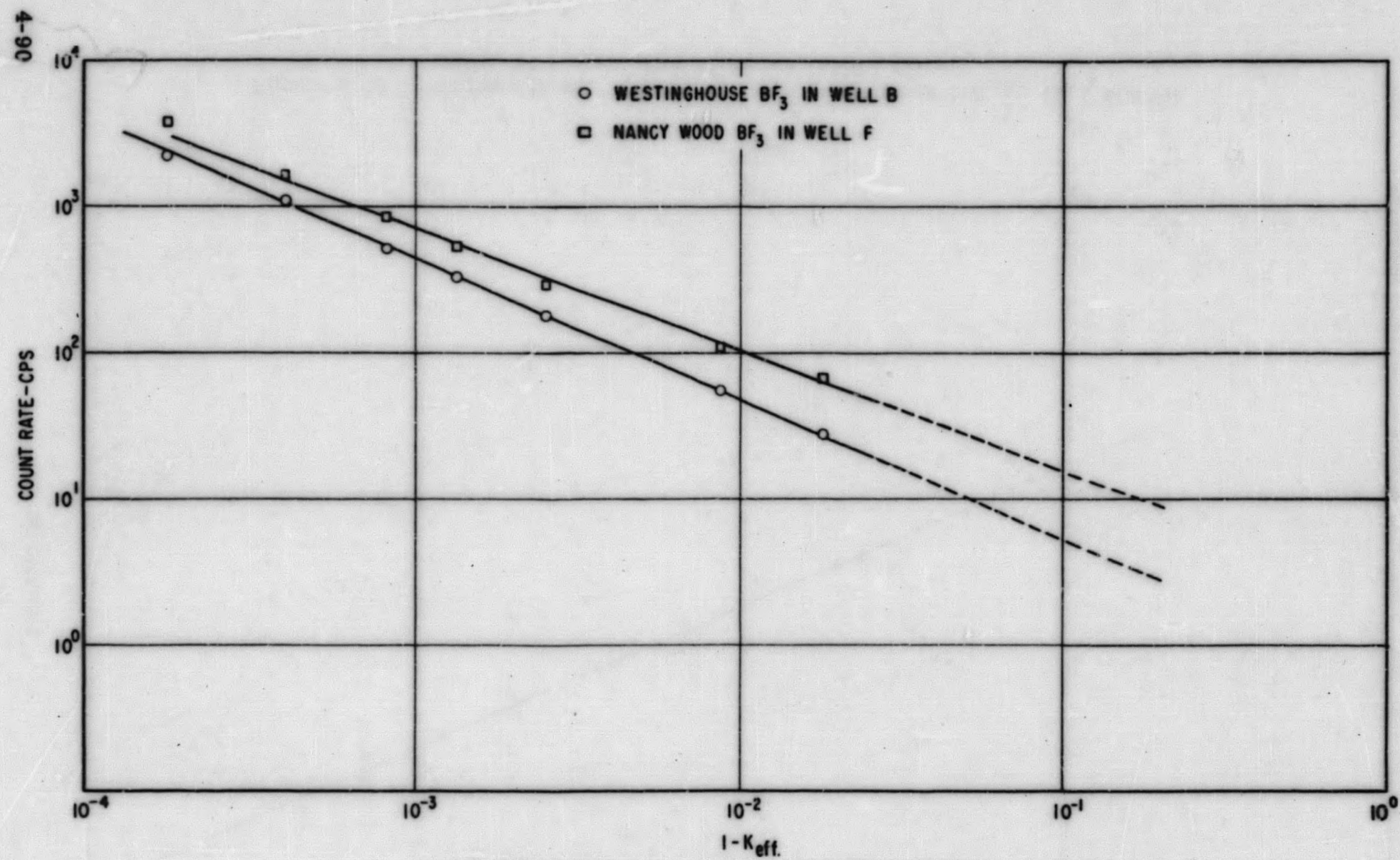
Figure 4.53.   Startup Channel Count Rate as a Function of 1-K_{eff}, 13.5 MWYR, 115°F, 111 Hours after Shutdown, SM-1 Core I
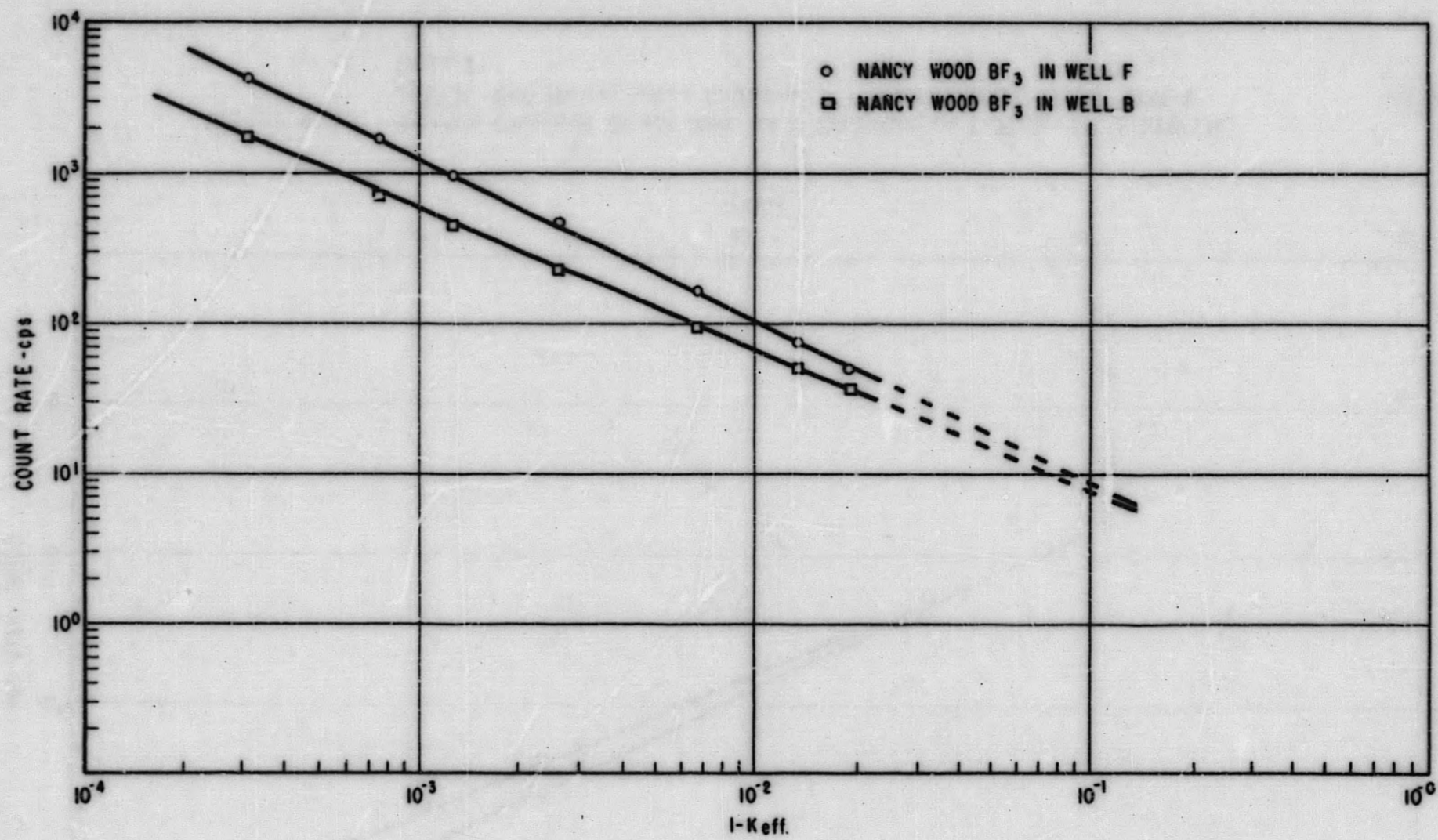
Figure 4.54. Startup Channel Count Rate as a Function of $1-K_{eff}$, 16.4 MWYR, $134^{\circ}F$, 240 Hours after Shutdown, SM-1 Core I
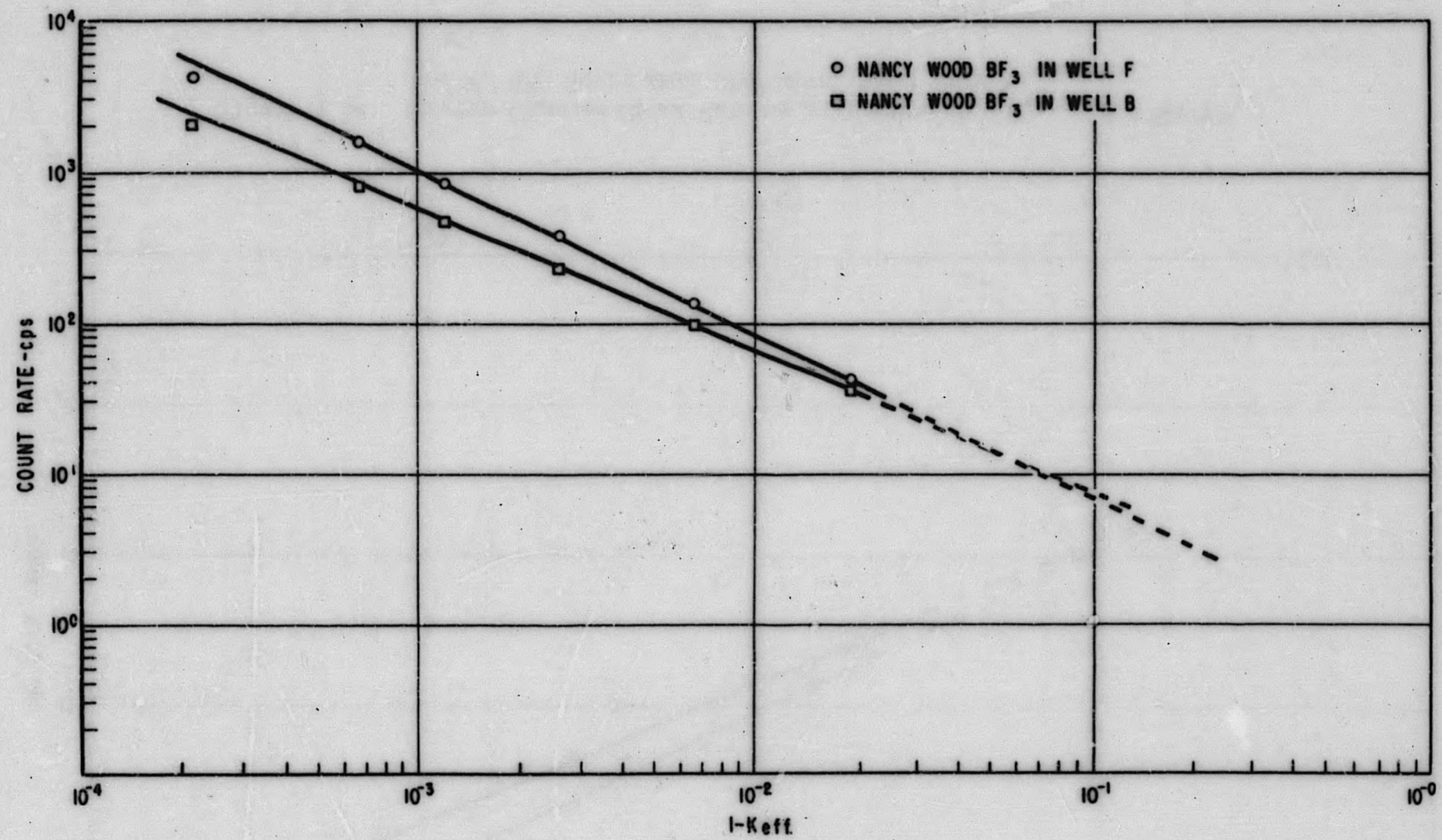
Figure 4.55. Startup Channel Count Rate as a Function of $1-K_{eff}$, 16.4 MWYR, 125°F, 240 Hours after Shutdown, Photoneutron Source, SM-1 Core I
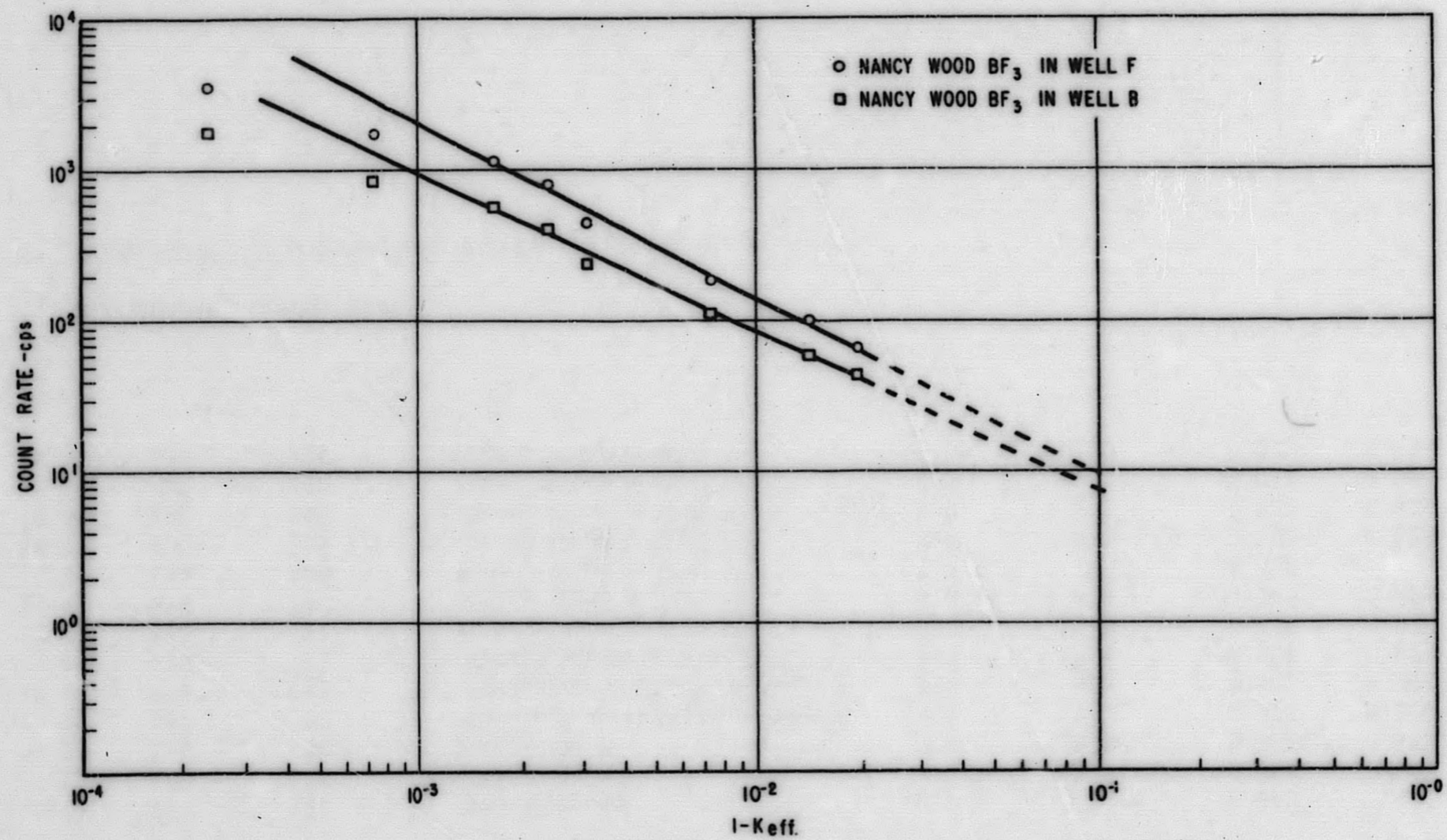
Figure 4.56.   Startup Channel Count Rate as a Function of $1-K_{eff}$, 16.4 MWYR, 135°F, 240 Hours after Shutdown, Photoneutron Source and New Dual Po Be-Sb Be Source, SM-1 Core I

TABLE 4.24
SHUTDOWN K_{eff} AND STARTUP CHANNEL COUNT RATES, SM-1 CORE I

Energy Release MWYR	Temp. °F	Time After Shutdown Hours	BF₃ Chamber Identification	Count Rate CPS		Shutdown K_{eff}	
				All Rods Inserted	5 Rod Bank Inserted A&B at 19 in.	All Rods Inserted	5 Rod Bank Inserted A&B at 19 in.
6.15	110	122	Westinghouse	4.0	-	0.942	-
7.22	100	156	Westinghouse	1.4	3.5	0.929	0.967
9.10	115	88	Nancy Wood	7.8	13.5	0.880	0.932
12.1	130	97	Westinghouse #75225 in Well B	4.4	7.0	0.872	0.920
12.1	130	97	Westinghouse #75234 in Well F	5.3	9.8	0.895	0.944
13.5	115	111	Westinghouse in Well B	4.2	6.5	0.875	0.921
13.5	115	111	Nancy Wood in Well F	13.0	20.0	0.875	0.926
16.4	134	240	Nancy Wood in Well B	3.6	9.5	0.780	0.921
16.4	134	240	Nancy Wood in Well F	7.4	-	0.885	-
16.4*	125	240	Nancy Wood in Well B	7.5	10.0	0.902	0.928
16.4*	125	240	Nancy Wood in Well F	3.0	5.3	0.790	0.876
16.4**	135	240	Nancy Wood in Well B	8.5	11.0	0.914	0.933
16.4**	135	240	Nancy Wood in Well F	12.5	15.0	0.922	0.934

*   Photoneutron source alone

**   Photoneutron source and new dual Po-Be plus Sb-Be source.

TABLE 4.25
FIVE AND SEVEN ROD BANK SHUTDOWN MARGIN AND WORTH OF RODS A AND B AS ESTIMATED FROM SHUTDOWN K_{eff} DATA, SM-1 CORE I[+]

Energy Release, MWYR	Seven Rod Bank Shutdown Margin, Dollars	Five Rod Bank Shutdown Margin, Dollars	Worth of Rod A & B, Dollars
6.15	8.3	---	---
7.22	10.0	4.8	5.2
9.10	16.8	9.7	7.1
12.1	18.1	11.5	6.6
12.1	14.9	8.2	6.7
13.5	17.5	11.2	6.3
13.5	17.5	10.5	7.0
16.4	30.7	11.4	19.3
16.4	16.3	---	---
16.4*	13.9	10.3	3.6
16.4*	29.3	17.5	11.8
16.4**	12.4	9.8	2.6
16.4**	11.3	9.6	1.7

+ All values corrected to temperature of 70°F.
* Photoneutron source alone.
** Photoneutron source and new dual Po-Be plus Sb-Be source.

    E. Chambers are partially in direct line of sight of the source; this is especially true of the chamber in well F (reference Fig. 2.1 and 2.2).

    F. Changes in chambers, core conditions, and chamber pulse height and high voltage over the lifetime of the core prevent comparisons of measurements made during burnup.

2. Because of the large spread in the data and the inherent experimental errors, it is not possible to ascertain the effect on K_{eff} of core burnup. However, the source multiplication data does provide an estimate to the subcritical K_{eff} of the core at various startup channel count rates, at the particular time at which the calibration of count rate versus negative reactivity is performed.

3. The shutdown rate data at 16.4 MWYR energy release seems to be erratic and should be disregarded. Evaluation of the 16.4 data at higher count rates shows that the removal of the old Po-Be source did not change the count rate, Fig. 4.54 and 4.55 indicating that all neutrons were from the Be photoneutron source. The addition of the new 45 curie dual source

resulted in an increase in count rate by a factor of two to three, Figs.
4.55 and 4.56.

4. Examination of the five and seven rod bank shutdown margin data, dis-
regarding the 16.4 MWYR data, shows an increase in shutdown margin
with core burnup. A more conclusive evaluation being prevented by the
relatively large experimental uncertainties.

5. The worth of rods A and B seems to remain constant during core life
with an average value of $6.5 ± 0.2. This is in agreement with the
value of $6.6 determined in Section 4.5.6.

4.10 ADDITIONAL MEASUREMENTS

4.10.1 Xenon Override by Temperature Compensation

The xenon override by temperature compensation experiment, test number
A-320, was designed to determine the minimum amount of time required for re-
turn to normal full power operation from peak xenon concentration near the end
of SM-1 Core I life.[4] The reactor was run continuously at full power for 129.07
hr to buildup equilibrium xenon concentration before the reactor was scrammed.
Peak xenon concentration was allowed to build up, and 7 hr 13 min after the scram,
the rods were raised to approach criticality. Criticality was achieved 7 hr 41 min
after scram with a core outlet temperature of 307°F and approximately peak xenon
concentration (approximately 8 hr after shutdown) in the core. Full power of 2050
gross kwe was produced 4 hr 44 min after going critical at peak xenon concentra-
tion. This compares with a time of approximately 12 hr (20-8 hr, see section 4.7)
in allowing peak xenon to decay to equilibrium xenon concentration. Figures 4.57
through 4.59 show the power output, reactor outlet temperature, and five rod bank
position as a function of time after criticality, respectively.

Up to three hours after criticality, no significant power was generated beyond
that required for heatup. The bank was full out at 3-1/2 hr after criticality and
the reactor was at rated power 4.7 hr after criticality.

4.10.2 Danger Coefficient

Test number A-319, was designed to determine the danger coefficient as-
sociated with the insertion of a new SM-1 Core I elements into the burned out
Core I. This experiment was performed at 16.4 MWYR energy release during the
Core I end of life physics measurements.[4]

Critical rod positions were recorded for the original core configuration, for
a fresh SM-1 Core I element in position 62, for a fresh SM-1 Core I element in po-
sition 35, and for a SM-1 Core I fresh element in position 16. The change in re-
activity between the original core configuration and the configurations with the
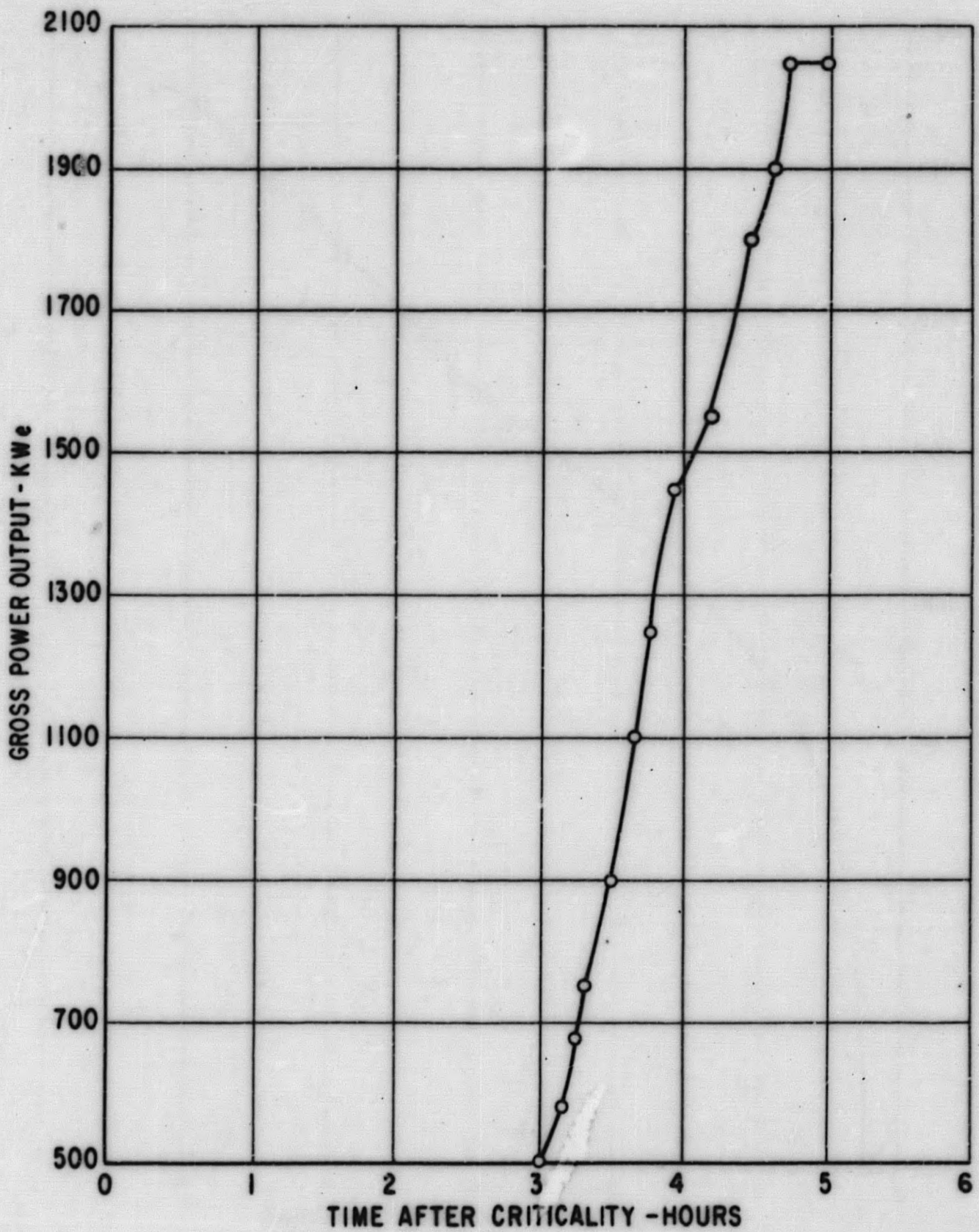
Figure 4.57.   Gross Power Output Vs. Time after Criticality, SM-1 Core I
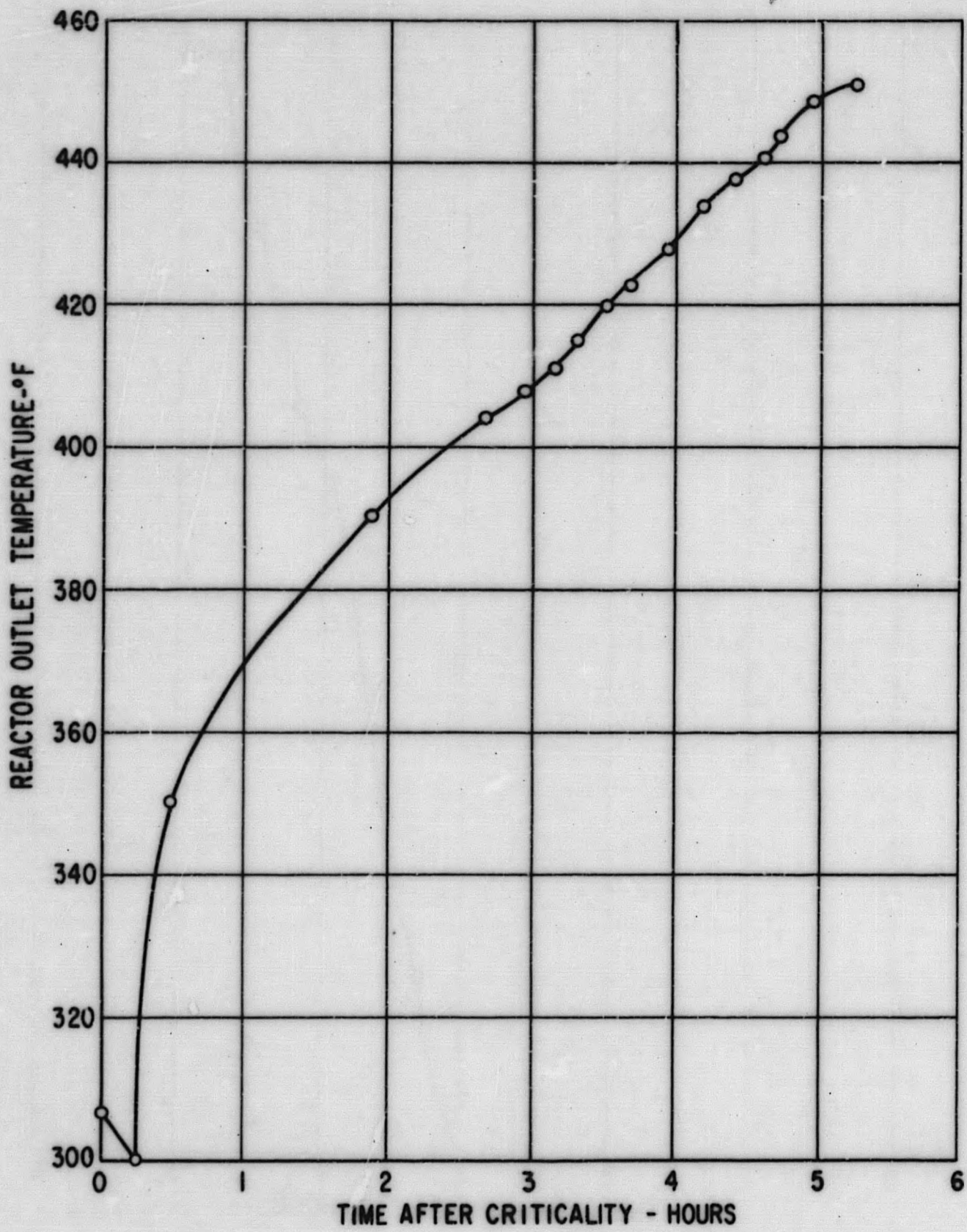
Figure 4.58.   Reactor Outlet Temperature Vs. Time after Criticality, SM-1 Core I
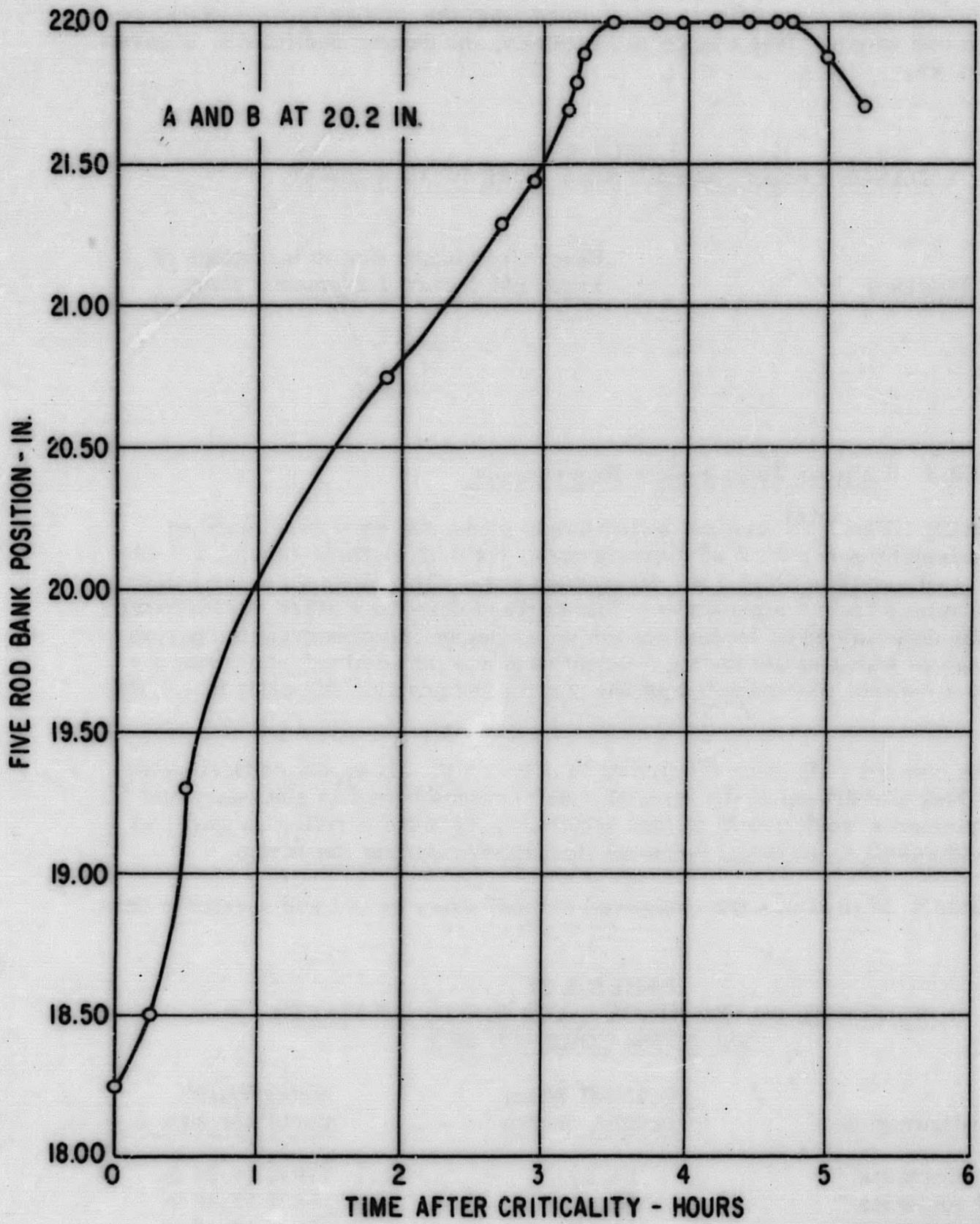
Figure 4.59.   Five Rod Bank Position Vs. Time after Criticality, A and B at 20.2 Inches, SM-1 Core I

fresh SM-1 element inserted was determined from the change in rod critical position and rod worth. This change in reactivity, the danger coefficient, is given in Table 4.26.

TABLE 4.26
DANGER COEFFICIENT SM-1 CORE I - 16.4 MWYR

Element Position	Reactivity Change due to Insertions of Fresh SM-1 Core I Element - Cents
62	+ 47.9
35	+ 94.7
16	+ 11.0

4.10.3 Critical Water Height Experiments

During ZPE-2[14] critical water height measurements were made on 5 x 5 21 element core, 5 x 5 25 element core, 6 x 6 32 element core, 7 x 7 44 element core, and the SM-1 7 x 7 45 element core. The absolute water height was determined from a sight glass. The worth of the water at the critical water height was determined by increasing the water height and observing the period. The change in water height during a calibration was determined by a probe attached to a control rod and noted on the control rod position indicator to ± 0.002 inches.

The control rods were withdrawn to only 0.5 in. above the critical water height. Full withdrawal of the control rods to align the fuel in stationary and control elements would result in fuel addition to the bottom reflector upon rod scram and result in an initial increase in reactivity during the scram.

Table 4.27 presents the measured critical water height and reactivity data.

TABLE 4.27
CRITICAL WATER HEIGHT AND WORTH OF WATER
SM-1 ZPE CORE, [14] 68°F

Core Configuration	Critical Water Height, Inches	Water Worth, Cents per Inch
5 x 5 21 elements	14.20	119 @ 14.26 in.
5 x 5 25 elements	12.41	156 @ 12.46 in.
6 x 6 32 elements	10.12	251 @ 10.16 in.
7 x 7 44 elements*	8.82	329 @ 8.85 in.
7 x 7 45 elements	8.64	---

* Position 47 missing

4-100

The equivalent bare core K_{eff} equation can be approximated by the expression,[21]

$$K_{eff} = \frac{k_\infty}{1 + M^2 B^2}$$

(1)

where k_∞ = infinite multiplication constant

M^2 = migration area

The water worth at critical water height is[22]

$$\frac{\Delta \rho}{\Delta h} = \frac{2 \pi^2 M^2}{k_\infty} \frac{1}{(h + S_z)^3}$$

(2)

where h = critical water height

S_z = total axial reflector savings

This relationship indicates that the reactivity worth is a unique function of $h^{-1/3}$ which is independent of the K_{eff} of the core if

$\frac{M^2}{k_\infty}$ and S_z are not functions of core height.[12]

Since the worth is a unique function of $h^{-1/3}$ it is possible to plot the reciprocal cube root of the worth, $(\Delta \rho / \Delta h)^{-1/3}$, as a linear function of the height,

$$\left(\frac{d\rho}{dh}\right)^{-1/3} = \left(\frac{2\pi^2 M^2}{k_\infty}\right)^{-1/3} (h + S_z).$$

Figure 4.60 presents the reciprocal cube root of the worth data as a function of the height. The curve shown was obtained by a least squares linear fit to the data. The slope of the curve is equal to

$$\left(\frac{2\pi^2 M^2}{k_\infty}\right)^{-1/3}$$ and the intercept is equal to S_z.

The excess reactivity was obtained by integrating equation (2) from the critical water height h_c, to the 22 in. water height condition. Thus

$$\rho = \frac{1}{2} \left(\frac{2\pi^2 M^2}{k_\infty}\right) \left[\frac{1}{(h_c + S_z)^2} - \frac{1}{(22 + S_z)^2}\right]$$

4-101
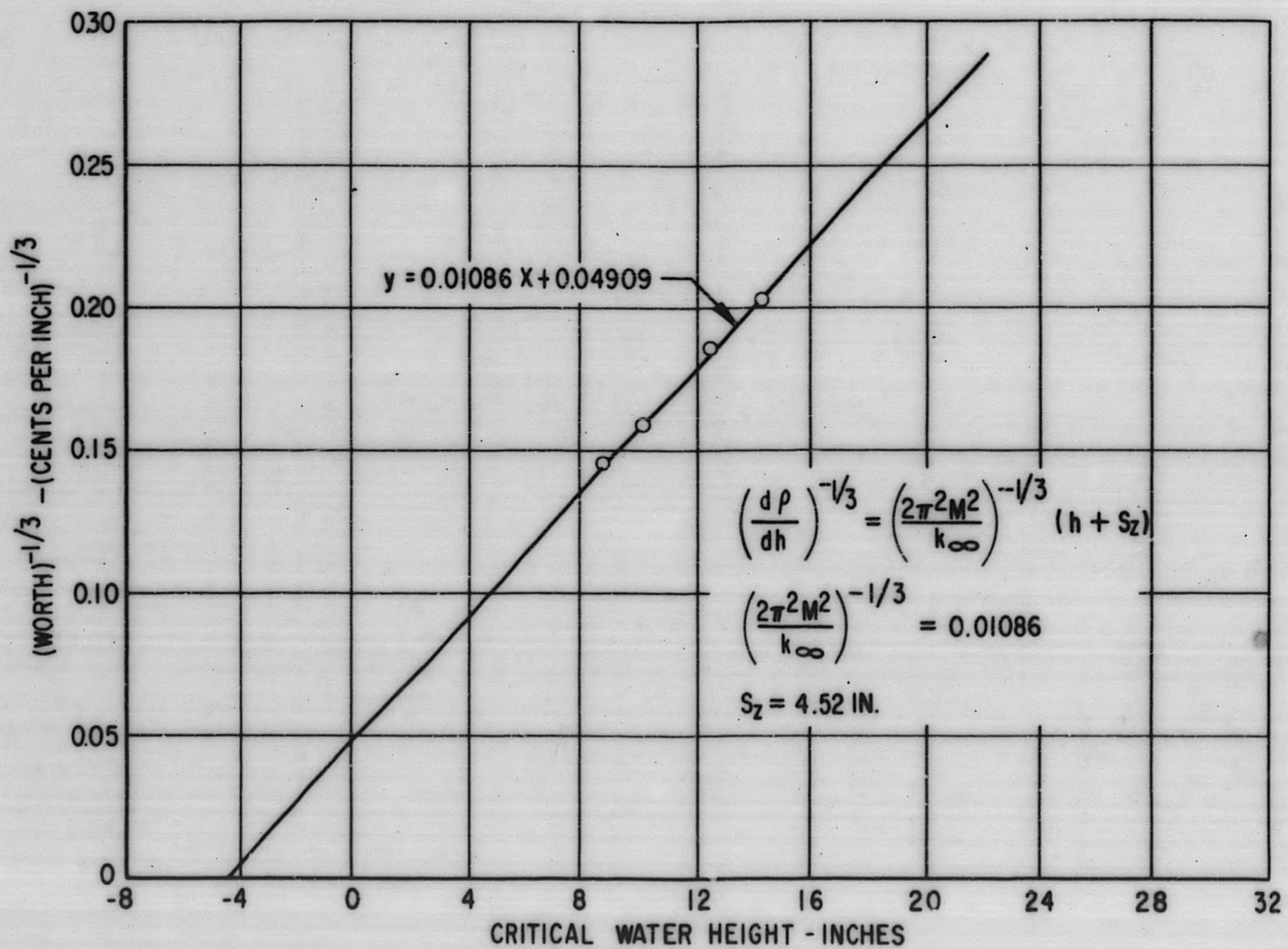
Figure 4.60. Water Height Worth, SM-1 ZPE-2, 68°F

where $\dfrac{2\pi^2 M^2}{k_\infty}$ and S_z were determined from Fig. 4.60.

The excess reactivity was found to be $17.2 using the above method. This is considerably lower than the value of $23.8 obtained by integrating the five rod bank calibration curve from the cold clean critical bank position to 22 in. Other than possible inadequacies in the model, this deviation may be due partially to the following factors:

1. The total axial reflector savings as determined from the critical water height measurements is for a water and steel bottom reflector and an air, fuel and steel top reflector. The actual core with the rods out has an active height of 22 in. and the same water and steel bottom reflector, however, the top reflector is water, steel and portions of the absorber section. This indicates that the total axial reflector savings for the 22 in. water height would be higher, which in turn means a higher excess reactivity.

2. The critical water height and water worth measurements were made as a function of core size by varying the core radius.

Further work is necessary to adequately resolve the difference in excess reactivity determined by critical water height measurements and integration of the five rod bank calibration curve.

5.0 CORE PHYSICS MEASUREMENTS ON SM-1 REARRANGED AND SPIKED CORE I

5.1 INTRODUCTION

Following the physics measurements performed at the end of Core I life, the core was shutdown rearranged and spiked as shown in Fig. A.3. The initial operation of the reactor resulted in a significant increase in the fission product concentration in the primary coolant of the SM-1. The core was shutdown and the release of fission products localized to the PM-1-M element. This element was then removed and the core arranged as shown in Fig. A.4. Operation was continued till April 11, 1961, for a total Core I energy release of 18.0 MWYR. At this time, the core was arbitrarily shutdown for changeover to Core II.

5.2 STARTUP PHYSICS MEASUREMENTS ON THE INITIAL SM-1 REARRANGED AND SPIKED CORE I

5.2.1 Introduction

The startup physics measurements on the initial SM-1 Rearranged and Spiked Core I (Fig. A.3) consisted of tests A-305, A-306, A-308, A-309, A-312, A-315 and A-316 integrated into an operating procedure to provide a systematic sequential testing program.

5.2.2 Five Rod Bank Positions

The critical positions of the five rod bank at the hot and cold, low xenon conditions were measured and are tabulated in Table 5.1.

TABLE 5.1

FIVE ROD BANK POSITIONS FOR VARIOUS CORE CONDITIONS
Initial SM-1 Rearranged and Spiked Core I (Fig. A.3)
16.5 MWYR

Core Conditions	Five Rod Bank Critical Position - inches
Low Xenon, 70°F, A and B at 19"	8.31*
Low Xenon, 195°F, A and B at 19"	8.91
Low Xenon, 200°F, A and B at 19"	8.94
Low Xenon, 437°F, A and B at 19"	12.55
Low Xenon, 440°F, A and B at 19"	12.62*
Low Xenon, 442°F, A and B at 19"	12.67

* Corrected for temperature.

5.2.3 Control Rod Calibrations

Control Rod A and the two rod bank (rods A and B) were calibrated as a function of the five rod bank position at 199°F and 435°F, respectively. Tables 5.2 and 5.3 and Figs. 5.1 and 5.2 summarize these data.

TABLE 5.2
CONTROL ROD A CALIBRATION AT LOW XENON, 199°F
Initial SM-1 Rearranged and Spiked Core I (Fig. A.3)
16.5 MWYR

Rod A Position, Inches	Rod A Worth, Cents per Inch	Five Rod Bank Position, Inches
2.98	25.73	11.49
6.05	37.86	10.70
6.63	41.54	10.54
7.35	38.96	10.33
9.46	30.22	9.85
11.10	22.28	9.60
13.56	14.75	9.35
16.58	10.28	9.15

TABLE 5.3
CONTROL ROD A AND B BANK CALIBRATION AT LOW XENON, 435°F
Initial SM-1 Rearranged and Spiked Core I (Fig. A.3)
16.5 MWYR

Rod A and B Position, Inches	Rod A and B Worth, Cents per Inch	Five Rod Bank Position, Inches
8.91	90.00	22.00
10.18	108.57	17.22
12.18	66.74	14.82
14.50	47.37	13.50
16.59	26.54	12.90
18.23	19.00	12.53

Figure 5.3 presents the integral worth of rod A as a function of position at 199°F. The total integral worth of rod A is $4.30 with an estimated uncertainty of ± $0.30. This represents an increase in rod A worth of approximately $1.1 over the integral worths of rod A cold measured during the original SM-1 Core I life and reported in Table 4.8.
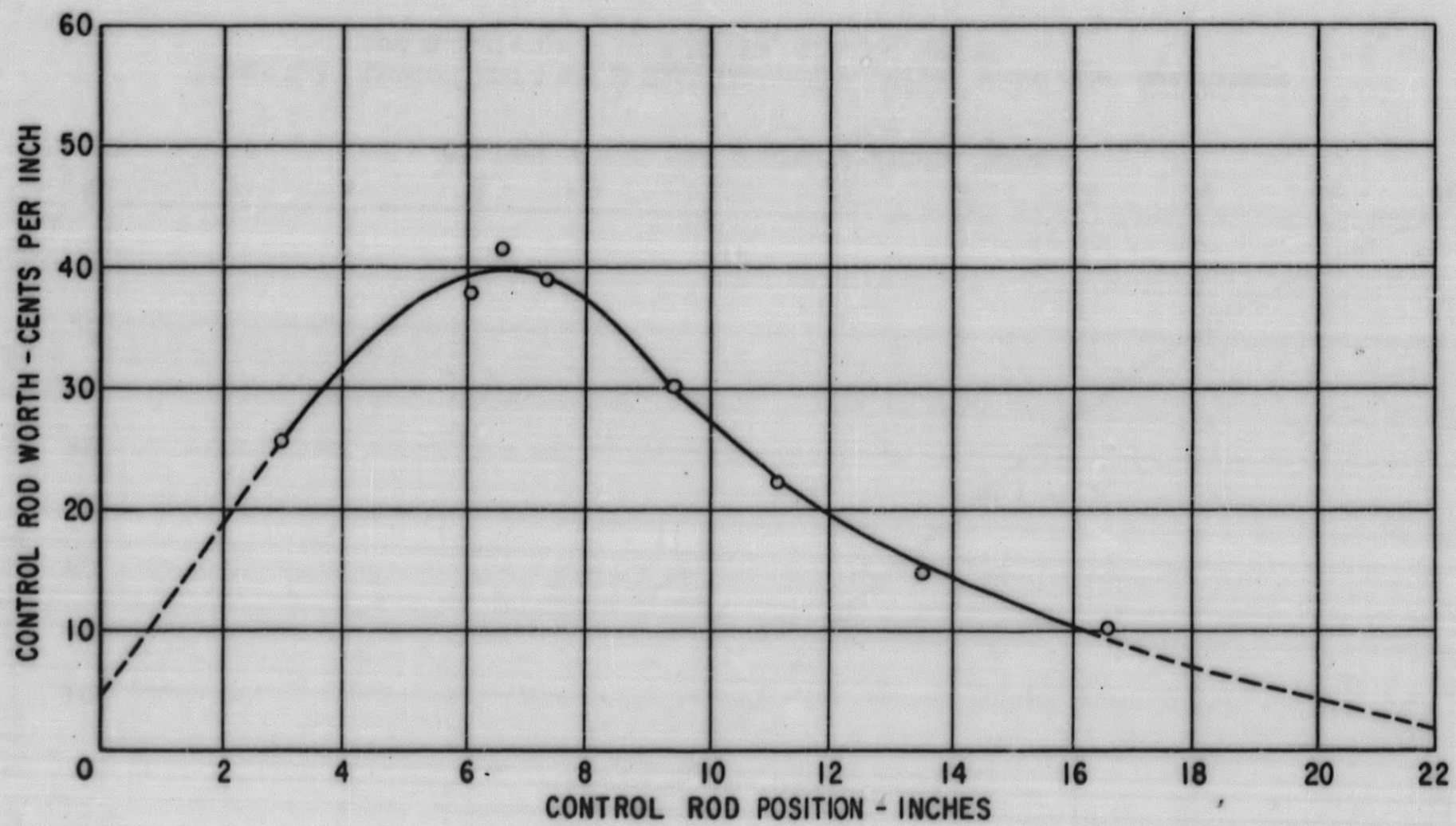
Figure 5.1. Control Rod A Calibration Curve, Initial SM-1 Rearranged and Spiked
Core I, 16.5 MWYR, Low Xe, 199°F
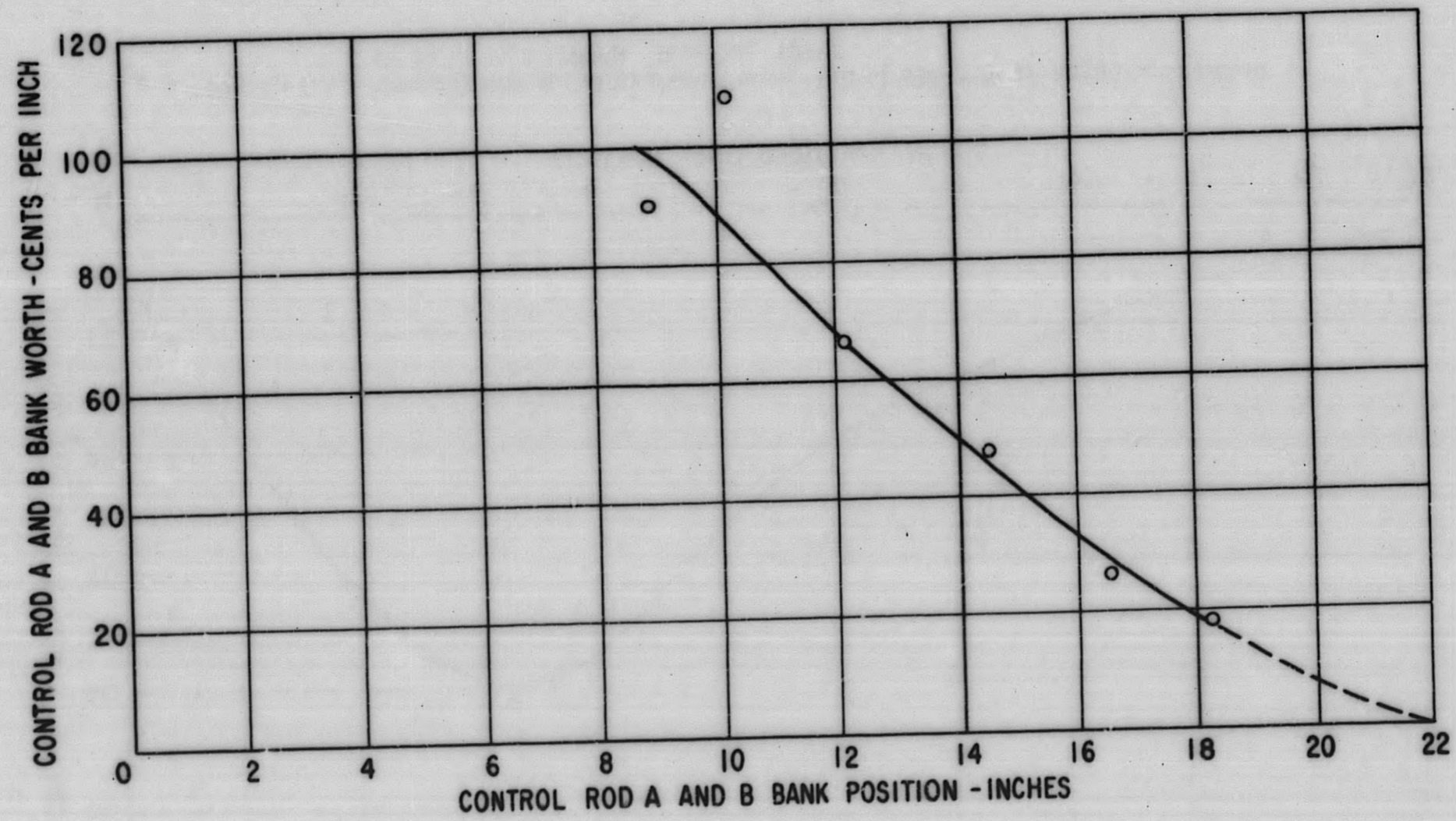
Figure 5.2. Control Rod A and B Bank Calibration Curve, Initial SM-1 Rearranged and Spiked Core I, 16.5 MWYR, Low Xe, 435°F
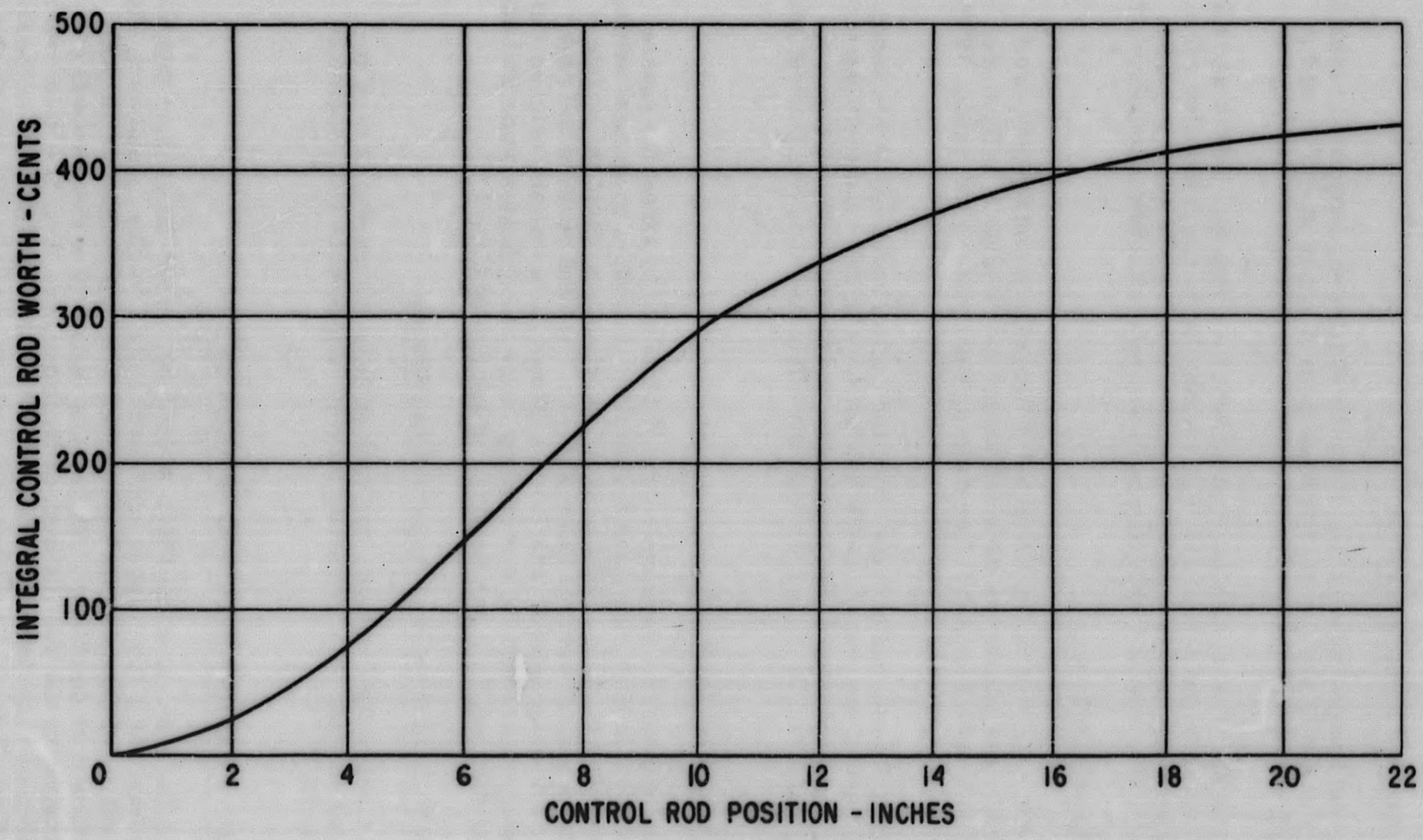
Figure 5.3. Control Rod A Integral Worth, Initial SM-1 Rearranged and Spiked Core I, 16.5 MWYR, 199°F, Low Xe

5.2.4 Five Rod Bank Calibration

The five rod bank calibration was determined from the integrated reactivity values of rod A at 199°F and the two rod bank (rods A and B) at 435°F, and is shown in Fig. 5.4.

The data at 435°F is in good agreement with the composite ZPE-1 and CE-1 calibration curve while the data at 199°F is slightly below the calibration curve. The lower temperature data is expected to show a lower worth since rod A has been indicating a decrease in worth corresponding to a decrease in temperature.

5.2.5 Excess Reactivity

The excess reactivity of the initial SM-1 Rearranged and Spiked Core I was determined by integrating the bank calibration curve (Fig. 5.4) from the critical bank position to 22 inches. The excess reactivities at low xenon, 70°F, and low xenon, 440°F are $12.9 and $5.7, respectively.

At 16.4 MWYR, the end of Core I life, the excess reactivity at low xenon, 70°F was $10.2 and at low xenon, 440°F was $3.4. The difference between the excess reactivities at startup of the rearranged and spiked core and at end of life of the original core, $2.7, is the reactivity effect due to rearrangement and spiking.

5.2.6 Axial Flux Distribution

The relative axial flux distribution was determined by taking the square root of the rod A calibration curve and normalizing the values to an axial average of unity as shown in Fig. 5.5. The flux peak occurs 6.5 in. from the bottom of the core and has a peak to average value of 1.53. The bank position and peak location values are in agreement with Table 4.23 and fit in with the original Core I values. The peak-to-average ratio is slightly lower and indicates some flattening of the axial flux distribution in the Rearranged and Spiked Core I.

5.2.7 Effects of Core Rearrangement and Spiking

Table 5.4 shows the reactivity and bank position effects due to core rearrangement and spiking. The reactivity increase due to core rearrangement and spiking was $2.7.

5.3 FINAL SM-1 REARRANGED AND SPIKED CORE I

Following the removal of the PM-1-M element, an SM-2A element was inserted and the final SM-1 Rearranged and Spiked Core I loading established, Fig. A.4. A brief series of tests was then performed to establish the five rod bank position at various core conditions. The excess reactivity of the core was determined by integrating the five rod bank calibration curve, Fig. 5.4, obtained for the initial Rearranged and Spiked Core I from the critical bank position to the fully withdrawn position. Table 5.5 presents bank position and reactivity values obtained for the final SM-1 Rearranged and Spiked Core I loading.

5-6
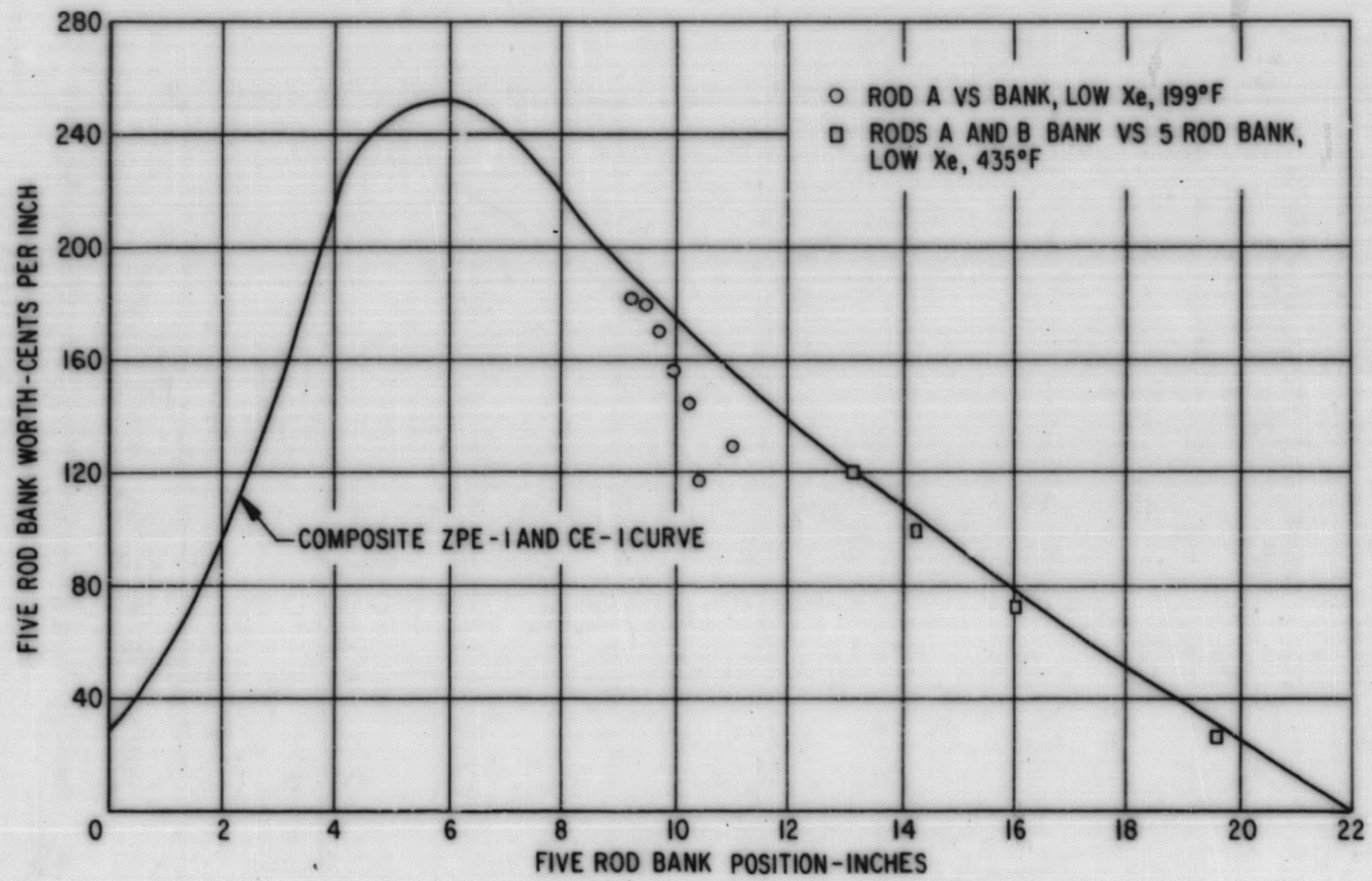
Figure 5. 4.   Five Rod Bank Calibration Curve, Initial SM-1 Rearranged and Spiked
Core I, 16. 5 MWYR
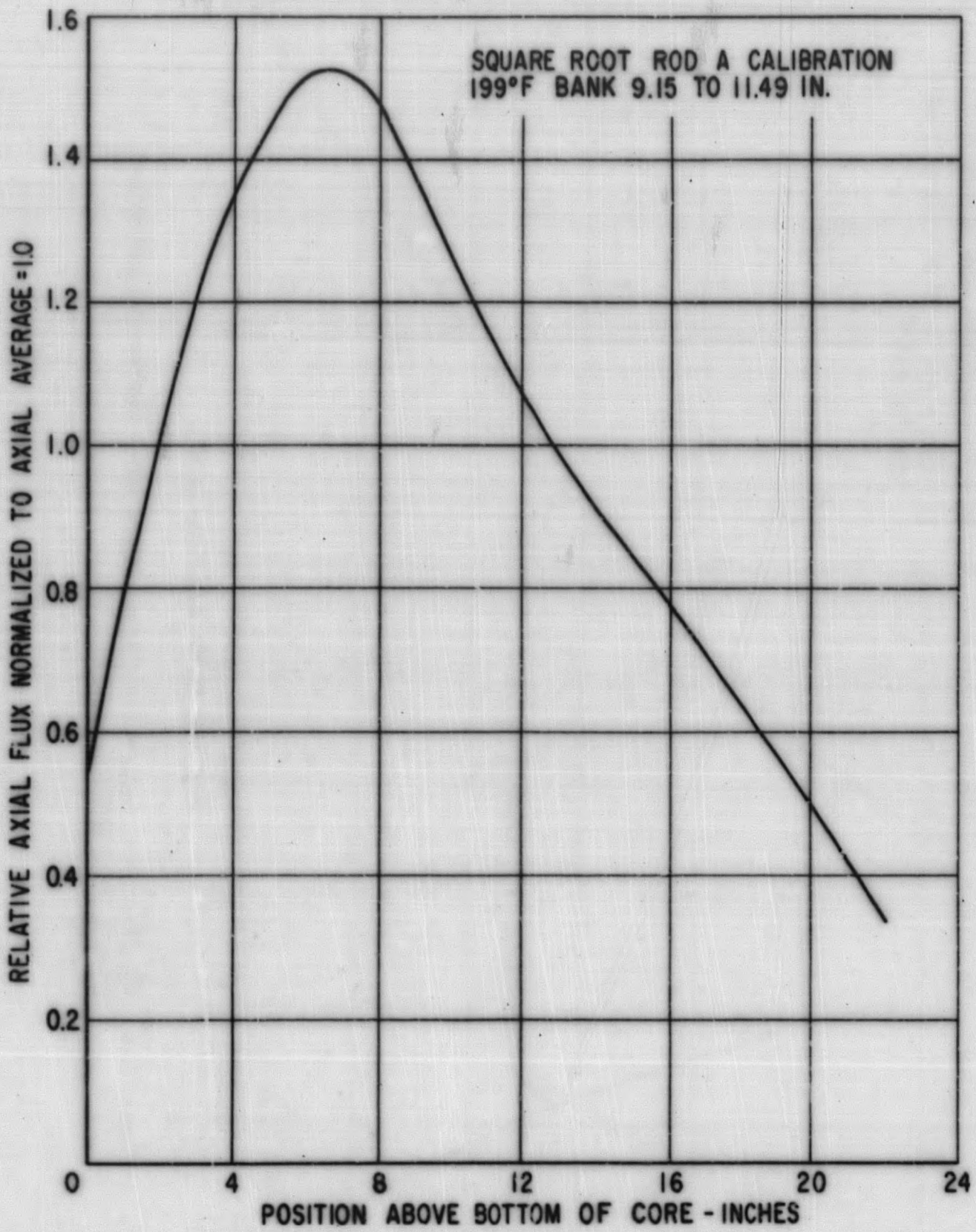
Figure 5.5. SM-1 Rearranged and Spiked Core I Axial Flux Distribution, 16.5 MWYR

TABLE 5.4
EFFECTS OF INITIAL CORE REARRANGEMENT AND SPIKING

	SM-1 Core I 16.4 MWYR	SM-1 Rearranged and Spiked Core I - 16.5 MWYR
Bank Position, Low Xe, 70°F (in.)	12.10	8.31
Bank Position, Low Xe, 440°F (in.)	17.10	12.62
Excess Reactivity, Low Xe, 70°F (dollars)	10.2 ± 0.5	12.9 ± 0.6
Excess Reactivity, Low Xe, 440°F (dollars)	3.4 ± 0.2	5.7 ± 0.3
Hot to Cold Reactivity Change (dollars)	6.8 ± 0.4	7.2 ± 0.4

TABLE 5.5
EXPERIMENTAL VALUES OBTAINED AT 16.5 MWYR
SM-1 REARRANGED AND SPIKED CORE I
Final Loading, Fig. A.4

Core Conditions	Five Rod Bank Critical Position, Inches	Excess Reactivity, Dollars
Low Xe-70°F	8.32*	12.9 ± 0.6
Low Xe-188°F	8.92	-
Low Xe-400°F	11.92	-
Low Xe-432°F	12.50	-
Low Xe-440°F	12.70*	5.6 ± 0.3
Equilibrium Xe-440°F	15.65**	2.6 ± 0.1

* Value corrected for temperature.

** Measured at 16.6 MWYR.

Comparison of Table 5. 5 with Table 5. 4 indicates only a slight reactivity difference between the initial rearranged and spiked core loading and the final loading following the removal of the PM-1-M element.

5. 4 CORE PHYSICS MEASUREMENTS AT THE END OF LIFE OF THE SM-1 REARRANGED AND SPIKED CORE I

5. 4. 1 Introduction

The purpose of this section is to report the core physics measurements performed at shutdown of the SM-1 Rearranged and Spiked Core I at 18. 0 MWYR. It may be assumed that these measurements are typical of those performed throughout core life and as such the data processing will be reported in detail including an error analysis where possible.

5. 4. 2 Temperature Coefficient

The temperature coefficient was measured at 18. 0 MWYR following test procedure number A-311. Measurements were started after the core had attained a low xenon concentration at operating temperature. The five rod bank was positioned at 14. 67 in. , rod B at 19 in. and rod A at 18. 00 inches. The increase in reactivity during cooldown was followed by inserting rod A; the other rods remained constant. At 247°F, it was not possible to compensate for the increase in reactivity with rod A fully inserted, so the five rod bank was inserted to 10. 87 in. and rod A withdrawn to 19. 00 inches. The continued increase in reactivity associated with cooldown was again followed by inserting rod A; the other rods remained constant. Table 5. 6 presents the data obtained during the temperature coefficient experiment.

The temperature coefficient as a function of temperature was calculated from the data in Table 5. 6 and the rod A calibration curves presented in Fig. 5. 8. A sample calculation is shown below:

T_1 = initial temperature = 449°F.

X_1 = rod A position at T_1 = 18. 00 in.

T_2 = new temperature ($T_2 < T_1$) = 434°F

X_2 = rod A position at T_2 = 14. 85 in.

W = rod A worth at $\dfrac{X_1 + X_2}{2}$ obtained from rod A calibration curve at 430°F

low xenon, Fig. 5. 8 (assuming the change in worth is essentially linear over the interval from X_1 to X_2) = 18. 5 cents per in. at 16. 43 in.

C = temperature coefficient at temperature $\dfrac{T_1 + T_2}{2}$ in cents per °F.

$$C = \frac{W (X_1 - X_2)}{(T_1 - T_2)} = \frac{18. 5 (18. 00 - 14. 85)}{(449 - 434)} = 3. 89 \text{ cents per °F at } 442°F.$$

TABLE 5.6
DATA OBTAINED DURING TEMPERATURE COEFFICIENT EXPERIMENT
SM-1 REARRANGED AND SPIKED CORE I - 18.0 MWYR
ROD B AT 19 INCHES

Temperature, °F	Rod A Position, Inches	Five Rod Bank Position, Inches
449	18.00	14.67
434	14.85	14.67
410	12.14	14.67
392	10.76	14.67
375	9.51	14.67
357	8.55	14.67
336	7.01	14.67
327	6.44	14.67
313	5.42	14.67
301	4.45	14.67
272	1.36	14.67
247	19.00	10.87
234	16.00	10.87
218	14.20	10.87
203	12.70	10.87
186	11.50	10.87
168	10.50	10.87
146	9.60	10.87
131	9.05	10.87
120	8.79	10.87

Figure 5.8 shows two rod A calibration curves obtained at low xenon. The curve at 120°F was obtained as a function of the 5 rod bank position from 4.83 in. to 12.74 in. The curve at 430°F was obtained as a function of the 5 rod bank from 14.11 to 20.20 in. The proper calibration curve to use in the temperature coefficient calculation is determined from the bank position during the measurement. For our sample calculation the bank was at 14.67 in., indicating that we should use the rod A calibration curve obtained at 430°F over a bank variation of from 14.11 to 20.20 in. It should be noted that an uncertainty is introduced in not using a calibration obtained for an identical configuration.

Table 5.7 and Fig. 5.6 present the temperature coefficient values as a function of temperature at 18.0 MWYR. The uncertainties in the temperature coefficient were calculated by the method of least squares assuming uncertainties of ± 1°F, ± 1 cent per in., and $\pm .03$ in. in the temperature change, rod A worth, and change in rod A position, respectively.

The curve shown in Fig. 5.6 is the composite SM-1 Core I curve as presented in Fig. 4.5. From the scatter in the data and the uncertainties it is seen that this curve may be used for the SM-1 Rearranged and Spiked Core I. The temperature coefficient at 440°F is -3.6 cents per °F with an estimated probable error of ± 0.1 cents per °F. The probable error was estimated from the spread in the data over core life.

5.4.3 Five Rod Bank Position as a Function of Temperature

During the temperature coefficient measurements as the core cooled down five rod bank critical positions were determined at approximately 4 hr intervals. Rods A and B were positioned at 19 in. and the critical five rod bank position determined and recorded along with the core temperature. Following this measurement the five rod bank and Rod A were repositioned to their original settings to continue the temperature coefficient measurements as outlined in the preceding section.

Table 5.8 presents the five rod bank critical positions measured as a function of temperature during 18.0 MWYR. Since no points were obtained at 440°F and 70°F, these values were calculated from the closest measured position using the temperature coefficient and bank worth from Fig. 5.11.

Figure 5.7 shows the five rod bank critical position as a function of temperature during core life. The 18.0 MWYR data for the Rearranged and Spiked Core I falls slightly above the data obtained at 13.5 MWYR for the original Core I.

TABLE 5.7
TEMPERATURE COEFFICIENT VS. TEMPERATURE DATA
SM-1 Rearranged and Spiked Core I - 18.0 MWYR

Temperature, °F	Temperature Coefficient Cents per °F
442 ± 2	3.89 ± .34
442 ± 2	3.34 ± .18
401 ± 2	2.74 ± .18
384 ± 2	2.79 ± .19
366 ± 2	2.01 ± .14
347 ± 2	2.57 ± .15
332 ± 2	1.96 ± .25
320 ± 2	2.02 ± .17
307 ± 2	1.88 ± .19
387 ± 2	1.55 ± .12
241 ± 2	1.73 ± .
226 ± 2	1.49 ± .15
211 ± 2	1.77 ± .16
195 ± 2	1.54 ± .12
177 ± 2	1.42 ± .11
157 ± 2	1.19 ± .08
139 ± 2	1.17 ± .11
126 ± 2	0.79 ± .12

TABLE 5.8
FIVE ROD BANK POSITION AS A FUNCTION OF TEMPERATURE
SM-1 Rearranged and Spiked Core I - 18.0 MWYR
Low Xe - A and B at 19 Inches

Temp., °F	Five Rod Bank Position, Inches
440	14.55*
365	12.64
283	11.40
247	10.83
192	10.24
129	9.76
124	9.73
120	9.71
70	9.47*

* Calculated.
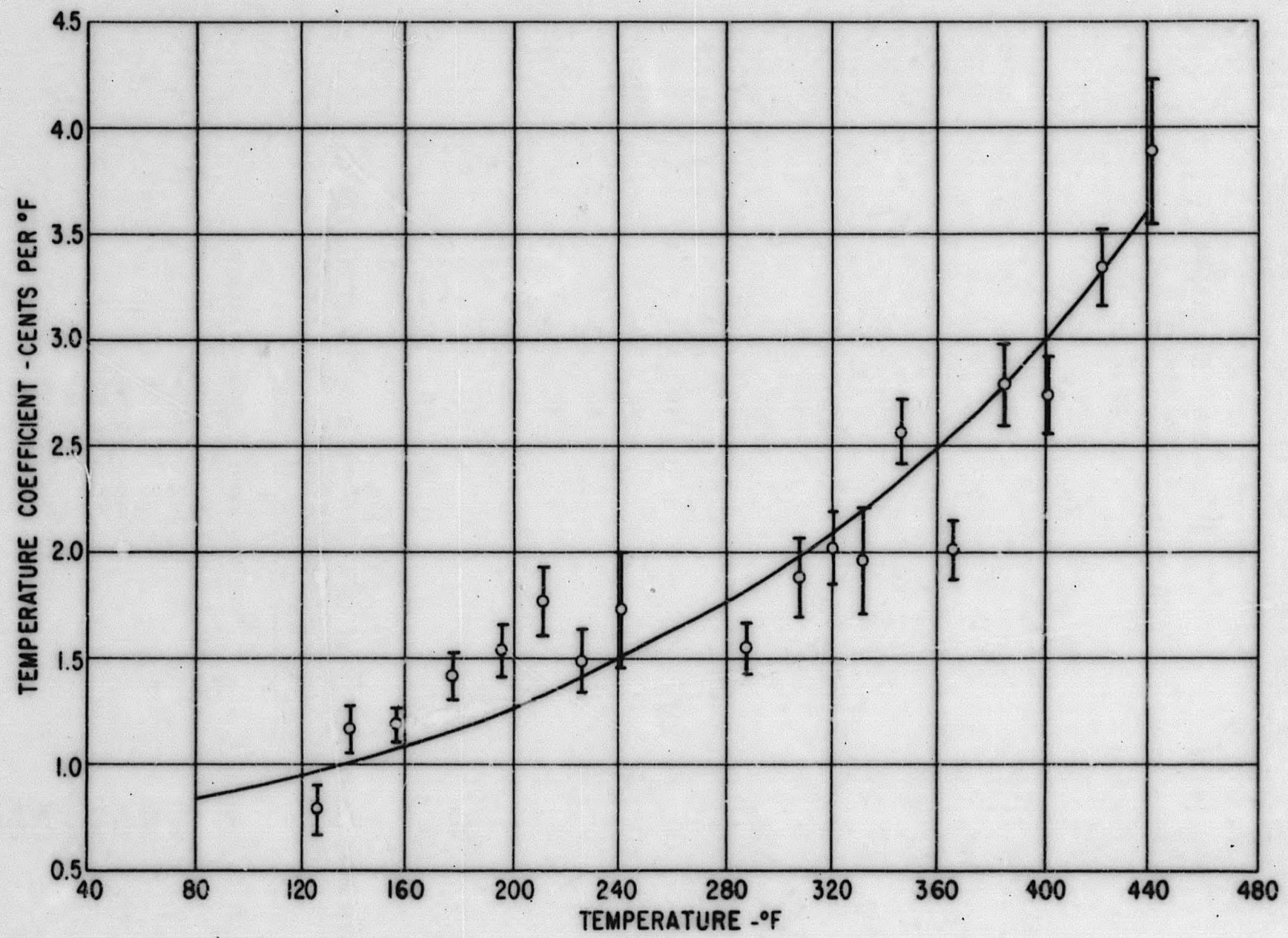
Figure 5.6. Temperature Coefficient Data, 18.0 MWYR, SM-1 Rearranged and
Spiked Core I
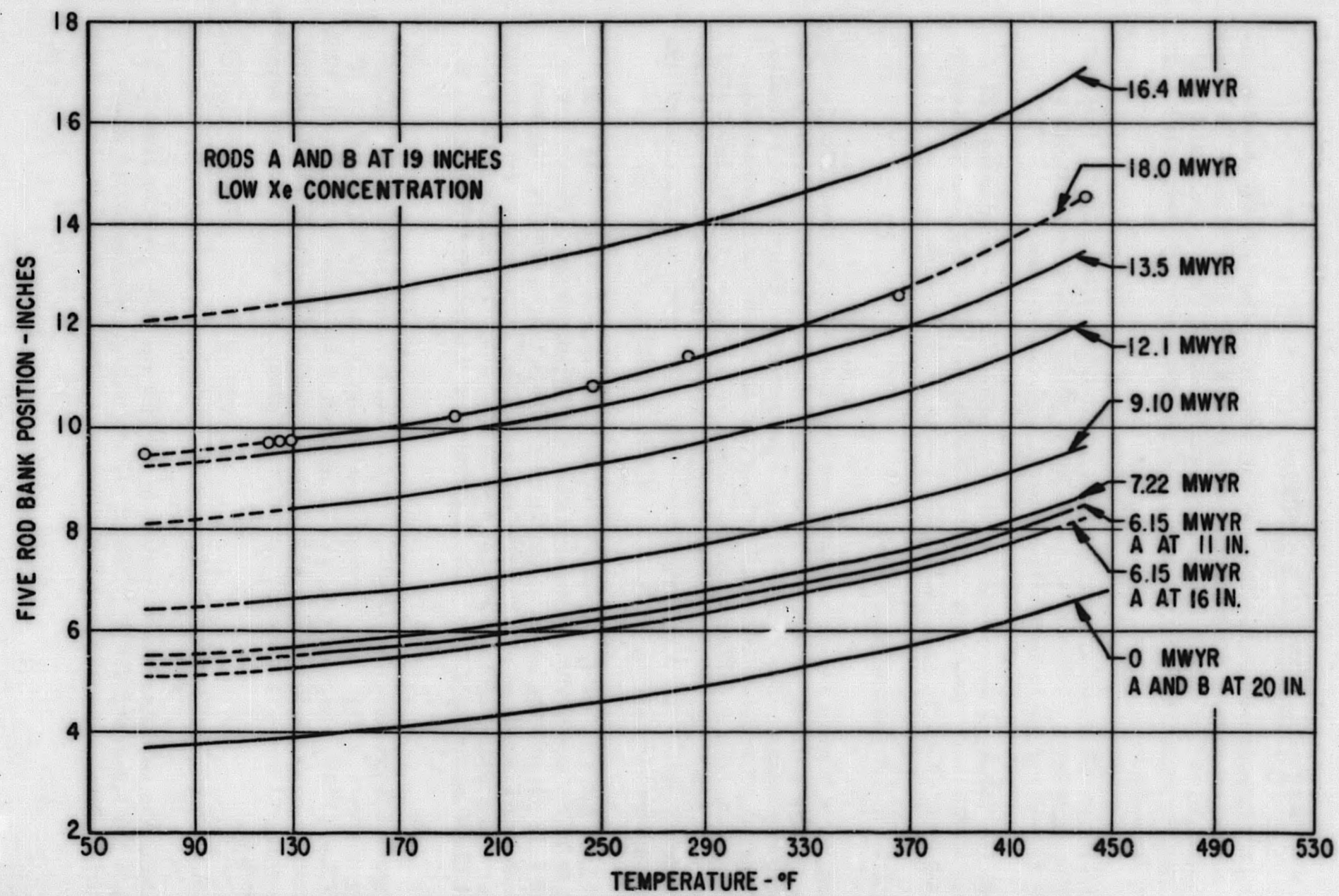
Figure 5.7. Five Rod Bank Position Vs. Temperature, Rods A and B at 19 Inches, Lw Xenon Concentration, SM-1 Core I and SM-1 Rearranged and Spiked Core I, 18.0 MWYR

5.4.4 Hot-to-Cold Reactivity Change

The hot to cold reactivity change as determined by the integral of the temperature coefficient versus temperature curve from $440^\circ F$ to $70^\circ F$ is 6.66 ± 0.50. This is identical to that determined for the original SM-1 Core I (Section 4.2.4) since within the experimental uncertainty the temperature coefficient curve was assumed the same.

The hot to cold reactivity change as determined by integrating the five rod bank calibration curve from 9.47 to 14.55 in. is $7.20 with an estimated uncertainty of $\pm$ $0.40 due to uncertainties in the bank calibration.

The two values of hot to cold reactivity change, 6.66 ± 0.50 and 7.20 ± 0.40, are within their respective uncertainties and in agreement with the values previously determined for the original SM-1 Core I (Table 4.4).

5.4.5 Rod A Calibration Curves

Single rod control rod calibrations were performed using the period technique. With the core in a steady state critical condition; the control rod to be calibrated was withdrawn a small amount resulting in a supercritical condition and positive reactor period. The positive reactor period was related to the core reactivity change by means of the in-hour equation. The control rod worth was calculated from the core reactivity change divided by the rod position change and plotted at the average rod position. A calibration over the length of travel of a control rod was accomplished by varying the position of the remaining control rods.

At 18.0 MWYR, rod A was calibrated as a function of the five rod bank position at $120^\circ F$ and $430^\circ F$ low xenon and at $434^\circ F$ peak xenon. Tables 5.9, 5.10 and 5.11 present the rod A calibrations as a function of the five rod bank position at $120^\circ F$ low xenon, $430^\circ F$ low xenon and $434^\circ F$ peak xenon, respectively. The three calibration curves are presented on Fig. 5.8. The maximum rod A worth at $120^\circ F$ occurs at 7.1 in.; the maximum rod A worth at $430^\circ F$ occurs at 9.6 in.

Figure 5.9 presents the integral worth of the two complete rod A calibration curves shown in Fig. 5.8. Rod A has an integral worth of $4.18 and $4.70 at $120^\circ F$ and $430^\circ F$, respectively, with an estimated uncertainty of $\pm$ $0.30. This represents an increase in rod A worth of approximately $1.0 at $120^\circ F$ and $430^\circ F$ over the integral worths measured during the original SM-1 Core I life and reported in Table 4.8.

5.4.6 Rod C Calibration Curve

Rod C was calibrated as a function of the four rod bank position rods (1, 2, 3 and 4) at low xenon and $430^\circ F$. Table 5.12 and Fig. 5.10 present the Rod C calibration data.

TABLE 5.9
CONTROL ROD A CALIBRATION AT LOW XENON, 120°F
SM-1 Rearranged and Spiked Core I - 18.0 MWYR

Rod A Position, Inches	Rod A Worth, Cents per Inch	Bank Position, Inches
1.08	11.3	12.74
2.95	21.8	12.51
4.81	31.4	12.09
6.78	37.2	11.50
8.78	33.5	10.93
10.75	26.6	10.48
12.98	15.3	10.17
15.16	13.4	9.98
17.37	10.1	9.83

TABLE 5.10
CONTROL ROD A CALIBRATION AT LOW XENON, 430°F
SM-1 Rearranged and Spiked Core I - 18.0 MWYR

Rod A Position, Inches	Rod A Worth, Cents per Inch	Bank Position, Inches
1.30	8.9	20.20
3.21	15.7	19.69
4.71	20.6	19.10
5.88	30.0	18.61
6.60	30.4	18.17
7.36	32.6	17.80
8.04	34.7	17.47
8.80	36.3	17.09
9.57	43.9	16.69
10.58	37.3	16.12
11.81	32.6	15.62
13.50	30.7	15.04
15.59	19.0	14.61
17.99	10.0	14.31
20.50	5.8	14.11

TABLE 5.11
CONTROL ROD A CALIBRATION AT PEAK XENON, 434°F
SM-1 Rearranged and Spiked Core I - 18.0 MWYR

Rod A Position, Inches	Rod A Worth, Cents per Inch	Bank Position, Inches
18.05	20.4	21.97
18.24	22.4	21.97
18.65	18.3	21.97
19.87	12.5	21.25
21.00	8.0	20.43
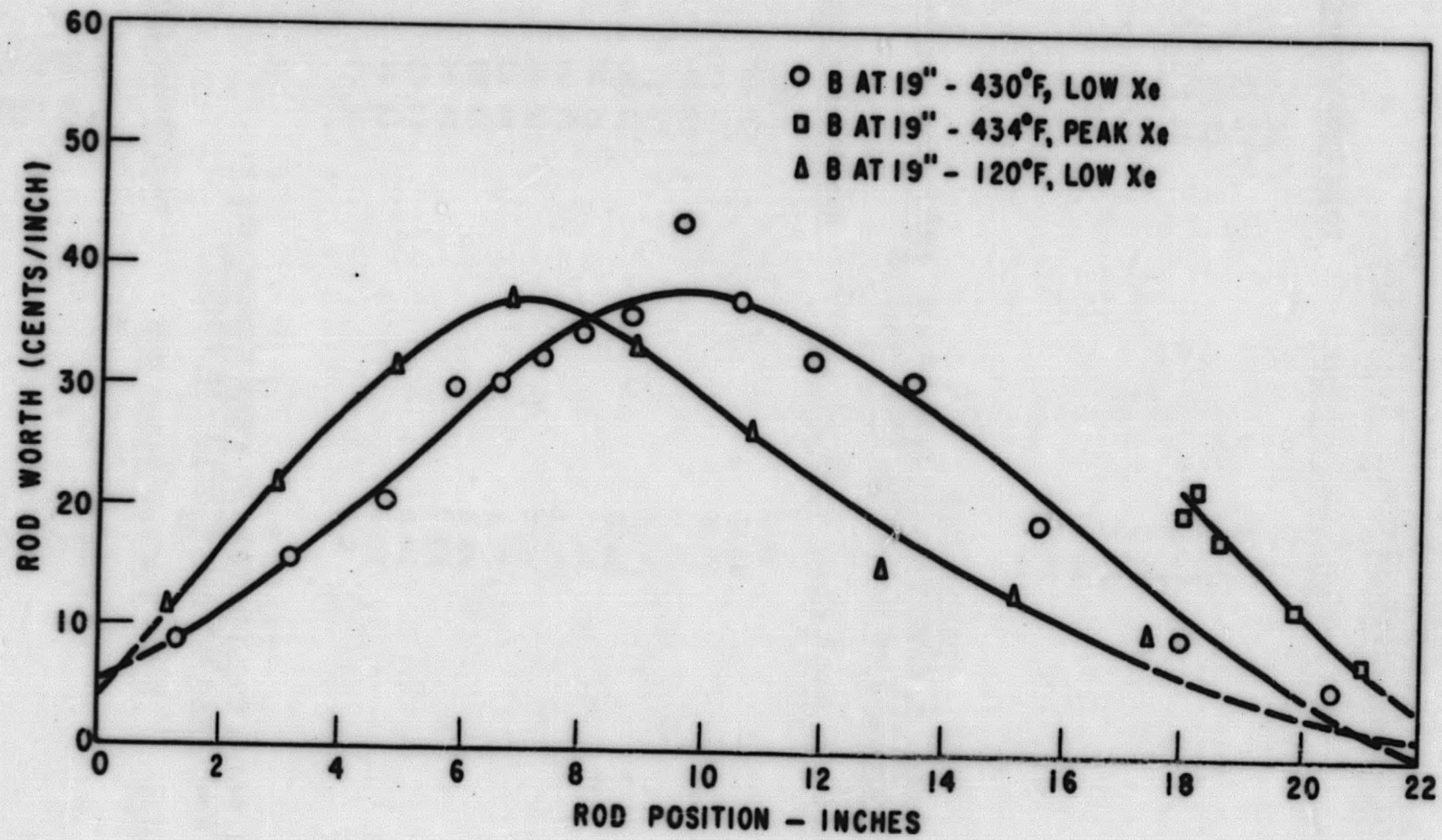
Figure 5.8. Rod A Calibration Curves, 18.0 MWYR, SM-1 Rearranged and Spiked Core I
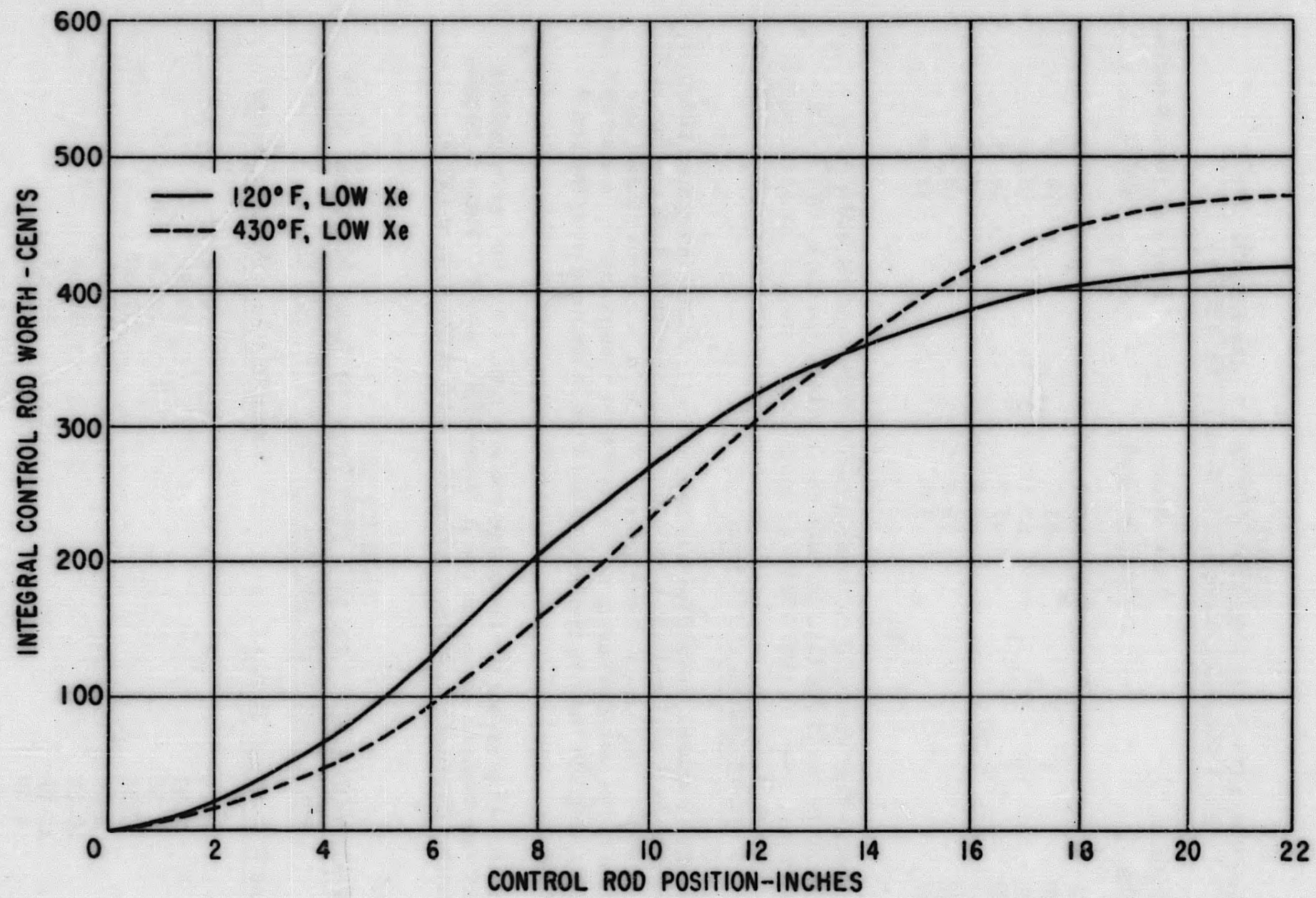
Figure 5.9. Control Rod A Integral Worth, 18.0 MWYR, SM-1 Rearranged and Spiked Core I

TABLE 5.12
CONTROL ROD C CALIBRATION CURVE AT LOW XENON, 430°F
SM-1 Rearranged and Spiked Core I - 18.0 MWYR

Rod C Position, Inches	Rod C Worth, Cents per Inch	Four Rod Bank Position, Inches
8.33	59.7	21.93
9.60	63.7	18.49
10.96	53.1	16.69
12.60	41.7	15.11
14.37	40.9	14.10
16.51	19.6	13.25
20.27	3.7	12.78

It is seen that the rod C calibration curve obtained at 18.0 MWYR is similar in shape to the rod C calibration curve obtained at 13.5 MWYR (Fig. 4.15); however, rod C at 18.0 MWYR seems to have a greater maximum worth.

5.4.7 Five Rod Bank Calibration

The five rod bank calibration was determined from the integrated reactivity values of control rod A; rod A was calibrated as a function of bank position at 120°F and 430°F, low xenon concentration. Section 4.5.2 gives an adequate description of the technique used, so the treatment here is limited to a sample calculation showing how the five rod bank calibration is obtained from the rod A calibrations.

Table 5.13 presents the measured rod A positions and the corresponding bank positions obtained during the rod A calibration at 430°F. Table 5.14 presents similar information obtained during the rod A calibration at 120°F.

TABLE 5.13
CONTROL ROD A POSITION AS A FUNCTION OF BANK POSITION, 430°F
SM-1 Rearranged and Spiked Core I - 18.0 MWYR

Rod A Position, Inches	Five Rod Bank Position, Inches
0.11	12.74
2.50	12.51
4.50	12.09
6.50	11.50
8.50	10.93
10.50	10.48
12.50	10.17
14.50	9.98
16.50	9.83

5-20
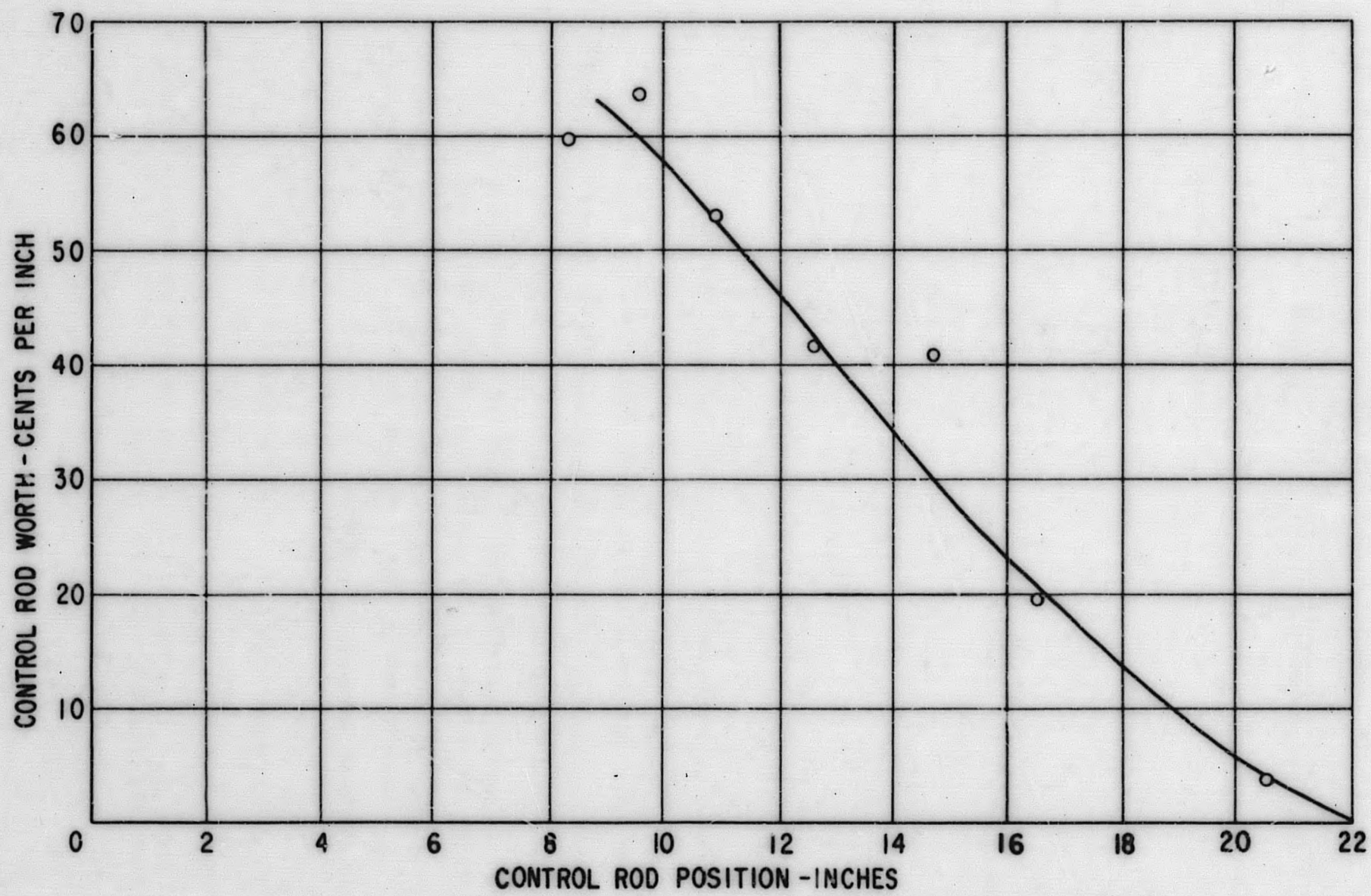
Figure 5.10. Control Rod C Calibration Curve, 18.0 MWYR, SM-1 Rearranged and
Spiked Core I, 430°F, Low Xe

TABLE 5.14
CONTROL ROD A POSITION AS A FUNCTION OF BANK POSITION, 120°F
SM-1 Rearranged and Spiked Core I - 18.0 MWYR

Rod A Position, Inches	Five Rod Bank Position, Inches
0.10	20.20
2.50	19.69
4.20	19.10
5.50	18.61
6.25	18.17
7.00	17.80
7.72	17.47
8.50	17.09
9.30	16.69
10.30	16.12
11.50	15.62
13.20	15.04
15.00	14.61
17.00	14.31

The bank calibration is obtained from the rod A calibration at 430°F as follows:

A_1 = initial rod A position = 0.11 in. (from Table 5.13)

B_1 = five rod bank position when rod A is at A_1 = 12.74 in. (from Table 5.13)

A_2 = adjusted rod A position = 2.50 in. (from Table 5.13)

B_2 = position to which five rod bank is inserted to compensate for withdrawing rod A from A_1 to A_2 = 12.51 in. (from Table 5.13)

I_A = rod A integral worth; obtained by integrating the 430°F, low xenon, rod A calibration curve (Fig. 5.8) from A_1 to A_2 = 21.6 cents

W_B = five rod bank worth at $\dfrac{B_1 + B_2}{2}$

$$W_B = \frac{I_A}{B_1 - B_2} = \frac{21.6}{12.74 - 12.51} = 42.4 \text{ cents per in. at } 19.95 \text{ in.}$$

Table 5.15 and Fig. 5.11 summarize the 5 five rod bank worths as a function of position as determined from the rod A calibrations.

TABLE 5.15
FIVE ROD BANK WORTH AS A FUNCTION OF POSITION
SM-1 Rearranged and Spiked Core I - 18. 0 MWYR

Five Rod Bank Position, Inches	Five Rod Bank Worth, Cents per Inch
19. 95	42. 4
19. 40	36. 9
18. 86	60. 5
18. 39	46. 9
17. 99	62. 2
17. 64	73. 1
17. 28	73. 7
16. 89	75. 0
16. 41	66. 7
15. 87	88. 3
15. 33	97. 6
14. 83	115. 1
14. 46	134. 7
14. 21	122. 0
12. 63	128. 9
12. 30	119. 0
11. 80	115. 6
11. 22	129. 8
10. 71	138. 9
10. 33	154. 2
10. 08	185. 3
9. 91	161. 3
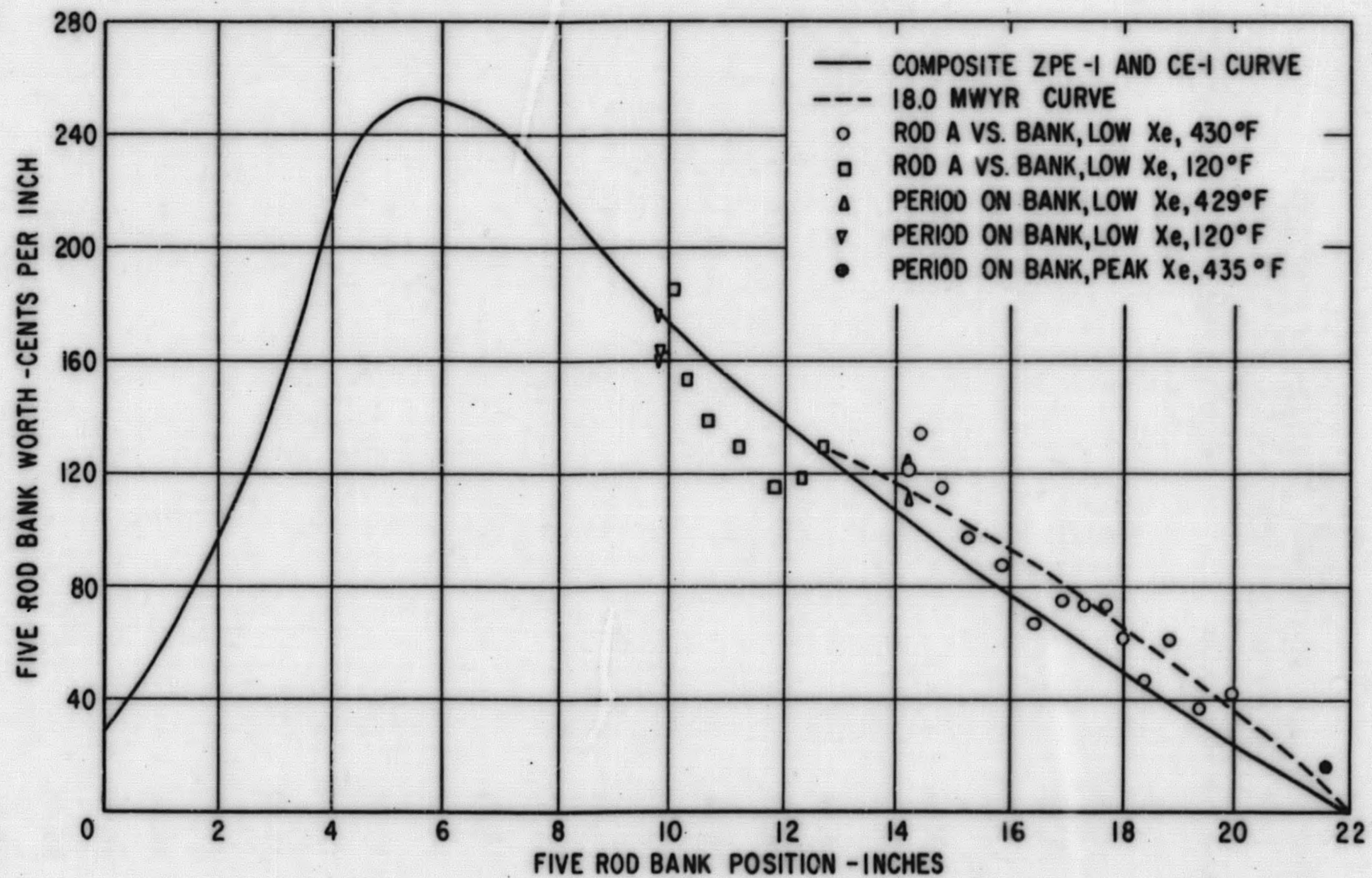
Figure 5.11. Five Rod Bank Calibration, SM-1 Rearranged and Spiked Core I, 18.0 MWYR

As a check on the five rod bank worth a number of five rod bank calibration points were obtained using the period technique. Because of the large reactivity the bank controls, it was necessary to move one rod at a time when going on a period. The amount of time needed to adjust the bank position coupled with limitations on the power level reduced the interval over which the period was taken introducing some additional uncertainties. An effort was therefore made to take a number of period measurements at each point to provide an average value with a lower uncertainty. The five rod bank period measurements taken at 18.0 MWYR are tabulated in Table 5.16, and also presented in Fig. 5.11.

TABLE 5.16
FIVE ROD BANK WORTH AS DETERMINED BY PERIOD
MEASUREMENTS ON THE BANK
SM-1 Rearranged and Spiked Core I - 18.0 MWYR

Core Condition	Five Rod Bank Position, Inches	Bank Worth, Cents per Inch
Peak Xe - 435°F	21.57	16.4
Low Xe - 429°F	14.25	124.5
Low Xe - 428°F	14.22	111.4
Low Xe - 124°F	9.78	164.0
Low Xe - 120°F	9.78	176.0
Low Xe - 120°F	9.78	160.0
Low Xe - 120°F	9.77	163.0

The agreement between the measured bank worth by period technique and that determined indirectly from single rod calibrations is shown to be quite good. Figure 5.11 shows the change in bank worth in comparison with the composite ZPE-1 and CE-1 curve. This increase in worth is in agreement with the data measured at 12.1 MWYR (Fig. 4.35).

5.4.8 Excess Reactivity

The excess reactivity of the SM-1 Rearranged and Spiked Core I at 18.0 MWYR was determined by integrating the bank calibration curve (Fig. 5.11) from the critical bank position to 22 in. The excess reactivities for various core conditions at 18.0 MWYR are tabulated in Table 5.17.

TABLE 5.17
EXCESS REACTIVITY AT 18.0 MWYR
SM-1 Rearranged and Spiked Core I

Core Condition	Bank Position, Inches	Excess Reactivity, Dollars
Low Xe - 70°F	9.47	11.56
Low Xe - 440°F	14.55	4.36
Equilibrium Xe - 440°F	18.10	1.39
Peak Xe - 440°F	21.96	~ 0

5.4.9 Transient Xenon

The reactor was operated continuously at full power for 45 hr to build up equilibrium conditions. At this time, the power was reduced to 100 Kw to allow the xenon concentration to buildup while maintaining temperature. The possibility existed that there would not be sufficient excess reactivity in the core to maintain criticality at peak xenon concentration so the core temperature was lowered from 440°F to 431°F to provide an additional 32 cents reactivity. It later turned out that this was unnecessary and the core was able to override peak xenon at 440°F.

The reactivity associated with the xenon transient was determined from the change in critical bank position as xenon built up to a peak concentration and then started decaying. Table 5.18 and Fig. 5.12 and 5.13 summarize the transient xenon data. It should be noted that the reactivity values were determined from the change in five rod bank positions (Table 5.18) and the bank worth shown in Fig. 5.11.

Peak xenon was reached approximately 7.5 hr after power reduction and had a negative reactivity of $1.39* relative to equilibrium concentration. The xenon concentration had decayed back to equilibrium concentration approximately 20 hr after power reduction. Equilibrium xenon relative to low xenon concentration had a negative reactivity of approximately $2.97*.

---

* Estimated uncertainty of ± 6%.

TABLE 5.18
XENON TRANSIENT
SM-1 Rearranged and Spiked Core I - 18.0 MWYR

Time After Power Reduction, Hours	Five Rod Bank Position, Inches	Temperature, °F ± 2°F	Reactivity Change Relative to Equilibrium Concentration, Cents
0	18.10*	440	0
7.50	21.96**	439	-138.8
12.10	19.61	431	-113.3
19.83	17.67	431	- 2.7
24.05	16.86	433	59.7
27.72	16.19	431	117.3
31.70	15.72	432	161.5
36.25	15.26	431	207.3
41.22	14.91	431	243.7
45.17	14.60	430	258.5
49.38	14.42	431	278.5
53.83	14.39	432	281.9
57.33	14.29	431	293.2
58.30	14.26	432	296.6

* Corrected to 17.63 in. at 431°F.

** Corrected to 20.30 in. at 431°F.
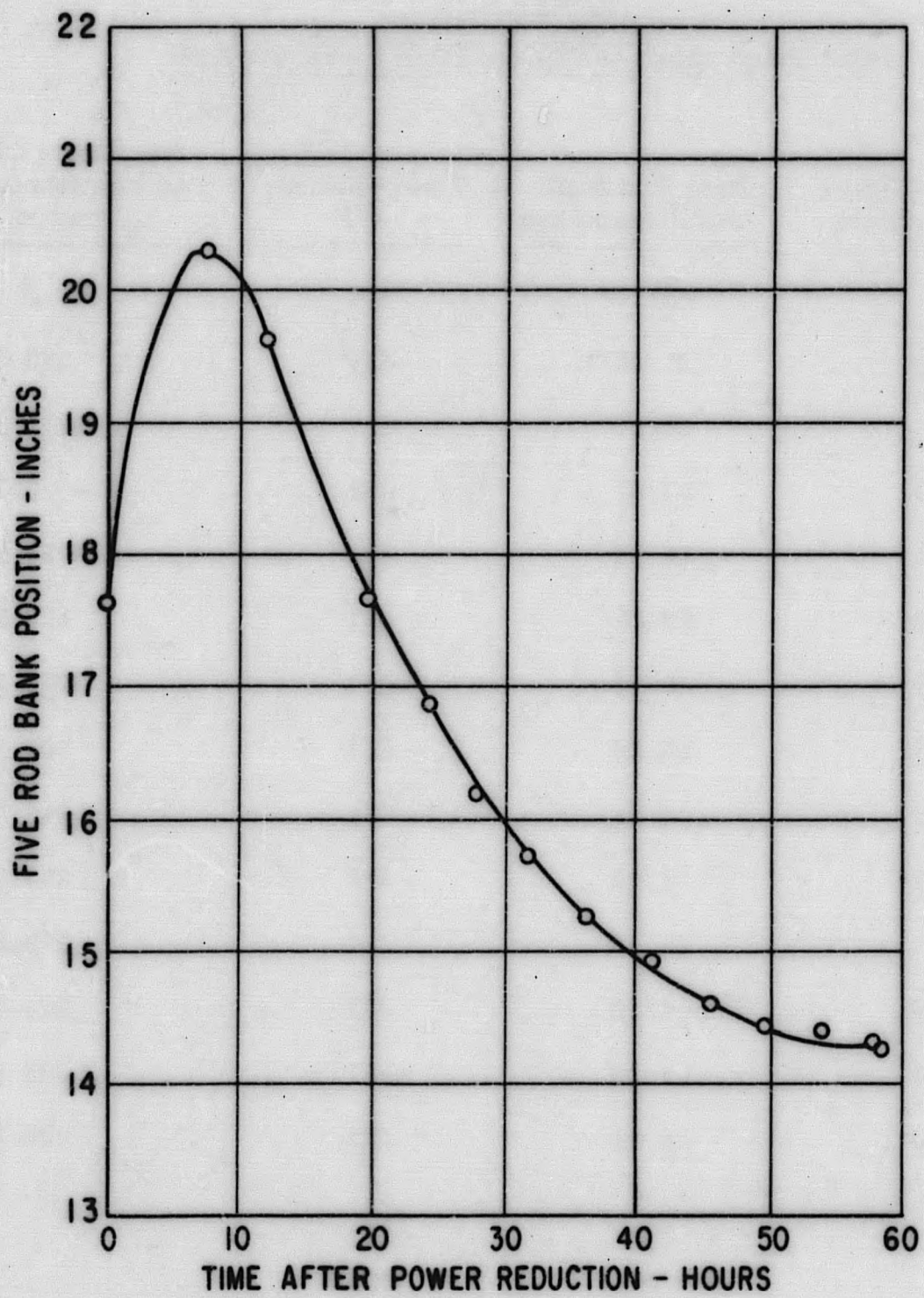
Figure 5.12. Xenon Transient, Five Rod Bank Position Vs. Time after Power Reduction, 18.0 MWYR, SM-1 Rearranged and Spiked Core I, 431°F
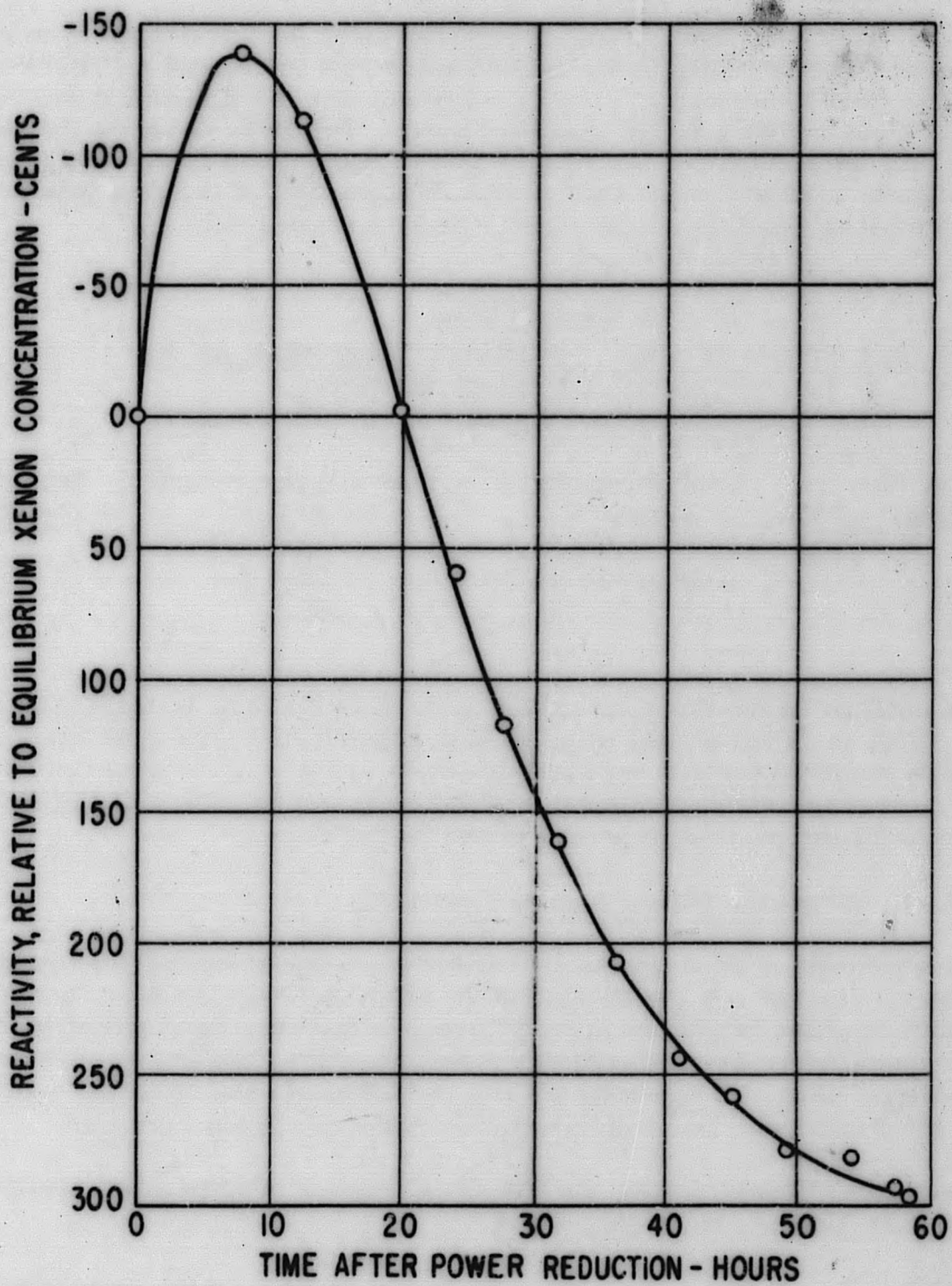
Figure 5.13. Reactivity Introduced by Transient Xenon, 18. 0 MWYR, SM-1 Rearranged and Spiked Core I, 431°F

5.4.10 Axial Neutron Flux Distribution

The relative axial neutron flux distribution may be determined by assuming the axial flux shape is proportional to the square root of the rod A calibration curve. This validity assumption was checked in Section 4.8.2 and shown to be in close agreement with gold foil measurements. Figure 5.14 shows the relative axial flux distributions at 120°F and 430°F, normalized to an axial average of unity. Table 5.19 shows the shift in the axial location of the flux peak as the bank was withdrawn and the variation in peak to average ratio.

TABLE 5.19
LOCATION OF AXIAL NEUTRON FLUX PEAK AS A
FUNCTION OF BANK POSITION
SM-1 Rearranged and Spiked Core I - 18.0 MWYR

Location of Flux Peak, Inches	Bank Position, Inches	Core Temperature, °F	Peak to Average Ratio
7.1	9.83 to 12.74	120	1.48
9.6	14.11 to 20.20	440	1.42

The position of the flux peak moves upward as the bank is withdrawn from the core. This is in agreement with the data reported in Table 4.23 and the 18.0 MWYR bank position and peak location values fit in with the original Core I values. The peak to average ratios are considerably lower and indicate a flattening of the axial flux distribution in the Rearranged and Spiked Core I.

5.4.11 Shutdown Neutron Source Evaluation

The shutdown neutron source evaluation experiment was performed at 18.0 MWYR energy release approximately 100 hr after shutdown from full power operation. Optimum pulse height and high voltage settings were determined for the startup channels after which shutdown count rates were obtained every 8 hr for the following 13 days. At this time all the fuel elements and absorber sections were removed from the core and the startup count rate again recorded.

The startup channel count rate data as a function of time after shutdown is presented in Table 5.20 and Fig. 5.15.

The well B and well F data show the startup channel count rate decaying with a half life of 14.0 and 20.7 days, respectively. Since a constant count rate is expected from the dual Po-Be plus Sb-Be source during the time of these measurements, the primary source of neutrons is the Be plate photoneutron source which depends on the gamma activity due to fission product buildup.
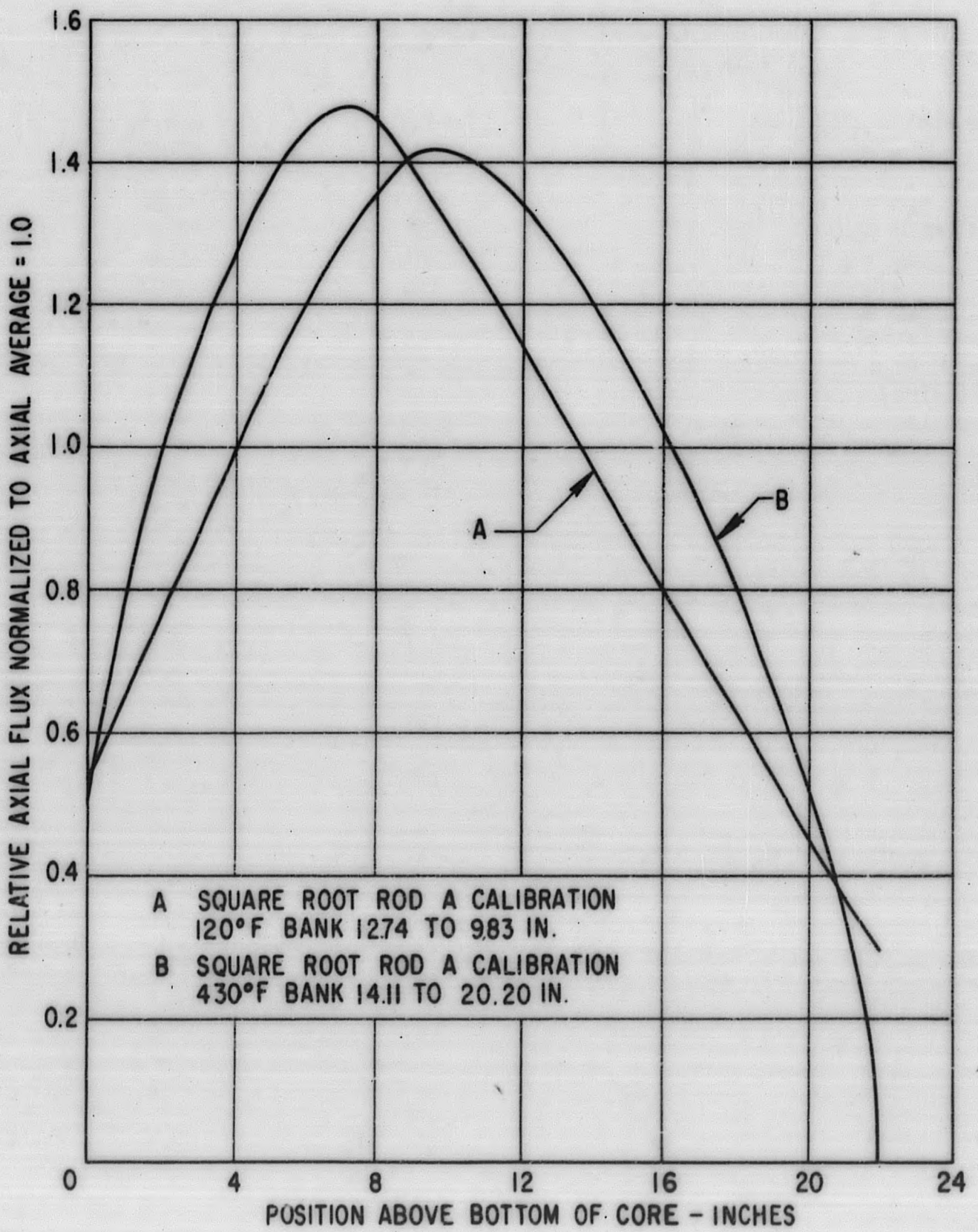
Figure 5.14.   SM-1 Rearranged and Spiked Core I Axial Flux Distribution, 18.0 MWYR

The graph shows Relative Axial Flux Normalized to Axial Average = 1.0 (y-axis) versus Position Above Bottom of Core – Inches (x-axis).

Legend:

A   SQUARE ROOT ROD A CALIBRATION
    120°F BANK 12.74 TO 9.83 IN.

B   SQUARE ROOT ROD A CALIBRATION
    430°F BANK 14.11 TO 20.20 IN.

TABLE 5.20
STARTUP CHANNEL COUNT RATE DATA
SM-1 Rearranged and Spiked Core I - 18.0 MWYR

Time After Shutdown, Hours	Startup Channel Count Rates, cpm	
	Well B	Well F
110.3	241	326
114.9	225	322
122.4	201	326
132.5	206	307
137.9	193	283
147.6	193	257
157.1	173	274
164.9	178	286
170.3	183	267
178.7	172	291
186.8	164	293
203.4	160	277
220.2	158	276
228.1	158	278
234.7	152	254
244.1	145	291
255.6	150	244
259.0	142	246
268.4	147	247
274.8	149	247
281.5	146	238
291.2	137	239
297.9	135	234
305.9	120	237
318.6	129	215
323.7	131	228
331.9	130	233
339.4	122	221
347.1	125	244
360.8	131	221
363.7	117	208
371.5	112	210
379.3	112	204
388.1	116	204
396.3	113	198
456 *	9.5	50.5

* All fuel elements and absorber sections removed from core.
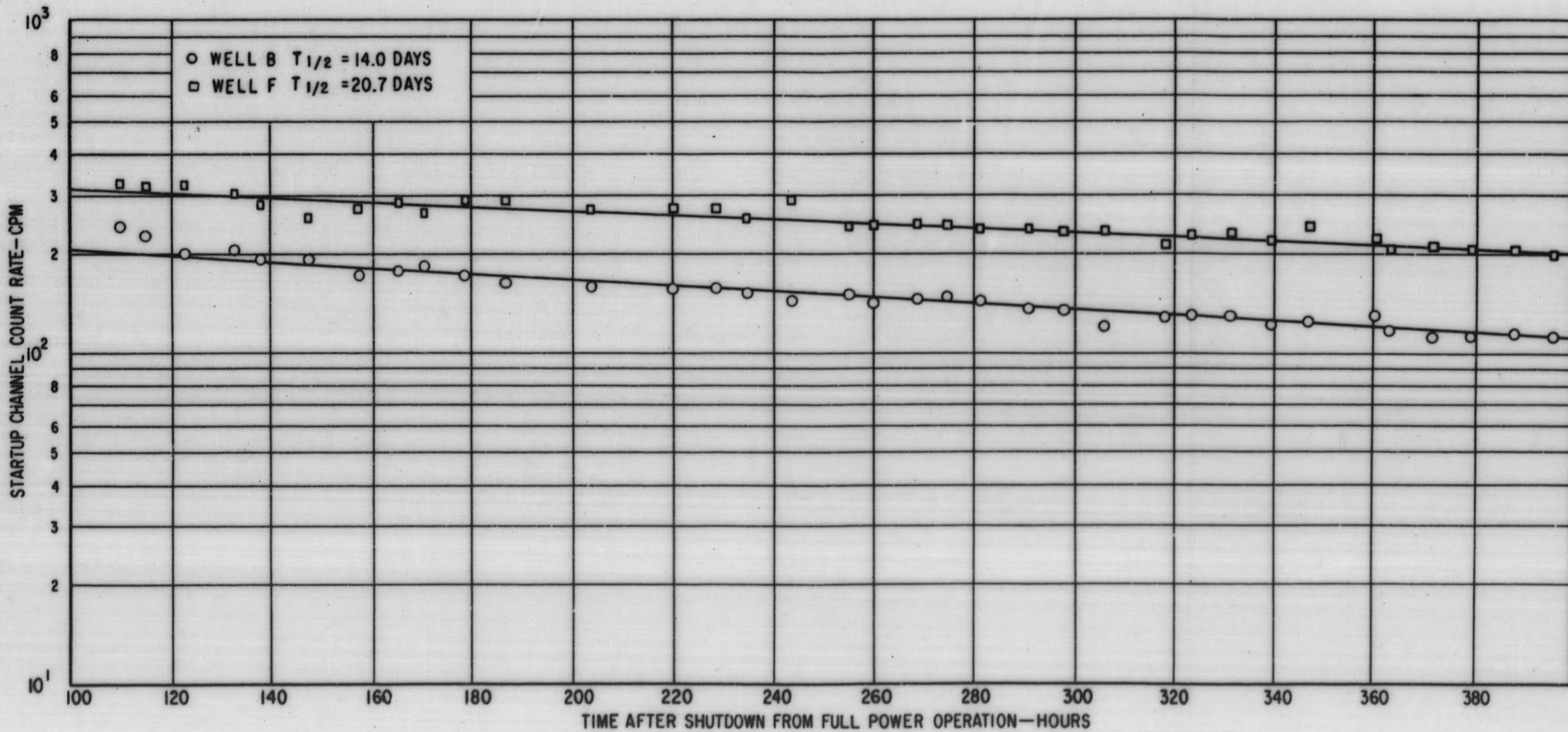
Figure 5.15. Startup Channel Count Rate as a Function of Time after Shutdown, SM-1
Rearranged and Spiked Core I, 18.0 MWYR

The threshold energy for the (γ,n), reaction in Be is 1.6 mev.[12] The only significant long lived fission product with a gamma activity above this threshold occurs in the fission product decay chain of mass 140.[23]

$$54 \ Xe^{140} \xrightarrow[\ 55\ ]{16.0 \ sec} Cs^{140} \xrightarrow[\ 56\ ]{1.1h} Ba^{140} \xrightarrow[\ 57\ ]{12.8d} La^{140} \xrightarrow[\ 58\ ]{1.68d} Ce^{140}$$

Yield 0.037

Yield 0.023

Yield 0.003
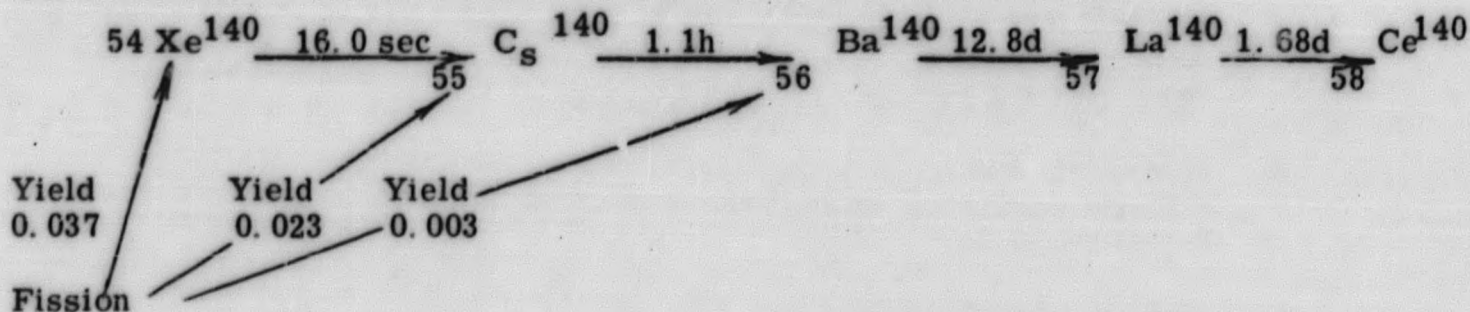
Fission

La-140 decays to Ce-140 by β^{-} and gamma emmission (1.60 mev gamma with intensity of 0.99 photons per disintegration),[23] thus providing the gamma activity at the necessary threshold energy for the (γ,n) reaction in Be. Further substantiation as to the neutron source is provided by the partial agreement of the measured decay rate (measured half life of 14.0 and 20.7 days) with the decay rate of Ba-140 to La-140 (half life of 12.8 days).

With all the fuel elements and absorber sections removed from the core, the startup channels registered count rates of 9.5 cpm and 50.5 cpm in wells B and F, respectively. These neutrons are primarily from the dual Po-Be plus Sb-Be source because there is no gamma activation from fission products for the (γ,n) reaction with Be with the fuel removed. The count rate in well F is greater than that in well B, because well F is located closer to the dual source (as seen in Fig. 2.1).

5.4.12   Five Rod Bank Positions

Figure 5.16 presents a summary of the five rod bank critical positions measured as a function of core energy release for the SM-1 Core I and the SM-1 Rearranged and Spiked Core I. Extrapolating the curve obtained at equilibrium xenon, 440°F, to 22 in. indicates a total core life conservatively estimated at 18.9 MWYR energy release, an extension of the original core life by 2.5 MWYR.

5.4.13   Summary of Experimental Results at 18.0 MWYR Energy Release

1. Within the experimental uncertainties, the temperature coefficient as a function of temperature was the same as for the original Core I. The temperature coefficient at 440°F is -3.6 cents per °F with a probable error of $\pm$0.1 cents per °F.

2. The hot-to-cold reactivity change as determined by integrating the five rod bank calibration curve from the hot critical position to the cold critical position is $7.20 $\pm$ 0.40.

3. The rod A integrated worth at 120°F, low xenon, is $4.18 +0.30. This represents an increase in worth of approximately $1.$\overline{0}$ over similar measurements made on Core I prior to rearrangement.

4. The rod A integral worth at 440°F, low xenon is $4.70 +0.30. This represents an increase of $0.9 over similar measurements made on Core I prior to rearrangement.

5. Rod C over the interval calibrated (8.3 to 22 in.) has a greater integral worth than similar measurements made on Core I prior to rearrangement.

6. The five rod bank calibration measurements show an increase in worth from $5.2 at 0 MWYR to $6.4 at 18.0 MWYR in the interval from 13 to 22 in.

7. The excess reactivity at 18.0 MWYR, equilibrium xenon concentration, 440°F, is $1.39.

8. Peak xenon concentration was reached approximately 7.5 hr after power reduction and had a negative reactivity of $1.39 relative to equilibrium concentration. The xenon concentration decayed back to equilibrium concentration approximately 20 hr after power reduction.

9. Equilibrium xenon relative to low xenon concentration had a negative reactivity of approximately $2.97.

10. The axial neutron flux distribution at 120°F had a peak to average ratio of 1.48. The peak was located 7.1 in. above the bottom of the core.

11. The axial neutron flux distribution at 440°F had a peak to average ratio of 1.42. The peak was located 9.6 in. above the bottom of the core.

12. The shutdown neutron count rate recorded on the startup channels after 100-hr shutdown indicated a decay rate with a half-life of 14.0 and 20.7 days from wells B and F, respectively.

13. With all the fuel elements and absorber sections removed from the core, the startup channel registered count rates of 9.5 cpm and 50.5 cpm in wells B and F, respectively.
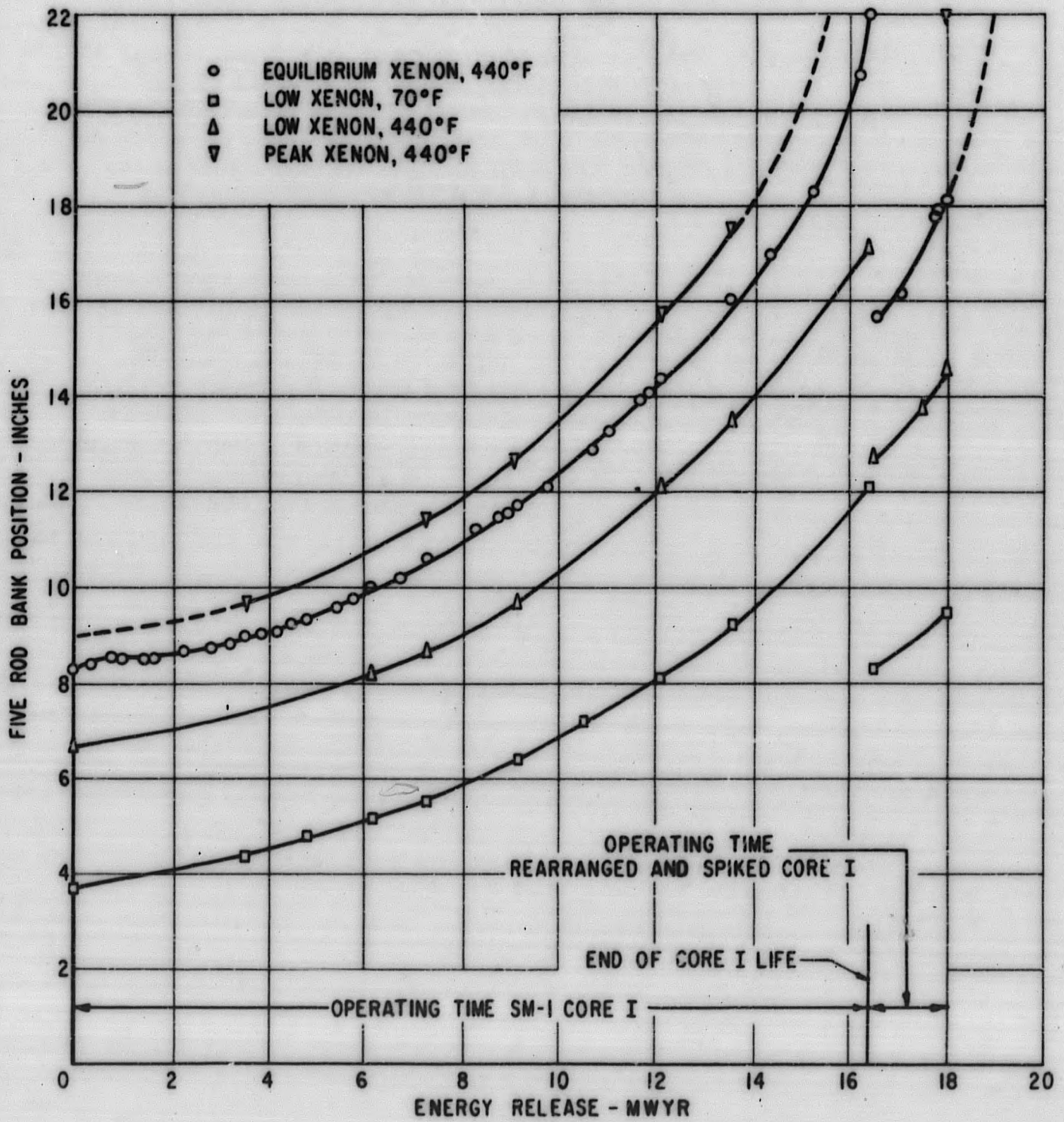
FIGURE 2.2

Figure 5.16. Five Rod Bank Position as a Function of Energy Release, Various Core Conditions, SM-1 Core I, SM-1 Rearranged and Spiked Core I

5.5 EFFECT OF CORE REARRANGEMENT AND SPIKING ON CORE LIFE

Extrapolating the five rod bank critical position at equilibrium xenon, 440°F, to 22 in. yields a total potential energy release of 18.9 MWYR for the SM-1 Core I and Rearranged and Spiked Core I. This is an increase of 2.5 MWYR in the lifetime of the SM-1 due to the rearrangement of the elements and spiking the core. When the reactor was shutdown for core changeover at the end of 18.0 MWYR, it was estimated that 0.9 MWYR was still available in Rearranged and Spiked Core I.

In Section 5.4.8 the excess reactivity, at equilibrium xenon, 440°F, was estimated as \$1.39. Assuming the Rearranged and Spiked Core I will burn out in approximately the same manner as the original Core I (refer to Fig. 4.37) an excess reactivity, at equilibrium xenon, 440°F, of \$1.39 is equivalent to 1.2 MWYR energy release (16.4 - 15.2). The total potential energy release of the core is 19.2 MWYR, which is in good agreement the value of 18.9 MWYR as determined by extrapolating the bank position as a function of energy release to 22 in. Using an average value, the estimated total potential energy release of the SM-1 Core I and the Rearranged and Spiked Core I is 19.1 MWYR.

6.0 CONCLUSIONS

6.1 SM-1 CORE I EXPERIMENTAL RESULTS

A. SM-1 Core I life was 16.4 MWYR. *

B. Temperature coefficient measurements did not indicate any change in temperature coefficient during burnup. At $440^{\circ}F$, low xenon concentration, the temperature coefficient is -3.6 ± 0.1 cents per $^{\circ}F$.

C. The hot to cold reactivity change, with low xenon concentration in the core, is 6.7 ± 0.5, and remained constant with burnup within experimental uncertainty.

D. The average pressure coefficient at low temperature is 1.06 ± 0.33 cents per 100 psi and at operating temperature is 3.35 ± 0.68 cents per 100 psi.

E. The total rod A integral worth showed little variation with burnup. The increase in total integral worth with cold to hot temperature change is of the order of 20 percent.

F. The total rod C integral worth showed a 4.4 percent decrease with cold to hot temperature change, and a decreasing integral worth with burnup.

G. Rod C and rod 3 integral worth curves obtained during zero power experiments show a decrease in rod worth as poison is added to the core and the bank withdrawn.

H. The worth of the five rod bank increases with burnup in the upper regions of the core. In the interval from 13 to 22 in. ,the bank worth increased from $5.2 at 0 MWYR to $9.0 at 16.4 MWYR.

I. The five rod bank integral worth at 0 MWYR and $70^{\circ}F$ is 27.4 ± 1.0 from the fully inserted to fully withdrawn position.

J. The seven rod bank integral worth at 0 MWYR and $70^{\circ}F$ is 34.0 ± 2.0.

K. The integral worth of rods A and B at 0 MWYR and $70^{\circ}F$ is 6.6 ± 2.2.

L. The shutdown margin of the five rod bank plus rods A and B at 0 MWYR, $70^{\circ}F$, is $10.2.

---

* The energy release of the SM-1 Core I, unperturbed by the insertion of two new elements at 2/3 core life is estimated at 16.1 MWYR.

M. The 80 percent stuck rod shutdown requirement was met throughout core life.

N. The most reactive core configuration met the 80 percent requirement by -30 cents.

O. Peak xenon concentration was reached 7 to 9 hr after power reduction and had decayed to equilibrium concentration after a total of 19 to 21 hr.

P. Least squares fits of transient xenon reactivity data indicate:

1. A slight decrease in the reactivity of equilibrium xenon relative to low xenon of from 325 cents to 309 cents during 16.4 MWYR.

2. A slight increase in the reactivity of peak xenon relative to equilibrium xenon of from 133 cents to 157 cents.

3. A slight increase in reactivity of peak xenon relative to low xenon of from 458 cents to 466 cents.

Q. The relative axial neutron flux distribution curves indicate that as the bank is withdrawn from the core, the location of the flux peak moves upward

R. At a constant energy release, the peak-to-average flux ratio decreased as the core temperature increased.

S. The peak-to-average flux distribution ratio decreased with core burnup.

T. Source multiplication data shows an increase in shutdown margin with lifetime and that the worth of rods A and B appeared to remain constant with core life at 6.5 ± 0.2.

U. The excess reactivity of the core based on critical water height and worth was $17.2. This is considerably lower than the value of $23.8 obtained by integrating the five rod bank calibration curve from the cold clean critical bank position to 22 inches.

The following recommendations on improving present core physics measurements and techniques would add greatly to the accuracy and usefulness of the data.

A. A training program for the military operating crew on the reasons for measurements, the techniques used, the need for strict adherence to the test procedures, and the need for accuracy in all measurements.

B. An improvement in temperature measuring instrumentation, including provision for calibration prior to core physics tests.

C. The maintaining an accurate log book of all maintenance, calibrations, and adjustment to Δt integrator.

D. It would also be desirable to investigate the possibility of inserting a different BF_3 chamber into one of the instrument wells for the source multiplication experiment. This chamber would be removed afterward and used just for this test during core life in order to obtain better data.

6.2 SM-1 REARRANGED AND SPIKED CORE I EXPERIMENTAL RESULTS

A. The SM-1 Rearranged and Spiked Core I operated for 1.6 MWYR for a Core I total energy release of 18.0 MWYR, at which time it was arbitrarily shut down for core changeover.

B. The estimated total potential energy release of the SM-1 Core I and the Rearranged and Spiked Core I is 19.1 MWYR, had operation been allowed to actual end of life.

C. The reactivity increase due to core rearrangement and spiking is $2.7.

D. The removal of the defective PM-1-M element and substitution of the SM-2A element had a negligible effect on core reactivity.

E. The total Rod A integral worth, cold, low Xe, shows an increase in worth of approximately $1.0 over similar measurements made on Core I prior to rearrangement. The total Rod A integral worth, hot, low Xe, shows an increase of $0.9 over similar measurements.

F. Rod C shows a greater integral worth than measured on Core I prior to rearrangement.

G. Within the rather large experimental uncertainties, there was no change in temperature coefficient in comparison to the measurements made prior to Core I rearrangement and spiking.

H. The hot to cold reactivity change, with low xenon concentration in the core, is $7.2 $\pm$ 0.4.

I. Five rod bank calibrations at the startup of the Rearranged and Spiked Core I (16.5 MWYR) are similar to the 0 MWYR measurements. Calibrations at the end of life of the Rearranged and Spiked Core I (18.0 MWYR) show an increase in worth of $1.2 from 16.5 MWYR in the interval from 13 to 22 in. This increase in worth is in agreement with the measurements made on Core I as a function of burnup prior to rearrangement and spiking.

6-3

J. The positions of the relative axial neutron flux distribution curves were in agreement with the data obtained from Core I prior to rearrangement and spiking.

K. The peak-to-average flux ratios were lower than the ratios obtained for Core I prior to rearrangement. This indicates a flattening of the flux in the Rearranged and Spiked Core I.

L. Peak xenon concentration was reached 7.5 hr after power reduction and had decayed to equilibrium concnetration after a total of 20 hr; agreeing with the measurements obtained prior to rearrangement and spiking.

M. Peak xenon relative to equilibrium xenon had a negative reactivity of $1.39.

N. Equilibrium xenon relative to low xenon had a negative reactivity of $2.97.

6.3 RECOMMENDATIONS

It is suggested that the following work be considered, for the purpose of clarifying and evaluating further the data presented here.

A. Resolve the difference in excess reactivity of the core obtained by critical water height measurements and by the integral bank worth. This would involve an evaluation of the techniques used at other facilities as well as experimental checks at the Critical Facility.

B. Determine if better procedures are available to obtain accurate temperature coefficient measurements. Possibilities are to do the temperature coefficient during heatup, maintaining criticality with the calibrated five rod bank or with a calibrated control rod. The bank or rod would be calibrated during the heatup as a function of temperature. In this manner, the calibrations would be obtained for the actual core conditions, and there is also a better control of system temperature during heatup.

C. Investigate the possibility of measuring the temperature coefficient at power, with equilibrium xenon concentration in the core, using a method similar to that used at PWR.

D. Investigation of bank calibration techniques to determine the bank worth over its full length of travel.

E. Rod A calibrations as a function of various B-10 poison loadings. This would be similar to the Rod C and Rod 3 calibrations performed in ZPE-1 and could be performed at the Alco Critical Facility in Schenectady. This experiment would aid in separating the burnup, bank position, and temperature effects on the Rod A calibrations obtained at the SM-1.

7.0 BIBLIOGRAPHY

1. Rosen, S. S., Editor, "Hazards Summary Report for the Army Package Power Reactor, SM-1, Task XVII," APAE No. 2, Revision 1, May 1960.

2. Meem, J. L., Editor, "Initial Operation and Testing of the Army Package Power Reactor APPR-1," APAE No. 18, August 9, 1957.

3. Obrist, C. H., et al, "SM-1 Reactor Core Inspection at 2/3 Core Life," APAE No. 55, January 13, 1960.

4. Kemp, S. N., et al, "SM-1 Research and Development Program Test Report, Core Physics Measurements at 16.43 MWYR, Tests 301-317, 319, 320," AP Note No. 291, October 15, 1960.

5. Kemp, S. N., et al, "PWR Research and Development Program Test Report, Gamma Scanning Spent SM-1 Core I Fuel Elements, Test 318," APAE Memo No. 281, April 6, 1961.

6. Hasse, R. A., et al, "Army PWR Support and Development Program Test Report, Flux Mapping of SM-1 Spent, Rearranged and Spiked Cores - Test 321," AP Note No. 321, January 5, 1961.

7. O'Brien, J. P., Project Engineer, "A Boron Determination for the APPR-1," MND-E-1718-1, May 25, 1959.

8. Noaks, J. W., and Johnson, W. R., "Army Package Power Reactor Zero Power Experiments, ZPE-1," APAE No. 8, February 8, 1957.

9. Marlowe, O. J., and Ombrellaro, P. A., "Candle - A One-Dimensional Few-Group Depletion Code for the IBM-704, Addendum 1 Candle-2," WAPD-TM-53, Addendum 1, October 1957.

10. MacKay, S. D., et al, "SM-1 Research and Development Program, Interim Report on Core Measurements, Task No. VII," APAE Memo No. 178, March 1, 1959.

11. MacKay, S. D., and Stueck, C. J., "Program No. 67, Temperature Coefficient," AP Note No. 114, September 15, 1958.

12. Christman, R. P., and Jones, D. H., "Summary of Calculational and Experimental Physics Results for Shippingport PWR-1 Seed-1," WAPD-234, January 1961.

13. MacKay, S. D., and Tubbs, D. C., "Procedures for Core Measurements, TP-301 - TP-316."

14. Noaks, J. W., Editor, "Extended Zero Power Experiments on the Army Package Power Reactor, ZPE-2," APAE No. 21, November 15, 1957.

15. Noaks, J. W., et al, "SM-2 Critical Experiments, CE-1," APAE No. 54, November 30, 1959.

16. DeYoung, R. C., Letter to H. L. Weinberg, "Stuck Rod Experiment 2," January 20, 1958.

17. DeYoung, R. C., Letter to H. L. Weinberg, "Stuck Rod Experiment 1," January 20, 1958.

18. Murray, R. L., "Nuclear Reactor Physics," Prentice Hall, Inc., Englewood Cliffs, N. J., (1957).

19. Clancy, E. F., "Neutron Startup Sources for the SM-1 Core II," AP Note No. 213, January 8, 1960.

20. Etherington, H., Editor, "Nuclear Engineering Handbook," McGraw-Hill Book Company, Inc., New York (1958).

21. Glasstone, S., and Edlund, M. C., "The Elements of Nuclear Reactor Theory," D. VanNostrand Co., Inc., Princeton, New Jersey (1952).

22. Byrne, E. J., and Oby, P. V., "Analysis of Extended Zero Power Experiments on the Army Package Power Reactor, ZPE-2," APAE No. 27, May 7, 1958.

23. Scoles, J. F., "Calculated Gamma Ray Spectra from U-235 Fission Products," NARF-58-37T, August 29, 1958.

24. MacKay, S. D., and Fried, B. E., "Evaluation of Hazards Associated with SM-1 Core I Modification," APAE Memo No. 194, May 8, 1959.

25. Edgar, E. C., and Robertson, R. D., "Materials Specifications for APPR-1 Core II Control Rod Fuel Element and Absorber Sections," APAE Memo 159, December, 1958.

26. Birken, S., "Hazards Report for SM-1 Rearranged and Spiked Core," AP Note 225, May 25, 1960, and Addendum, 8-11-60; Addendum 3 (B. J. Byrne, 10-24-60); Addendum 4 (B. J. Byrne, 10-26-60).

27. O'Brien, J. F., "Evaluation and Results of the Irradiation Testing of the PM-1-M Fuel Element," MND-M-2583, June 1961.

28. Lee, D. H., Editor, "Experiments and Analysis for SM-1 Core II with Special Components," APAE No. 85, April 1961.

7-2

APPENDICES

APPENDIX A - FUEL ELEMENT LOCATION

A.1 ORIGINAL SM-1 CORE I LOADING

Figure A.1 presents the fuel element locations as initially loaded in the SM-1 Core I. [2] The number in the upper left corner of the lattice position is the position number. The number in the lower right corner is the element number.

A.2 MODIFICATIONS AT 10.5 MWYR

Figure A.2 presents the fuel element loadings following modification at 10.5 MWYR [3], [24]

A. The boron absorbers in control rods 1, 2, 3, 4 and C were replaced by europium absorbers [25] numbered 1, 5, 4, 6 and 8, respectively.

B. Fuel element number 13 in control rod 3 was replaced by fuel element number 12 from control rod 4. A new control rod fuel element, number 15, containing an integral europium flux suppressor [25] was placed in rod 4.

C. Stationary element number 46 was rotated 180° and used to replace the element, number 72, removed from position 57.

D. A spare, unused Core I stationary fuel element, number 62 was placed in position 56.

A.3 INITIAL SM-1 REARRANGED AND SPIKED CORE I

Figure A.3 presents the fuel element loadings for the initial Rearranged and Spiked Core I. At the end of life of Core I, 16.4 MWYR, the elements were rearranged by placing the low burnup elements in the center of the core and the high burnup elements along the edges. [26]   The core was spiked with:

A. PM-1-M [27] element in position 26.

B. SM-2B [28] element in position 52.

C. A fresh SM-1 element, number S-84, in position 21.

D. Elements number 79, 52, and 74 were removed from the core.

Code
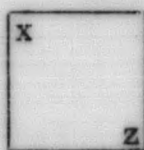
x = position number
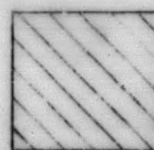
z = element number

Control rod element

Total Kg. of U^{235} = 22.50 Kg.

Source

12	13	14	15	16
S56	S54	S51	S52	S53

21	22	23	24 C.R. #1 10	25	26	27
S41	S55	S67		S68	S45	S70

31	32	33 C.R. A 11	34	35	36	37
S40	S47		S80	S64	S69	S71

41	42 C.R. #4 12	43	44 C.R. C 9	45	46 C.R. #2 14	47
S57		S79		S81		S82

51	52	53	54	55 C.R. B 16	56	57
S42	S48	S66	S65		S46	S72

61	62	63	64 C.R. #3 13	65	66	67
S44	S43	S49		S50	S74	S73

72	73	74	75	76
S58	S78	S77	S76	S75

Plates
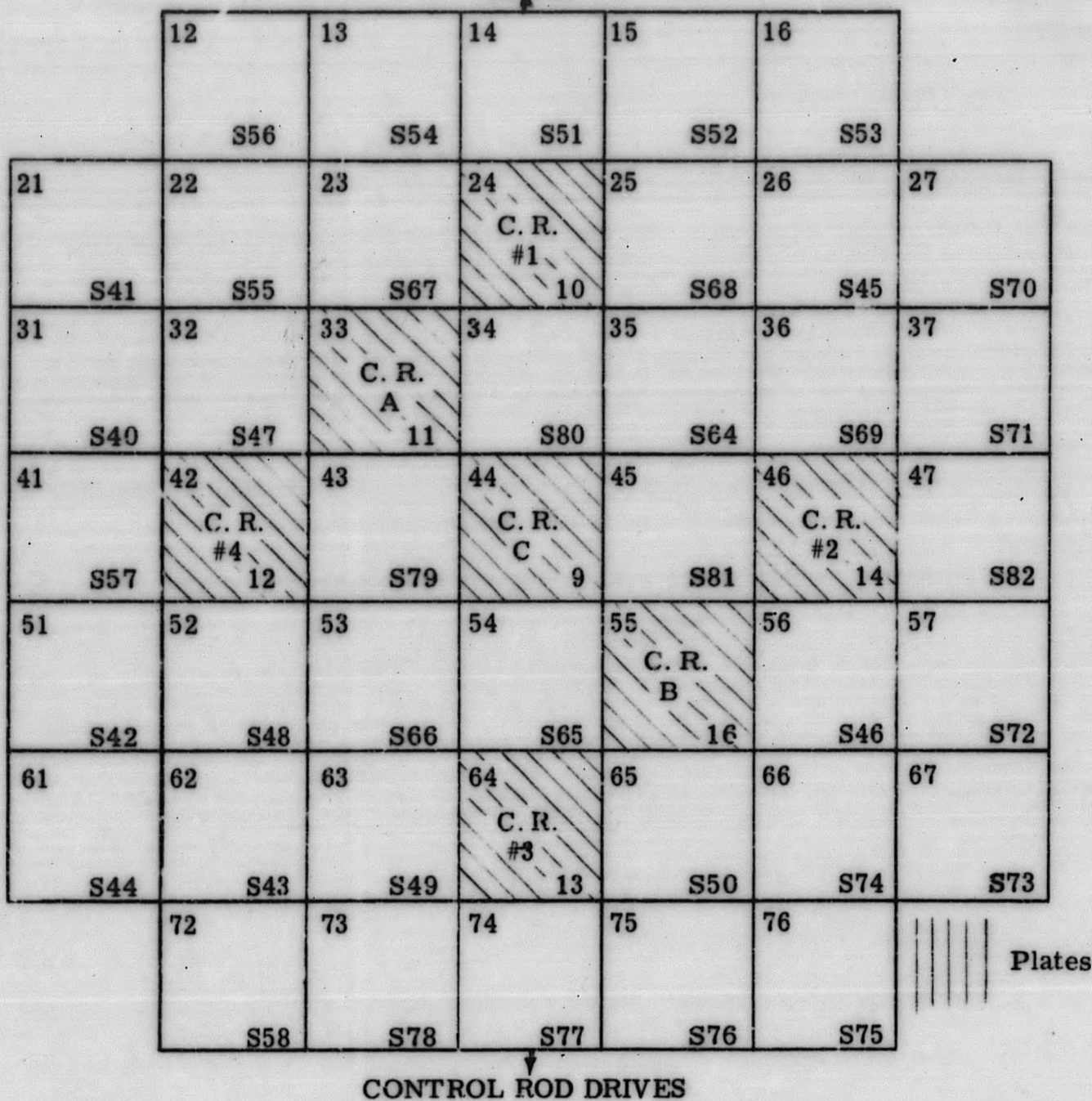
CONTROL ROD DRIVES

Figure A. 1.   SM-1 Core I Initial Loading
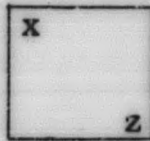
A-2
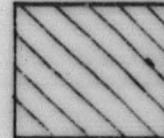
Code

x = position number
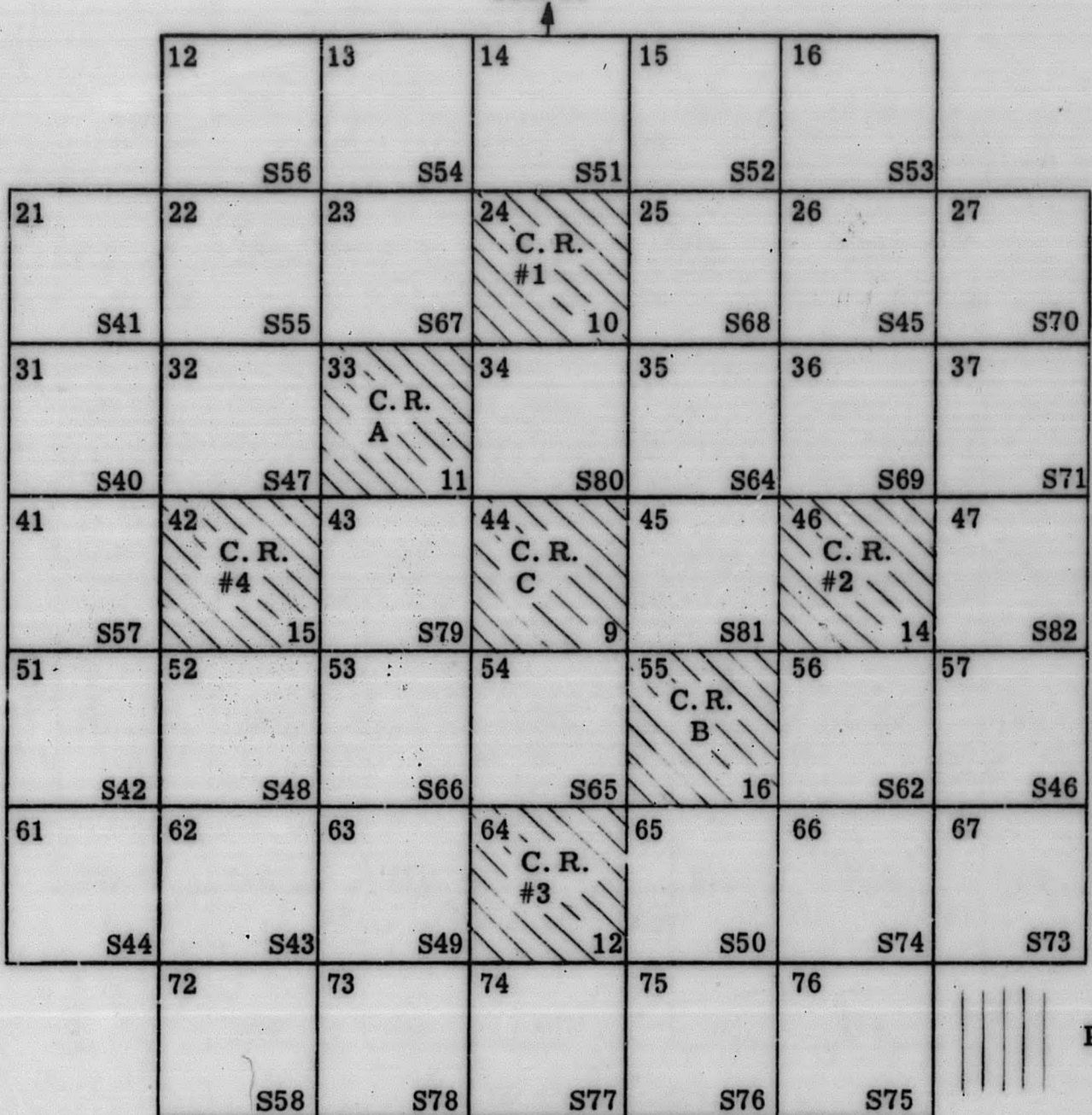
z = element number

Control rod element

Figure A.2. SM-1 Core I as Modified at 10.5 MWYR

Code

x		x = position number
	z	x = element number

control rod element

Source

12	13	14	15	16
S64	S45	S51	S68	S81

21	22	23	24 C.R. #1	25	26	27
S84	S56	S41	11	S53	PM-1-M	S80

31	32	33 C.R. A	34	35	36	37
S67	S40	12	S54	S82	S70	S69

41	42 C.R #4	43	44 C.R. C	45	46 C.R. #2	47
S55	18	S57	CR-15	S62	14	S42

51	52 SM-2B	53	54	55 C.R. B	56	57
S47	SM-2	S78	S76	10	S73	S46

61	62	63	64 C.R. #3	65	66	67
S48	S58	S44	9	S75	S71	S50

72	73	74	75	76
S65	S43	S77	S49	S66

Plates
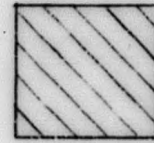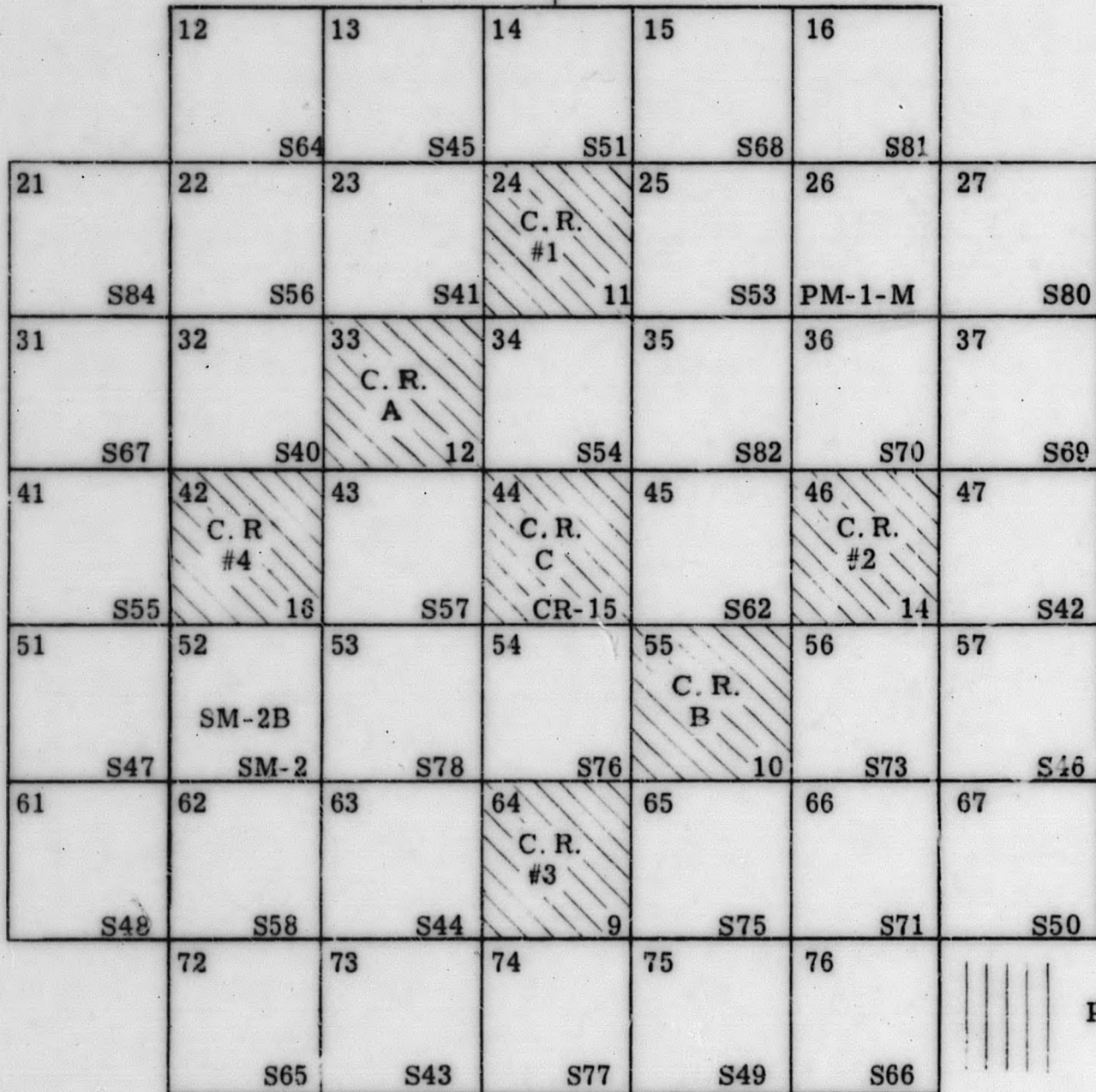
CONTROL ROD DRIVES

Figure A.3. Initial SM-1 Rearranged and Spiked Core I

A.4   FINAL SM-1 REARRANGED AND SPIKED CORE I

The startup operations of the initial Rearranged and Spiked Core I resulted in a significant increase in the fission product concentration in the primary coolant. The core was shutdown and the release of fission products localized to the PM-1-M element. [27] This element was then removed and replaced by element number 75 from position 65. An SM-2A element [28] was placed in position 65. Figure A.4 shows the final loading of the SM-1 Rearranged and Spiked Core I.

A.5   ORIENTATION OF FUEL ELEMENTS BY DOWEL PIN DIRECTION

The orientation of fuel elements in the core is further specified by the direction faced by a dowel pin which protrudes from one side of the stationary fuel element end boxes. The dowel pin directions are tabulated in Table A.1. These directions were kept constant throughout core rearrangement.

TABLE A.1
DOWEL PIN DIRECTION

| | Dowel Pin Direction | |
Element	Toward Rod Drives	Toward Source
S81		X
S62		X
S73	X	
S50		X
S75		X
S66	X	
S78	X	
S43	X	
S58	X	
S65		X
S76		X
S49	X	
S44		X
S48	X	
S42		X
S47	X	
S40	X	
S67		X
S41	X	
S79		X
S57	X	
S55	X	
S56		X
S64	X	

TABLE A.1 (CONT'D)

Element	Dowel Pin Direction	
	Toward Rod Drives	Toward Source
S82	X	
S74	No dowel pin	
S71		X
S69		X
S70		X
S80	X	
S54	X	
S45		X
S52		X
S68	X	
S53		X
S81		X
S79	-	-
S84		X
S75	-	-

Code

x = position number

z = element number

Control Rod Element

Source ↑

12	13	14	15	16
S64	S45	S51	S68	S81

21	22	23	24 C.R. #1	25	26	27
S84	S56	S41	11	S53	S75	S80

31	32	33 C.R. A	34	35	36	37
S67	S40	12	S54	S82	S70	S69

41	42 C.R. #4	43	44 C.R. C	45	46 C.R. #2	47
S55	16	S57	CR-15	S62	14	S42

51	52 SM=2B	53	54	55 C.R. B	56	57
S47	SM-2	S78	S76	10	S73	S46

61	62	63	64 C.R. #3	65 SM-2A	66	67
S48	S58	S44	9	SM-2	S71	S50

72	73	74	75	76	Plates
S65	S43	S77	S49	S66	
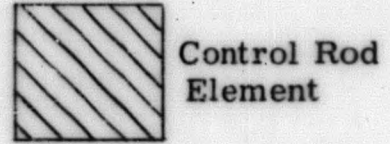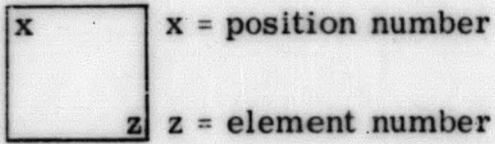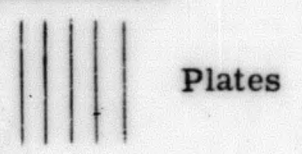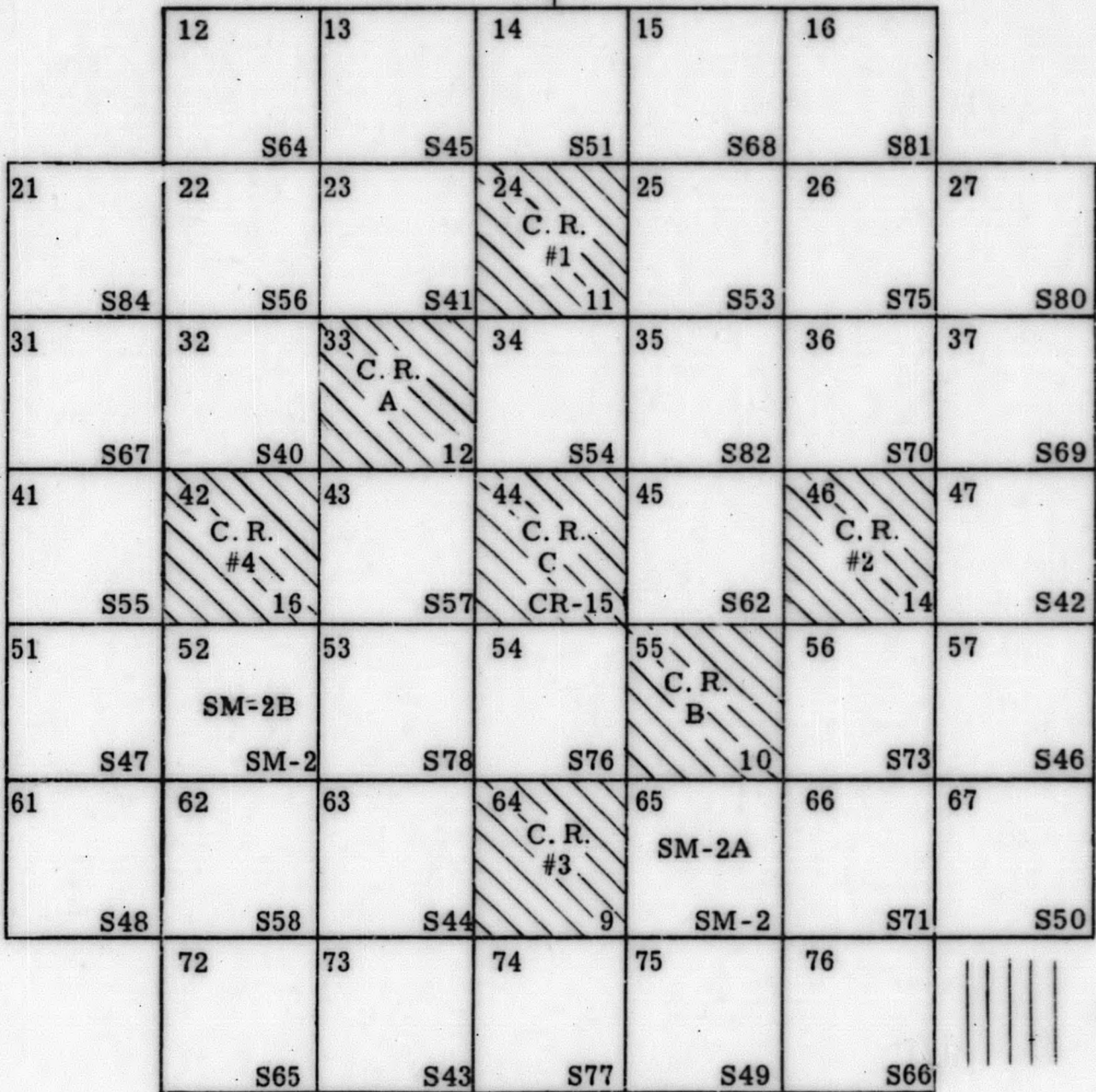
CONTROL ROD DRIVES ↓

Figure A. 4.   Final SM-1 Rearranged and Spiked Core I
Total Kg of U^{235} = 16. 92 Kg

A-7

APPENDIX B - CORE PHYSICS TEST PROCEDURES

B.1 TEST NO. A-301 - TRANSIENT XENON

The test objective of the transient xenon test is to evaluate the reactivity associated with the xenon concentration in the core as a function of the time after reactor shutdown. This test objective is attained after the establishment of equilibrium xenon concentration in the core. The reactor is then brought down to a low power level and the changing core reactivity associated with the buildup and decay of xenon in the core is followed by maintaining core criticality with a previously calibrated control rod.

B.2 TEST NO. A-302 - EQUILIBRIUM XENON

The test objective of the equilibrium xenon test is to evaluate the reactivity associated with the equilibrium xenon concentration in the core. This test objective is attained after the reactor is operated continuously for approximately 48 hr at a constant power level to establish an equilibrium xenon concentration in the core. Operational data is recorded hourly during the run until the critical bank positions attain a constant value. The reactivity associated with the equilibrium concentration is established from the difference between the no xenon (operational conditions) critical bank position and the final equilibrium xenon critical bank position and the previously determined bank worth.

B.3 TEST NO. A-303 - FIVE ROD BANK POSITION, PEAK XENON CONCENTRATION, 440°F

The test objective is the determination of the critical position of the five rod bank at (440°F), with peak xenon concentration in the core. This test objective is attained after the reactor is operated at full power for about 48 hr to achieve near equilibrium conditions. The reactor is then shutdown and the xenon builds up to peak concentration at which time the five rod critical bank position will be determined. The five rod bank position is to be measured as a function of core life to show core burnout characteristics at operating temperature with peak xenon concentration.

B.4 TEST NO. A-304 - FIVE ROD BANK POSITION, EQUILIBRIUM XENON CONCENTRATION, 440°F

The test objective is the determination of the critical position of the five rod bank at 440°F with equilibrium xenon concentration in the core. This test objective is attained after the reactor is operated continuously at full power for at least 48 hr to achieve equilibrium xenon concentration in the core. The five rod critical bank position will be determined with equilibrium xenon concentration in the core. The five rod bank position is to be measured as a function of core life to show core burnout characteristics at operating temperature with equilibrium xenon concentration.

B. 5 TEST NO. A-305 - FIVE ROD BANK POSITION, LOW XENON
CONCENTRATION, 440°F

The test objective is the determination of the critical position of the five rod bank at 440°F with a low xenon concentration in the core. This test objective is attained after the reactor is operated for 48 hr at the minimum power level necessary to maintain the operating temperature, yielding a low xenon concentration in the core. The five rod bank critical position will then be determined. The bank position is to be measured as a function of core life to show core burnout characteristics at operating temperature with little or no xenon concentration in the core.

B. 6 TEST NO. A-306 - FIVE ROD BANK POSITION, LOW XENON
CONCENTRATION, LOW TEMPERATURE

The test objective is the determination of the critical position of the five rod bank at an operating temperature of approximately 70°F with little or no xenon concentration in the core. This test objective is attained after the reactor is shutdown from operation for at least 60 hr allowing a very low xenon concentration in the core to be established, with the primary system at low temperature. The five rod bank critical position will then be determined. The bank position is to be measured as a function of core life to show core burnout characteristics at room temperature with little or no xenon concentration in the core.

B. 7 TEST NO. A-307 - CONTROL ROD A CALIBRATION AT PEAK
XENON, 440°F

The test objective is to provide a basis for evaluating the reactivity change introduced by peak xenon concentration in the core, and for calibrating the five rod bank. This test objective is attained after the reactor is operated at full power for about 48 hr to achieve near equilibrium conditions. The reactor is then operated at a low power level and the xenon builds up to a peak concentration with the core at operating temperature. At the condition of peak xenon concentration, control rod A is calibrated as a function of the bank position by the period method.

B. 8 TEST NO. A-308 - CONTROL ROD A CALIBRATION AT LOW
XENON, 440°F

The test objective is to provide a basis for evaluating the reactivity change introduced by xenon, calibrating the bank, showing the relative axial flux distribution at the operating temperature and evaluating the temperature coefficient. This test objective is attained after the reactor is operated for 48 hr at the minimum power level necessary to maintain the operating temperature, yielding a low xenon concentration in the core. At the condition of low xenon concentration, the rod is calibrated as a function of the bank position by the period method.

B-2

B. 9 TEST NO. A-309 - CONTROL ROD A CALIBRATION AT LOW
XENON, LOW TEMPERATURE

The test objective is to provide a basis for: evaluating the temperature coefficient, showing the relative axial flux distribution at room temperature, calibrating the bank, and to generate data for use in neutron source evaluation. This test objective is attained after the reactor is shut down from operation for at least 60 hr, allowing a very low xenon concentration in the core to be established, with the primary system at room temperature. At the condition of low xenon concentration, the rod is calibrated as a function of the bank position using the period method.

B. 10 TEST NO. A-310 - CONTROL ROD C CALIBRATION AT LOW
XENON, 440°F

The test objective is to provide a basis for calibrating the four rod bank. Several calibrations throughout the core life may determine the change in central control rod worth as a function of core burnout. This test objective is attained after the reactor is operated for 48 hr at the minimum power level necessary to maintain the operating temperature, yielding a low xenon concentration in the core. At the condition of low xenon concentration, the central control rod is calibrated as a function of the bank position using the period method.

B. 11 TEST NO. A-311 - TEMPERATURE COEFFICIENT

The test objective of the temperature coefficient test is to determine the temperature coefficient of reactivity as a function of temperature and core life. The procedure followed will be to operate the reactor at a very low power level and allow the temperature to decrease from operating temperature to approximately 120°F. While the temperature is decreasing, criticality is maintained with a calibrated control rod. The change in temperature with the corresponding change in critical position of the calibrated control rod is interpreted to yield the temperature coefficient of reactivity.

B. 12 TEST NO. A-312 - SOURCE MULTIPLICATION

The test objective of the source multiplication test is to establish the adequacy of the neutron sources for providing sufficient flux to the nuclear instruments for safe startup under various core conditions. This objective is attained after the reactor has been shutdown from power operation for at least 60 hr, and the primary system is at room temperature. The reactor is brought critical at low power level, at which time a calibrated control rod is inserted stepwise and the sub-critical count rates measured.

B. 13 TEST NO. A-312-A - NEUTRON SOURCE EVALUATION

This test objective is to obtain information in order to evaluate the neutron sources used in the SM-1. This test objective will be attained by taking shutdown count rate measurements with:

1. The original Po-Be source and Be photoneutron emitter.

2. The Be photoneutron emitter alone.

3. The new Po-Be and Sb-Be dual source and Be photoneutron emitter.

These measurements will be analyzed to determine the adequacy of the new source to provide sufficient neutrons to safely startup the reactor at any time during core life.

B. 14 TEST NO. A-313 - GAMMA HEATING IN THE PRESSURE VESSEL

The test objective is to measure the gamma heating in the pressure vessel wall during operation at various power levels. The procedure followed will be to operate the reactor continuously for 48 hr at a constant power level; operating and gamma heating data are recorded hourly. Runs will be made at various power levels to obtain the gamma heating data as a function of power level.

B. 15 TEST NO. A-314 - FIVE ROD BANK CALIBRATION, PEAK TO EQUILIBRIUM XENON

The test objective is to measure the maximum rate of change of reactivity available and provide a means for evaluating the reactivity of the core as a function of core life. The procedure will be to achieve full power equilibrium xenon concentration in the core by operating the reactor at full power for at least 48 hours. A five rod bank critical position is obtained at the equilibrium xenon concentration condition, the power is reduced, and the xenon transient initiated. The reactivity introduced by the xenon transient is determined by maintaining criticality with a calibrated control rod. A five rod bank critical position is taken when the xenon concentration reaches its peak. The motion of the five rod bank associated with the reactivity introduced by the xenon provides a calibration for the five rod bank.

B. 16 TEST NO. A-315 - FIVE ROD BANK CALIBRATION FROM ROD A CALIBRATION, LOW XENON, 440°F

The test objective is to measure the maximum rate of change of reactivity available, to provide a means for evaluating the reactivity of the core as a function of core life, and to indicate the five rod bank worth as a function of temperature. The test objective is attained after the reactor is operated for 48 hours at the minimum power level necessary to maintain the operating temperature,

B-4

yielding a low xenon concentration in the core. Critical positions for the bank are taken with control rod A fully withdrawn. Control rod A is then calibrated over its length by the period method. A calibration for the bank is determined from the change in bank position associated with the change in reactivity as determined from the integral worth of the calibrated rod.

B. 17 TEST NO. A-316 - FIVE ROD BANK CALIBRATION FROM ROD A CALIBRATION, LOW XENON, LOW TEMPERATURE

The test objective is to measure the maximum rate of change of reactivity available and to provide a means for evaluating the reactivity of the core as a function of the core life. This test objective is obtained after the reactor is shut down from operation for at least 60 hr, allowing a very low xenon concentration to be established in the core, with the primary system at low temperature. At the condition of low xenon concentration, critical positions of the bank are determined with calibrated control rod A fully inserted and fully withdrawn. A calibration for the bank is determined from the change in bank positions associated with the change in reactivity as determined from the integral worth of the calibrated rod.

B. 18 TEST NO. A-317 - SPENT CORE REARRANGEMENT

The test objective is to determine the extension in SM-1 Core I lifetime possible by rearrangement of the fuel elements and to provide a basis for the estimation of the increase in lifetime possible by rearrangement techniques for other cores of the APPR type. This test objective is accomplished by removing the elements from the core and then placing the low burnup elements in the center positions of the core and the high burnup elements in the outer positions. The excess reactivity in the core will be measured from the integral bank worth allowing the extension in core life to be estimated.

B. 19 TEST NO. A-318 - GAMMA SCANNING OF SPENT FUEL ELEMENTS

The objective of this test is to determine the gross uranium burnout distribution of the spent fuel elements. The test procedure will be to remove each element from the core to the spent fuel pit and then scan it along the active fuel length with the spectrometer apparatus. The gamma distribution obtained will be related to the fuel burnup distribution.

B. 20 TEST NO. A-319 - DANGER COEFFICIENT MEASUREMENTS

The objective of this test is to provide information from which the danger coefficient associated with the insertion of a new SM-1 Core I element may be evaluated. The test procedure will be to use the change in critical position of calibrated control rods to determine the change in core reactivity associated with the insertions of the new element in several core positions.

B.21 TEST NO. A-320 - XENON OVERRIDE BY TEMPERATURE COMPENSATION

The test objective is the determination of the minimum time required to
return to normal operation with peak xenon concentration in the core, by temp-
erature compensation. The procedure will be to operate the reactor for 48 hr
at full power to obtain equilibrium xenon concentrations in the core. The reactor
will then be scrammed and allowed to cool for 8 hr while peak xenon concen-
tration in the core is built up. After 8 hr shutdown, rod withdrawal will begin
as in a normal startup. Once the rods are withdrawn to this original critical
position, they will not be adjusted for the duration of test, and the reactor will
be allowed to return to full power while recording the temperature as a function
of time. As the xenon burns out, the core reactivity and power level will in-
crease allowing the temperature to increase. The period between the initial
rod withdrawal and the return to full power operations will be considered the
minimum time required for return to full power operation at peak xenon concen-
tration by temperature compensation.

B.22 TEST NO. A-321 - FLUX MAPPING

The objective of the flux mapping test is to obtain a map of the relative
flux distribution in the core. The test procedure will be to locate the foils in
one quadrant of the core, and then irradiate them at 0.01 percent of full power
for a specified time interval. The induced activity of each foil will be determined
relative to a single foil. The neutron flux in the quadrant is then obtained rela-
tive to the flux in which the single foil was exposed.

B.23 TEST NO. A-322 - SHUTDOWN NEUTRON SOURCE EVALUATION

The objective of this test is to evaluate the neutron source used in the
reactor. The test is initiated after the reactor has been shut down from power
operations for at least 60 hr, in order to minimize the xenon concentration in
the core. Optimum pulse height settings will be determined for the startup
channels and shutdown count rate measurements will be taken at predetermined
intervals over a specified period of time. This data will be interpreted to yield
an evaluation of the adequacy and time dependent behavior, of the neutron source
and photoneutron emitters.

B.24 TEST NO. A-325 - CALIBRATION OF FIVE ROD BANK

The objective of this test is to determine the differential worth of the
five rod bank as a function of burnup and other core changes. The test method
is to determine the differential bank worth by the period method. The differential
worth at a number of bank positions will be obtained by changing reactor tempera-
ture or xenon concentration. This information will be used to evaluate the re-
activity of the core and to check calibrations by other methods.

B-6

APPENDIX C - PROBABLE ERROR ANALYSIS

C.1 THEORY OF ERRORS

C.1.1 Introduction

There are four types of errors:

1. Constant or systematic errors (meter calibrations wrong; zero off; results influenced by some secondary phenomenon which has been neglected; etc.).

2. Personal Errors (setting cross hair to one particular side of center; actuating stop watch too soon, etc.). If the individual is consistent in these errors, they are merely a subdivision of the first type.

3. Mistakes (errors in reading a scale, i. e. 6.3 for 5.7; errors in recording data such as transposition, i. e. 165 for 156; etc.). If sufficient data have been taken, and the discrepancy of one observation with the mean is large enough to be certain, the observation can be legitimately rejected.

4. Accidental errors. These are errors due to the combined effect of a number of causes, each of which is just as likely to have a (+) effect as a (-) effect.

The first and second types are (in general) consistent or systematic, the third type is erratic, the fourth statistical. The fourth is therefore the only type that can be treated mathematically.

A number of methods have appeared for the mathematical treatment of this fourth type of error. Of these, the only one which can be shown by experiment to conform with the actual behavior of nature is that of "least squares." Least squares obtains its name from the fact that it makes the sum of the squares of the "residuals," rather than the sum of the residuals, have the smallest possible value. A residual is the difference of any given observation from the value predicted by all the observations combined (i. e., the distance of a point from a curve: or the difference of a single observation from the average of all; etc.).

C.1.2 Probable Errors of Averages

There are two types of probable errors, namely external, Re, and internal, Ri, that apply to the average, or mean, of several similar observations. The external p. e. (probable error) depends on the difference of each of the similar observations from their mean. It is, in short, a measure of the consistency of

the quantities entering into the mean value. If, however, each of the quantities which are averaged have known probable errors (which may be different for each quantity), then an internal p. e. of the mean can be computed which depends entirely on these individual probable errors (and is therefore independent of their consistency).

In expressing the p. e. of a mean, common practice is to be conservative and use the larger of the internal or external p. e. The ratio of the two probable errors Re/Ri should be approximately unity. The deviation of this ratio to values above unity is a gauge of the presence of constant or systematic errors. To be specific: if n is five, a ratio of two is an indication, and a ratio of three almost certain evidence, of the presence of constant or systematic errors; while if n is 20, a ratio of 1. 5 is an indication, and a ratio of two almost certain evidence of such errors.

Both the value of the mean and its p. e. are influenced by the relative weights, p, of the results entering into it. Obviously if one observation is considered twice as reliable as another, it should influence the result twice as much as the other. If the observations are all of equal reliability, we assign a weight of one to each. These observations are commonly referred to as "unweighted."

The residual, v, is simply the difference between an individual observation, x, and the mean, $\bar{x}$, of all the observations, i. e., $v = x - \bar{x}$.

The following cases are described:

1. The external p. e., Re, of the weighted mean $\bar{x}$ of n observations x_1, x_2, . . . x_n having relative weights p_1, p_2, . . . p_n.

The weighted mean is

$$\bar{x} = \frac{\sum (px)}{\sum p} \tag{1}$$

In Eq. (1) and in all the following equations, the summations run from one to n.

The external p. e. of the mean is

$$Re = \pm 0.6745 \sqrt{\frac{\sum (pv^2)}{(n-1) \sum p}} \tag{2}$$

The result would then be expressed as

$$\bar{x} \pm Re$$

The weights p used in these formulas may be assigned arbitrarily (from experimental conditions) or they may be from known probable errors as in Sec. 3, Eq. 5.

2. The external p. e., Re, of the mean of n observations x_1, x_2, . . . x_n having equal weights. Equations (1) and (2) become

$$\bar{x} = \frac{\sum x}{n}$$

$$Re = \pm 0.6745 \sqrt{\frac{\sum (v^2)}{(n-1) n}} \qquad (4)$$

3. The internal p. e., Ri, of the weighted mean $\bar{x}$ of n observations x_1, x_2, . . . x_n, the probable errors of which are r_1, r_2, . . . r_n, and the weights of which are p_1, p_2, . . . p_n. If the p. e. is known, the weight of a quantity is usually taken as proportional to the reciprocal of the square of its p. e., i. e.

$$P_j = \frac{c}{r_j^2} , \quad j = 1, 2, ... n \qquad (5)$$

Here c is a purely arbitrary constant. It may be taken as unity, but is commonly chosen to make the arithmetical work as easy as possible. Its value does not affect the results.

The weighted mean is (same as Eq. (1))

$$\bar{x} = \frac{\sum (px)}{\sum p} \qquad (6)$$

Its internal p. e. is

$$Ri = \pm \sqrt{\frac{c}{\sum p}} = \pm \sqrt{\frac{1}{\sum (\frac{1}{r^2})}} \qquad (7)$$

4. The internal p. e., Ri, of the mean $\bar{x}$ of n observations x_1, x_2, . . . x_n, the p. e. of which is the same, namely r.

Equations (6) and (7) became

$$\bar{x} = \frac{\sum x}{n} \tag{8}$$

$$Ri = \pm \frac{r}{\sqrt{n}} \tag{9}$$

It is to be emphasized that the probable errors r in both Sections 3 and 4 must be completely independent. In particular, they must not involve any error that is common to all of them.

C.1.3 Probable Errors of Functions

In general terms suppose

$$Z = f(z_1, z_2, z_3, \ldots) \tag{10}$$

where z_1, z_2, etc. are observed quantities with probable errors r_1, r_2, etc. We desire to find the p.e. R of Z.

$$R = \pm \sqrt{\left(\frac{\partial Z}{\partial z_1}\right)^2 r_1^2 + \left(\frac{\partial Z}{\partial z_2}\right)^2 r_2^2 + \left(\frac{\partial Z}{\partial z_3}\right)^2 r_3^2 + \ldots} \tag{11}$$

The results for several common functions are summarized in the accompanying table.

Function	Probable Error R	
$Z = z_1 + z_2 + z_3 + \ldots$	$R = \pm \sqrt{r_1^2 + r_2^2 + r_3^2 + \ldots}$	(12)
$Z = z^n$	$R = \pm Zn \dfrac{r}{z}$	(13)
$Z = z_1 z_2 z_3$	$R = \pm Z\sqrt{\left(\dfrac{r_1}{z_1}\right)^2 + \left(\dfrac{r_2}{z_2}\right)^2 + \left(\dfrac{r_3}{z_3}\right)^2 + \ldots}$	(14)
$Z = z_1^a z_2^b c_3^c$	$R = \pm Z\sqrt{\left(\dfrac{r_1}{z_1}\right)^2 a^2 + \left(\dfrac{r_2}{z_2}\right)^2 b^2 + \left(\dfrac{r_3}{z_3}\right)^2 c^2 + \ldots}$	(15)
$Z = a z$	$R = \pm a\,r$	(16)
$Z = \log_e z$	$R = \pm \dfrac{r}{z}$	(17)
$Z = \log_{10} z$	$R = \pm 0.4343 \dfrac{r}{z}$	(18)
$Z = a f(z_1, z_2, \ldots)$	$R = a$ times the p.e. of $f(z_1, z_2, \ldots)$	(19)

C-4

C.2 PROBABLE ERROR IN FIVE ROD BANK POSITION

There is an estimated error of ± 0.03 in. in determining the position of a single control rod. This is due both to the uncertainty in reading the rod position indicator and uncertainties in the indicating mechanism due to backlash, etc. During core physics five rod bank measurements, the control rods in the bank were kept within 0.1 in. of one another. The procedure to determine the five rod bank position and its probable error is as follows:

1. The first rod (of the five rod bank) is at position X_1. The remaining four rods have to be within 0.1 inches of X_1 and 0.1 inches of one another. The worst case being $X_2 = X_1 + 0.05$, $X_3 = X_1 - 0.05$, $X_4 = X_1 + 0.05$, and $X_5 = X_1 - 0.05$.

2. There is an experimental error of ± 0.03 inches in the position of each rod.

3. The bank position is calculated from the average of the five individual rod positions.

4. The probable error is calculated assuming the individual rod positions are equally weighted similar observations of the bank position.

Rod Position	v	v^2
X_1	0	0
$X_2 = X_1 + 0.05$	$+ 0.05$	25×10^{-4}
$X_3 = X_1 - 0.05$	$- 0.05$	25×10^{-4}
$X_4 = X_1 + 0.05$	$+ 0.05$	25×10^{-4}
$X_5 = X_1 + 0.05$	$- 0.05$	25×10^{-4}

Average position = X_1 $\qquad\qquad\qquad\qquad\qquad$ $\sum (v^2) = 100 \times 10^{-4}$

From equation (4) the external probable error is

$$Re = \pm 0.6745 \sqrt{\frac{\sum v^2}{(n-1)(n)}} = \pm 0.6745 \sqrt{\frac{100 \times 10^{-4}}{(4)(5)}}$$

$$Re = \pm 0.015 \text{ in.}$$

From Equation (9) the internal probable error is

$$R_i = \pm \frac{r}{\sqrt{n}} = \pm \frac{0.03}{\sqrt{5}}$$

$$R_i = \pm 0.013 \text{ in.}$$

The larger value, ± 0.015 in., is then used as the probable error of the five rod bank position.

C-6

APPENDIX D - ENERGY RELEASE DETERMINATION

D.1 CONVERSION OF ^{o}F DAYS TO MWYR

Core energy release is obtained from a Δt integrator which measures the Δt across the core and integrates it as a function of time to obtain ^{o}F days. The conversion from ^{o}F days to MWYR is derived as follows:

$$MWYR = m \ c_p \Delta t$$

where

m = coolant flow rate (the two SM-1 pumps have capacities of 1.66 x 10^6 and 1.60 x 10^6 lb/hr so average is used) = 1.63 x 10^6 lb/hr.

c_p = specific heat of water at 440°F and 1200 psi (interpolated from Reference (20)) = 1.1022 BTU/lb^{o}F.

Δt = Δt integrator reading in ^{o}F days.

Therefore:

$$MWYR = 1.63 \times 10^6 \ \frac{lb}{hr} \times \frac{1.1022 \ BTU}{lb^o F} \times \Delta t \ ^o F \ days \times \frac{yr}{365 \ day} \times \frac{MW \ hr \times 10^{-3}}{3412.75 \ BTU}$$

$$MWYR = \frac{\Delta t}{693.28}$$

APPENDIX E - SUMMARY OF SM-1 CORE I NUCLEAR DATA

Five Rod Bank Position, Low Xenon, 70°F, 0 MWYR	3. 70 in.
Seven Rod Bank Position, Low Xenon, 70°F, 0 MWYR	5. 50 in.
Five Rod Bank Position, Low Xenon, 440°F, 0 MWYR	6. 68 in.
Five Rod Bank Position, Equilibrium Xenon, 440°F, 0 MWYR	8. 30 in.
Five Rod Bank Position, Peak Xenon, 440°F, 0 MWYR	8. 98 in.
SM-1 Core I Energy Release	16. 4 MWYR
SM-1 Core I (Unperturbed) Energy Release*	16. 1 MWYR
SM-1 Rearranged and Spiked Core I Actual Energy Release	1. 6 MWYR
SM-1 Rearranged and Spiked Core I Estimated Potential Energy Release	2. 7 MWYR
Temperature Coefficient, Low Xenon, 440°F	-3.6 ± 0.1 ¢/°F
Hot to Cold Reactivity, Low Xenon	
A. SM-1 Core I	$6. 7 \pm 0.5
B. SM-1 Rearranged and Spiked Core I	$7. 2 \pm 0.4
Pressure Coefficient, Low Xenon	
A. Low Temperature	$1. 06 \pm 0.33$ ¢/100 psi
B. Operating Temperature	$3. 35 \pm 0.68$ ¢/100 psi
Five Rod Bank Integral Worth, 70°F, 0 MWYR	$27. 4 \pm 1.0
Seven Rod Bank Integral Worth, 70°F, 0 MWYR	$24. 0 \pm 2.0
Shutdown Margin, Five Rod Bank and Rods A and B, 70°F, 0 MWYR	$10. 2
Excess Reactivity, Low Xenon, 70°F, 0 MWYR	$23. 8
Excess Reactivity, Low Xenon, 440°F, 0 MWYR	$16. 5

---

* Unperturbed by the insertion of two new elements at 2/3 core life.

Excess Reactivity, Equilibrium Xenon, 440°F, 0 MWYR $12.9

Excess Reactivity, Peak Xenon, 440°F, 0 MWYR $11.5

Time Required to Reach Peak Xenon Concentration after
Reduction from Full Power Operation   7-9 hr

Time Required to Reach Peak Xenon and Decay Back to
Equilibrium Xenon Concentration after Reduction
from Full Power Operation   19-21 hr

Least Squares Fits of Transient Xenon Reactivity Data
Indicate:

    A. Reactivity of Equilibrium Xenon Relative to Low
        Xenon during Core I Life   -325¢ to -309¢

    B. Reactivity of Peak Xenon Relative to Equilibrium Xenon
        During Core I Life   -133¢ to -157¢

    C. Reactivity of Peak Xenon Relative to Low Xenon
        During Core I Life   -458¢ to -466¢

END